Physical analysis of solid solution formulations

By

LINA AKIL

A thesis submitted to the Strathclyde Institute of Pharmacy and Biomedical Sciences, University of Strathclyde, in fulfilment of the requirement for degree of Doctor of Philosophy

October 2018

Declaration of Authenticity and Author's Rights

This thesis is the result of the author’s original research. It has been composed by the author and has not been previously submitted for examination, which has led to the award of a degree.

Signed: _____

Date:

Acknowledgements

I would like to thank my supervisors Professor Gavin Halbert and Dr Steven Ford for their support, advice and encouragement throughout my PhD and for giving me this lifetime opportunity, without them I would have not be here now. Also, I would like to thank CRUK for funding my project.

I would like to thank Dr Ibrahim Khadra for his help and training on Sirius T3. Also, I send my gratitude to Prof Clive Wilson to invite me to his group meetings and his guidance. Dr Alan Martin for his time and patience in the VT XRPD experiments.

To my friends in RW215/217 lab and RW601F office thank you for the good times we spent together.

I would like to thank my big family (mum, dad, sisters and brothers) for their moral support and encouragement. Finally, I cannot find words to thank and appreciate my small family (Husband, Hadi and Majd) for their endless support, sacrifice and believing in me.

Abstract

Amorphous solid dispersion is one of the techniques used for enhancing dissolution rate of drugs with low aqueous solubility. The physical stability of the amorphous solid dispersion is the main challenge for their formulation development and commercialisation by pharmaceutical industry. The aims of the project were to prepare amorphous solid solution of a poorly aqueous soluble drug using different molecular weight mixtures of PEG and PEG mixed with other polymers such as PVP and poloxamers, the formulations were prepared using melt method, solvent evaporation and quench cooled from melt method. Also, to find a system with controlled instability to study the impact of various features on the stability of the formulation. A series of physicochemical characterisation techniques were used to evaluate the different formulations such as XRPD, VT XRPD, DSC, dissolution and microscopy. The cooling temperature of the formulation from melt has a great impact on forming amorphous CBZ in PEG mixture. PEG 300 did show the ability to reduce the crystallinity in the other PEG used and to reduce the enthalpy of CBZ recrystallisation which indicates that less crystals been formed. The higher the PEG concentration in the formulation, the more stable the CBZ amorphous form. The best performing formulations in terms of controlling the recrystallisation of the CBZ from melt were the PEG 4000 and 6000 mixed with PEG 300, but their dissolution profile was not as good as the formulations with one PEG. The substitution of just 5% of PEG weight with PVP did show an increase in CBZ amorphous form stability. The quench cooling method did not show any decomposition of CBZ and that was proven by the HPLC method used.

CBZ amorphous solid solution can be achieved by formulating the drug with PEG using melt method and the addition of secondary polymer such as PVP to the formulation at low concentration can inhibit the CBZ recrystallisation from the glassy/ liquid state and increases CBZ physical stability.

Table of Contents

Table of figures

List of tables

Abbreviation

API	Active pharmaceutical ingredient
CBZ	Carbamazepine
DSC	Differential scanning calorimetry
FT-IR	Fourier transform – Infra Red
HME	Hot Melt Extrusion
HMPC	Hydroxypropylmethylcellulose
HPLC	High Performance Liquid Chromatography
HSM	Hot Stage Microscopy
mg	Milligram
ml	Millilitre
Nif	Nifedipine
NMR	Nuclear magnetic resonance
PEG	Polyethylene glycol
PVA	Polyvinyl alcohol
PVP	Polyvinylpyrrolidone
T_g	glass transition
UV	UltraViolet
XRD	X-ray Diffraction

Chapter 1 Introduction

1.1 General introduction

In drug administration routes, oral administration is the most popular and common method for drug administration because it is convenient, relatively safe and inexpensive (Florence, 2011). The major drawback for this route is the low bioavailability, which depends on drug aqueous solubility, drug permeability, dissolution rate, first-pass metabolism, and presystemic metabolism (Savjani et al., 2012). For orally administered drugs to appear in the blood stream and have a therapeutic effect, the drug has to go through a dissolution process and then permeation across the gastric membrane. In recent years, the number of potential active pharmaceutical ingredients (API) has increased very quickly as a result of the use of combinatorial chemistry and high throughput screening (Sarode et al., 2012). These new APIs have problems hindering their development and commercialisation into effective drugs due to showing low aqueous solubility, which will have an impact on the dissolution rate and hence their bioavailability (Sinha et al., 2010). According to the Biopharmaceutics Classification System (BCS) drugs are divided into four different classes according to their solubility and permeability (Amidon et al., 1995). Butler and colleague did propose a revised version of the BCS system which is designed to focus more on drug developability such as intestinal solubility and permeability in the small intestine and an estimate of the particle size needed to overcome dissolution rate limited absorption were all considered in the revised system which been named as developability classification system (DCS) (refer to Figure 1.1-1). Most of these discovered drugs are of class II where the solubility is very low but they exhibit high permeability (Butler and Dressman, 2010). The figure below was reproduced from Butler and Dressman, 2010.

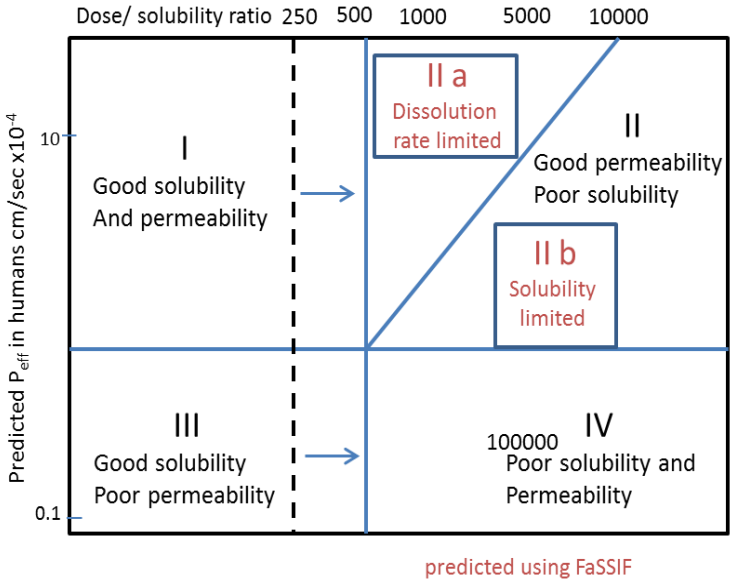

Figure 1.1-1 DCS drug classification

Solubility is the ability of a substance to dissolve in a solvent, in this situation aqueous systems are the most relevant. Solubility measurements of a drug can be divided into four groups (Box et al., 2009):

- Equilibrium solubility (also known as thermodynamic solubility) is the concentration of a drug in a saturated solution when excess solid is present in the solution and both (solution and solid) are in equilibrium. It can be measured using the shake flask method.
- Intrinsic solubility is the equilibrium solubility of the drug at a pH where it is fully un-ionised. It can be measured using potentiometric acid/base titration.
- Supersaturated solutions contain excess neutral species in solution, which will carry on precipitating until the system reaches equilibrium.
- Kinetic solubility is the concentration of a drug in a super-saturated solution when induced precipitation first appears. The precipitation can be measured using light scattering.

Dissolution can be defined as the process by which a solid solute enters into a solution in the presence of solvent (Beyssac et al., 2005). Solubility is a thermodynamic process while dissolution is a kinetic process. The dissolution rate of a solute in a solvent is directly proportional to its solubility, as described by the Noyes-Whitney equation (Noyes and Witney, 1897):

$$Dissolution\ rate = \frac{dM}{dt} = \frac{DA}{h}(Cs - Ct)$$ Equation 1-1

dM/dt is the rate of mass transfer, D is the diffusion coefficient (cm^2/s), A is the surface area of the drug (cm^2), h is the static boundary layer (cm), Cs is the saturation solubility of the drug, Ct is the concentration of the drug at time (t). There are lots of factors which will affect the solubility and the dissolution of a drug such as the temperature, the pressure, different polymorphic forms and the polarity of the solute and solvent (Kansara et al., 2015).

The solubility and the dissolution rate of a drug can be improved by physically modifying the solid material such as decreasing the particle size of the powder, which will increase the surface area for dissolution, the use of surfactant or cyclodextrin, co-solvent, the use of the amorphous form of the drug and solid dispersion (Kansara et al., 2015). These methods have disadvantages, such as poor control of the particle size distribution in the sample and surfactants suffers from adsorption of the drug formulation at the container wall either during manufacturing or storage which will affect the potency and the stability of the drug formulation (Florence, 2011). Therefore, there is the need to develop a good, reliable and efficient technique to improve solubility of poorly soluble aqueous drugs and to enhance their bioavailability. Solid dispersion has gained a good reputation as a platform technology for the formulation of poorly-soluble drugs. Solid dispersion technology has been successfully applied to develop formulations with a high drug loading and containing drugs with a high tendency to crystallise, besides there are a

few drugs that have been approved and are on the market such Gris-peg™, Norvir™ and Sporanox™ (Huang et al., 2014).

There are many different methods can be used to prepare solid dispersion formulations such as co-precipitation, kneading, electrospinning and lyophilisation (Nikghalb et al., 2012).

1.2 Crystalline and amorphous solids

Solid drugs can be broadly divided in two categories: crystalline and amorphous forms. In the crystalline form the drug molecules are held together by non-covalent bond in a highly ordered repeated unit. The crystal form can be subdivided by polymorphism (the ability of a drug substance to exist in more than one structural arrangement), co-crystals (drug molecules mixed with other crystals to form a single phase materials), solvate and hydrates (they are crystalline solid adducts containing either stoichiometric or nonstoichiometric amounts of a solvent/ water incorporated within the crystal structure) (Florence, 2011).

These different crystal forms of an API solid can have different chemical and physical properties such as melting point, apparent solubility, and dissolution rate. These properties can have a direct impact on performance of drug products, such as stability, dissolution, and bioavailability. The disadvantages of these crystal forms are: for the polymorph the most thermodynamically stable form is the least soluble and the metastable form is more soluble but less stable. The metastable form can revert to the more stable form during storage or due to environmental conditions (Vippagunta et al., 2001).

Amorphous form has no long range ordering of molecules (as shown in Figure 1.2-1) which have a rigid structure and wide range of dissolving temperature. The solubility and stability of amorphous drug is different from the crystalline form. Amorphous solids have higher energy state than the crystalline form, which makes them thermodynamically unstable, and in favour of changing to more stable crystalline form during storage. Besides, the type of drug solid will have an effect on the solid dispersion dissolution behaviour as the dissolution of amorphous drug is higher than the crystalline form.

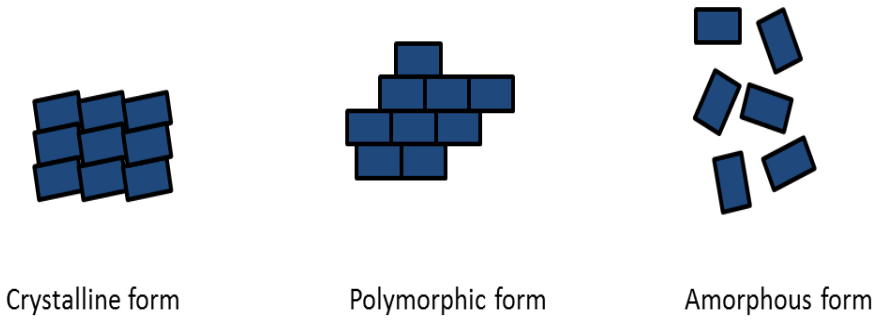

Figure 1.2-1 Crystalline, polymorph and amorphous arrangement

1.3 Solid dispersions

Solid dispersions can be described as the dispersion of one or more hydrophobic API(s) in a hydrophilic carrier. The carrier used in this process can be either crystalline (e.g. mannitol) or amorphous (e.g. polymers) and the drug can be dispersed in the carrier molecularly, in amorphous state or in crystalline particles (Varma et al., 2012). Solid dispersions can be divided into three categories: eutectic mixtures, solid solutions and glass suspensions (Sinha et al., 2010).

1.3.1 Eutectic mixtures

A eutectic mixture consists of two compounds (A and B) they are miscible in the liquid state but not moderately in the solid state. At a particular composition of A and B the eutectic point can be reached where the melting point of this composition is the lowest compared to any mixture of A and B and both compounds will crystallise simultaneously when cooled whereas at any other composition the components begin to crystallise consecutively (Figure 1.3-1). The advantages of the solid eutectic mixture are low processing temperature and a reduction in the particle sizes of A and B, hence, the increased surface area of the drug crystals which will enhance the dissolution of the eutectic mixture compared to the dissolution of A and B alone. Griseofulvin and succinic acid eutectic mixture was prepared as a solid dispersion by Chiou and colleague and showed an increase in the dissolution rate of griseofulvin from the formulation (Chiou and Niazi, 1976).

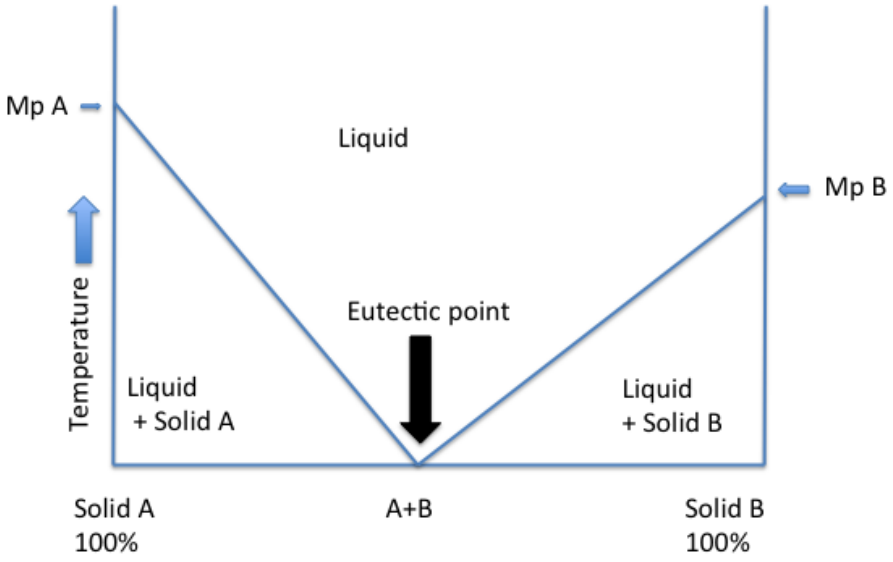

Figure 1.3-1 Eutectic mixture

1.3.2 Solid solution

In a solid solution, the drug will be molecularly dissolved in a good water-soluble solid carrier. The drug particle size has to be reduced and the dissolution rate will be determined by the dissolution rate of the carrier (Leuner and Dressman, 2000). Solid solutions can be divided into sub groups according to the drug and carrier miscibility (continuous and discontinuous) and the API distribution within the matrix (crystalline and amorphous solid solution) as shown in **Table 1.3-1** (Leuner and Dressman, 2000):

Table 1.3-1 Solid solution sub groups

Group	
Continuous solid solution:	The components of the solid dispersion are miscible at any composition in the solid state.
Discontinuous solid solution	The solubility of each of the components in each other is limited above certain temperature.
Crystalline solid solution	This section can be divided into two categories: • substitutional :The API molecules occupy crystal lattice sites, the miscibility can be continuous or discontinuous. • Interstitial: the API molecules can occupy the interstitial spaces in the crystal lattice, the miscibility can only de discontinuous.
Amorphous solid solution	The API is distributed irregularly within the amorphous solvent

As an example griseofulvin dispersed in PEG 4000 and 2000 (1:1) did show an increase in dissolution rate, also indomethacin dispersed in PEG 6000 did produce a faster dissolution rate and this is due to the formation of interstitial solid solution (Chiou and Riegelman, 1971).

1.3.3 Glass suspension

Glass suspension is when the amorphous drug is suspended in a homogeneous system with the matrix, which has a glass forming consistency (Shah et al., 2013). An example of this would be Griseofulvin in the citric acid glass suspension obtained from melt and this formulation did show an increase in dissolution rate Chiou and Riegelman, 1971).

1.3.4 Solid dispersion

This is the dispersion of an API in an inert carrier in the solid state prepared by solvent or melting method. Crystalline and amorphous solid dispersions can be produced.

A crystalline solid dispersion is prepared by dispersing crystalline drug in an amorphous carrier. This technique can be used for controlled drug release profile for fast soluble drug (Shah et al., 2013). The API in this technique is stable but the dissolution rate does not hugely increase compared to the pure API.

An amorphous solid dispersion is prepared by cooling of the drug-polymer melt at a rate that does not allow recrystallisation of the drug but the drug remains immiscible with the carrier. The advantage of this technique is the increase in the dissolution rate of the API; on the other hand, the amorphous API can revert back during storage or manufacturing to the stable crystalline form (Shah et al., 2013).

1.4 Methods of preparing solid dispersion

The most common routes for solid dispersion preparation are: fusion method, solvent evaporation, spray drying and hot melt extrusion (Nikghalb et al., 2012).

1.4.1 Fusion (melting) method

The method consists of the dispersion of an API in a matrix by melting using a physical mixture at eutectic composition followed by a cooling step. The matrix can be either crystalline or amorphous, the most common matrix used are urea, cyclodextrin and polymers. It is a very simple method; solvent free and only simple equipment is needed. (Shah et al., 2013) The first solid dispersion made using this method was the dispersion of Sulphathiazole in urea (Sekiguchi and Obi., 1961).

This method can only be used when drug and matrix are compatible and can be mixed well when heated to form a homogeneous solid dispersion. When the drug-matrix is cooled, the miscibility changes and separation can occur, which will affect the formulation, dissolution and stability. The use of this method can be affected by

the degradation of the drug or matrix if they are thermally unstable during the melting step.

1.4.2 Solvent evaporation

In this technique, the API and the polymer are dissolved in a solvent and then the solvent will be removed to produce a thin solvent free film and then dried as shown in Figure 1.4-1. The solvent should have the ability to dissolve both ingredients and to be removed completely using many methods such as freeze-drying and spray drying.

It is a useful technique in producing solid dispersion when other techniques fail (such as the hot melt extrusion technique) due to thermal issues but the main drawback of this technique is the solvent used has to be pharmaceutically acceptable and safe as some solvent residues can stay in the formulation. These residues can have adverse effects on the chemical stability of the API and on the patient health, it is also, considered to be an expensive technique (Sridhar et al., 2013). The first formulation prepared using this method was the formation of molecularly dispersed *B*-carotene in polyvinylpyrrolidone (PVP) and chloroform was used as the solvent (Tachibana and Nakamura, 1965).

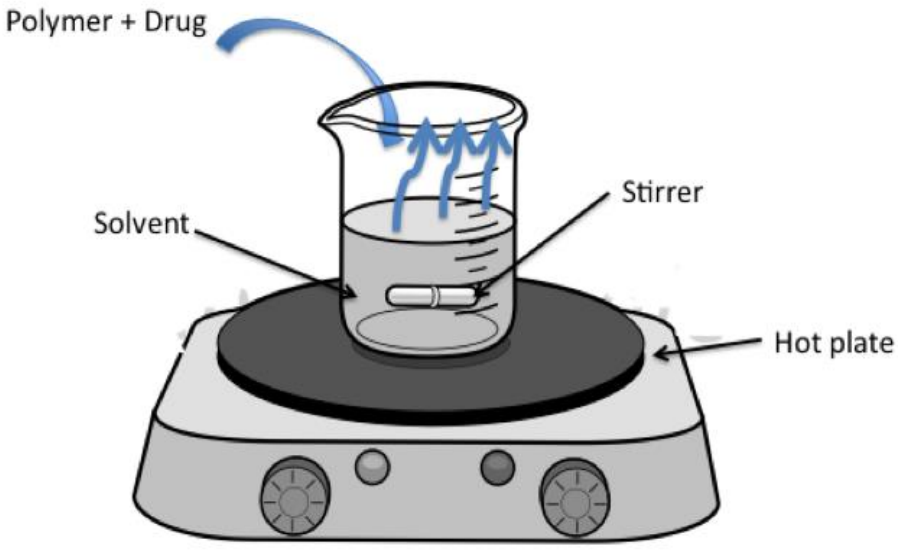

Figure 1.4-1 Solvent evaporation process

1.4.3 Spray drying

The spray drying technique transforms a liquid sample into dry particles by passing the liquid through hot gas as shown in Figure 1.4-2. This process consists of four steps:

1. Feed preparation: the feed should be homogenous and free from impurities. It can be solution, suspension or emulsion.

2. Atomization/droplet formation and hot gas contact: in this step the liquid is dispersed into fine droplets using two fluid nozzles, pressure nozzles, rotary disk atomizer or ultrasonic nozzles. The atomizer type is selected according to the rate of the feed and its nature also, on the required droplets size. (drying chamber in Figure 1.4-2)

3. Evaporation, particle shape formation and drying: The hot drying gas will evaporate the droplets. The morphology of the particles depends on the solvent, sample composition, flow rate of the drying gas and the temperature. The hot drying gas used is air but nitrogen is used when oxygen-free drying is required.

4. Separation of the dried product from the gas: The particles are separated from the gas by passing them into a cyclone. The fine particles will sediment after hitting the cyclone wall.

Spray drying technique is a rapid, robust and continuous process. It is very useful in controlling particle size, shape and morphology of the solid dispersion by altering the spray drying conditions. Also, the particles produced do not require additional process before tableting (Douroumis, 2013).

The disadvantage of this technique is that the drug and the polymer require a volatile solvent, which may leave some residue in the final product (Shah et al., 2013).

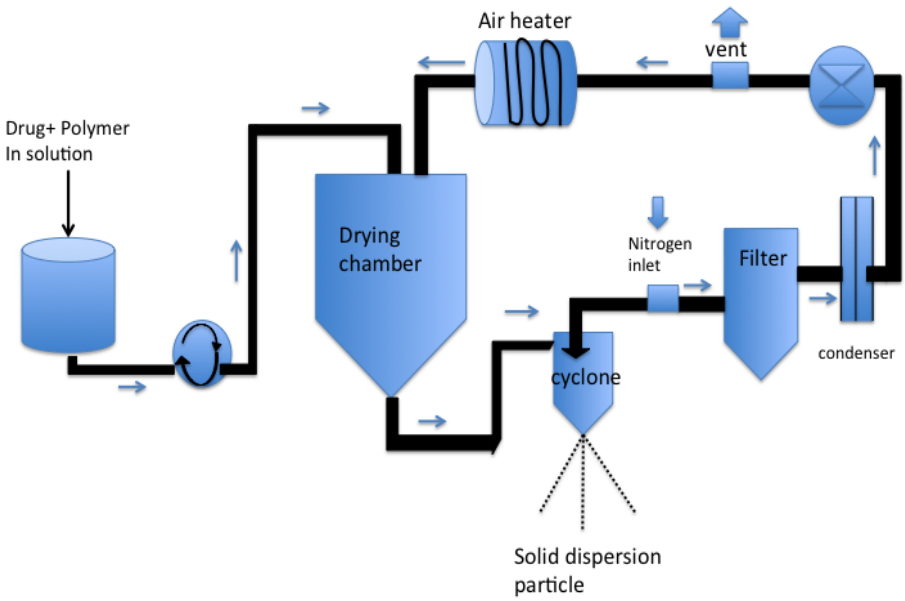

Figure 1.4-2 Spray drying technique

The figure above was reproduced from Akers et al., 2014

1.4.4 Hot melt extrusion (HME)

HME process can be defined as melting a mixture of API and carriers and forcing them through an orifice under controlled conditions to form a new material. HME involves the compaction and conversion of blends from a powder or a granular mix into a product of uniform shape.

The process involves four steps: (see Figure 1.4-3)

1. Feeding: feeding of the extruder through a hopper with the API and the polymer previously weighed according to the formulation prepared.

2. Mixing: A conveying and kneading system for mixing the API with the carrier (polymer) to reduce particle size.

3. Extrusion: a die system for forming the extrudates.

4. Downstream: auxiliary equipment where the cooling and the sample collection for further processing occurs.

An extruder consists of heated barrels which contain in the middle a rotating single or twin screw which transport and force the melt through a die to give the required shape in a continuous process. The screws can either rotate in the same direction (co-rotating) or in the opposite direction (counter-rotating).

The main drawback of the use of HME is the requirements of pharmaceutical grade polymers which have a low T_g to be used with thermally sensitive drugs. Also, all the components of the solid dispersion must be thermally stable at the required temperature during the heating process (Douroumis, 2013).

HME offers many advantages such as:

1. The molten polymers during the extrusion process can function as thermal binders and act as drug depots and/or drug release retardants or taste masking upon cooling and solidification.
2. Does not require solvents therefore, solvent residue free.
3. Water is not necessary, hence fewer processing steps and drying steps.
4. Uniform dispersion of the API.
5. Increased solubility and bioavailability.
6. Reduced processing time.
7. Continuous and efficient process.

Disadvantages of HME:

1. Drug/polymer stability at high temperature.
2. A limited number of polymers can be used.

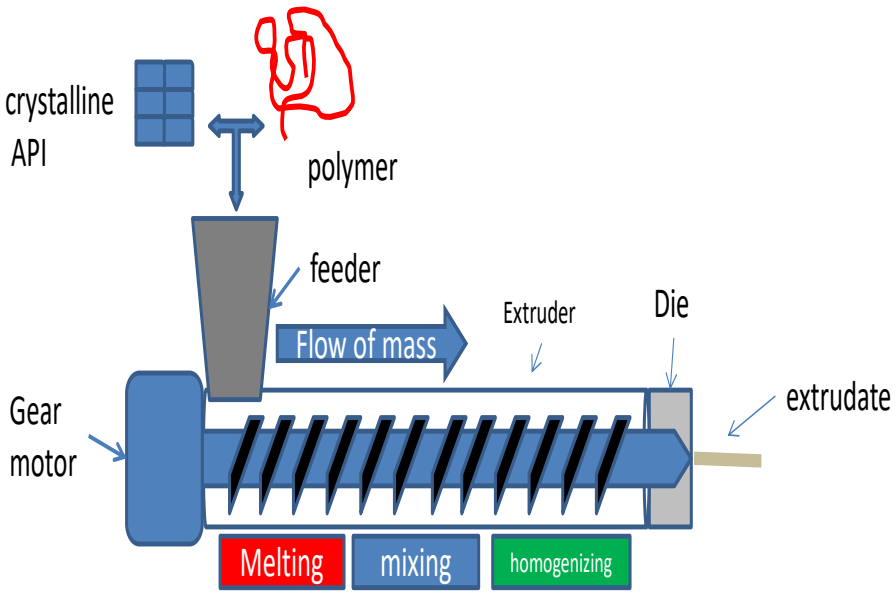

Figure 1.4-3 HME process

The figure was reproduced from Patil et al., 2015

1.5 Carriers used in Solid Dispersion

Over the years, a wide range of substances have been used as a carrier in solid dispersion formulations to enhance dissolution and stability of poorly aqueous soluble drugs. The first solid dispersion used Urea in the preparation of sulfathiazole solid dispersion by Sekiguchi and colleague in 1961. Sugars like mannitol, sorbitol and sucrose were also used to prepare solid dispersion and to enhance the dissolution rate of Prednisone (Allen et al., 1977).

Synthetic or semi- synthetic polymers are also used as a carrier in formulating amorphous solid dispersion such as polyethylene glycol (PEG), polyvinylpyrrolidone (PVP) and hydroxypropyl methylcellulose (HPMC) are the most commonly used polymers (Leuner and Dressman, 2000). Each polymer has different characteristics and properties which make it suitable in the formation of the solid dispersion using different methods. PEG has a low melting point which make suitable to prepare solid dispersion with melt method whereas, PVP has a high Tg value which is better used with solvent evaporation method (Leuner and Dressman, 2000).

Surfactants were also used as a matrix especially when mixed with one of the polymers stated above. The surfactant (Tween 80, Sodium Lauryl Sulphate (SLS) and Pluronic 68) used in a study made by Ghebremeskel and colleagues was found to help the stability of the formulations prepared by hot melt extrusion by lowering the viscosity of the melt also, by decreasing the API melting temperature, Tg of the polymer and the combined Tg of API and polymer (Ghebremeskel et al., 2007).

Carriers in solid dispersion play a big role not only in enhancing the dissolution rate of a drug but also, in the stability of drug as an amorphous form within the formulation or preventing precipitation and maintain supersaturation of the drug in solution (Alonzo et al., 2010).

1.5.1 Polyethylene glycols (PEG)

1.5.1.1 Properties of PEG

Polyethylene glycols (PEG) (Figure 1.5-1) are manufactured by polymerisation of ethylene oxide (EO) with water, ethylene glycol or diethylene glycol under alkaline conditions (Herzberger et al., 2015). PEG can have a molecular weight between 200- 100000 g/mol.

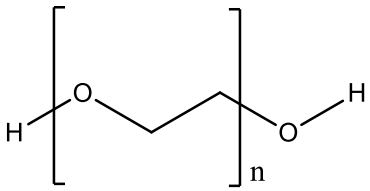

Figure 1.5-1 PEG structure

(Rowe et al. Handbook of Pharmaceutical Excipients, Sixth edition, 2009)

Low molecular weight PEGs with a mean molecular weight up to 600 are non-volatile liquids at room temperature, the melting point of the PEG increases with increasing molecular weight.

The most important property of all PEGs is their solubility in water. Liquid PEGs up to PEG 600 are miscible with water in any ratio, as the molecular weight of PEG increases the solubility decreases slightly (As shown in **Table 1.5-1**).

Table 1.5-1 PEG properties with increasing molecular weight

Name	n	Molecular weight average	Melting or freezing point	Appearance	Solubility in water at 20°C, % by weight
PEG 300	6	285-315	-15 - -8°C	Liquid	miscible
PEG 1500	32	1305-1595	42 - 46°C	Solid	72
PEG 4000	90	3600-4400	53 - 59°C	Solid	66
PEG 20000	455	16000-24000	63 - 66°C	Solid	52
PEG 35000	795	35000-no range	64 - 66°C	Solid	50

* This table was produced from 'carbowax polyethylene glycols' brochure from Dow published October 2011 and from the MSDS of each PEG from Sigma-Aldrich website

PEGs have been used for many years in cosmetics, food industry and the pharmaceutical industry because they are non-ionic substances; they have low toxicity, low cost and they solidify quickly which make them useful for many applications (Papadimitriou et al., 2012).

High molecular weight PEGs have a good water solubility, they are in the solid form and they have higher melting point (~65°C) than the low molecular weight PEGs which make them ideal in the formation of solid dispersion using the melt method. On the other hand, PEGs are soluble in many organic solvents which make them very

useful in the formation of solid dispersion using solvent evaporation method (Price et al., 1994).

1.5.1.2 PEG based solid dispersion

The dissolution rate of a solid dispersion will be affected by the PEG molecular weights. A study made by Kapsi and colleagues shows, that the itraconazole solid dispersion with PEG 20000 has a higher dissolution rate than the one prepared with PEG 8000 and PEG 3350 (Kapsi et al., 2001). The performance of a solid dispersion is directly related to the drug: PEG ratio and it should be studied carefully before the formation of solid dispersion. The higher the drug load the more chances for the drug to be in the crystal form not molecularly dispersed within the matrix hence, a lower dissolution rate will be observed (Lin and Cham, 1996). On the other hand, the crystallinity of the drug within the solid dispersion has an influence on the dissolution rate. The quick release of carbamazepine and nifedipine from the solid dispersion with PEG 1500 over the other formulations prepared with a mixture of PEG1500 with different polymers (1:1 PEG1500: PVP30, PVP12, PVP/VA, Eudragit EPO) is due to the reduced crystallinity of the APIs (Bley et al., 2010).

The stability of the PEG based solid dispersions are affected by crystal growth during manufacturing process or during storage (Shah et al., 1995). Also, PEGs with low molecular weights used in solid dispersion will result in a sticky or soft solid dispersion which makes the formulation hard to handle and to be processed as a final product (Bley et al., 2010).

1.5.1.3 Formulations prepared with PEG

The most studied drug in PEG dispersion is griseofulvin and it did result in a marketed formulation (Gris-PEG) (Leuner and Dressman, 2000). Ritonavir which is an antiviral drug which exists in two crystal forms that will affect its solubility was made into a solid dispersion in PEG8000 in a study made by Law and colleagues. The study shows an increase in the dissolution rate, bioavalibility and stability of ritonavir (Law et al 2001).

The table below show some drugs formulated in PEG based solid dispersion.

Drug	Polymer	Method used	Comments	Reference
Nimodipine	PEG 2000 20 and 40% drug loading	melt method	Formulations did recrystallize during storage at elevated temperature and humidity.	Urbanetz et al., (2005)
Sirolimus	PEG 6000 Poloxamer-188 Mannitol	Solvent evaporation, melt method	Formulations containing PEG6000 were amorphous and the 1:1 (drug: PEG 6000) showed highest dissolution rate	Preetham et al., (2011)
Gliclazide	PEG6000	Solvent evaporation, melt method	Drug was in microcrystalline or amorphous state within the formulation. the dissolution rate was enhanced in all the formulations.	Biswal et al., (2008)
Itraconazole	PEG 6000 mixed with HPMC 2910E5	Spray drying extrusion	20% Itraconazole in 15/85 w/w PEG 6000:HPMC formulation was the best performing formulation and the drug was in amorphous state	Jassens et al.,(2008)
Nifedipine	PEG 1500, blended with PVP/VA, PVP 30, PVP 12 and Eudragit	Melt method	nifedipine: PEG1500 alone showed the best dissolution rate. All the formulations with polymer blend were amorphous except nif: PEG1500	Bley et al., (2010).

Phenylbutazone	PEG 8000	Melt method	Increased dissolution rate compared to the physical mixture	Khan et al., (2011)
Naproxen	PEG 3350	Melt method	API-PEG interaction slows the crystallisation of the API compared to the pure drug. Also, PEG 6000 help increase the dissolution rate of naproxen.	Zhu et al., (2013)
Valdecoxib	PEG 4000 PVP K30 And a mixture of both	Melt method	a complete transformation of the drug from crystalline to amorphous form and enhanced dissolution rate in both polymer and in combination.	Shah et al., (2008)
Carbamazepine	PEG6000	Melt method	CBZ form II crystallises from the melt and PEG 6000 favours this crystallisation. CBZ and PEG 6000 interact in the liquid state.	Naima et al., (2001)

1.5.2 PolyVinylPyrrolidone (PVP)

1.5.2.1 Introduction and properties of PVP

PVP is a water-soluble polymer; it is polymerised from vinylpyrrolidone monomer (Figure 1.5-2) and has a molecular weight ranging from 2500 to 1000000 (Haaf et al., 1985). PVP are named according to their K-value (thermal conductivity value) as each molecular weight has a different K-value.

PVP exhibits some useful properties (PVP PolyVinylPyrrolidone polymers, Ashland, brochure, n.d) such as:

1. High solubility in water as well as in a range of polar solvents.
2. Adhesive and dispersive properties.
3. Film formation ability.
4. Complex formation especially with H donors.
5. Stable in wide pH range.
6. Hygroscopic.

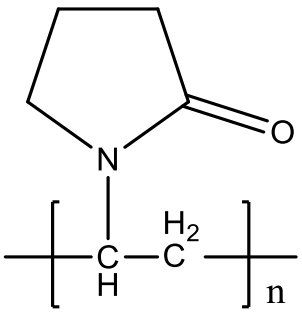

Figure 1.5-2 PVP structure

(Rowe et al. Handbook of Pharmaceutical Excipients, Sixth edition, 2009)

The glass transition temperature (T_g) of PVP is generally high but it will increase as K-value increases. The T_g value for PVP K12 is around 101°C and for PVP K90 is

174°C. The high glass transition temperature limits the use of PVP in the formation of solid dispersions by hot melt extrusion but it can be used by the solvent method.

Table 1.5-2 Properties of different PVP

PVP	Molecular weight g/mol	Tg °C	n	Appearance
K12	4,000–6,000	120	36-54	Off-white powder
K15	6000-15000	130	54-135	Off-white powder
K30	40000-80000	163	360-720	Off-white powder
K90	900000-1500000	174	8108-13513	Off-white powder

(The table was reproduced from Ashland. (2013). PVP/VA polyvinylpyrrolidone/Vinyl Acetate copolymers Intermediates. brochure)

The dissolution rate of PVP in any solvent is affected by its molecular weight, the longer the polymer chain length the lower the dissolution rate. The solubility decreases as the K-value of PVP increases and the viscosity increases as the K-value increase, which will decrease the dissolution rate (Rowe et al., Handbook of Pharmaceutical Excipients, Sixth edition, 2009).

PVP has the ability to inhibit and retard the recrystallization process of an amorphous API by forming a network around the crystal surface or between the drug molecules, hence limiting the molecular mobility of the API in the matrix (Tantishaiyakul et al., 1999).

1.5.2.2 Solid dispersion prepared with PVP

The dissolution rate from the solid dispersion will be affected by the ratio of drug to polymer in the formulation. This was observed in the study made on Bicalutamide (BL) solid dispersions prepared with PVP K25 using hot melt method. The solid dispersions had different drug to polymer ratio (1:10, 2:10 and 3:10 (w/w)). The result of the study shows that all the solid dispersions had a single glass transition temperature indicating that the drug was totally miscible with the polymer. The release rate from the dispersion was higher than the pure compound but the concentration of BL released depended on the polymer ratio in the dispersion, the higher the polymer to drug ratio the greater the dissolution rate was observed (Andrews et al., 2009).

Some studies suggested that the use of polymer mixtures i.e. PVP/PEG with drugs in the formation of solid dispersion will enhance their dissolution and the stability. One study showed (Shah et al., 2008), that the solid dispersions prepared from a mixture of polymers PVP and PEG enhanced the dissolution rate of Valdecoxib compared to the formulations prepared from one polymer and the drug was transformed into an amorphous state. Another study used PVP K30 with PEG 200 to prepare Felodipine solid dispersion by melt mixing. The low molecular weight of PEG200 had a plasticiser effect on PVP and reduced its glass transition temperature. The drug was found in the amorphous state, nano-dispersed in the matrix blend. These solid dispersions showed a higher dissolution profile than the pure drug, but the dissolution rate was dependent on the drug to polymer blend ratio, the lower the drug load the higher the dissolution rate (Papadimitriou et al., 2012).

The table below shows some of the solid dispersion formulations prepared with PVP

Drug	Polymer	Method used	Comments	Reference
Bicalutamide	PVP K25	Hot met extrusion	Formulations showed higher dissolution rate and were stable for 12 months at 20°C, 40%RH	Andrews et al., (2010)
Carvedilol	PVP K30	Solvent evaporation	Drug was found to be in amorphous form in the formulation and the dissolution rate was enhanced compared to pure drug.	Sharma et al., (2010)
Piroxicam	PVP K25	spray drying and precipitation with compressed antisolvent	1: 4 (w/w drug: polymer) formulations. The results show better dissolution rate compared to pure drug.	Wu et al., (2009)
Felodipine	PVP K30, HPMC (606), HPMCAS (AS-MF)	Solvent evaporation	All the polymers used did reduce the crystal growth from the supersaturated solution. PVP was less effective in enhancing the dissolution compared to the other polymers used.	Konno et al., (2008)
	PVP K30, HPMC, Poloxamer	Solvent wetting 1:5 w/w	All the formulations were in amorphous state. PVP and poloxmer formulations showed better dissolution than the HPMC formulations.	Kim et al., (2006).
Gliclazide	PVP K90	Solvent evaporation	Increased dissolution rate compared to the physical mixture	Biswal et al., (2009)

Tibolone	PVP	Fumed with SiO_2	the formulations with PVP were amorphous and showed immediate release dissolution profile.	Papadimitri et al., (2009)
T-OA (anti-tumour lead compound)	PVP K30	Solvent evaporation	The highest dissolution rate was observed in the 1:5 (drug: PVP K-30) formulation, followed by the 1:3 then 1:8.	Hou et al., (2013)
Mefenamic acid	PVP K12	cryomilling	The solid dispersions were amorphous and the dissolution rate significantly increased.	Kang et al., (2015)
Carbamazepine	PVP K30 Gelucire 44/14 or Vitamin E TPGS (1:5 w/w)	solvent evaporation and supercritical fluid process	CBZ: PVP K30 prepared by superficial fluid process showed the best dissolution profile. The drug was amorphous in the formulations.	Sethia et al., (2004)

1.5.3 PVP copolymers

1.5.3.1 Properties of PVP copolymers

Polyvinylalcohol (PVA), crospovidone (PVP-CL) and polyvinylpyrrolidone-polyvinyl acetate (PVP/VA) copolymers are three different polymers belonging to the polyvinyl group.

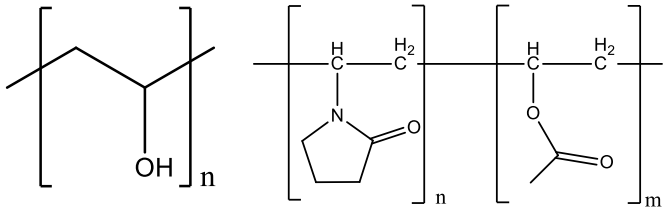

PVA PVP/VA

Figure 1.5-3 PVA and PVP/VA structures

(Rowe et al., Handbook of Pharmaceutical Excipients, Sixth edition, 2009)

Crospovidone is a cross-linked polyvinyl-based polymer; it is insoluble in water and most organic solvents. It shows a wettability effect on hydrophobic drugs due to its swelling ability. PVP/VA is used in the pharmaceutical industry as a disintegrating agent, excipient and solubilising agent (Mohamed et al., 2012).

PVA is made by dissolving polyvinyl acetate (PVAc), in an alcohol such as methanol and treating it with an alkaline catalyst such as sodium hydroxide. The resulting hydrolysis reaction removes the acetate groups from the PVAc molecules without disrupting their long-chain structure. PVA is highly soluble in water and insoluble in almost all organic solvents. (https://www.britannica.com/science/polyvinyl-alcohol)

PVP/VA copolymer, is formed from PVP and VA at different ratios such as 6:4 and 3:7. The Tg value of different ratios decreases as the PVP content in copolymer decreases (PVP/VA, Ashland brochure, 2014 http:// ragitesting.com/ resourcePortfolio/ wp-content/ uploads/2014/09/ ASH- PC8092_PVP_VA_ Brochure_VF.pdf). PVP/VA used in the pharmaceutical industry as dry binders for direct compression tableting; also it can be used in hot melt extrusion processes. In

the formulation PVP/VA acts as solubilising agent, dispersant and crystallisation inhibitor (Kollidon-VA64, basf, brochure, (https://pharmaceutical.basf.com/en/Drug-Formulation/Kollidon-VA64.html)

1.5.3.2 Solid dispersion prepared with PVP copolymers

A study prepared furosemide in crosspovidone (1:2) solid dispersion which showed a 6-fold increase in dissolution rate compared to the pure drug due to the drug amorphous state in the dispersion (Shin et al., 1998).

In another study carried out using carbamazepine and nifedipine solid dispersions prepared with 1:1 mixtures of PEG 1500 and PVP/VA, Eudragit EPO, PVP 30 or PVP 12. The results show that the higher dissolution rate from carbamazepine was shown in the formulation prepared with PEG 1500 alone and PVP K30 followed by PVP/VA then PVP 12. For nifedipine the highest dissolution rate was shown in the formulations prepared PEG1500 alone followed by PVP/VA then the formulations prepared PVP K30 and PVP 12. From the same study, after 6 months storage both drugs had the highest release rate from the formulation with PEG 1500/PVP/VA (Bley et al., 2010).

1.5.4 HPMC/HPMCP

1.5.4.1 Properties of HPMC polymers

Cellulose is a long chain un-branched polysaccharide with very high molecular weight (162 g/mol for one monomer) naturally found in every plant. Semi synthetic cellulose derivatives can be produced by alkylation such as methyl cellulose (MC), hydroxypropylmethylcellulose (HPMC) and hydroxypropylmethylcellulose phthalate (HPMCP).

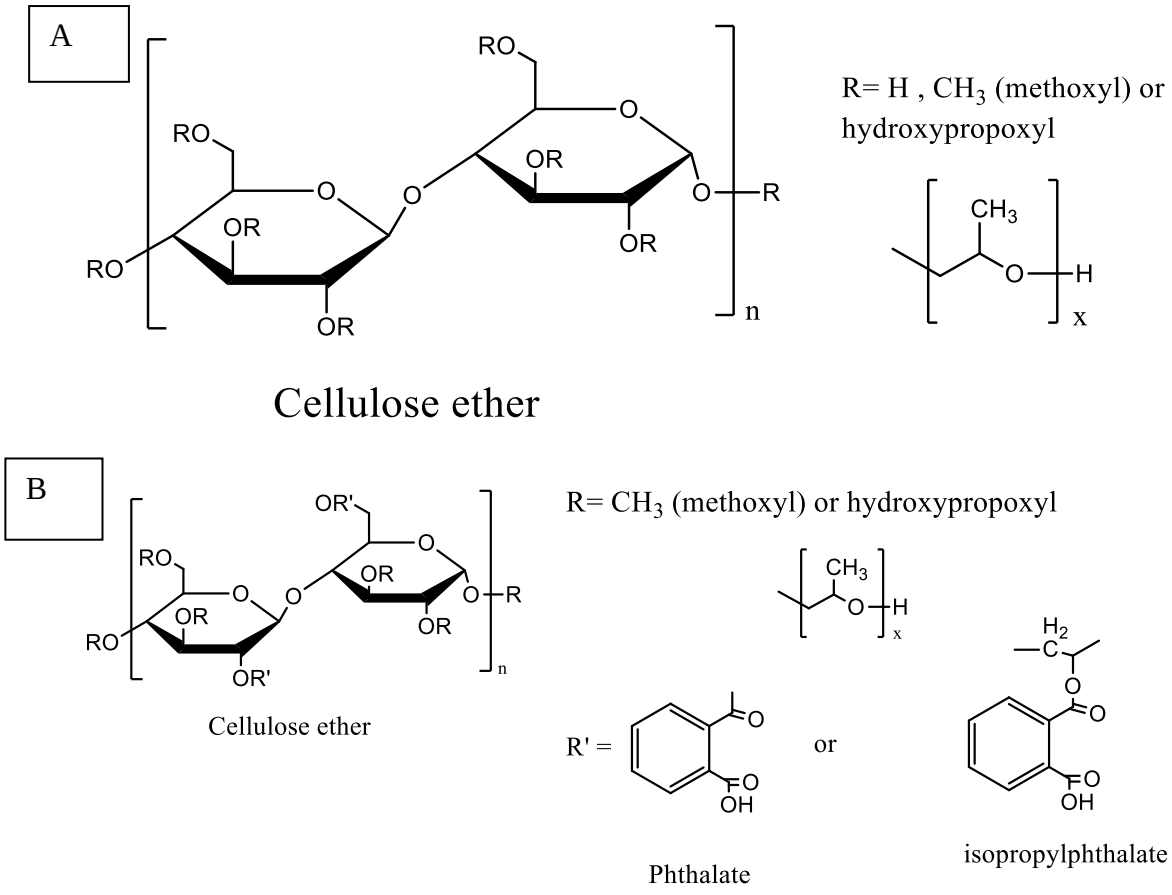

Figure 1.5-4 HPMC structure (A) HPMCP structure (B)

(Rowe et al., Handbook of Pharmaceutical Excipients, Sixth edition, 2009)

HPMCs have a mixture of ethers, some of the hydroxyl groups are methylated and the others are derivatised with hydroxypropyl groups. HPMCs have a molecular weight of around 10000 to 1500000, they are solid at room temperature, non-toxic and they are non-ionic water-soluble polymers (Ford, J., 2014). The solubility of HPMC is pH independent, stable at a wide range of pH and resistant to enzymatic degradation (Tiwari et al., 2008). HMPC is used as a food additive for thickening and emulsifying liquids as well as in pharmaceutical industry in tablet coating, granulation, controlled or modified release formulations (Methocel cellulose ethers, Dow, brochure, 2013).

1.5.4.2 Solid dispersions prepared with HPMC

Studies with Itraconazole solid dispersion prepared by spray drying using different carriers such as Eudragit E100 (Butylated Methacrylate Copolymer), PEG 20000, PVP and HMPC showed that the dissolution rate of all solid dispersions is higher than the itraconazole pure drug. The dissolution rate of the solid dispersion made from HMPC is higher than the one prepared with PVP and similar to the one prepared with PEG 20000 but the highest dissolution rate was shown from the solid dispersion with Eudragit E100. The best performing formulation was the one prepared with 1:1 (w/w) (drug: polymer) (Jung et al., 1999).

A study made by Leuner and colleague to prepare solid dispersion using HPMCP as the matrix with anti-fungal drug (MFB-1041) prepared by spray drying, showed increase in the dissolution rate of the drug and enhancing its bioavailability (Leuner and Dressman, 2000).

1.5.5 Poly (meth) acrylate

1.5.5.1 Polymethacrylate polymer structure and properties

Poly (meth) acrylate is the commercial name of polymethacrylate polymer. It is produced from the polymerisation of acrylic and methacrylic acid (Nikam et al., 2011).

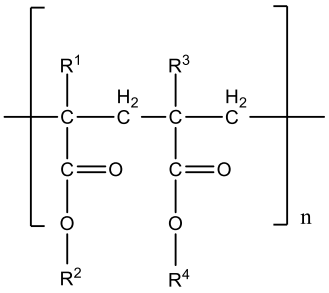

For form E: $R^1$and R^3 = CH_3 R^2= $CH_2CH_2N(CH_3)_2$ R^4= CH_3, C_4H_9
For form L and S: $R^1$and R^3 = CH_3 R^2= H R^4= CH_3
For form RL and RS: R^1 = H, CH_3 R^2= CH_3, C_2H_5 R^3 = CH_3 R^4= $CH_2CH_2N(CH_3)_3^+Cl^-$ a

Figure 1.5-5 Polymethacrylate polymer structure

(The figure above was reproduced from Date et al., 2010)

Polymacrylate polymer can be divided into two groups according to the pH dependent behaviour. The pH dependent forms are polymethacrylate L, S and E and pH independent forms are polymethacrylate RS and RL.

The table below shows some properties of the different Poly(methacrylate) forms (Joshi M., 2013).

Table 1.5-3 Properties of various Poly(methacrylate) copolymers

Form	Availability	Dissolution properties	Applications
L 100	powder	Dissolution above pH 6	Enteric coatings
L 100-55	powder	Dissolution above pH 5.5	Enteric coating
S 100	powder	Dissolution above pH 7	Enteric coatings
E 100	granules	Soluble in gastric fluid up to pH 5 and permeable above pH 5	Film coating
RL 100	granules	High permeability	Sustained release
RS 100	granules	Low permeability	Sustained release
NE 40 D	40% aqueous dispersion	Swellable, permeable	Sustained release

1.5.5.2 Polymethacrylate based solid dispersion

In a study carried out on the solid dispersions prepared by hot melt extrusion for three drugs (indomethacin, itraconazole and griseofulvin) with one of these polymers (Eudragit E PO, Eudragit L100-55, kollidon VA-64, HPMCAS-LF and HPMCAS-MF), showed the highest dissolution rate from the solid dispersion of indomethacin prepared with Eudragit E PO, itraconazole with the polymer HPMCAS-LF and griseofulvin with the polymer Eudragit L100-55 (Sarode et al., 2013).

1.5.6 Other carriers

Urea was one of the first carriers used to produce solid dispersions in order to enhance dissolution and bioavailabity of sulphathiazole drug. It is the waste product from the decomposition of protein in human body; it is highly water soluble and non-toxic.

Emulsifiers can also be used to enhance wettability and the dissolution of a drug along with other polymers such as polysorbate 80 (Okonogi et al., 2006), sodium lauryl sulphate (SLS) (Urbanetz, 2005). Poloxamers have been used as a carrier and they are block of copolymers of Poly(EthyleneOxide) (PEO) and Poly(PropyleneOxide) (PPO). Poloxamers are available in a broad range of molecular weight and PPO/PEO ratios such as: poloxamer 188 and poloxamer 407 (Bodratti and Alexandridis, 2018).

1.6 Characterisation of solid dispersions

Analytical characterization of the solid dispersion is very important in determining the solid state of the drug in the matrix, the drug/polymer miscibility and crystallization. There are a number of thermal, spectroscopic and microscopic techniques, which can be used to provide information on the solid dispersion.

1.6.1 Thermal techniques

Differential Scanning Calorimetry (DSC)

Differential Scanning Calorimetry is an important technique for detecting phase transformations. The sample and a reference sample are heated at the same rate. The difference in electrical signals arising from identical temperature sensors placed in the sample and reference holders are recorded. The sample may require more or less power to be maintained at the same temperature as that of the reference. During a phase transition of a sample, for example from solid to liquid state (melting), heat is absorbed and therefore, heat flow to the sample is higher than that to the reference, hence heat flow is positive. This process is called endothermic process as the transition absorbs energy. On the other hand, crystallisation is an exothermic process; due to the heat flow is negative and the transition releases energy. This

differential power is represented as a plot between temperature and the peak area or the energy of transition.

This technique can be used as a primary screening technique to indicate the drug/polymer miscibility and give information about the property of the sample such as: melting points, enthalpies of melting, crystallisation temperatures, glass transition temperatures and degradation temperatures (Shah et al., 2013).

There are two types of DSC instruments:

1. The power compensation DSC in which the sample and reference temperatures are controlled separately by identical furnaces.

2. The heat flux DSC in which the sample and reference are enclosed together in a single furnace and their temperatures are controlled by a single temperature sensor.

A standard DSC curve for a particular polymer is shown in Figure 1.6-1 it shows a glass transition where the amorphous materials of the polymer are molten and in a rubber like state, crystallisation where the material gains energy to arrange their self into a solid crystal form and melting of the polymer where all the bonds are lost and the polymer is in the liquid state.

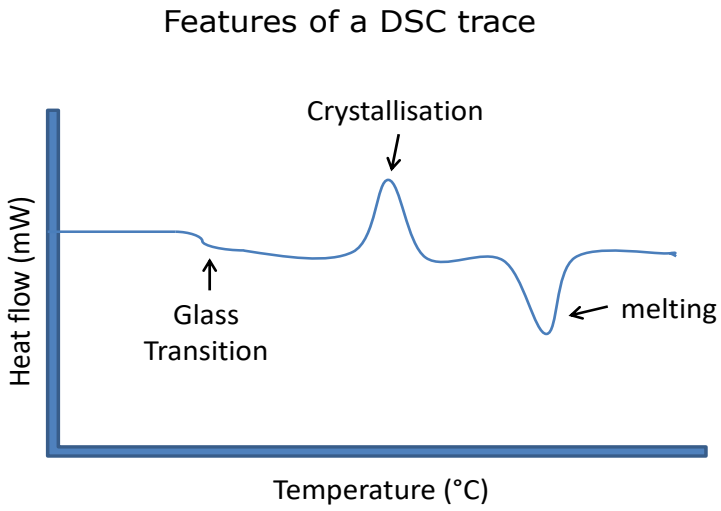

Figure 1.6-1 Typical DSC curve

(http://www.flemingptc.co.uk/our-services/dsc-tga/)

DSC can be used in the pharmaceutical industry to study the polymorphic form and purity of a compound as well as melting point. Also, it can be used in the food industry to test storage and process temperature.

1.6.2 Spectroscopic techniques

Molecules can absorb energy when hit by a photon. This energy allows the molecule to vibrate. Vibrational spectroscopy measures which wavelengths of light are absorbed by a molecule. Infrared and Raman spectroscopy are both vibrational spectroscopy methods. These techniques are very useful in identifying unknown molecules by comparing its absorbance to the other molecule. The absorbance peaks are dependent on the structure and the conformation of the molecule.

1.6.2.1 Fourier Transform- Infra Red (FT-IR)

Infrared generally referred to any electromagnetic radiation falling in the region from 0.7 μm to 1000 μm wavelength, it is divided into three regions: near-IR (0.8–2.5 μm), mid-IR (2.5–25 μm) this region includes the frequencies corresponding to the fundamental vibrations of nearly all of the functional groups of organic molecules, and far-IR (25–1000 μm).

Infra Red (IR) spectroscopy is a very useful technique used in identifying unknown samples by assigning the chemical group to the specific absorption bands. Infrared light passes through a sample and certain frequencies of the light are absorbed by the chemical bonds of the substance, leading to molecular vibrations due to a change in the dipole moment of the molecules.

Infrared spectrum usually presented as % transmittance versus wavenumber (cm^{-1}) (wavenumber = 1/ wavelength in cm) ranging from 4000-200 cm^{-1}. The absorption spectrum of the sample will create a molecular fingerprint of the sample, (fingerprint region 900-1500 cm^{-1}) this region is a very specific and important as this region can be used as confirmation of identity because it is unique for each substance.

Fourier transformed IR uses an optical device called an interferometer to collect an interferogram of the IR light. Using a beam splitter and a moving mirror (refer to Figure 1.6-2) the interferometer measures all the IR frequencies simultaneously.

When interferogram signal is transmitted through or reflected off the surface of a sample, specific IR frequencies are absorbed. In the detector the interferogram signal (which is a complex wave pattern) has to be decoded by the mathematical Fourier transformation into absorbance or transmission data.

Advantages of FT-IR techniques are: non-destructive, precise measurement, increase speed (collecting a scan every second), good sensitivity, specific and the ability to differentiate between polymorphs.

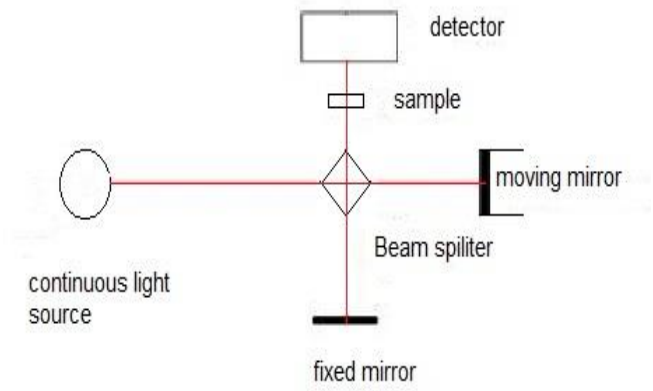

Figure 1.6-2 FT-IR instrument

(Ismail et al., 1997)

FT-IR is a very useful technique because it provides specific information on molecular structure and chemical bonding. For this reason, FT-IR is widely used in multiple areas such as pharmaceutical industry to study chemical structure, in the agriculture industry to analyse the soil, food industry, biochemistry and in environmental area to measure air pollution.

1.6.2.2 Raman spectroscopy

Raman spectroscopy is a vibrational spectroscopic technique provides information about molecular vibrations that can be used for sample identification and quantification. This technique is based on inelastic scattering of monochromatic light, usually from a laser source. Photons of the laser light are absorbed by the sample and then reemitted into three forms (Rayleigh, Stokes and anti-Stokes) refer to Figure 1.6-3. The photons emitted by Stokes scattering have a lower energy and frequency than that of the photons absorbed by the molecule. The anti-Stokes scattering is when the photons emitted have a higher energy and frequency than the photons absorbed. Inelastic scattering means that the frequency of photons in monochromatic light changes upon interaction with a sample (ie. Stokes and anti-Stokes). Raman spectroscopy is a useful technique used in collecting the unique chemical fingerprint of molecules because each molecule has a different set of vibrational energy levels depending on their structure and confirmation, and the photons emitted have unique wavelength shifts.

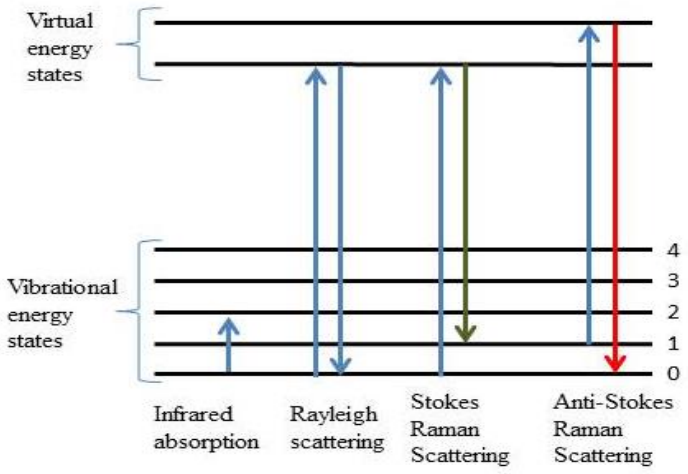

Figure 1.6-3 Jablonski energy diagram

(Frackowiak, 1988)

1.6.3 X-Ray Diffraction (XRD)

X-ray diffraction is a non-destructive analytical technique which can identify crystalline material and measure the dimension of the crystals. When an X-ray beam is applied to a crystal, the atoms in the crystal interact with the x-ray to produce interference bands as shown in Figure 1.6-4. The angle at which the interference bands were detected depends on the wavelength applied and the geometry of the sample. This can be described as the Bragg's law and can be summarised in the equation below.

$$n\lambda = 2d\sin\theta$$

Equation 1-2

Where n is the integer (order of the diffracted beam), λ is the wavelength of the incident X-ray beam, d is the distance between adjacent planes of atoms, θ is the angle of incidence of the X-ray beam.

There is a region in the diffraction pattern called the fingerprint region and it can only be observed when drug in crystalline form is detected.

The fingerprint region is very specific and it is possible to distinguish between the crystallinity of the drug from the crystallinity of the carrier (Leuner and Dressman, 2000).

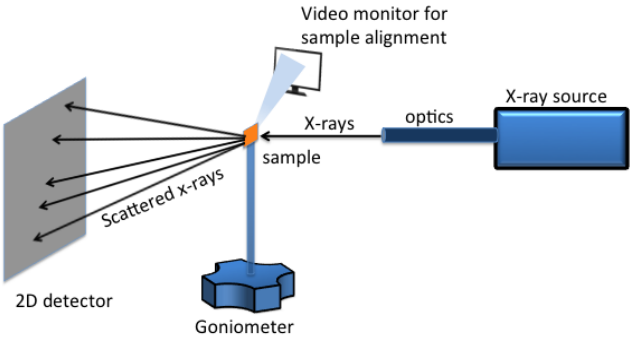

Figure 1.6-4 X-Ray diffraction

(klug et al., 1974)

This technique is widely used to identify unknown crystalline materials, characterisation of crystalline materials and in determining sample purity.

The advantages of XRD are sample preparation is minimal, data interpretation is straight forward and it is a rapid technique. The disadvantages are peak overlay may occur and large sample quantity in powder form is needed

XRD technique is used to identify the composition of a pharmaceutical compound. It is also used in forensic science for trace analysis of stains, glass and paint flakes. It is a very useful technique in geological studies.

1.6.4 Microscopy techniques

Light microscopy is used to visualise the crystal shape and the appearance of sample at high magnification. A light source on the opposite side of the sample is shone on the sample and then the light passes through a condenser to focus it on the sample to get a maximum illumination. After the light passes through the sample it goes through the objective lens to magnify the image of the sample and then to the oculars, where the enlarged image is viewed.

Hot stage microscopy is identical to the light microscopy but has a temperature controlled stage. The sample can be heated or cooled any changes occurring in the sample with temperature can be visualized and this information can be used along with the DSC curve.

Polarised light microscopy uses plane-polarised light to analyse birefringent materials (materials that have their refractive index dependent on polarisation). The microscopy techniques are used study the surface morphology of the solid dispersion and to detect crystallinity in amorphous formulation.

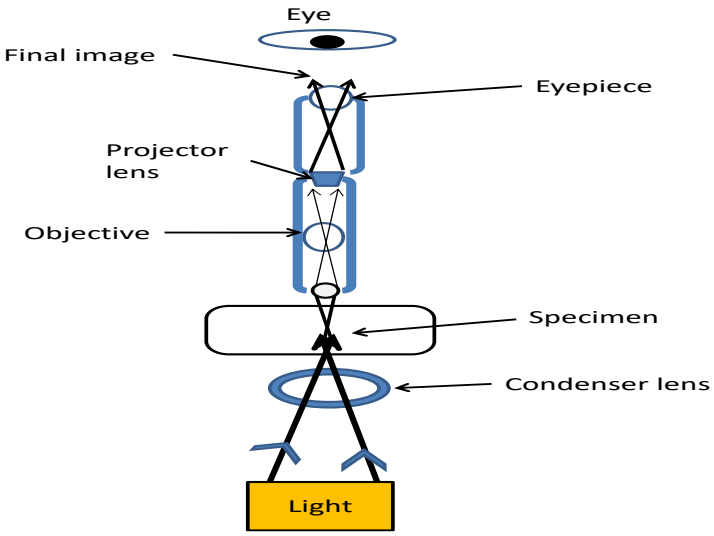

Figure 1.6-5 Light microscope schematic

(Keller, 2003)

1.6.5 Dissolution testing

Dissolution is a kinetic process and can be defined by the rate at which the solute dissolves. The higher the dissolution rate for a drug enhances the drug bioavailability if it has a good gut permeability (refer to Figure 1.1-1).

There are many apparatus for dissolution test but the main ones for testing tablets and capsules are the basket and the paddle (refer to British Pharmacopoeia, Appendix XII B. dissolution, BP 2017). In both instruments, the sample is placed in a vessel with 900 ml or 1000 ml dissolution medium contained within a thermostated water bath. The stirring rate which will affect the dissolution rate can be varied. Sample aliquots can be removed at regular interval time and the concentration of the drug can be measured using High Performance Liquid Chromatography (HPLC) or UV spectrometry.

In recent years, small-scale dissolution apparatus are becoming more available in the pharmaceutical industry such as Sirius T3 or Sirius SDI. These instruments are used during the pre-formulation stage using powder-based assays or compressed discs. These instruments can determine the dissolution rate using minimal amounts of

material, also it has a UV dip probes to read concentration over time and a pH meter where the pH of the dissolution medium can be controlled. These instruments are useful in giving an idea on the drug behaviour in solution and can accelerate pre-formulation development.

1.7 Problems with solid dispersion

There are lots of factors affecting the behaviour of solid dispersions with different effects on performance (refer to Figure 1.7-1). The main problem facing solid dispersion production is the maintenance of their physical stability.

The main aim of producing solid dispersion is to enhance dissolution of the drug and to keep the dissolution profile unchanged during storage. The physical state and the molecular structure of the drug within the solid dispersion have to stay the same during storage in order to obtain consistent dissolution results.

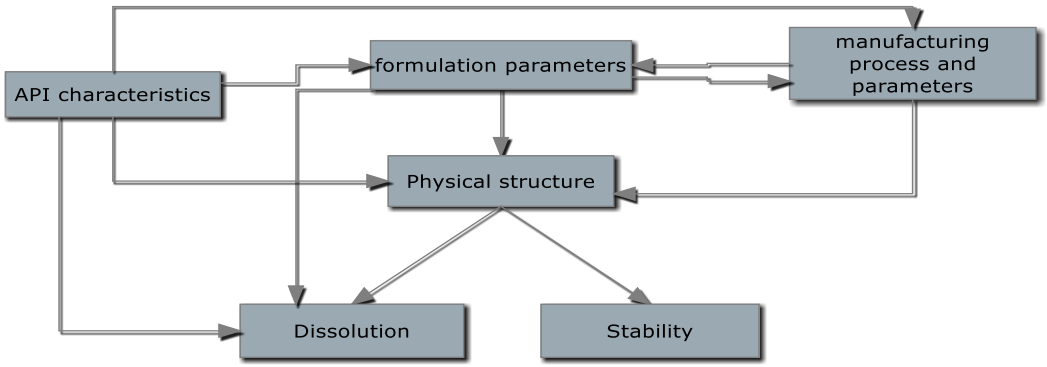

Figure 1.7-1 Factors affecting solid dispersion performance

(Reproduced with modification ref. Van den Mooter)

In the crystalline solid dispersions, the crystal particle can act as nuclei where further crystals can grow. In the amorphous solid dispersion, the crystallisation can occur but a nucleation step is needed. Therefore, a small amount of drug crystal in the amorphous dispersion will be the start point for crystallisation. If the drug was molecularly dispersed in the amorphous solid dispersion, the drug has to move within the matrix before nucleation and crystallisation will occur. Therefore, the molecular mobility should be kept as low as possible. The molecular mobility can be measured by solid state NMR. The stability of amorphous solid dispersion depends

not only on the crystallisation of drug but also to the molecular distribution of the drug and the ability of the polymer to inhibit the crystallisation.

Amorphous materials are thermodynamically unstable and tend to go back to lower energy crystalline state but they are kinetically stable below their glass transition temperature (T_g) where they have low molecular mobility and slow recrystallisation. When a drug mixed with a matrix which has a high T_g, the solid dispersion will have a higher T_g than the pure drug and it will result in low drug mobility. Also, more research is needed to identify why some carriers stabilise some drugs and other not (Van der Mooter, 2012).

1.7.1 Spring and parachute mediated supersaturation

Amorphous solid dispersion when placed in water release its potential energy and a thermodynamically unstable supersaturated drug solution will be generated this is referred to as 'spring'. As this solution is unstable it tends to crystallise and precipitate quickly which will affect absorption of the drug. The theoretical idea is that the polymer used in the formulation has to act as a 'parachute' to maintain the supersaturation state by preventing the drug crystallisation and to ensure maximum drug absorption (Brough et al.,2013). Therefore, the choice of the polymer is very important; it should have the 'parachute' effect in order to hold the supersaturation.

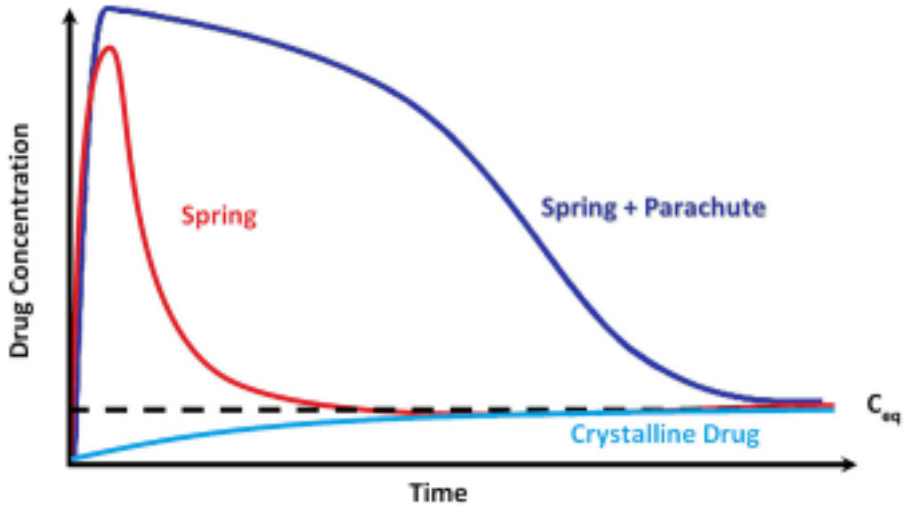

Figure 1.7-2 'Spring ' and 'parachute' concept for supersaturation

(Brough et al., 2013)

1.8 Marketed formulations

A list of some of the marketed drugs prepared using different solid dispersion technique and polymers are shown in the **Table 1.8-1**.

Table 1.8-1 Name of some marketed drugs produced using solid dispersion technique

Trade name	Drug	Carrier	Processing technique	Company	FDA approval
Kaletra	Lopinavir/ Ritonavir	PVP/VA	Melt extrusion	Abbot	2007
Onmel	Itraconazole	CL-PVP	Melt extrusion	Merz Pharma	2010
Prograf	Tacrolimus	HPMC	Spray drying	Astellas Pharma	1994
Zortress	Everolimus	HPMC	Spray drying	Norvatis	2010
Intelence	Etravirine	HPMC	Spray drying	Janssen	2008
Cesamet	Nabilone	PVP	Solvent evaporation	Meda Pharmaceuticals	1985

(Brough et al., 2013 and Guy Van den Mooter, 2012)

1.9 Conclusion

The number of discovered drugs which exhibit low solubility has risen in the past two decades (Shah et al., 2013) and there is a need to find a suitable formulation for these drugs. The formation of these drugs into solid dispersions using the method discussed above (section 1.3) and especially by HME is becoming increasingly popular due to the promising results in enhancing dissolution.

In the literature, substantial research describes how to prepare solid dispersions and how the solid dispersion enhances bioavailability and solubility but the number of marketed drug using this technique is very low. Only a few drugs have reached the market. This is due to the problems solid dispersion has with physical stability and the crystal growth during the dissolution step or during storage (Van den Mooter, 2012). Before formulating a drug as a solid dispersion, there are parameters (such as melting point, solubility, Tg temperature and toxicity) should be taken into account regarding the physico-chemical properties, stability and miscibility of the excipient. The drug/polymer and the appearance of the final dosage form should also be considered. The use of polymer blends is gaining attention due to the better physico-chemical contributions to the pharmaceutical properties dosage form compared to the use of a single polymer. The benefit of forming a solid dispersion is that the carriers that are used in the formation of solid dispersions are already being used in the pharmaceutical industry as excipients so there is no need to do toxicity studies on them.

Finally, there is a need to fully understand the solubility enhancement mechanism of the solid dispersion over the pure drug to use it as a guide in the formation of best performing solid dispersion. Also, there is a potential to use this technique in different area such as controlled release or target release dosage form.

1.10 Aims and objectives

The aims of this project are to generate a procedure for the preparation of solid dispersion in PEG based formulation for oral administration of poorly soluble drugs using simple melting, solvent evaporation and quench cooling from melt to enhance the solubility and the stability of these formulations. A range of formulations with different ratios of active pharmaceutical ingredient and polymer will be prepared to produce the best performing formulation.

The drug solid state within the polymer of the final formulation will be assessed using differential scanning calorimeter, spectroscopic techniques FTIR and Raman, microscopy technique and dissolution studies. These techniques will be used in order to build an idea on the drug-matrix interaction, the drug solid state within the formulation and to check if the dissolution has improved. The stability of these formulations will be assessed under different temperature storage.

PEG mixes have been used in a range of CRUK formulation unit formulations and instability was noticed in some of the formulations therefore, the aim was to find a system where we can control the instability and study the impact of various features on stability.

Chapter 2 Materials and methods

2.1 Materials

Details of the model drugs, excipients and instruments are listed in the sections below.

2.1.1 Model drugs

Carbamazepine (MW 236.27 g/mol) > 98% pure was purchased from Sigma-Aldrich, Dorset, UK.

Nifedipine (MW 346.33 g/mol) >98% pure was purchased from Sigma-Aldrich, Dorset, UK.

Carvedilol, Probucol, Fenofibrate, Naproxen, Itraconazol and Indomethacin were gifted from Dr Ibrahim Khadra (ORBITO)

2.1.2 Excipients used

PEG of different molecular weights (300, 1500, 4000, 6000, 20000 and 35000) , Pluronics F127, F68, P103, P123 and PVP K12 were purchased from Sigma-Aldrich, Dorset, UK

2.1.3 Other materials used

Sodium acetate buffer	Sigma-Aldrich, Dorset, UK.
Circular glass coverslips no 1.5,16mm diameter	Fischer scientific, Loughborough, UK
40 µl aluminium DSC pan	Mettler Toledo, Leicester, UK
Potassium chloride (KCl)	Sigma-Aldrich, Dorset, UK.
Glacial acetic acid	Fischer Scientific, Leicestershire, UK.

Sodium dihydrogen phosphate	Sigma-Aldrich, Dorset, UK.
XRPD Capillaries	Capillary Tube Supplies Ltd, Cornwall, UK.
Liquid nitrogen	SIPBS store
Hydranal coulomat A	Sigma-Aldrich, Dorset, UK.

2.1.4 Instrument used

Differential Scanning Calorimetry, DSC model 822e Sample robot, TS0801RO	Mettler Toledo Ltd, Leicester, UK.
Sirius T3	Sirius Analytical, East Sussex, UK
Disc press connected to TR150 Load Cell Indicator	Applied measurement, Reading, UK LCM Systems, Newport Isle of Wight, UK
Varian Cary eclipse fluorescence spectrophotometer Cuvette used: Material: Suprasil quartz Light length: 10x10mm Volume: 3500 µl	Agilent technologies, United States. Hellma- analytics, Müllheim,Germany
Karl Fischer (DL39)	Mettler Toledo, Leicestershire, UK

D8 advance II, capillary XRPD	Bruker, MA, USA
Hot stage (TMS-91)	Linkam scientific, Tadworth, UK
Polyvar microscope Equipped with Infinity 1camera (1.3Megapixel, 640x480 resolution)	Reichert inc, NY, USA Lumenera Corporation, Ontario, Canada
Mettlet MT5 analytical balance	Mettler Toledo, Leicestershire, UK
JASCO 4200 FTIR	Jasco, Maryland, USA
D8 advanced II, plate XRPD	Bruker, MA, USA
DXR Raman	Thermo scientific, MA, USA
Thermo Finnigan Surveyor HPLC	Thermo scientific, MA, USA

2.1.5 Software used

Thermal analysis software, STARe	Mettler Toledo Ltd, Leicester, UK.
Minitab version 14	Minitab Ltd, Coventry, UK.
FTIR spectra manager	JASCO, Maryland, USA
Diffrac plus xrd commander	Bruker, MA, USA
Sirius T3 control version 1.1.3.0	Sirius analytical, East Sussex, UK
Infinity analyse microscope software	Lumenera Corporation, Ontario, Canada
Chromquest Hplc software (version 4.2.34)	Thermo scientific, MA, USA

2.2 Methods of solid dispersion preparation

2.2.1 Preparation of PEG mixtures (no drug)

PEG mixtures were prepared to investigate the effect of its molecular weight on heat of fusion, melting point and the freezing point.

Mixtures of PEGs (see **Table 2.2-1** for ratios used) were weighed into a glass vial then heated to the liquid state (at around 70°C) with continuous stirring to mix well then left to cool in a desiccator for further analysis.

The table below shows the different ratios of PEG 300 used with higher PEG molecular weight (PEG 4000, PEG 6000, PEG 20000 and PEG 35000).

Table 2.2-1 The different ratios used to study the melting and freezing point of different PEG mixtures

PEG300 (%w/w)	Higher molecular weight PEG (%w/w)
100	0
90	10
75	25
50	50
25	75
10	90
0	100

2.2.2 Preparation of drug solid dispersion in PEG

2.2.2.1 Physical mix

Physical mixture is the mixing of drug with the polymer. This method was used in formulations with PEG 300 alone since PEG 300 is liquid at room temperature.

Physical mixtures of Carbamazepine (CBZ) or Nifedipine (NIF) were prepared with PEG 300 at different ratios. The ratios used in this experiment were 1:1, 1:5 and 1:10 (w/w). In an Eppendorf tube, 10 mg of the drug was added to the appropriate amount of PEG, mixed thoroughly using a vortex for 2 minutes and then analysed.

2.2.2.2 Melt method

The required amount of the polymer was weighed and then heated to the melting point (i.e. for PEG the melting point around 60°C) then the drug was added and mixed thoroughly for few minutes until the drug crystals are dissolved and the drug was fully solubilised in the molten polymer.

2.2.2.3 CBZ: PEG mixture 300:4000 using melt method

The drug was mixed with PEG 300 and 4000 mixtures at different ratios (refer to **Table 2.2-2**). The PEG mixtures were heated on a hot plate to 60°C where it melts then the required amount of drug was added and mixed quickly where the drug dissolves in the hot PEG. The formulation was left to cool at room temperature, and then placed in a closed desiccator containing silica beads.

The mixtures were analysed in the DSC using ‘the normal cool DSC’ method.

Table 2.2-2 Compositions of the different CBZ: PEG300: 4000 mixtures

		Compositional ratio		
Formulation	Drug	Total PEG mixture	PEG300	PEG4000
A	1	1	0.75	0.25
B	1	1	0.5	0.5
C	1	1	0.25	0.75
D	1	5	3.75	1.25
E	1	5	2.5	2.5
F	1	5	1.25	3.75
G	1	10	7.5	2.5
H	1	10	5	5
I	1	10	2.5	7.5

Formulation A, B and C have 1:1 drug: PEG mixture. Formulation D, E and F contains 1:5 drug: PEG mixture and the formulation G, H and I have 1:10 drug: PEG mixture.

2.2.2.4 Solvent evaporation method

PEG mixtures were weighed, and then the drug was added. Methanol was used as a solvent; 1ml of Methanol was added for every 5 mg of drug. The solution was placed on a heated plate at 50°C with continuous stirring until the solvent evaporated.

2.2.2.5 Quench cooled method

Quench cooled solution was prepared by either method stated above (melt or solvent evaporation), then placed in an oven heating the sample from 20-210°C. Once the sample reaches 210°C, it was quickly transferred to -80°C freezer for 10 minutes. Then placed at the required temperature for further studies.

2.2.2.6 CBZ solid dispersion with PEG and Pluronic

Pluronic of different molecular weights and different ratio of PEO-PPO (refer to chapter 7) such as P103, P123, F68 and F127 was added to the CBZ formulation. The melting method was used to prepare the formulations. The polymers (PEG and Pluronic) were weighed and then heated to the molten state then the drug was added and mixed well until the drug dissolves in the polymer mix. A 10%w/w of PEG was replaced by the pluronic used in the CBZ: PEG300: 4000 and CBZ: PEG6000 formulations.

P103 was added to the CBZ: PEG300: 4000 formulation at different concentrations (1, 2, 5, 7 and 10 %w/w of the PEG mixture). The formulations were prepared by the same method mentioned above.

2.2.2.7 CBZ Formulations with PEG and PVP

The formulations were prepared using solvent method mentioned in section 2.2.2.4.

The formulations contain different PVP concentrations. The concentration of CBZ in the formulations was fixed and the Polymer mixture ratio to drug was also fixed to 50:50 %w/w. The PVP concentration used were 1, 5, 10 and 20%. The PEG used in this experiment were 1500, 4000, and 6000.

2.2.3 Stability of the solid solution

Mixture B (refer to the **Table 2.2-2**) showed evidence of an exothermic event after rapid cooling (refer to 4.3.2.2). To further investigate the temperature dependence of this phenomenon two samples of mixture B were prepared by physical mixing. One sample was kept in the fridge at 4°C and the other in the freezer at -20°C.

2.2.3.1 Stability of the solid solution with increasing temperature

The stability of the solid solution with increasing temperature was studied by preparing samples of mixture B and then analysed in the DSC, by following a heating – quench cooling (30°C/min)- isothermal hold at required temperature (0, 10, 20 and 30°C) for 1hour then reheat to melting point.

2.2.4 Method used in the characterisation of the solid dispersion

2.2.4.1 Thermal analysis of the physical mixtures using differential scanning calorimetry (DSC)

An accurately weighed quantity (between 5-15mg) of the sample to be analysed was placed in a 40µl aluminium DSC pan then covered with a pierced aluminium cover and then sealed. The DSC instrument is purged with nitrogen at 50ml/min rate. The DSC trace data was exported and plotted using Microsoft Excel version 2010 operated on windows 7. Two main DSC thermal profiles - normal cooling and quench cooling (sections 2.2.4.1.1- 2.2.4.1.3), employed where other profiles were used these will be stated with the experimental details specified within the results section.

The methods used in the DSC were:

2.2.4.1.1 Normal cooling method

The samples were heated from -20 to 210°C at a rate of 10°C/min then cooled to -20°C at the same rate.

2.2.4.1.2 Quench cooling method

The samples were heated from -20-210°C at a rate of 10°C/min then cooled to -20°C at the rate of 30°C/min.

2.2.4.1.3 PEG mixture DSC method

The mixtures were analysed in the DSC using the following method:

Heating from -20-70°C at 10°C/min, hold for 2 minutes at 70°C then cool to -20°C at the same rate.

2.2.5 Mixture B stability DSC method

The DSC method used to study the stability of the solid solution of mixture B was heating the samples from -20-210°C at a rate of 10°C/min then cooled to -20°C at the rate of 30°C/min. The sample was held at -20°C for 60 minutes then reheated again to 210°C at 10°C/min.

2.2.5.1 Mixture B stability at different temperature DSC method

The DSC method used in this experiment was: heating the sample to 210°C at 10°C/min then rapidly cooled at 30°C/min to -20°C then held at different temperature for one hour (0, 10, 20 and 30°C) then heated again to examine at which temperature the exothermic peak will convert back to melting peak.

Also, the stability at higher temperature was investigated by storing one sample at 25°C and another one at 40°C for 12 hours in a temperature controlled incubator then the sample was investigated using the DSC with the quench cooling method.

2.2.6 Hot stage microscopy

In order to visualise the effect of thermal changes on the solid dispersion, HSM was used. The experiments were carried out on Linkam TMS91 hot stage using the same cycles in the DSC. For the cooling part, the hot stage was connected to Linkam LNP1 cooling pump attached to liquid nitrogen Dewar. The cycles were examined under Polyvar microscope equipped with Infinity1 camera. The microscope was set

to take a picture every minute for the duration of the experiment. The contrast of the images was balanced using preview software in order to see clearly the crystals.

A very small amount of the solid dispersion was placed on a glass circular cover slide then placed on the hot stage.

The hot stage was calibrated using caffeine. The result was in agreement with the melting point range of caffeine which is 235-238°C (Agyemang-yeboah, et al., 2013)

2.2.7 Fourier Transform-Infra Red

Around 1 mg of the drug physical mix were accurately weighed and then mixed well with KBr. The mixtures were pressed to form a thin disc. The discs were placed in the FT-IR instrument and analysed from 400-4000 cm^{-1}.

2.2.8 Dissolution rate

Sirius T3 was used to study the dissolution rate of the formulations. The experiments were conducted at a temperature of 25°C under an argon atmosphere. The apparatus was controlled from Sirius T3 control software. The T3 set up includes a Ag/AgCl double junction reference pH electrode, a Peltier temperature control device, with thermocouple temperature probe, an overhead stirrer (variable speed, computer controlled). The spectrophotometer was a MMS UV–vis Carl Zeiss Microimaging spectrophotometer with an ultra-mini immersion probe attached (Welwyn Garden City, Hertfordshire, UK)

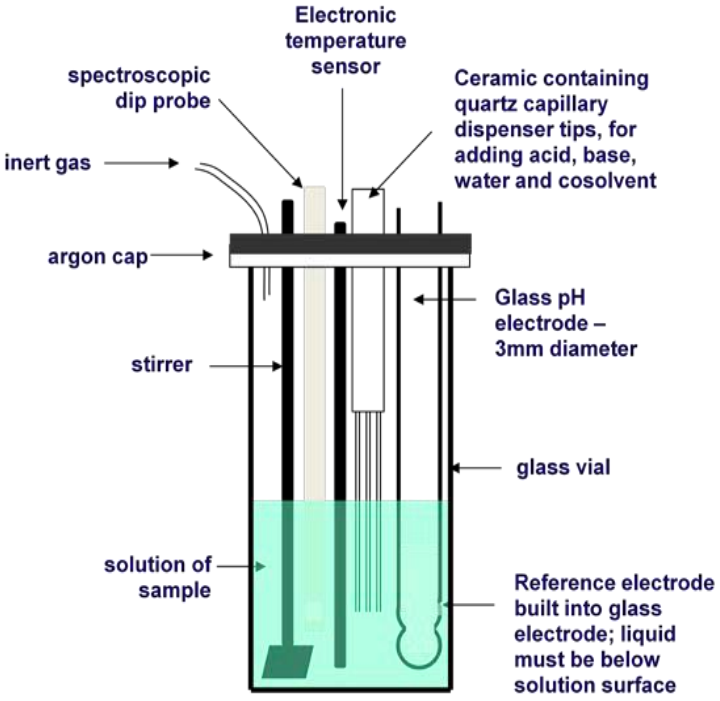

Figure 2.2-1 T3 probes

The formulations were made into a thin disc of 5-7 mg using hydraulic disc press. The powdered sample was placed in a metal disc holder and the compression compartment then placed. A pressure of 60 Kg was put on the sample, the sample was held for 2 minutes when the pressure is constant to form a disc.

The disc was analysed at four different pH 2.0, 4.0, 5.5 and 7.0 over 2 hours period, half an hour for every pH starting from low pH to high pH. The dissolution medium used was GI fluid at pH2 (refer to 2.2.8.1).

A clean up and calibration of the probe were performed every time before the experiment starts.

2.2.8.1 GI buffer preparation

The GI buffer was prepared according to Sirius GI dissolution manual.

KCl 11.18g ± 0.1g were weighed into a clean weighing boat then transferred to a 1000ml volumetric flask using funnel. The weighing boat and funnel were rinsed

with deionized water and the water was added to the flask. 1.37g ± 0.1g of sodium dihydrogen phosphate (monohydrate) were weighed and added to the flask. 572 μL of glacial acetic acid was added to the flask. The flask was sealed and shaken well until all the components were fully dissolved.

The pH was adjusted to 2 with HCl using a pH meter. The flask was filled to the mark with deionized water from the MilliQ water tank in the lab.

2.2.9 XRPD

2.2.9.1 Powder pattern experiment for the formulations:

The Powder X-ray diffraction was carried out on D8 advance (Bruker AXS). The scan parameters are:

1. Measurements made under $K\alpha_1$ radiation at 1.5406Å
2. Scan Range: 4-35° with 2θ.
3. Step Size: 0.02°
4. Count time: 1 sec/Step
5. Generator Voltage: 40 kV and 50 mA.

The sample was placed on a multiwell plate then analysed using the parameters stated above.

2.2.9.2 Variable temperature XRPD experiments.

Sample was powdered using a mortar and pestle. The powder than was transferred to an XRPD glass capillary. The capillary then sealed and mounted into a holder for analysis. A scan was taken at room temperature, and then the capillary was heated to 210°C another scan was taken. The capillary was cooled to -20°C using liquid nitrogen flow from the cryostream then a scan was taken. The sample was heated to the required temperature and a scan was taken.

For the stability at 25°C, the same procedure is followed and when the temperature was 25°C a scan was taken every hour for 24hours.

The parameters of scan used were:

A 2θ scan from 4°-35° with a step size of 0.02° and 1s/step. A 0.6mm anti diversion slit was employed with a Cu monochromated source tuned to kα1 x-ray emission. A LynxEYE PSD detector was used operating in 1D mode.

2.2.10 HPLC and forced degradation study for CBZ

A gradient HPLC method was developed for identifying the degradent of CBZ. The mobile phase used 10 mM acetate buffer at pH 5.2 (mobile phase A) and methanol (mobile phase B). The mobile phase composition at the start of the run is 95% A then it decrease to 5% in 30 mins. A 15 mins equilibration time at the initial mobile phase ratio is added. The flow rate used is 1.00ml/min and the wavelength used are 214 and 285nm. The column used was Luna C18 column, 15cm, 5µm.

2.2.10.1 Forced degradation for CBZ

A CBZ stock solution in methanol was prepared at a concentration of 1mg/ml. Then the required aliquots were taken from the stock to prepare a 100µg CBZ in 1.5M HCl, 1.5M NaOH, 3% H_2O_2 and in mobile phase stored at 80°C for 2 hours. The degradation solutions were also stored for 2 days at 55°C.

2.2.11 Design of experiment

Minitab software was used to produce a design of experiment for the occurrence of CBZ solid solution in different PEG mixtures (such as PEG300: 4000, PEG300: 6000 and PEG200: 4000). The formulations from the design of experiment were prepared using solvent evaporation method (section 2.2.2.4). The formulations then analysed on the DSC using the quench cooled DSC method (section 2.2.4.1.2). The results then entered into Minitab software and a contour plot was obtained.

2.2.12 Fluorescence experiment

The fluorescence of Carbamazepine and the different solid dispersions dissolved in methanol and in water was measured using the fluorescence spectrophotometer.

For the solid-state samples, the cuvette was filled with the powder then scanned from 300 to 500nm using integration time 1 second. An excitation spectrum was collected at 360nm and the emission spectrum was collected at 417nm at 5nm slit width.

For the methanol and water samples, a small amount of the powder sample (~50 mg) was dissolved in 3 ml of the specific solvent then filtered into the cuvette. The filtrate was then analysed at the same excitation and emission wavelengths as stated above.

2.2.13 Experiments with other drugs

The different model drugs were prepared as a PEG based solid dispersion. The solid dispersions were prepared using the melt method described in section 2.2.2.3. The ratios used were drug: PEG300: 4000 (50:25:25 %w/w).

The solid dispersions were analysed using DSC (using the method mentioned in section 2.2.4.1.2).

Chapter 3 Thermal analysis of different molecular weights PEG

3.1 Introduction

PEG in the solid state contains amorphous and crystalline regions whose occurrence is dependent upon the way the polymer was synthesised and its thermal history. The crystalline molecules of the polymer exist as a helical structure packed in layers called lamellae (Gines et al, 1996).

Most PEGs have one endothermic peak when heated, but PEG 4000 and 6000 have two due to the presence of two polymeric chain types (folded and extended). The folded chains are metastable compared to the extended ones (Gines et al, 1996).

PEG like most materials, can store thermal energy called latent energy. PEG has been classified as a good thermal energy storage material due to the large heat of fusion and the wide phase change temperature from solid to liquid depending on its molecular weight (Han et al., 1994). The large heat of fusion released when the PEG melts can affect the melting point of the drug used in the solid dispersion. PEG melts before the drug, and the drug can absorb the energy released therefore, the drug can melt at a lower temperature when forming eutectic formulation.

PEG has a wide molecular weight range and the melting / freezing point changes with molecular weight. The thermal history of PEG can slightly alter the melting and freezing points of the PEG; also, it might affect the crystal form of the drug in the final formulation and the dissolution rate of the drug. Therefore, the thermal transitions measured in the 1st heating cycle will be different than the 2nd heating cycle, which is more reproducible.

3.2 Method

In this chapter, PEG 300 was mixed with higher PEG molecular weights at different ratios to study the thermal behaviour of PEG mixtures. The mixtures were prepared by weight ratio then melted to form a homogeneous mixture, and then the mixtures were left to cool in a desiccator filled with silica for further analysis. The samples were analysed by the DSC according to section 2.2.4.1.3 to the molten state at 70°C.

The degree of crystallinity of PEG was calculated according to equation used from Wei et al., 2014.

$$x_c = \frac{\Delta H - \Delta H_a}{\Delta H^\circ_m} = \frac{\Delta H_m}{\Delta H^\circ_m} \qquad \text{Equation 3-1}$$

Where ΔH°_m is the melting of 100% crystalline polymer (determined to be 196.8 J/g) (Clariant, 2007) and ΔH_m is the melting enthalpy of the polymers investigated in this project.

3.3 Results

3.3.1 Thermal history

The table below shows the melting point and the enthalpy of PEG 4000 heated to the liquid state then cooled. This cycle was repeated three times on the same sample. The data shows that the melting point and the enthalpy are more consistent in the 2nd and 3rd cycle compared to the 1st cycle.

Table 3.3-1 The enthalpy and melting point of PEG after 3 heating cycles

Heat cycle	Peak min °C	Endothermic enthalpy J/g
1	46.9	-46.45
2	48.7	-46.08
3	48.9	-46.05

3.3.2 Melting and freezing points of the different PEGs

PEG 300 has a reported melting/freezing point between -8 to- 15°C (Carbowax brochure, 2011) and at room temperature is therefore liquid. However, in this study PEG 300 did not show any freezing event despite going to -20°C (Figure 3.3-1) this is might be due to the difference in the batch used compared to the literature or due to the PEG molecular weight is usually an average and it might have lots of ethlyene glycol (used as antifreeze) which might affect the freezing temperature.

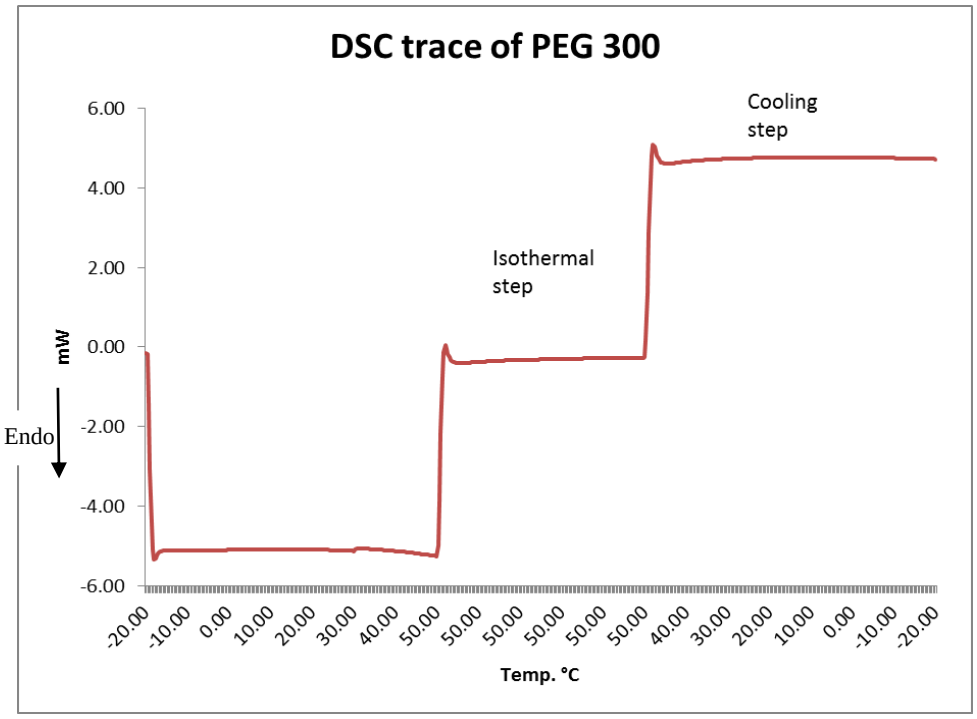

Figure 3.3-1 Heating and cooling DSC trace of PEG 300

The data of melting and freezing point of the different PEG molecular weights along with the enthalpy are presented below in **Table 3.3-2**.

Table 3.3-2 The melting and freezing results for the different PEG

PEG Mw	Mpt °C	Enthalpy of melting J/g	Mpt °C literature*	Enthalpy of melting J/g literature	Fpt °C	Enthalpy of freezing J/g	X_c (%)
300	N/A	N/A			N/A	N/A	N/A
1500	49	-174	59.35	-262	38	150	88.4
4000	63	-189	68.35	-281	42	156	96.0
6000	65	-208	73.65	-291	44	179	105.6
20000	67	-179	74.95	-273	49	176	90.9
35000	69	-195	73.85	-263	46	164	99.1

PEG 300 did not melt or freeze therefore, not data was recorded in the table above.
Mpt: melting point, Fpt: freezing point. Literature values are from Gines et al., 1996

PEG 4000 and PEG 6000 as discussed in section 3.1 shows two endothermic peak during melting this is due to the polymer has two polymeric chain types (folded and extended), this phenomena was also seen in the PEG used in this study. The DSC data of the different PEG shows that the melting point of PEG increases as the molecular weight increases. From PEG 1500 to PEG4000 there is a 14°C increase but from PEG 4000 to PEG 6000 the increase is only 2°C. This is due to the degree

of crystallinity since higher molecular weight PEG, above 4000, are nearly 100% crystalline (Wei et al., 2014).

The enthalpy of melting of the different PEGs increases as the molecular weight increases except for PEG 20000 and PEG 35000, where the enthalpy values were lower than the melting enthalpy of PEG 6000. The same phenomenon was seen by a study reported by Pielichowski et al., 2002. The results for PEG melting used in this project were compared to the literature and it shows that the PEG used had a lower melting point than the literature by around 7°C, but the results did follow the same trend as the molecular weight of PEG increases the melting point increases than a drop for PEG 20000 and 35000. The enthalpies of melting in the literature value were also higher than the one in our study but the same trend was observed. The slight difference in the values between the PEG used and the literature may be due to the thermal history of the PEG and the difference in the source of the PEG.

The freezing point also increases as the molecular weight increases, but the freezing point of PEG 20000 was higher than the expected result (49°C). In the literature, the freezing point increases as the molecular weight of PEG increases. The highest freezing point for PEG 20000 was 42°C and for PEG 35000 was 44°C whereas for the materials in this project the freezing point for PEG 35000 was 46°C. (Pielichowski et al., 2002.)

3.3.3 Thermal analysis of different PEG molecular weight blend with PEG 300

The addition of PEG 300 to a higher molecular weight PEG affects the melting and freezing point as well as the melting and freezing enthalpy. The figure below (Figure 3.3-2) presents the DSC traces for some of the PEG mixtures tested. The addition of 10% w/w of PEG 300 to PEG 20000 (purple trace) decreases the melting point of PEG 20000 by 5°C and the freezing point by 2°C. The enthalpy of melting decreased by 19 J/g whereas the freezing enthalpy decreased 27 J/g. The small quantity of PEG 300 decreased the degree of crystallisation of the PEG 20000 by

10% (based on Equation 3-1) The results also showed that the higher the PEG 300 content in the mixture with PEG 6000 (75:25 w/w red trace) affects the melting and freezing points of PEG 6000 in the mixture, they were decreased by 12 and 15°C respectively but the enthalpy of melting was very low (47 J/g) and the degree of crystallinity of PEG 6000 dropped to 24% (based on Equation 3-1).

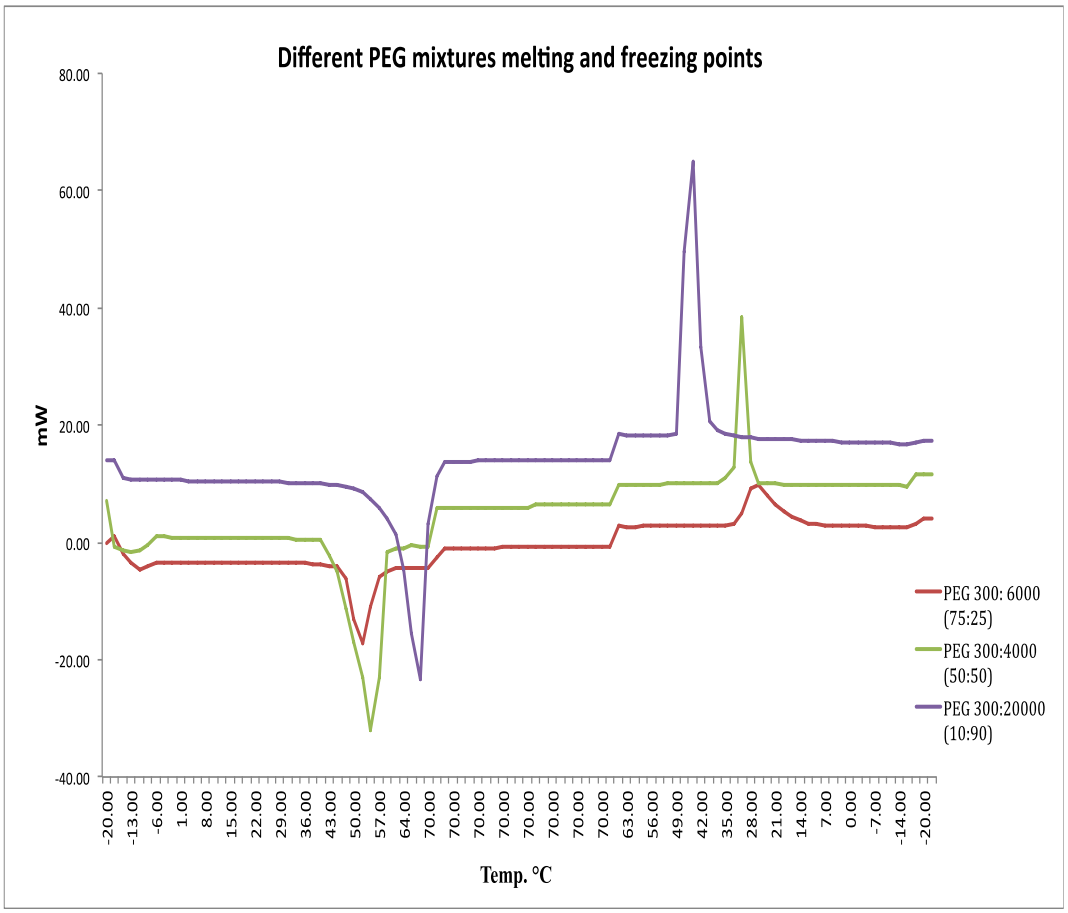

Figure 3.3-2 DSC traces for some of the PEG mixtures

The figure shows the difference in the melting and freezing point with the different PEG mixtures.

The results of the melting and freezing from mixtures of PEG 300 together with PEG's 4000, 6000, 20000 and 35000 are shown in Figure 3.3-3 to Figure 3.3-6. The results show that in all the mixtures of PEG the melting and freezing point changes with the different ratio of PEG 300 added.

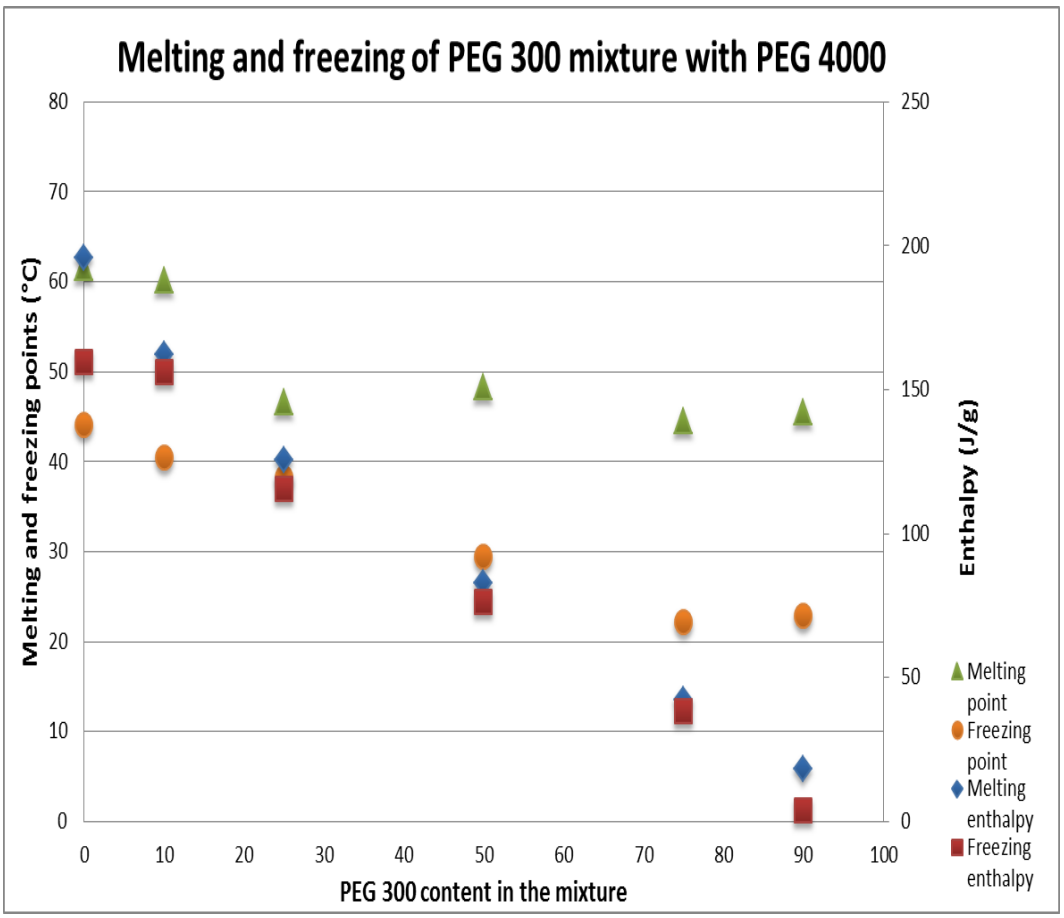

Figure 3.3-3 Melting and freezing point of PEG 300: 4000 mixtures

The melting point of PEG 4000 decreased as the PEG 300 ratio increased in the mixture. The figure above (Figure 3.3-3) shows that the enthalpy of melting is very close to the freezing enthalpy also, it illustrates that there is a gap of 15 to 25°C between the freezing and the melting point at each ratio except 25:75 PEG 300: PEG 4000 there was 8°C differences between the melting and freezing point. The lowest melting point (44.5°C) and freezing point (22.2°C) were observed in the 75:25 PEG 300: PEG 4000.

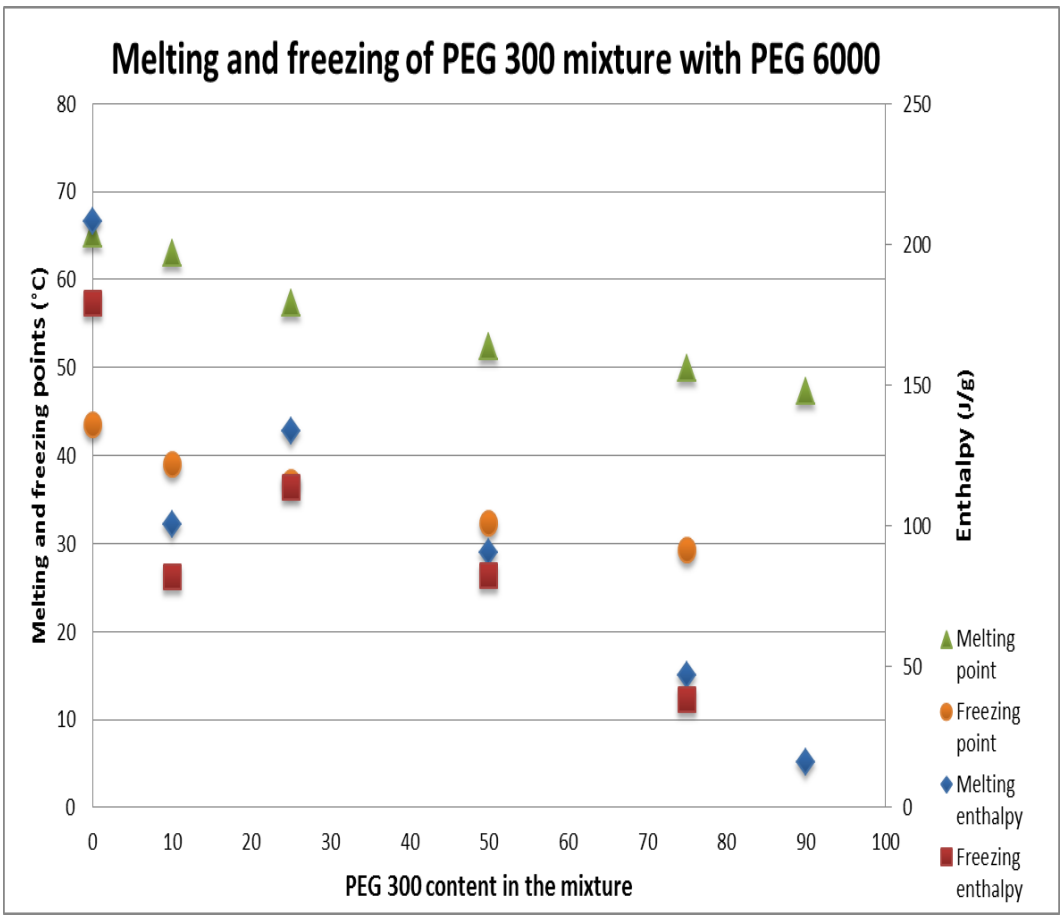

Figure 3.3-4 Melting and freezing point of PEG 300:6000 mixtures

The DSC data from the PEG 6000 mixtures results shows that the 90:10 mixture of PEG 300: 6000 did not freeze from melt during the cooling step. The melting points are consistently higher than the freezing points by 10 to 25°C. The melting and freezing points of all the mixtures did follow a trend, which decreases as the PEG 300 ratio increases in the mixture. The enthalpy of melting and freezing did follow the same trend except for 10:90 PEG 300: 6000 mixture where both enthalpies were lower than the other formulations. The lowest melting point was 47.3°C observed in the PEG 300: 6000 (90:10) mixture.

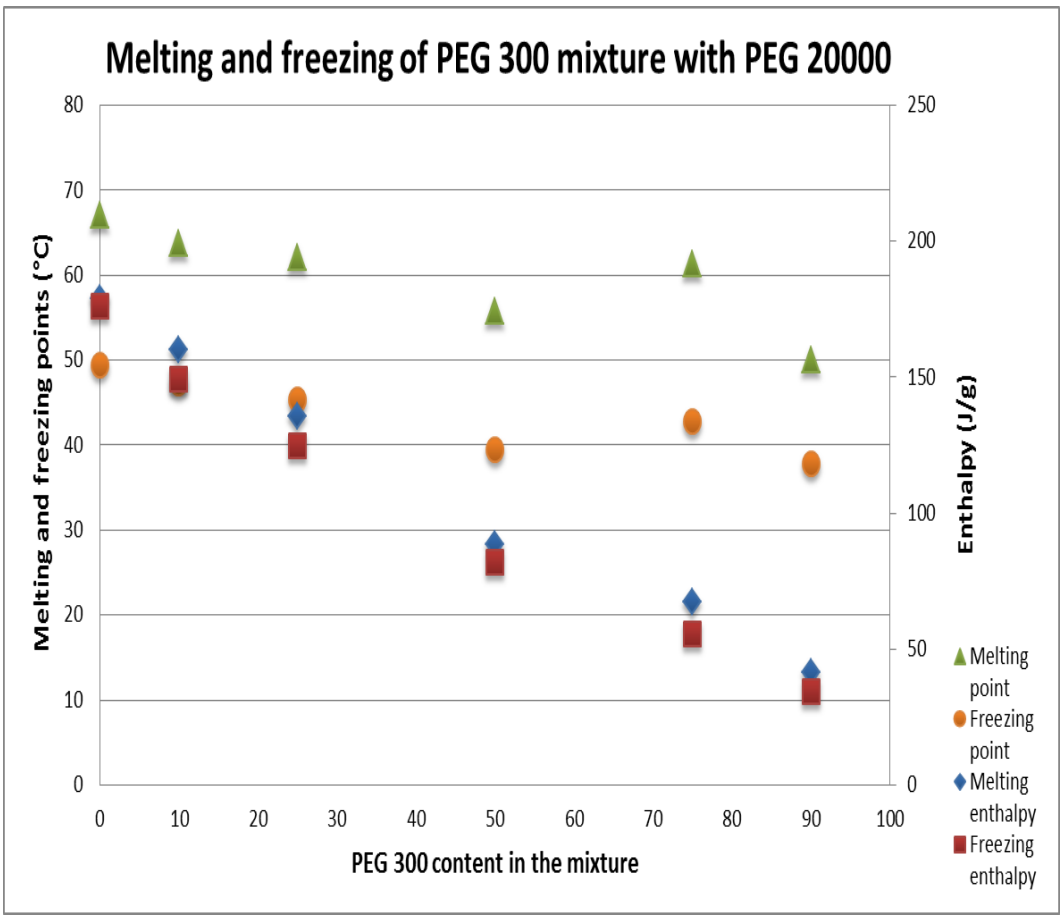

Figure 3.3-5 Melting and freezing point of PEG 300:20000 mixtures

For the PEG 20000 mixtures with PEG 300 the results show that the melting and freezing enthalpies are following the same trend by decreasing as PEG 300 increases in the mixtures. Besides, the values of melting enthalpy were similar to the freezing enthalpy.

The melting point did decrease as the PEG 300 in the mixture increases except for 75: 25 mixture where the melting point increases. The same trend was observed with the freezing point. The lowest melting point (50°C) was observed in the 90:10 mixture and the freezing point at this mixture was 38°C.

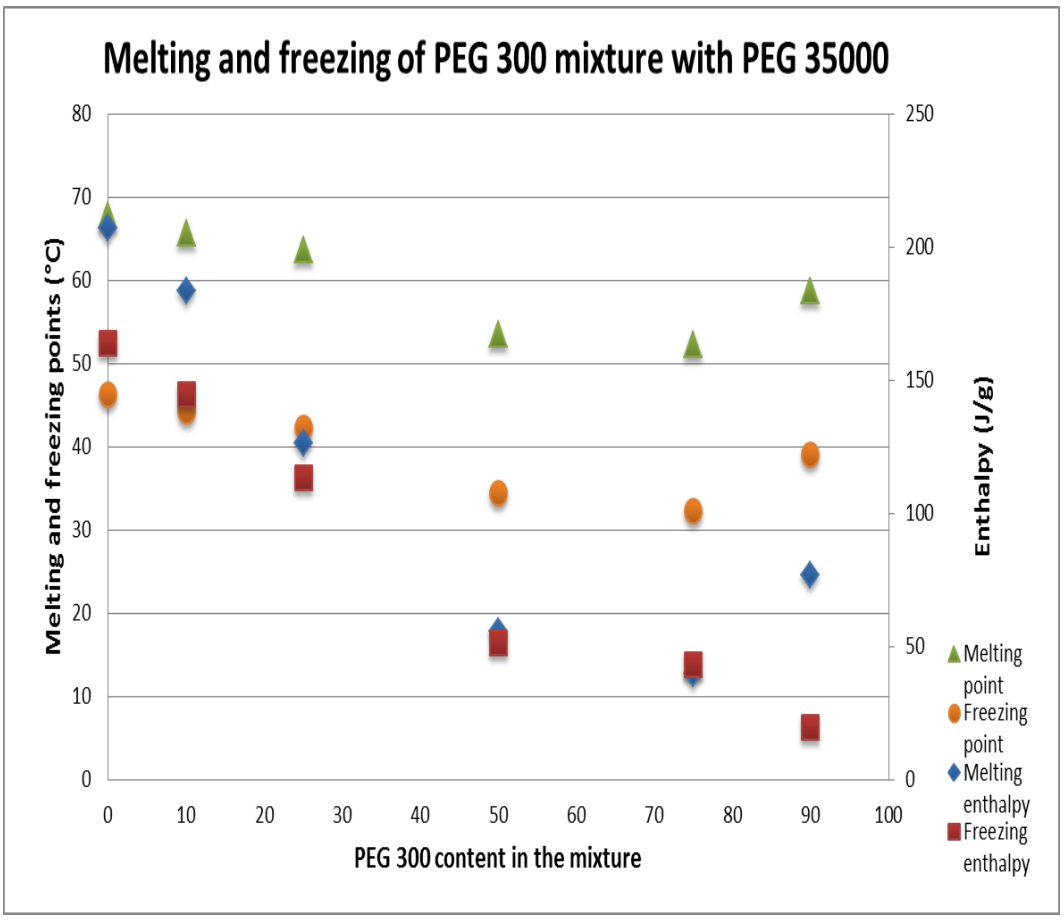

Figure 3.3-6 Melting and freezing point of PEG 300: 35000 mixtures

For the PEG 35000 mixtures, the enthalpies did not follow the same trends as the other PEGs stated before. The melting and freezing enthalpies of 25:75, 50:50 and 75:25 mixtures have similar values. For the other mixtures there was a big difference between the melting and freezing enthalpy. The freezing enthalpy of the mixtures decreases as the PEG 300 increases in the mixture. The melting enthalpy decrease as PEG 300 increase in the mixture but at 90:10 mixture increases again. The melting and freezing point of the mixtures followed the same trend as the melting enthalpy by decreasing and then increase at 90:10 mixture. The lowest melting point (52.4°C) was observed at 75:25 mixture with a freezing point of 32.4°C.

3.3.4 Effect of the cooling rate on the freezing point of PEG

The effect of the cooling rate on the freezing properties of PEG was investigated using PEG 300:4000 (50:50) mixture and the results shows that when the cooling rate increased the temperature of crystallization/freezing decreases, but the freezing enthalpy did not follow the same trend. The results shown in Figure 3.3-7 were in agreement with the Pielichowski, 2002 study on the crystallization temperature but different in the freezing enthalpy as the literature study stated that increasing cooling rate increased the freezing enthalpy.

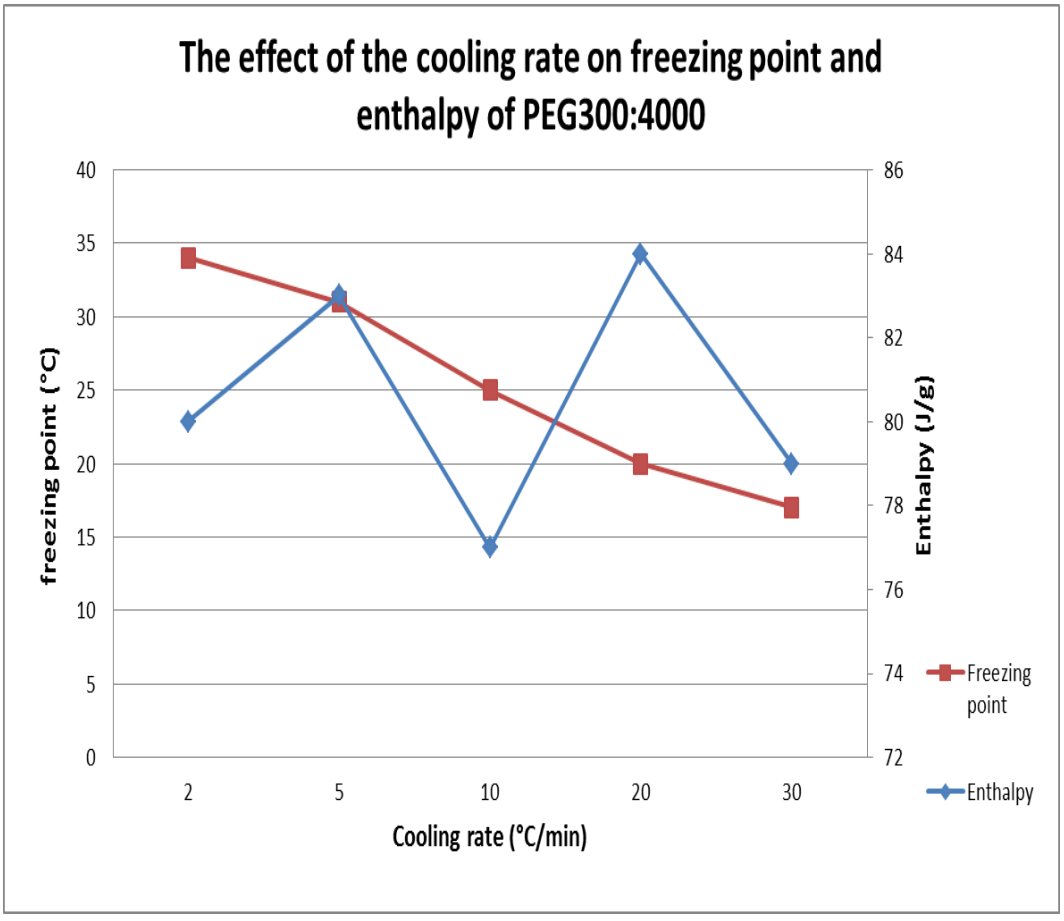

Figure 3.3-7 The freezing point and enthalpy at different cooling rate of PEG 300:4000

3.3.5 Hot stage microscopy of melting and cooling of PEG.

The effect of the cooling rate on PEG 4000 was investigated under hot stage microscopy. The sample was heated to the molten state than cooled at 10°C/min (normal cool) or 30°C/min (quench cooled). The hot stage microscopy images were taken at optical X10 magnification.

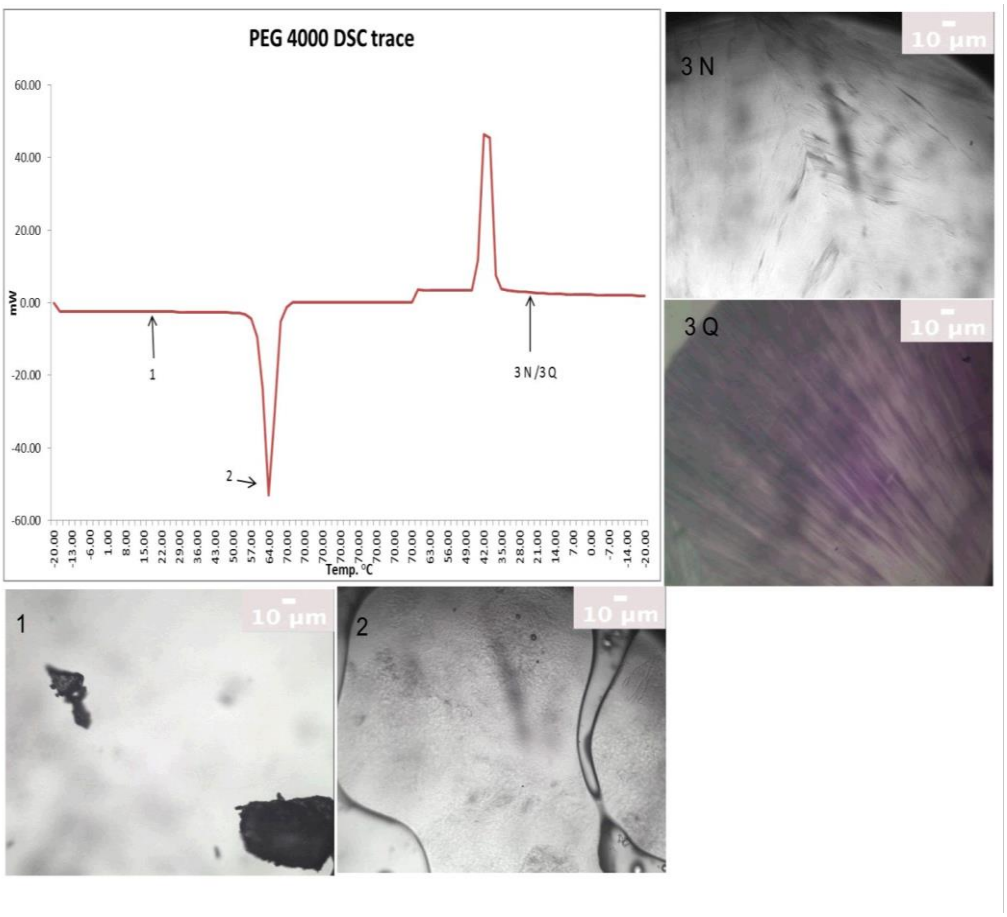

Figure 3.3-8 PEG 4000 DSC trace and hot stage microscopy images
(PEG 4000 at room temperature (1), PEG 4000 at 60°C (2), at 25°C after normal cooling (3 N) and at 25°C after quench cooling (3 Q))

At both cooling rates used, the PEG morphology was the same as both samples formed a striation sheet, but with the faster cooling rate the sheet was thicker. The PEG sheet appears thicker due to the number of folds in the PEG chain when cooled (Pielichowski et al., 2002).

3.4 Discussion

The thermal behaviour of PEG along with the effect of PEG 300 on the other higher molecular weight PEGs mixtures used in this project were studied. The melting and freezing point of PEG increases as the molecular weight increases; this is due to the degree of crystallinity of the PEG.

The blend of PEG 300 with higher molecular weight PEG did have an effect on the melting and freezing point of the mixture. The melting and freezing point of the mixtures were lower than the higher molecular weight PEG used alone. This temperature difference between the melting and the freezing point of PEG is due to the increase in polydispersity of the PEG and the decrease in degree of crystallisation during the preparation of the PEG mixture with PEG 300, also this temperature difference will increase with increasing molecular weight of PEG (Wei et al., 2014). The results from our study were similar to the one carried out by Pielichowki and colleagues, the freezing temperature of the blend they used (PEG 1000: 3400, PEG 1000:10000 and PEG 3400: 10000) was lower than the each PEG alone and they suggested that this is due to the PEG blend when cooled it has a morphological restrictions and it gets trapped in interlamellar regions which prevent them from freezing quickly (Pielichowki et al., 2002). The melting and freezing enthalpy in all the mixtures decreases as the higher molecular weight PEG content decreases in the mixture, which suggests that thermal event happening is due to the higher molecular weight PEG in the mixture and PEG 300 acts as a solvent. The PEG mixtures did give the ability to control or change the melting and freezing point as well as the enthalpy associated with them by changing the ratio or by using different PEG molecular weights. The melting and freezing enthalpies in all the PEG mixtures used did follow a straight line which is behaving as ideal solution according to Raoult Law whereas as the melting and freezing temperature were non ideal system as they were curved. These results were achieved from n of 1 and no statistical analysis could be done to show the differences.

The information gathered from this section was used to understand the behaviour of PEG alone and as blend before using it as the carrier for solid dispersion studies.

Chapter 4 Carbamazepine with PEGs mixtures solid dispersion

4.1 Introduction

4.1.1 CBZ background information

Carbamazepine is an effective antiepileptic drug widely used worldwide (Naima et al., 2001). CBZ belongs to the class II according to the biopharmaceutical classification system. It has poor gastrointestinal absorption after oral administration due to the reduced aqueous solubility and slow dissolution rate that will affect its therapeutic effect but exhibit high intestinal permeability (Liu et al., 2013).

The drug appears as a white crystalline powder with a molecular weight of 236.3 g/mol and melting point of 189 °C to 193 °C. (BP, volume I&II, 2014 online accessed). CBZ is a neutral drug, hence the drug will stay in unionised form with change of pH (Nghiem et al., 2005) and its glass transition temperature (T_g) is 60°C (Naima et al., 2001).

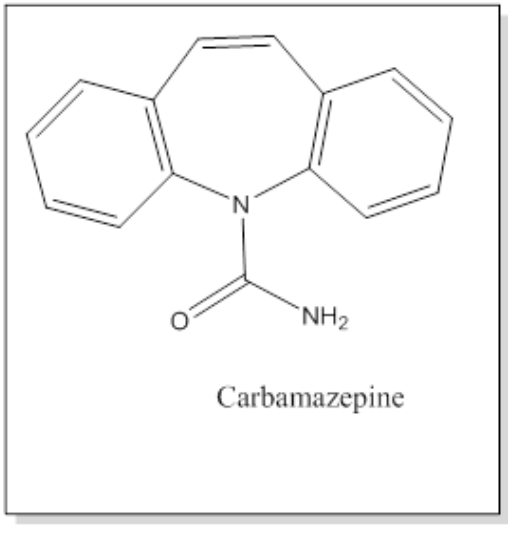

Figure 4.1-1 Carbamazepine chemical structure

Carbamazepine exists in four different polymorphic forms and a dihydrate: Triclinic (form I), Trigonal (form II), *P*-monoclinic (form III) and *C*-monoclinic (form IV) (Grzesiak et al., 2003). CBZ usually exists as form III which is the most thermodynamically stable form. Form I can be seen at elevated temperature (Grzesiak et al., 2003) therefore when CBZ form III is heated a change in polymorph can be seen on the DSC and the hot stage microscopy.

CBZ DSC trace along with hot stage microscopy images are shown below:

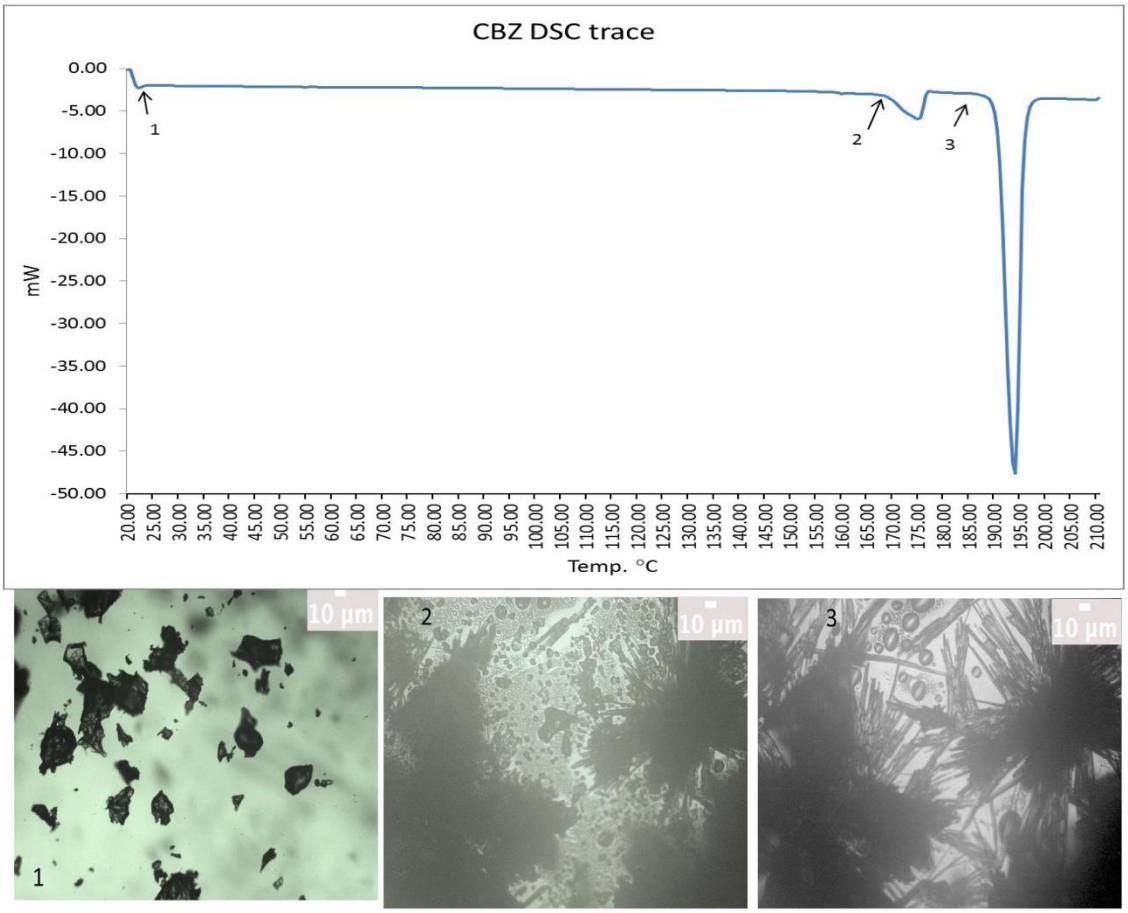

Figure 4.1-2 DSC and hot stage microscopy of CBZ

The figure above shows the thermal changes of CBZ crystals as they are heated. The transformation of form III to form I was observed under the microscope as the crystals change shape from rocky to needle shape at higher temperature before they melt.

The different forms of CBZ have different X-ray patterns. The figure below shows the different pattern (these pattern were generated using calculated pattern from Cambridge structure database)

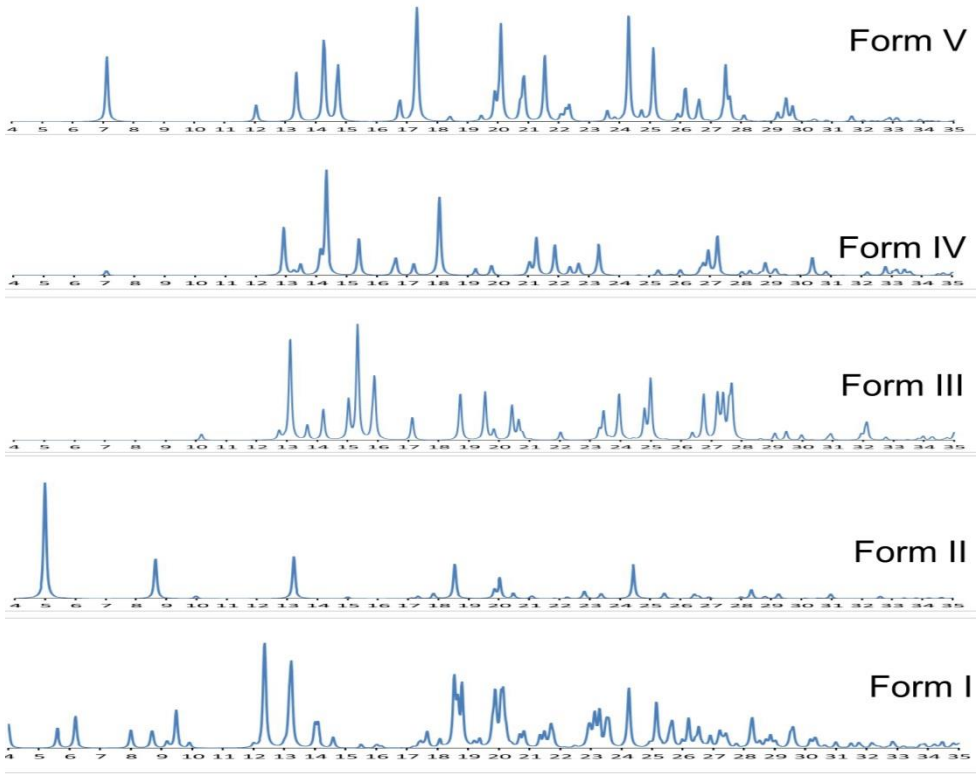

Figure 4.1-3 XRPD pattern of CBZ different forms

The main peaks for each form are:

Form I has peaks at 2θ= 7.92, 9.37, 12.28 and 19.99. Form II has peaks at 2θ= 8.68, 13.26, 18.56 and 24.54. Form III has peaks at 2θ= 15.36, 19.56, 25.00 and 27.47. Form IV has peaks at 2θ= 14.11, 17.89, 21.79 and 33.11. (Grzesiak et al., 2003) Form V has peaks at 2θ= 7.12, 17.32, 20.08 and 24.28.

4.1.2 Aims

As discussed in the introduction solid dispersions may be prepared by many different mechanisms, and in this chapter CBZ solid dispersions were prepared using the fusion (or melt) method. The solid dispersions were prepared with a mixture of PEG 300 and higher molecular weight PEG (such as PEG 4000, 6000, 20000 and 35000) varying both the drug to total PEG mixture ratio and ratio of PEG 300 to high molecular weight PEG. The aims of this chapter are to prepare the different formulations mentioned above and then they were analytically assessed by DSC, hot-stage microscopy and dissolution to study the effect of the various components on the quench cooled form of CBZ.

4.2 Method

In this chapter the formulations were prepared either by physical mixture (for PEG 300 only formulations) or by the melt method (for the formulations with higher PEG molecular weights) refer to section 2.2.2.

The CBZ: PEG 300 formulations were prepared at a ratio of 1:1, 1:5 and 1:10 w/w (CBZ: PEG 300), the other CBZ: PEG formulations were prepared according to **Table 3.3-2**. These formulations were assessed by DSC using both normal and quench cooling profiles (see section 2.2.4.1).

Solid solution terminology will be used to discuss the solution obtained after quench cooling (where no crystalline material was observed under the light microscope) and solid dispersion will be used to describe a crystalline material. Also CBZ dissolving will be used when no CBZ endothermic peak is observed and melting when the endothermic peak is observed.

4.3 Results

4.3.1 CBZ: PEG 300

A physical mixture of carbamazepine (CBZ) (melting point 189-194°C) was prepared with PEG 300 at different ratios. The DSC results for these formulations show that there was one endothermic event for the formulations (between 90-100°C

for CBZ) during the first heating cycle (refer to Figure 4.3-1). In these formulations no crystallisation or melting peak was observed during the second heating step except for CBZ: PEG 300 (1:1 w/w) formulation, where an exothermic event occurs at around 83°C followed by a melting event at 131°C. The exothermic event may be due to CBZ crystallisation from a supersaturated drug solution created during cooling, the temperature at which this event occurs is not for the PEG 300 as it does not have a solidification peak at the temperatures studied (see section 3.3.2).

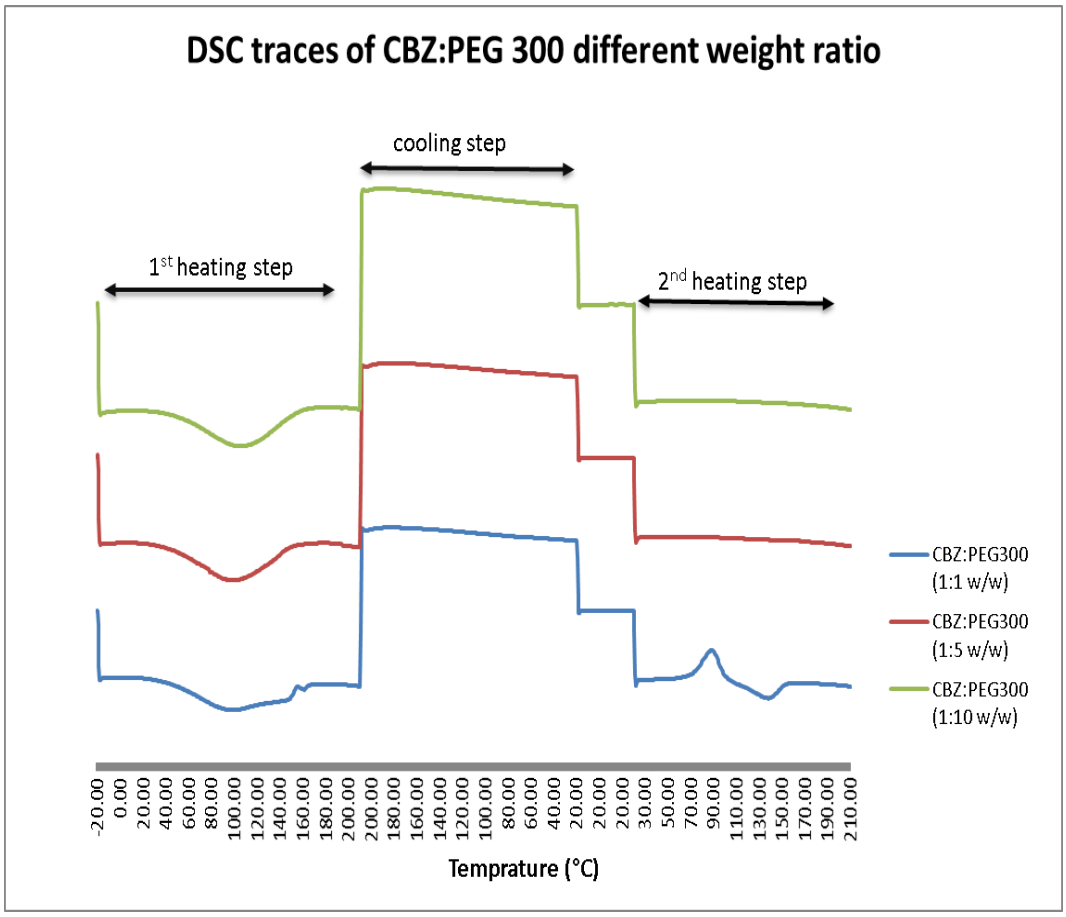

Figure 4.3-1 DSC traces of CBZ: PEG 300 different formulations

The results show that the sharp endothermic peak of CBZ at 194°C is missing and is replaced by a broad peak. The results suggest that CBZ molecules in the crystal are breaking apart requiring thermal energy. It could be proposed that the CBZ is dissolving in PEG 300 (see microscopy results below) rather than melting. The enthalpy of melting for the different CBZ: PEG 300 formulations remained the same

for the 1:1 and 1:10 (64 J/g) despite a 10 fold decrease in the drug concentration in the formulation. This may indicate that the underlying thermal event is independent of CBZ concentration, or that it is caused by a small amount of CBZ in the PEG, and so at higher CBZ concentrations no additional energy is released.

Table 4.3-1 CBZ: PEG 300 thermodynamic parameters

Drug to polymer ratio	Enthalpy J/g (of formulation)	Dissolving point °C	Crystallisation peak (2^{nd} heating)	Melting peak (2^{nd} heating)
1:1	-64.44	96.26	17.32 J/g 88.24°C	-13.29 J/g 137.76°C
1:5	-71.0	96.54	n/a	n/a
1:10	-64.16	105.48	n/a	n/a

4.3.2 Hot stage microscopy

CBZ: PEG 300 formulations were assessed using hot stage microscopy, with both thermal profiles used in the DSC. The results show that the solid particles of CBZ dissolves in the liquid PEG in all the formulations as the temperature increases until all the CBZ is dissolved before the solid state melting point (194°C) is reached. During both the normal and quench cooling steps no crystal growth was observed in the 1:10 and 1: 5 formulations.

During the 2^{nd} heating step only the CBZ: PEG 300 (1:1 w/w) formulation showed a crystallisation event at around 65°C irrespective of cooling rates used. The % CBZ crystallised in the formulation was around 30% (based on visual assessment) and as only a few crystals appeared then quickly dissolved in the liquid PEG.

4.3.2.2 CBZ: PEG 300 (1:1 w/w)

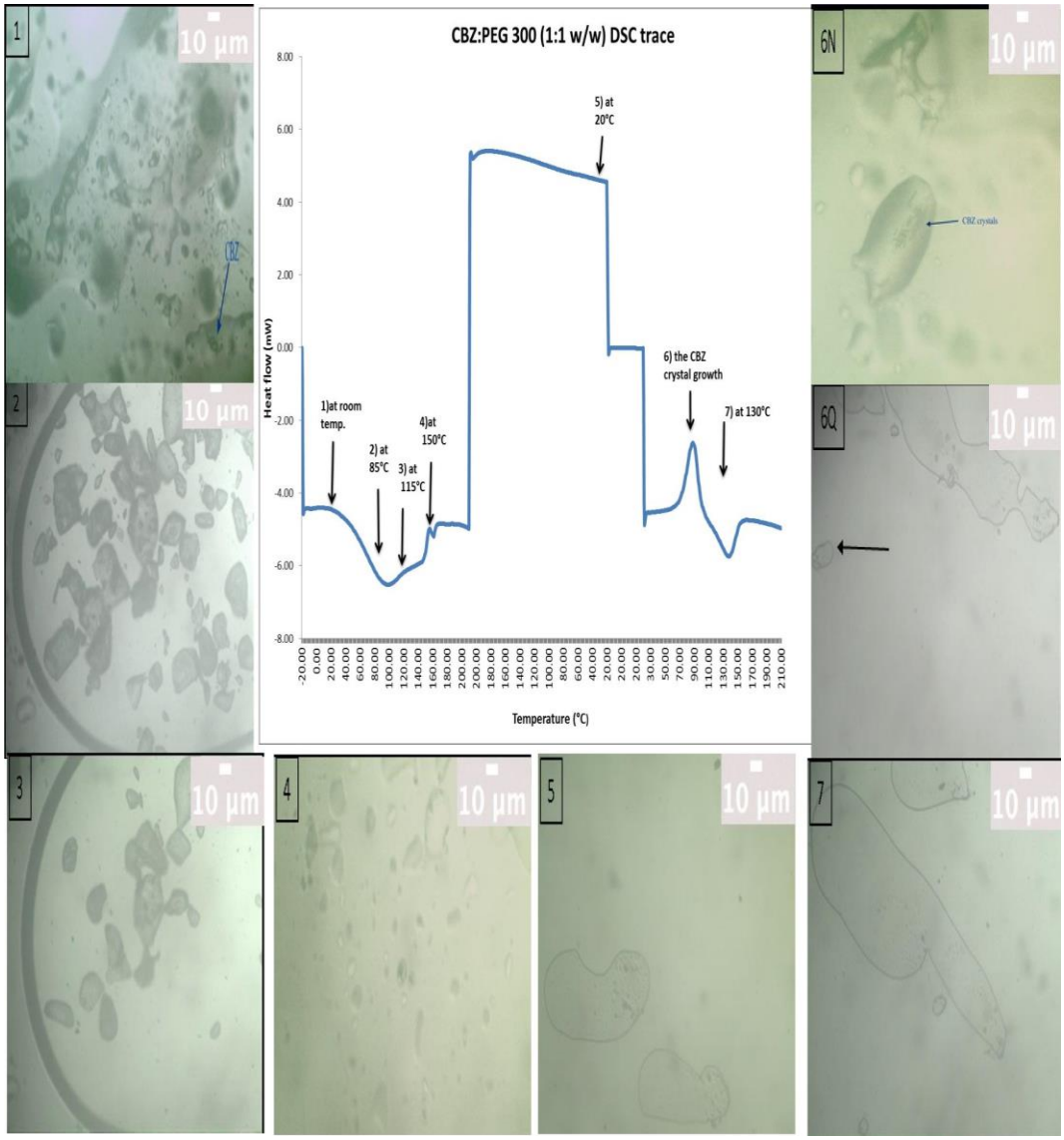

Figure 4.3-2 DSC trace of CBZ: PEG 300 1:1

(Image number relates to the DSC trace number)

The figure above shows the quench cooled DSC trace along with the hot stage microscopy of CBZ: PEG 300 (1:1 w/w). Image 1 was taken at 10X objective; it shows CBZ crystals in PEG 300 at room temperature (20°C), the CBZ can be seen covered by the PEG. As the sample was heated, the CBZ molecules start to dissolve in the liquid PEG 300. Image 2 was taken at 25X objective, it shows CBZ crystals in liquid PEG at 85°C and the CBZ crystals exists in form III as they have a rock shape. As heating continues, fewer crystals can be seen at 115°C (image 3). At

150°C (image 4), all the CBZ crystals have dissolved in PEG and there was no CBZ form change to form I as the crystals had all dissolved before they reach the required phase transition temperature of 180°C. During normal or quench cooling profiles no crystal growth was observed as image 5 shows (image 5 was taken during quench cooling). When the sample was reheated after quench cooling a crystal growth appears at around 100°C, the arrow in image 6Q pointing to the new crystal formed. For the normal cooled sample a crystal growth was also observed but at a higher temperature around 115°C (image 6N) but the crystals looked very fine. Image 7 was taken 130°C, where the re-formed crystals had all dissolved in the hot PEG.

4.3.2.3 CBZ: PEG 300 (1:10 w/w)

For this formulation the cooling rate did not affect the CBZ crystallisation behaviour during cooling or 2nd heating step; therefore only the hot stage microscopy images from normal cooling are shown in Figure 4.3-3.

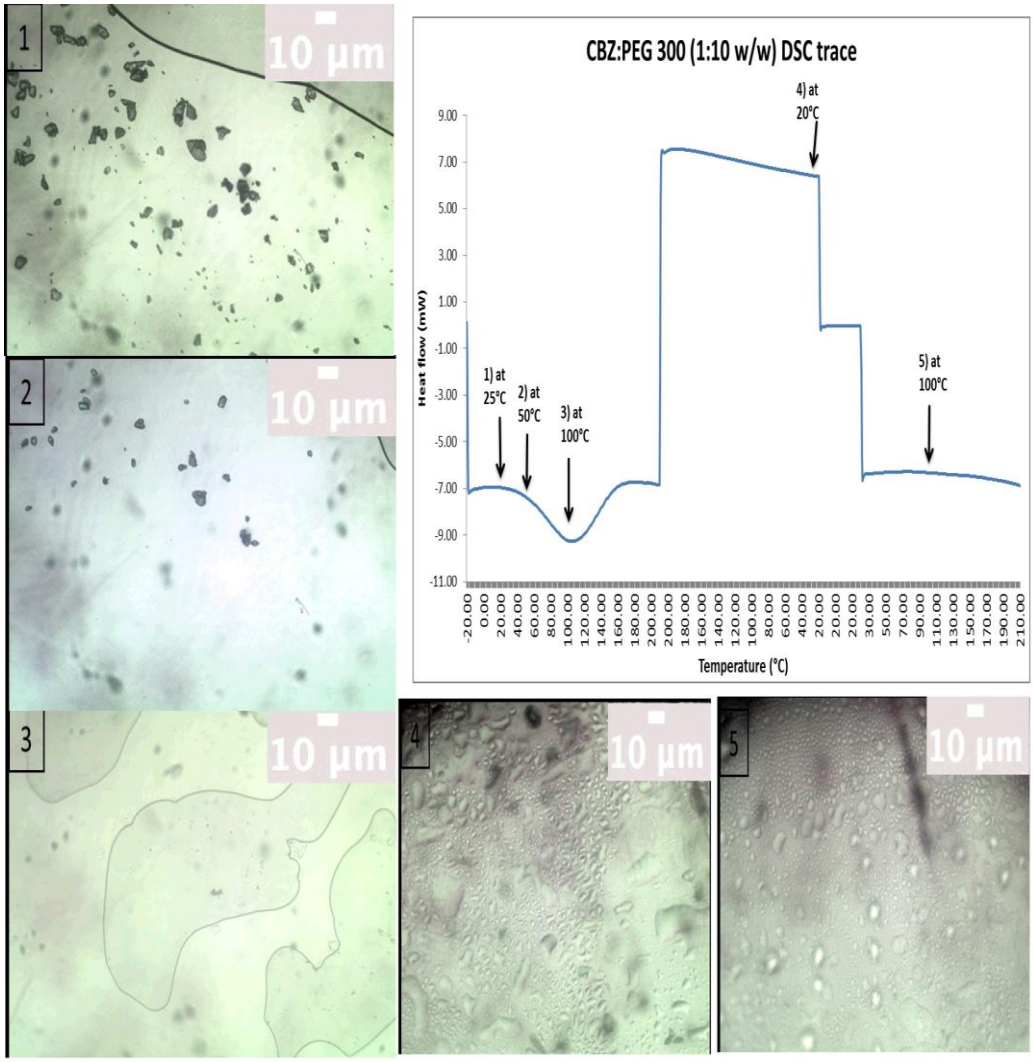

Figure 4.3-3 Hot stage microscopy and DSC trace of CBZ: PEG 300 (1:10 %w/w)

The figure above shows the phase transition of CBZ: PEG 300 (1:10) formulation with change of temperature. Image 1 was taken at 25°C, and the CBZ crystals can be seen dispersed in the liquid PEG 300. As the temperature increases the CBZ crystals become smaller, as they are dissolving in the hot PEG, as seen in image 2, taken at 50°C. Image 3 was taken at 100°C; all the CBZ crystals are dissolved in the

hot PEG. Image 4 was taken during cooling at 0°C, the CBZ molecules stayed in the liquid state (no crystallisation was observed). Image 5 was taken during the 2nd heating step, where no CBZ crystallisation was observed, the drug molecules stayed in the liquid state with PEG 300.

The DSC trace for CBZ: PEG 300 (1:10) did not show any crystallisation during the 2nd heating step, which indicates that the drug stayed in the amorphous or dissolved, state within the liquid PEG. The hot stage microscopy results showed similar pattern to the DSC results for CBZ: PEG 300 (1:1 and 1:10 formulations) where CBZ dissolved in the hot PEG during the 1st heating step then no crystallisation during cooling and 2nd heating step.

In order to study the re-crystallisation of CBZ further and to gain control of this process by pushing the exothermic event to a higher temperature, or if it could be observed in a wider range of CBZ: PEG ratios, higher molecular weights of PEG were mixed with the PEG 300 in order to stabilise the amorphous form.

4.3.3 CBZ: PEG 300: 4000 mixtures

4.3.3.1 CBZ: PEG 300: 4000

The effect of the addition of a higher molecular weight PEG to the CBZ formulations was assessed in this section. Nine formulations were prepared according to the weight ratio presented in **Table 2.2-2**. The figure below (Figure 4.3-4) shows the effect of the cooling rate on the molten CBZ formulation during the DSC experiment. During normal cooling (10°C/min), the CBZ molecules crystallise from the solution but when the same formulations were quench cooled (30°C/min) during the cooling step, some formulations showed crystallisation (of PEG and CBZ) during cooling and some remained as a solution until a certain temperature during the 2nd heating step where the crystallisation starts.

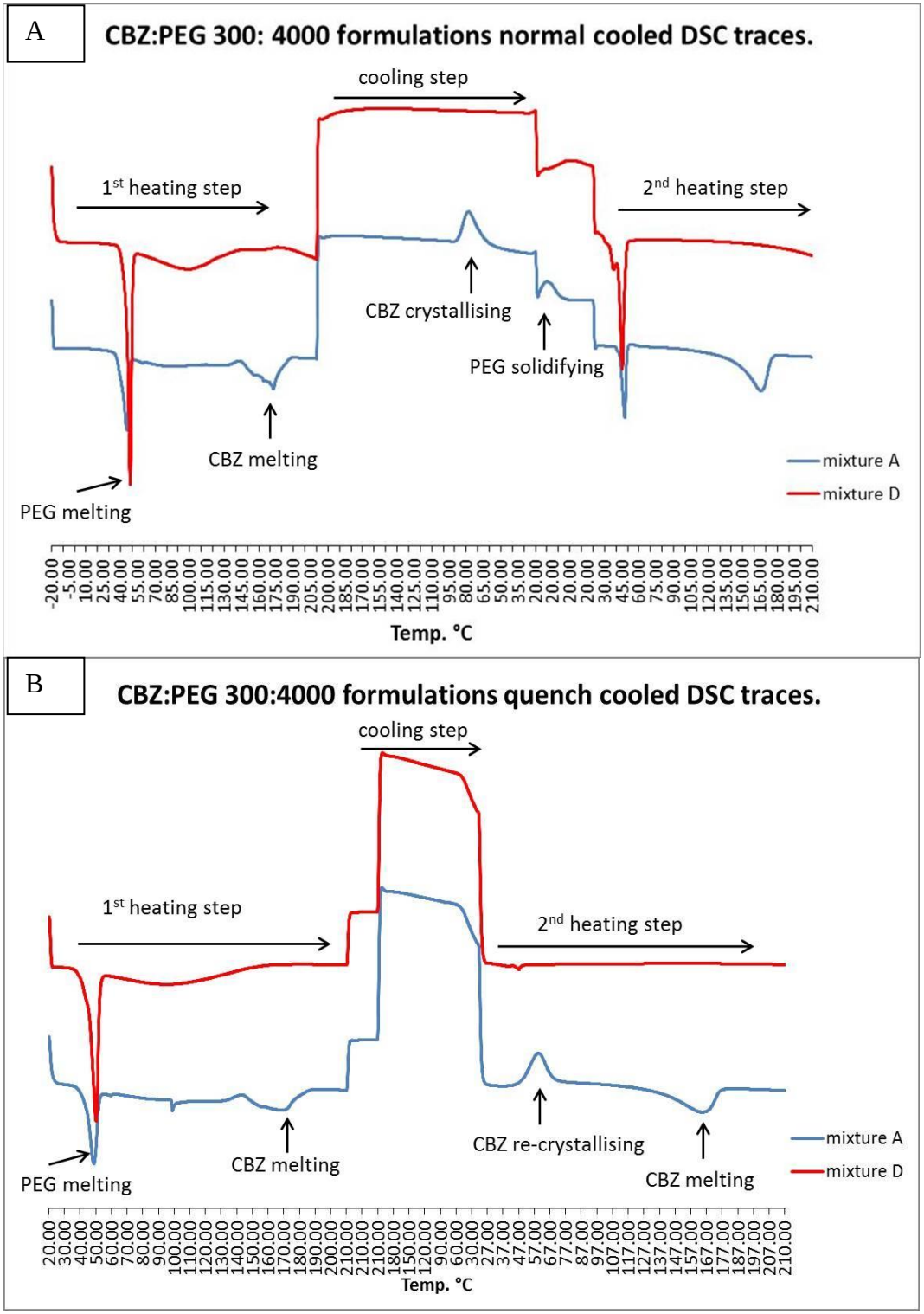

Figure 4.3-4 The effect of the cooling rate on the CBZ formulations

Figure A shows the thermal events of the samples normally cooled on the DSC and Figure B shows the thermal events of the samples quench cooled.

Figure 4.3-4 shows two different DSC traces as exemplars of the results found for the nine different formulations. Mixture A contains a 1:1 ratio of CBZ to PEG, with the PEG mixture being 0.75: 0.25 PEG 300: 4000, and mixture D contains a 1:5 drug to PEG mixture, with the PEG mixture ratio being the same as mixture A. The CBZ melting/ dissolving peak in the high PEG content formulation (mixture D) was observed in the 1st heating step but not in the 2nd heating step, this is due to the CBZ dissolved in the PEG and stayed in solution during cooling (normal and quench cooling). Image A shows the DSC traces of the formulations normally cooled and in mixture A a crystallization CBZ peak can be seen during the cooling step followed by a solidification of PEG peak during the isothermal step whereas in mixture D, CBZ dissolved in the hot PEG and only PEG recrystallised during cooling. In image B, mixture A shows no crystallisation during cooling and an exothermic peak being observed during the 2nd heating step at around 60°C, whereas for mixture D, no crystallisation occurred during cooling, and no exothermic peak was observed during the 2nd heating step. This suggests that at the normal cooling rate the PEG solidified in a way that produced an exotherm, and this solid form yielded a melting endotherm upon re-heating, whereas with quench cooling the PEG did not undergo any solidification that produced any energy, and so upon reheating no energy was required to re-melt the solid, or semi-solid. As the PEG did not solidify during quench cooling in mixture A, CBZ molecules as well stayed in the PEG as amorphous material until the sample was reheated and the sample reaches a temperature where the PEG molecules can freely move hence the CBZ molecules will have a higher mobility where they can come together and re-crystallise as the exothermic peak in the 2nd heating step shows.

The DSC traces of the different formulations were assessed and the results for the melting and freezing enthalpy of PEG 300:4000 peak in the formulations (normal cooled) are presented in the figure below (Figure 4.3-5).

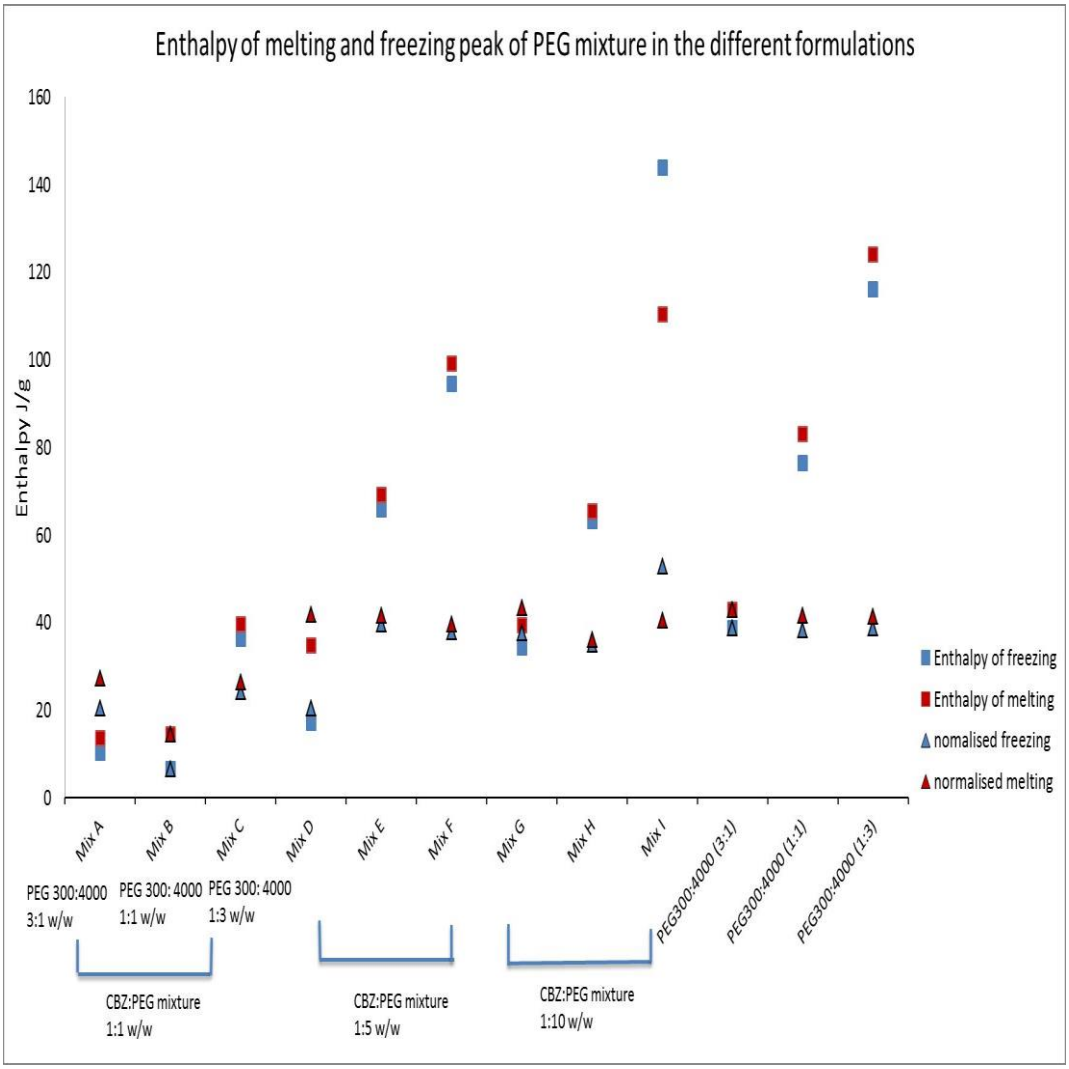

Figure 4.3-5 Enthalpy of melting and freezing of PEG 300:4000 in CBZ formulations (The enthalpy of the PEG mixtures in the formulations was normalised to the weight of PEG 4000 used in the formulation. The freezing enthalpy or the normalised freezing enthalpy is the exothermic peak of PEG during cooling.)

The results shows that as the PEG 300: 4000 to drug ratio increases in the formulation, the enthalpy of melting and freezing increases as well especially in the 1:10 (drug: PEG) formulations and that the higher the solid PEG (PEG 4000) in the formulation the higher the freezing and melting enthalpy, this was discussed before in section 3.3.3. The enthalpy of PEG mixture melting was higher than the freezing enthalpy (except for mix I), these results were similar to the results discussed in Figure 3.3-3. Although the PEG mixtures in the formulations did follow the same trends as PEG 300:4000 alone but the freezing and melting enthalpy values in the presence of CBZ were less than the PEG mixture alone even when the formulations

contains 10 times more PEG than CBZ. The normalised enthalpy did show that most of the formulations have a response similar to the PEG mixtures except for formulations A, B C and D where the normalised enthalpies were lower than the PEG mixtures which indicate that there is an interaction between the PEG mixture and the drug.

The quench cooling DSC traces of the formulations shows that the CBZ solid solution was only present in two formulations where the CBZ has an equal weight ratio as the PEG mixture (CBZ:PEG mixture 1:1 w/w). The two formulations were mixture A, where the PEG 300:4000 ratio was 3:1(w/w), and B where the PEG 300:4000 ratio was 1:1 (w/w). In both cases the crystallisation temperature was around 59°C.

The thermal stability of the solid solution in mixture B was studied to understand the effect of temperature on the CBZ crystal formation within the formulation. These experiments were performed as short-term studies, where the formulation was held at different temperatures for one hour in the DSC, and long term studies, where the formulation was stored in the fridge and freezer for up to a month.

4.3.3.2 Stability of the solid solution with increasing temperature

Mixture B was analysed in the DSC by heating the sample to 210°C followed by quench cooling and then held at an isothermal 'step' at different temperatures for one hour followed by heating again to examine at which temperature the exothermic peak will convert back to melting peak. (Refer to quench cooling method in section 2.2.4.1.2)

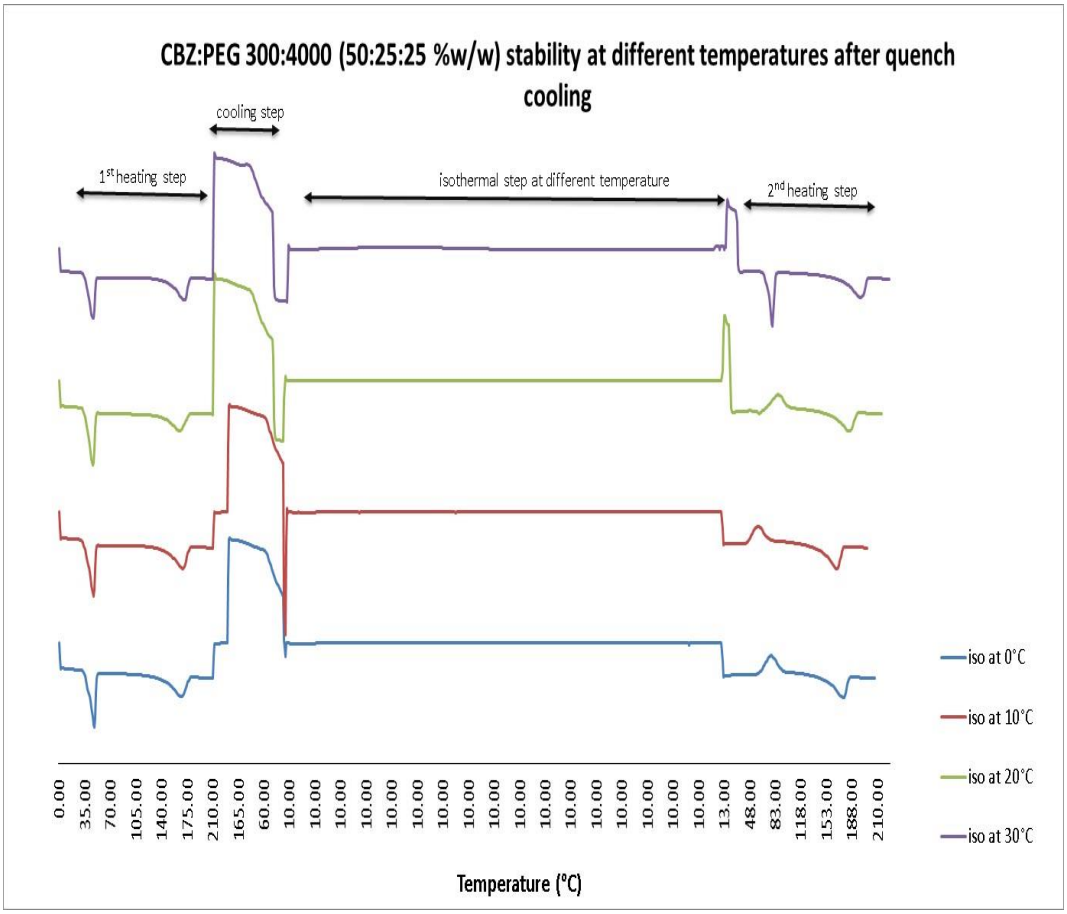

Figure 4.3-6 Isothermal stability of the solid solution at different temperature

The figure above shows the DSC traces of CBZ: PEG 300:4000 isothermally held at different temperatures, in the first heating part of the experiment, the first PEG melting peak can be observed at approximately 50˚C and the second peak, at approximately 175˚C, is due to the CBZ melting. In the second heating step: the first exothermic peak is due to CBZ crystallisation then the second peak is the melting peak of the resultant CBZ crystals. The results show that when the sample was held at 30°C, the exothermic CBZ peak had disappeared being replaced by the PEG melting peak, this due to PEG and CBZ crystallising during the isothermal step as the baseline changes with time. The solid solution was stable for one hour at 0, 10 and 20°C. (The shift in the CBZ melting point during the 2nd heating step at 20 and 30°C is due to the DSC experiment for these samples were slightly different than the others because of the removal of the 2 minutes equilibration time after the 1st cycle.)

The stability of mixture B at 25°C and 40°C for 12 hours were also analysed on the DSC, the results shows that the samples were not stable at these temperatures as the exothermic peak converts back to a melting peak (Result not shown).

4.3.3.3 Stability of the solid solution stored in the fridge and freezer

The stability of the exothermic peak in mixture B was studied by placing one sample in fridge at 4°C and the other sample in the freezer at -25°C. The samples were analysed at 0, 2, 7 and 30 days. The samples were prepared in an aluminum DSC pan with pierced lid, the sample was quench cooled after the experiment and stored at the required temperature. The DSC method presented in section 2.2.5

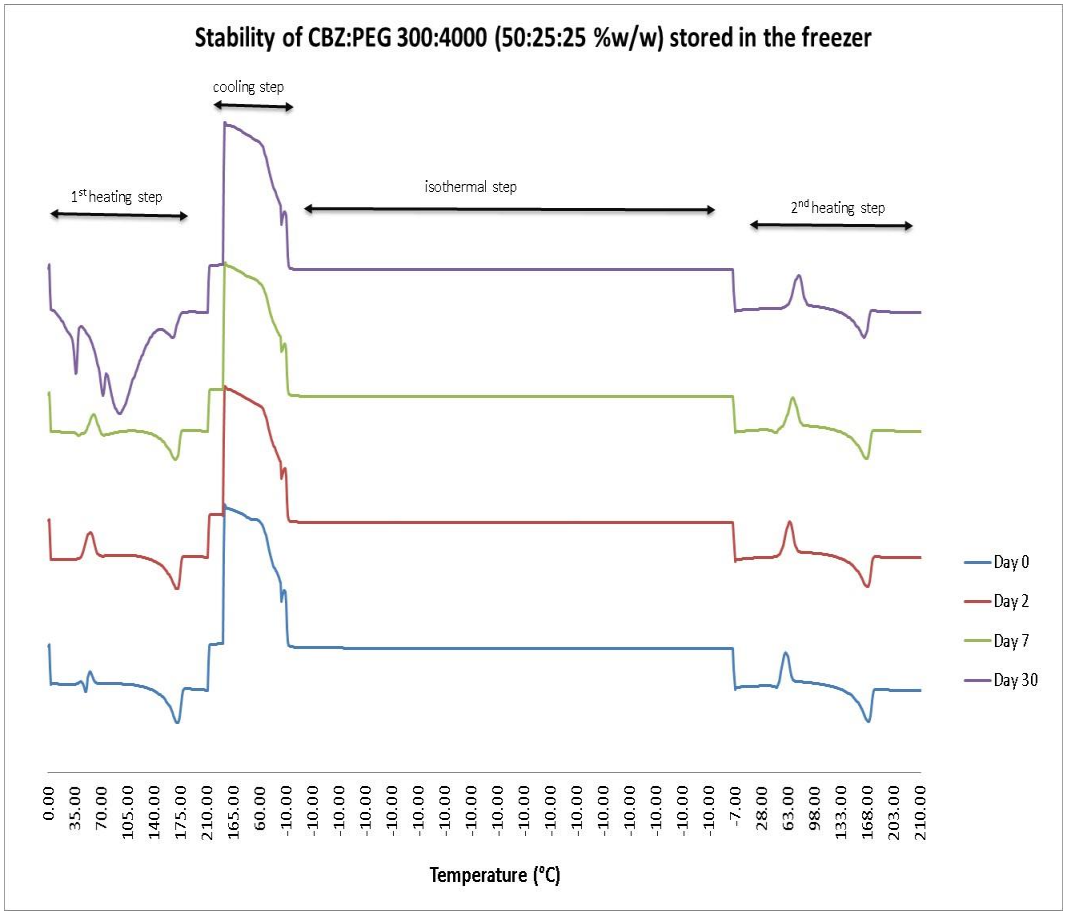

Figure 4.3-7 Stability of the exothermic peak in the freezer

The figure above shows the DSC curves of the stability sample stored in the freezer and the results shows that CBZ stayed in amorphous state as an exothermic peak was seen in the 1st heating cycle and this is due to when the sample was stored in the

freezer straight after the melt, the sample stayed in solution until it was reheated. This phenomenon was not seen at 30 days point where a broad and unresolved peak was seen and it was hard to fully interpret the events. This peak might be due to the dehydration of CBZ hydrate and the small endothermic peak around 180°C is due to the melting of CBZ form I as it was discussed by Liu et al., 2013. After quench cooling and reheating the samples were able to regenerate the solid solutions and the crystallisation temperature of exothermic peak during the 2nd heating step increased with time.

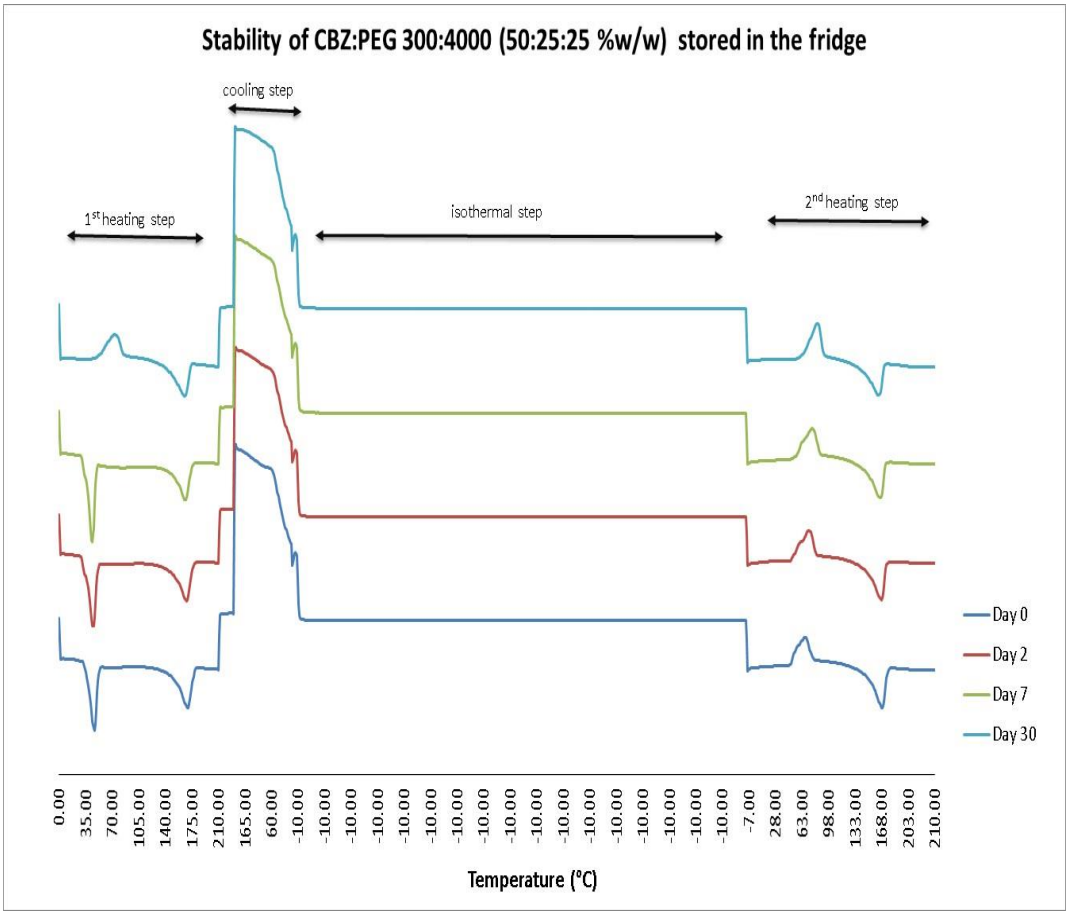

Figure 4.3-8 Stability of the exothermic peak hold in the fridge at 4°C.

For the sample stored in the fridge, the CBZ solid solution did revert back during storage with time as a PEG and CBZ melting peaks were observed except for day 30 where an exothermic peak was observed at high temperature followed by CBZ

melting peak (refer to the discussion). The sample was able to regenerate the solid solution once it was re-quench cooled and reheated.

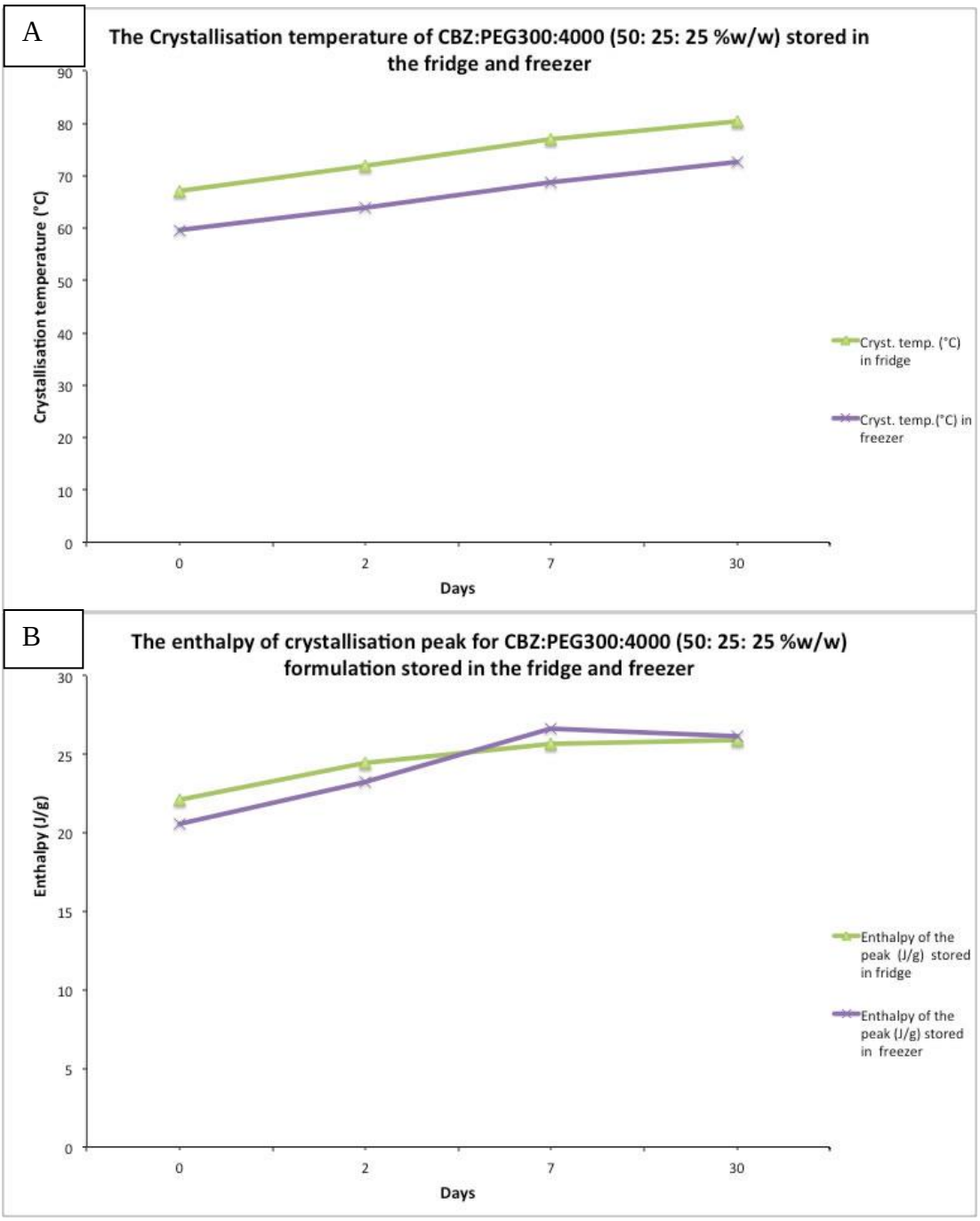

Figure 4.3-9 Crystallisation temperature (A) and enthalpy of peak (B) stored in the fridge and freezer

The above figure shows that the CBZ crystallisation temperature in the samples stored in the fridge and freezer increases with time, as well as the enthalpy of this

crystallisation. The crystallisation temperature of the sample stored in the fridge was higher than the one stored in the freezer by about 10°C whereas the enthalpies of both samples were very close to each other. This is due to the effect of the thermal history on the samples.

4.3.3.4 Hot stage microscopy

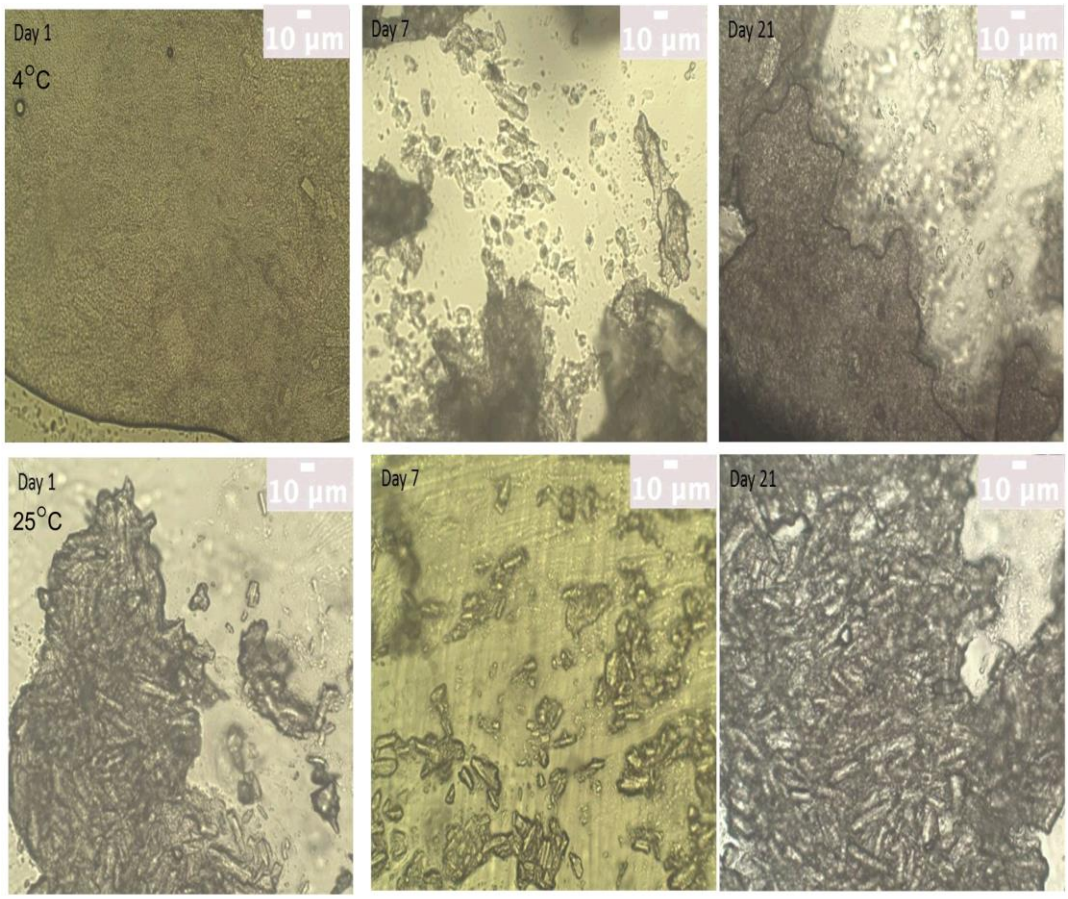

Figure 4.3-10 Hot stage microscopy for the stability sample at 25 and 4°C
The top 3 images are for the sample held at 4°C and the bottom 3 images are for the sample held at 25°C. The images were taken at 10x objective.

The microscopy results show that the sample held at 4°C at day 1 had a very fine and small crystals whereas the sample held at 25°C were much bigger and had rod shape. At day 7, in the 4°C the CBZ crystals can be seen trapped in the PEG mixture and in the 25°C the crystals stayed the same as day 1. In day 21, the sample held at 4°C

shows a few bigger crystals than before and the crystals in the sample held at 25°C stayed the same. From this experiment it was concluded that the sample held at 25°C crystallises within the first day and remains the same for the 21 days, whereas for the sample held at 4°C, the crystals were in a microcrystalline form, trapped in the PEG, but had grown in size by day 21.

4.3.3.5 Dissolution profile of stability samples at 4 and 25°C

The dissolution profiles of the stability samples were assessed on the Sirius T3 using a powder dissolution profile due to the sample was waxy and hard to press it into discs. The dissolution was carried out at 4 different pHs (30 minutes for each pH to mimic the release as the drug travel from the gut to the intestine) for 2 hours using GI buffer at pH2 as a dissolution media and the UV reading point was taken every 10 seconds.

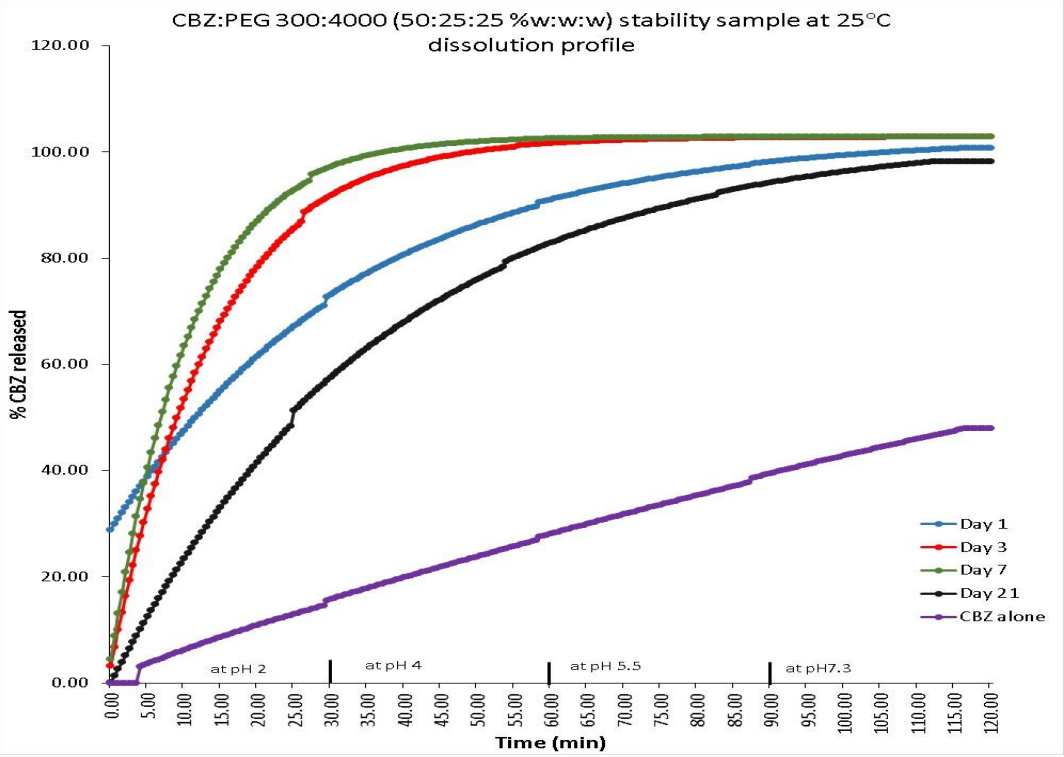

Figure 4.3-11 CBZ release profile from the quench cooled sample stored at 25°C

The dissolution profile of the sample stored at 25°C shows a better release than the drug alone. A drug release of 100% was measured for the sample at day 7 whereas day 21 showed the slowest this is due to the crystallisation in the sample during

storage. CBZ is not pH dependent therefore the change in pH will not affect the release. Day 7 did a 100% release in 30 minutes and the concentration did not change for the rest of the experiment.

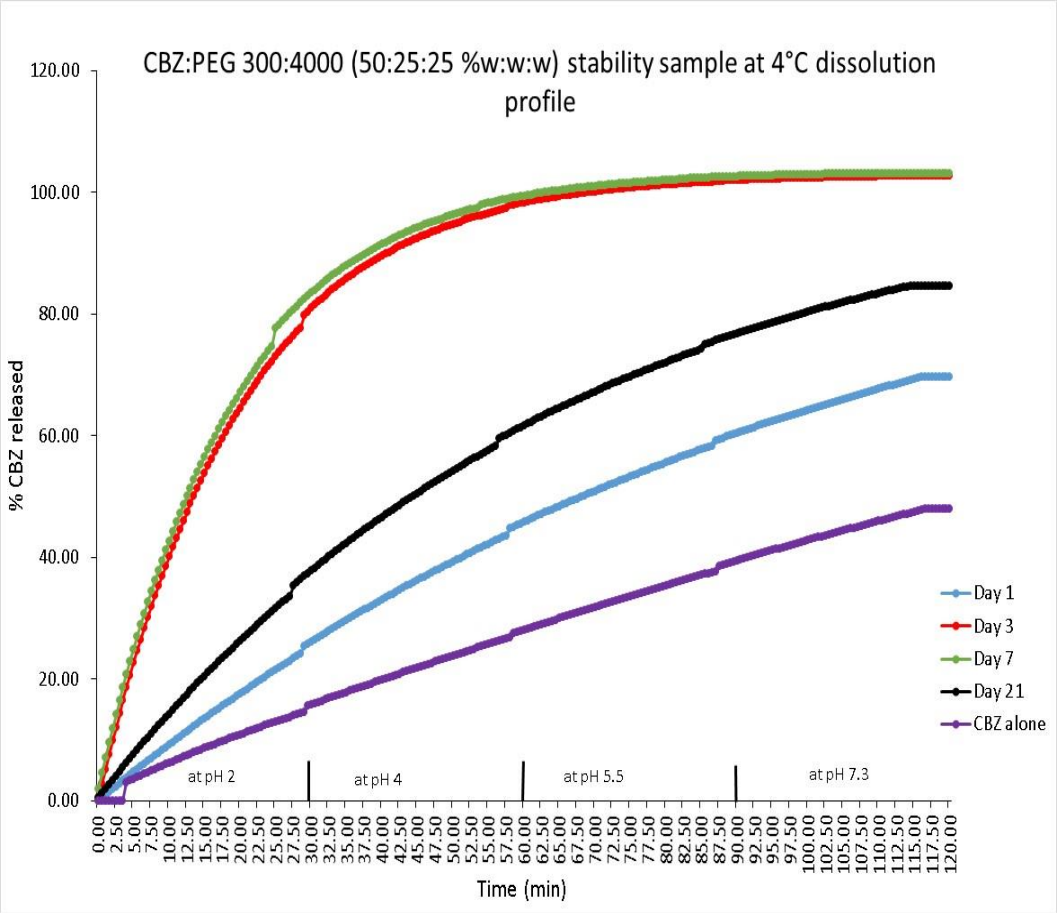

Figure 4.3-12 CBZ release profile from the quench cooled formulation stored at 4°C

The results for the mixture B stored at 4°C shows at the release was not hugely different than the drug alone for day 1 and day 21. Day 7 shows the higher release profile. The sample stored at 4°C did not show high release profile compared to the sample stored at 25°C this might be due to the processing of the sample, or that the dissolution is conducted at an elevated temperature with respect to the storage temperature which might affect the release.

4.3.3.6 XRPD Patterns

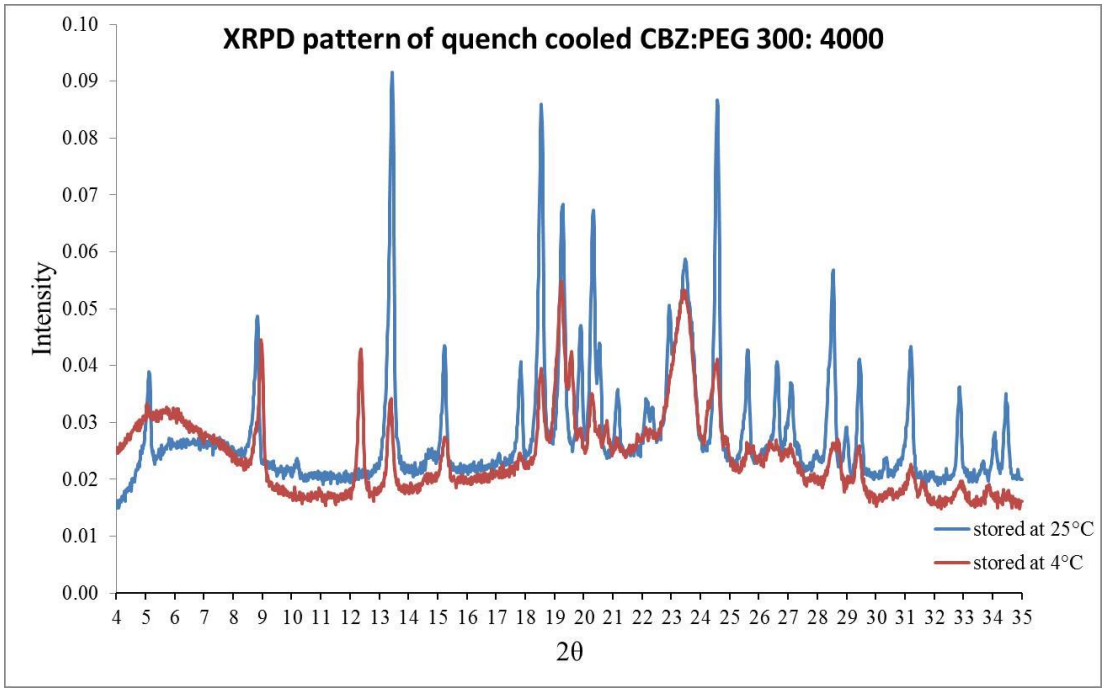

Figure 4.3-13 XRPD pattern of quench cooled CBZ: PEG 300:4000

(The figure above is for XRPD pattern of quench cooled CBZ: PEG 300:4000 (50:25:25 %w/w/w) formulation stored at 25 and 4°C for one day.)

The figure above shows that the formulation has some crystals had been formed when stored for one day at different temperature after quench cooling. The intensity from the sample stored at 25°C is higher than the one stored at 4°C which indicates that it contains more crystals. The CBZ exist as form II in the sample stored at 25°C whereas exist as form I in the sample stored at 4°C (refer to the XRPD pattern in Figure 4.1-3).

4.3.4 CBZ: PEG 300: high molecular weight PEG mixtures

From the DSC results of CBZ: PEG (300:4000) it was decided to repeat the experiment with higher PEG molecular weight mixed with PEG 300 to study the effect of higher molecular weight PEG in stabilising the solid solution. The same weight ratios were used. The PEG 300 was mixed higher PEG molecular weight (6000, 20000 and 35000). The formulations were prepared by melt method and analysed using the DSC quench-cooled method.

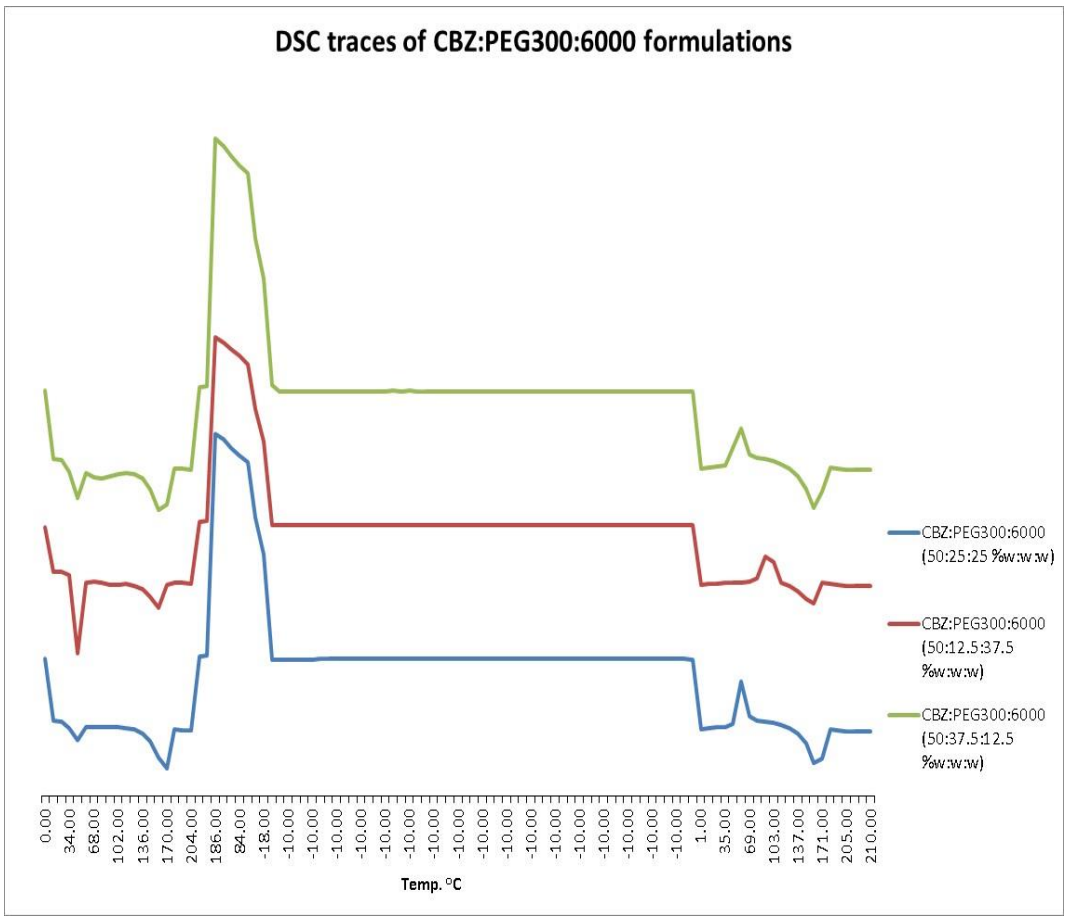

Figure 4.3-14 DSC traces of CBZ: PEG 300: PEG6000 formulations

An isothermal step at -10°C for 1 hour was added to the DSC method after the quench cooling step due to the crystallisation peak during the 2nd heating step having a very low enthalpy and could not be measured properly; this isothermal step was added to the DSC method for the formulations with PEG6000 and PEG35000.

The figure above (Figure 4.3-14) shows the DSC traces of CBZ: PEG 300:6000 formulations and the exothermic CBZ peak was observed in the three different formulations. The formulation containing more PEG 6000 than 300 showed a very high crystallisation temperature around 96°C whereas the other formulations had similar crystallisation temperature.

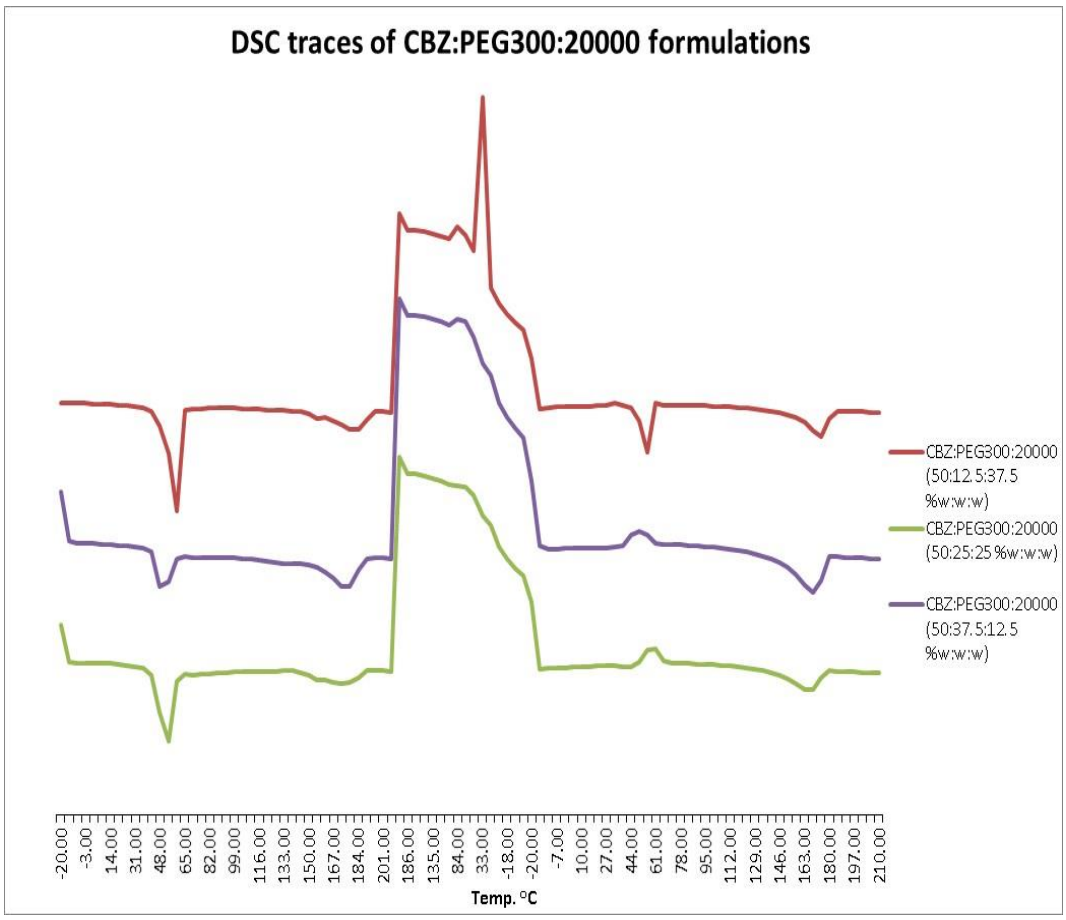

Figure 4.3-15 DSC traces of CBZ: PEG 300: PEG20000 formulations

For the formulations with PEG 20000, the results show that the CBZ and PEG in the formulation containing more PEG 20000 than PEG 300 did crystallise during cooling. The other formulations did show the CBZ crystallisation event during the 2nd heating step and the crystallisation peak temperature for the CBZ: PEG 300:20000 (50:25:25 %w/w/w) was 58°C which was 10°C higher than the other formulation such as CBZ: PEG 300:20000 (50:37.5:12.5 %w/w/w).

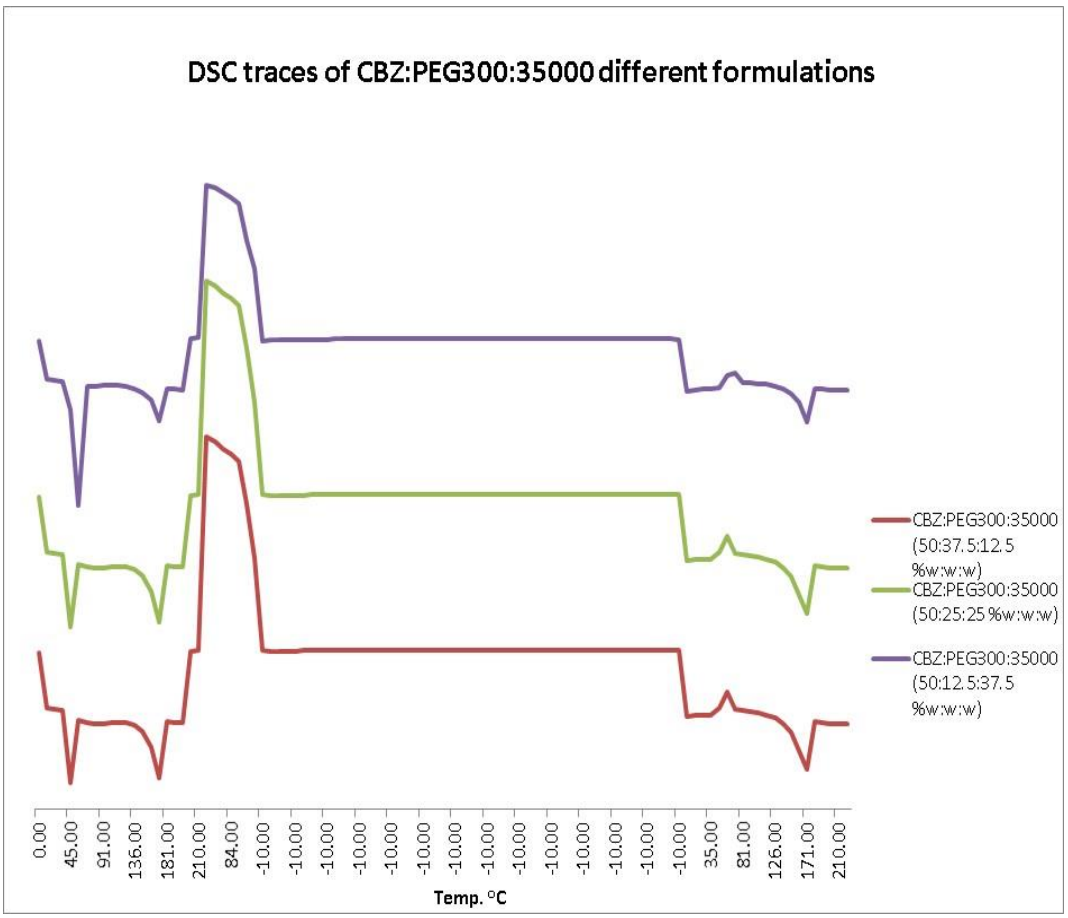

Figure 4.3-16 DSC traces of CBZ: PEG 300: PEG35000 formulations

For the formulations with PEG35000 the results were similar to the PEG 6000 where all the formulations did show the CBZ recrystallisation in the 2nd heating step. The results show that the formulation with high PEG 35000 content had the highest crystallisation peak temperature at 64°C followed by the CBZ: PEG 300:35000 (50:25:25) then (50:12.5:37.5) formulations.

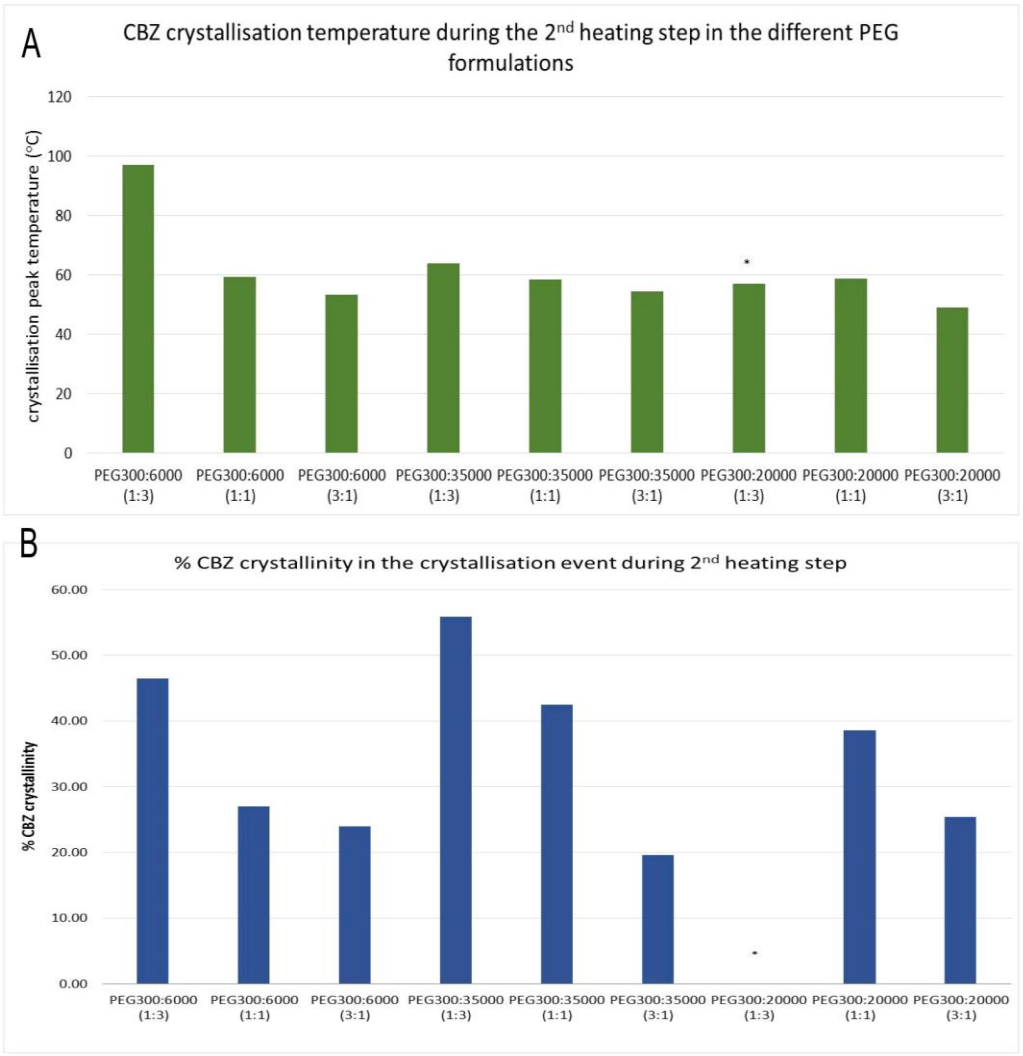

Figure 4.3-17 Comparison between the different CBZ: PEG mixtures formulations

The figure above summarise all the data from the three PEG mixtures used (n=1). The formulation with PEG 300:6000 (1:3) has the highest crystallisation temperature. Only one formulation did crystallise during cooling (PEG300:20000 1:3 based formulation). The enthalpies of these peaks were similar except for PEG 300:6000 (1:3) formulation where the enthalpy was the highest and in the formulation with PEG 300:35000 (3:1) was the lowest (comparison between the formulation which showed solid solution).

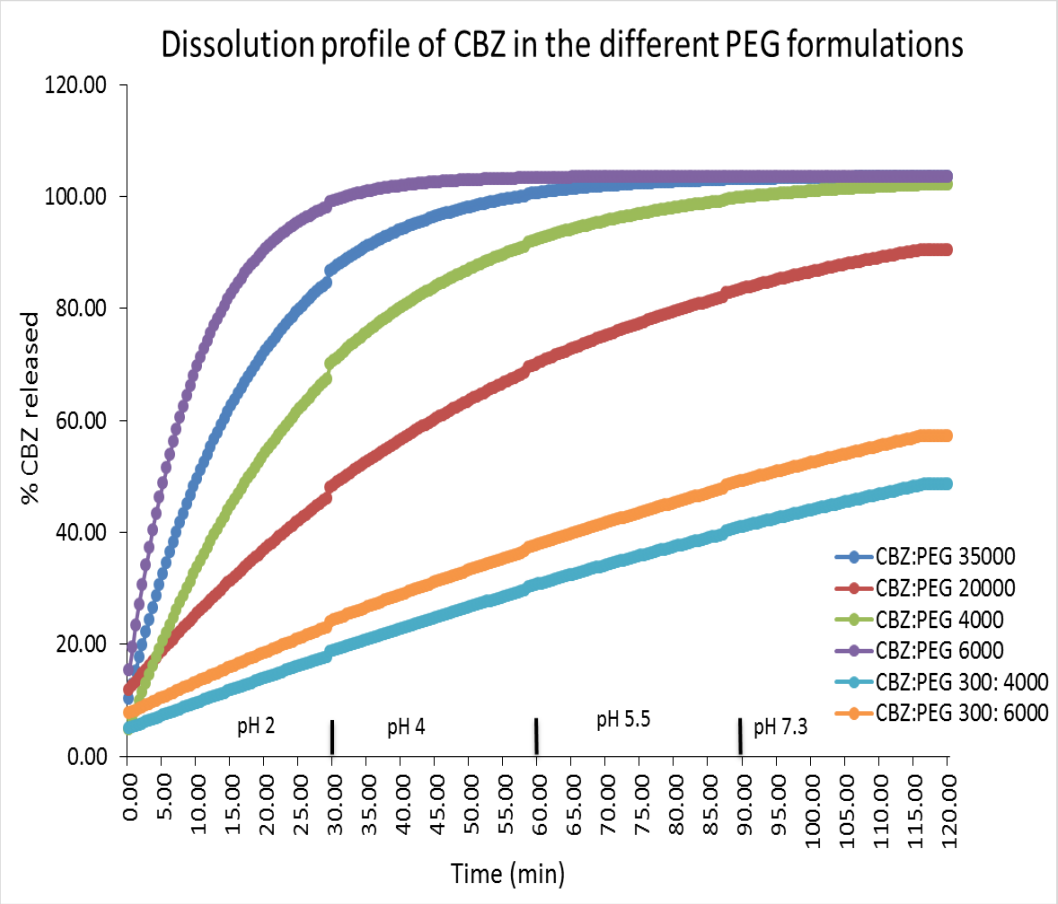

Figure 4.3-18 Dissolution profile of the different PEG based CBZ formulations

The figure above shows the different dissolution profiles of the CBZ formulation at CBZ: PEG (50:50% w/w). The result shows that the CBZ: PEG 6000 formulation has the highest and fastest release compared to the other formulations. Also, it shows that the formulation containing PEG300 mixture, the release was very slow and low compared with one PEG only.

4.4 Discussion

PEG 300 as discussed previously does not freeze or melt in the experiment parameters used in this project (refer to Figure 3.3-1). Therefore the melting and freezing peaks seen in the DSC traces are coming from the CBZ in the formulation and high molecular weight PEG. The CBZ crystals in the physical mixture with PEG 300 did show a broad endothermic peak during the first heating. This is due to the CBZ crystals dissolving in the hot PEG and converting to an amorphous or solution state during the heating cycle. This phenomenon was also seen when a CBZ solid dispersion prepared by hot melt extrusion was studied by Liu and colleague (Liu et al., 2013). The enthalpy of the peaks was similar in the three formulations (1:1, 1:5 and 1:10 %w/w) despite the decrease in the CBZ concentration in the 1:10 formulation. This may indicate that the underlying thermal event is independent of CBZ concentration, or that it is caused by a small amount of CBZ in the PEG, and so at higher CBZ concentrations no additional energy is released as the maximum solubility of CBZ in PEG 300 has been reached. The CBZ crystals in 1:5 and 1:10 %w/w formulation did not recrystallise during cooling which indicates that the CBZ is miscible with the PEG and they form an amorphous or solid solution after the heat-cool cycle (Liu et al., 2013). The hot stage microscopy results were in agreement with the DSC results where it was possible to visually follow the thermal changes happening. The CBZ crystals start to become smaller and smaller as the temperature increases which indicates that the crystals are dissolving in the hot PEG way before its melting temperature. During the second heating step, CBZ: PEG 300 (1:1%w/w) DSC trace shows an exothermic peak which correspond to the CBZ recrystallizing from the melt by forming a solid solution. This event was seen in the CBZ alone but not in a formulation with a polymer (Liu et al., 2013, Naima et al., 2001). In order to stabilise this formulation and to shift the recrystallisation temperature higher so the CBZ crystals in the formulation stays in amorphous form at room temperature for longer time, a higher PEG molecular weight was used with PEG 300 at different concentrations. PEG4000 was chosen as it has been used in solid dispersion formulation to enhance solubility and stability of low aqueous solubility API (Moneghini et al, 2001). Also, it was found that PEG 4000 upon co-solidification can affect the API behaviour in the final product (ie: API and polymer

fully amorphous, a combination of amorphous and crystalline region, only crystalline solid and eutectic mixtures Vasa et al., 2014). The solid solution was observed in the formulations when the CBZ content in the formulation is equal to the PEG mixture. The CBZ molecules in this formulation are in supersaturation state in the molten PEG and as the solution is heated the CBZ start to crystallise. The 1:5 and 1:10 w/w CBZ: PEG mixture did show a similar pattern as the CBZ: PEG 300 formulation where the CBZ crystals dissolves in PEG during the 1st heating cycle and stays in solution during cooling and reheating. The enthalpy of PEG mixture melting and freezing in the different formulations shows that when the enthalpy was normalised to the weight of PEG 4000 used the signal is the same in the different PEG mixture used (PEG 300: 4000 3:1, 1:1 and 1:3). The normalised PEG enthalpy of melting and freezing in the 1:5 and 1:10 w/w CBZ: PEG mixture showed similar values and pattern to the PEG mixture alone whereas the 1:1 w/w results were slightly different as the normalised enthalpies were lower than the PEG alone especially in mixture B (CBZ: PEG 300:4000 50:25:25 %w/w/w) which indicates that the CBZ at this ratio is interacting with the PEG. The cooling rate did have an impact on the formation of the solid solution this is due to quick cooling preventing the CBZ molecules from rearranging them self and crystallising during cooling (Einfalt et al., 2013). At slow cooling rate the CBZ molecules can rearrange and crystallise, besides at slow cooling rate there is more chance for iminostilbene (which is a form of CBZ impurity) to form a eutectic mixture with CBZ according to a study made by Naima et al., 2001 and this event can be seen in the DSC trace as a melting peak around 140°C. This event was not present in our study as the PEG used may prevent the CBZ from degrading at both cooling rates used. The stability study on the formulation which shows the solid solution was carried out on the DSC by holding the sample isothermally at different temperatures after quench cooling and the results shows that at high temperature (ie 30°C) the solution crystallises during the isothermal step this is due to the increase of the molecular mobility of the polymer, as at this temperature PEG 300 or 4000 will become more flexible which will affect the CBZ in the solution. The stability sample held in the fridge did show that the CBZ recrystallises during storage as the 1st heating step did show CBZ melting peak but at day 30 it did show that the sample was still amorphous as when

the sample was heated CBZ did recrystallise. The sample was held in a communal fridge where there was not a temperature controlled environment. When the sample was stored in the freezer, it did stay amorphous for up to 30 days where a broad (unresolved) melting peak was observed in the first heating cycle. The peak shows a sharp endothermic peak at around 40°C which may be the PEG melting followed by an exothermic peak which may be due to the CBZ recrystallising at 80°C. The melting peak at around 100°C may be due to melting of ice crystals (might have been formed on the lid of the pan). The hot stage microscopy results shows that the CBZ crystals stored at 25°C where larger than the ones stored at 4°C. The crystals at 4°C did not grow with time and they were very small whereas the crystals stored at 25°C did slightly grow with time. The dissolution results for both samples held at 4 and 25°C shows a better dissolution pattern than the CBZ alone. Day 1 release was lower than the other days where we expected the release to be higher as a greater percentage of CBZ in the formulation is in an amorphous state than the other days especially for the sample stored at 25°C where from the hot stage microscopy the crystals looked larger with time. The samples at day 3 and 7 stored at 25°C achieved a 100% release at a shorter time than the one stored at 4°C and the release at day 21 at both temperatures drop to 80% release. The PEG 4000 mixture with PEG 300 did show a better control in the solid solution formation than PEG 300 alone therefore it was decided to use a higher PEG molecular weight to study its effect on stabilising the CBZ solid solution. A 1:1w/w CBZ: PEG mixture was used as the solid solution was observed at this ratio with PEG 300: 4000. The CBZ solid solution was observed in almost all formulations except CBZ: PEG 300:20000 (50:12.5:37.5 w/w/w). The crystallisation temperature ranged between 58-65°C except for CBZ: PEG 300: 6000 (50: 12.5:37.5 w/w/w) which had a crystallisation temperature of 96°C but it did have a very high % crystallinity. The % crystallinity of CBZ was found to be around 25% for the formulations with high PEG 300 content and it increases as the solid PEG increases in the formulation, this can explained as the solid PEG are more crystalline than the liquid PEG which might induce the CBZ crystallisation also, PEG 300 was found from chapter 4 to decrease the crystallinity of the solid PEG when they are mixed. The lowest % crystallinity was observed in the CBZ: PEG 300:35000 (50:37.5:12.5% w/w/w) formulation and the crystallisation

temperature was around 58°C. The dissolution pattern for CBZ in the different PEG formulations was assessed and the results show that the highest and fastest dissolution rate was achieved with PEG 6000 alone followed by PEG 35000 formulations. It took 90 minutes to achieve a 100% CBZ release from PEG 4000 whereas the maximum release from PEG 20000 was 80%. The CBZ formulations with PEG mixture (ie PEG 300 mixture with PEG 4000 or 6000) showed a very slow release with maximum release of 40% CBZ which is similar to the release of CBZ alone and the release from the formulation containing PEG 6000 in the mixture was slightly better than the one with PEG 4000. The formulations containing PEG 300 should have less crystalline material than the higher molecular weight PEG alone as was discussed in chapter 4 but high molecular weight PEG alone did show better release and this is due to higher molecular weight PEG have a better solubilising effect than the low molecular weight one. The release from the PEG 6000 formulation was better than the PEG 4000 this due to the decrease in CBZ crystallinity content as from the XRPD data in the following chapters (7 and 8) shows that the formulations with PEG 6000 have less crystalline materials than the 4000 which may have helped in the dissolution.

Chapter 5 CBZ solid dispersions with different PEG molecular weights and concentration

5.1 Introduction

As was shown in the previous chapter, the CBZ recrystallisation from the solid solution during the 2nd heating step depends on the solid PEG concentration and also the PEG molecular weight, the cooling rate had a massive impact on the formation of the solid solution. It was decided to study the effect of PEG concentration and molecular weights on the CBZ recrystallisation from the melt when using one PEG molecular weight in the formulation.

5.2 Method

The different CBZ solid dispersions were prepared by solvent evaporation method (refer to 2.2.2.4). CBZ and PEG were weighed according to the different weight ratio (from 90:10 w/w to 10:90 w/w drug to polymer) and then mixed. The PEG used were PEG 300, PEG 3350, PEG 4000 and PEG 6000. The formulations were then assessed by DSC refer to 2.2.4.1.2.

5.3 Results

The peaks on the DSC trace were labelled as shown in the figure below to make it easier to discuss. In some formulations, during cooling no crystallisation events (labelled as peaks 3 and 4) were observed. It should be noted that the thermal events labelled as peak 5 may be related to PEG and/or CBZ re-crystallisation occurring at around 50˚C.

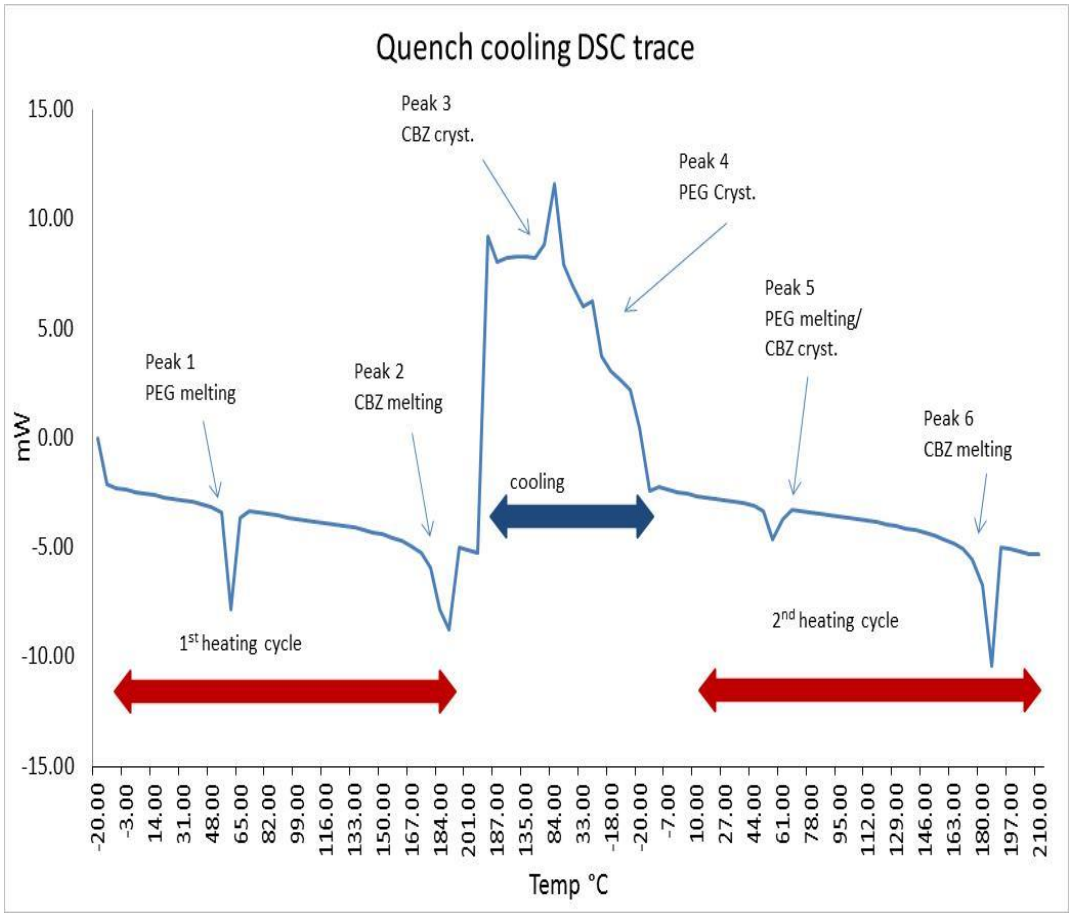

Figure 5.3-1 Quench cooled DSC trace

5.3.1 CBZ: PEG 300 formulations

PEG 300 is liquid at room temperature and did not freeze at low temperature (as discussed in previous section 3.4). Therefore, no melting peak for PEG 300 during the 1st heating step was observed with these formulations. The figure below shows some of the DSC traces of CBZ: PEG 300.

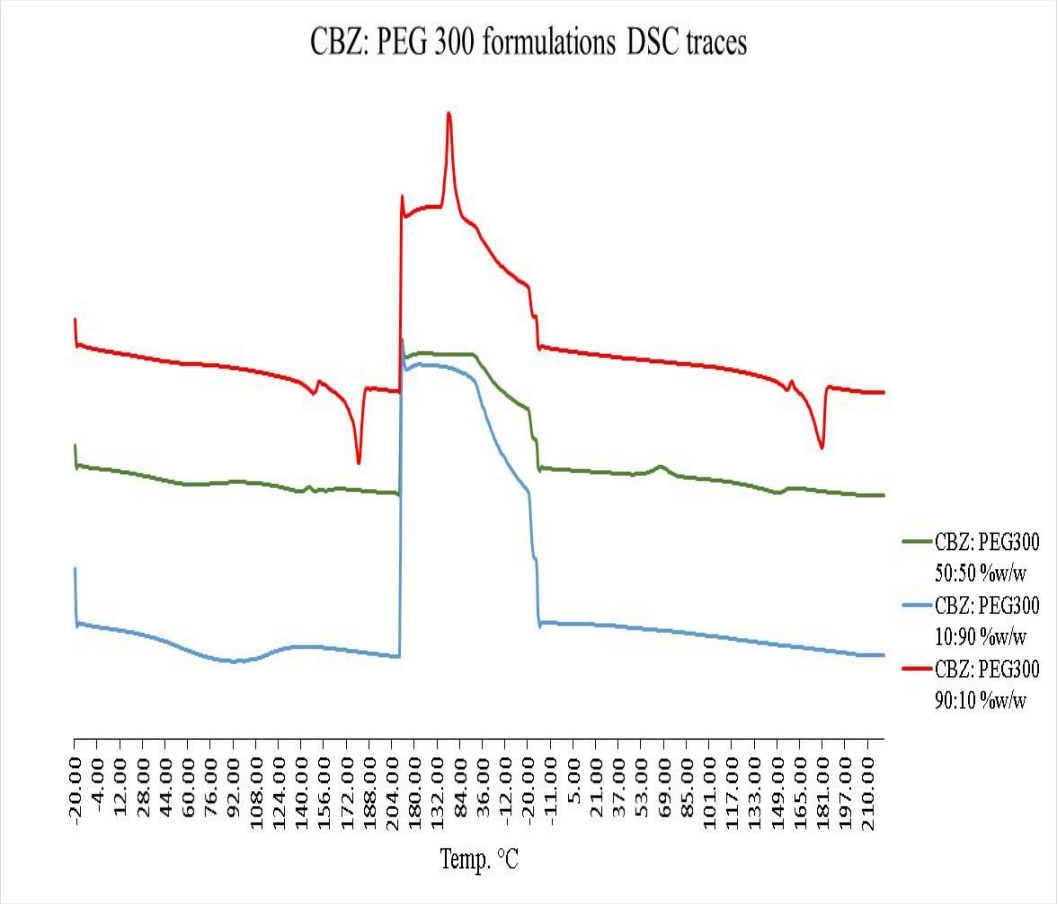

Figure 5.3-2 DSC traces for some of CBZ: PEG 300 formulations

(The figure above shows the DSC of three CBZ: PEG 300 formulations and it shows the effect of the PEG300 concentration on the thermal behavior of CBZ.)

Figure 5.3-3 summarises all the DSC data and shows the melting/ crystallisation temperature as well as the enthalpy associated with this thermal transition. In the formulations where PEG content was more than the CBZ, the first melting peak of CBZ (peak 2 in Figure 5.3-1) which is usually around 194°C disappears and replaced by a lower temperature broad peak due to the CBZ dissolving in the hot PEG. For some formulations such as 60:40 a portion of the CBZ dissolves in the PEG with the remainder melting at higher temperature and provides therefore two peaks. Formulations with high CBZ content did show recrystallisation during cooling and the formulations with low CBZ content did not show any crystallisation or melting during the 2nd heating step. The formulations which exhibited CBZ recrystallisation during 2nd heating were 70:30, 60:40, 50:50 and 40:60 (%w/w) CBZ: PEG 300. In

the formulation where CBZ recrystallised the melting point during the 2nd heating cycle was very close to the melting point during the 1st heating cycle.

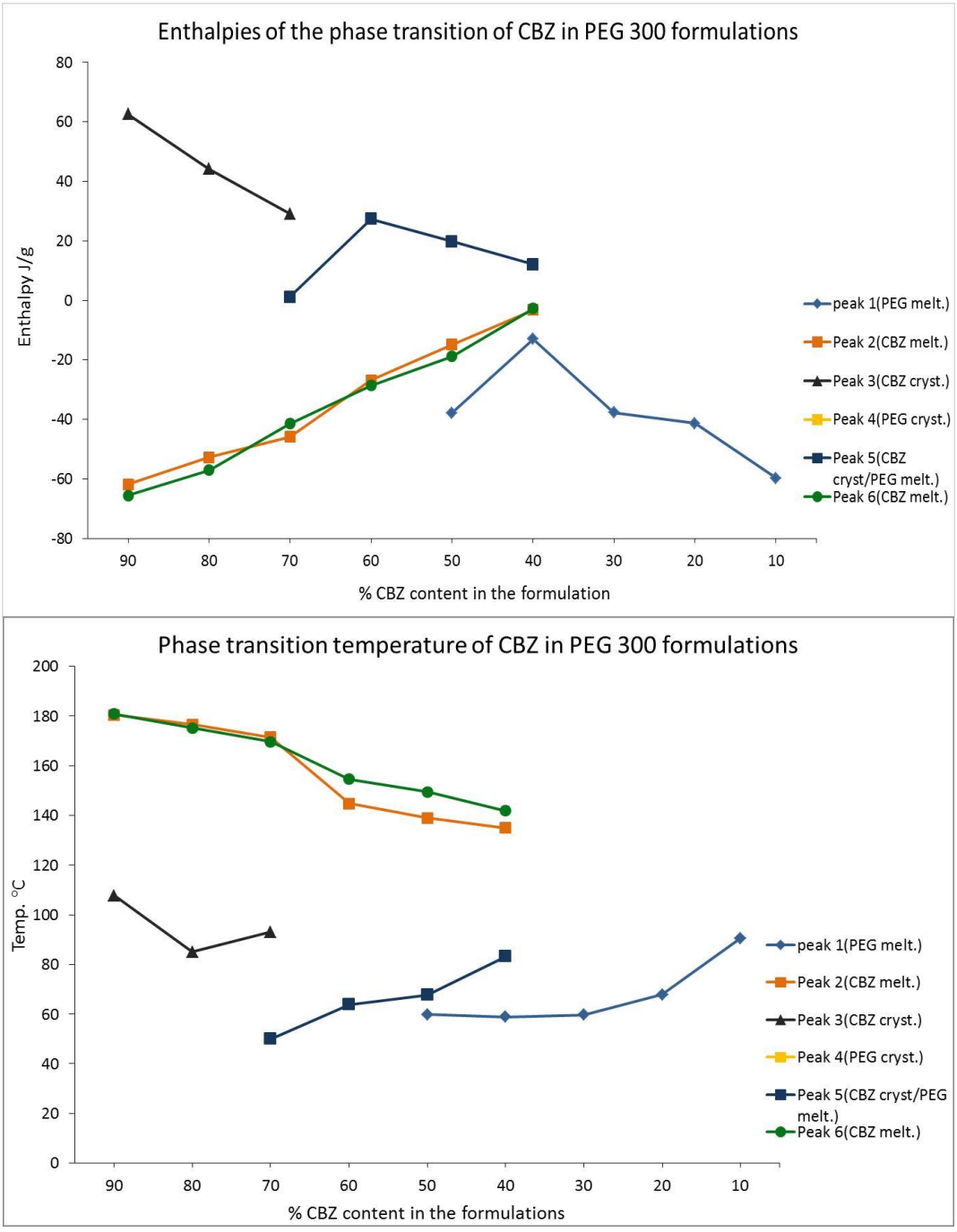

Figure 5.3-3 The melting/ freezing peaks and enthalpy of CBZ in PEG 300 formulations

(as PEG 300 is a liquid no melting and crystallisation peak as mentioned before therefore, Peak 4 has no data.)

Positive enthalpy value indicates crystallisation, negative enthalpy value indicates melting. PEG 300 does not have a melting peak and the melting peak 1 results are for CBZ dissolving in the hot PEG therefore, the enthalpy of melting is due to the CBZ. The enthalpy of CBZ melting peak in the 1st heating cycle matches with the enthalpy of CBZ in the 2nd heating cycle for the formulations where crystallisation was observed during cooling or 2nd heating step. The enthalpy of the CBZ recrystallisation (Peak 5) were also similar to the enthalpy of CBZ melting peak 6 except 70:30 formulation as some of the CBZ did crystallise during cooling. This can confirm that the crystals growing in peak 5 are CBZ crystals.

5.3.2 CBZ: PEG3350 formulations

The same experiment was repeated with PEG 3350. The figure below shows some of the DSC traces for the PEG 3350 formulations.

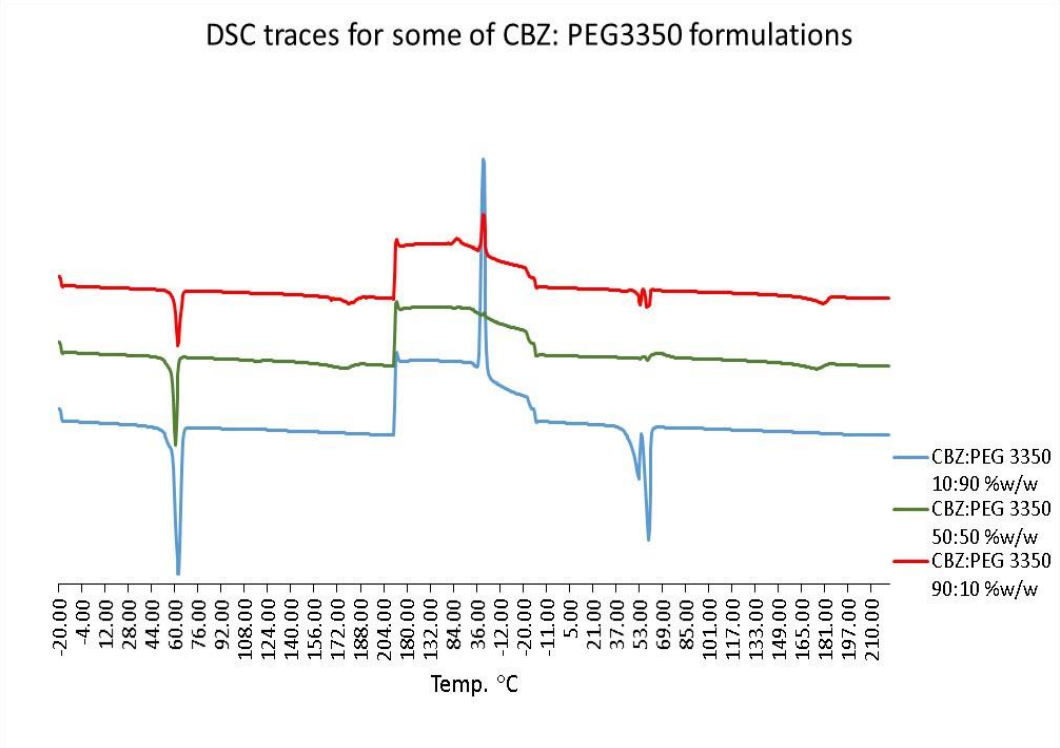

Figure 5.3-4 CBZ: PEG 3350 DSC traces

The DSC results show that the 50:50% w/w CBZ: PEG 3350 formulation did not crystallise during cooling, for the 90:10 % w/w CBZ: PEG 3350 formulation both PEG and CBZ melting and crystallisation peaks were observed. On the other hand, the 10:90 formulation did only show PEG melting and solidification peaks due to the low CBZ concentration where the CBZ crystals dissolves in hot PEG and the DSC cannot detect the signal as seen before or once the solid solution is formed the concentration of CBZ is too low for crystals to form.

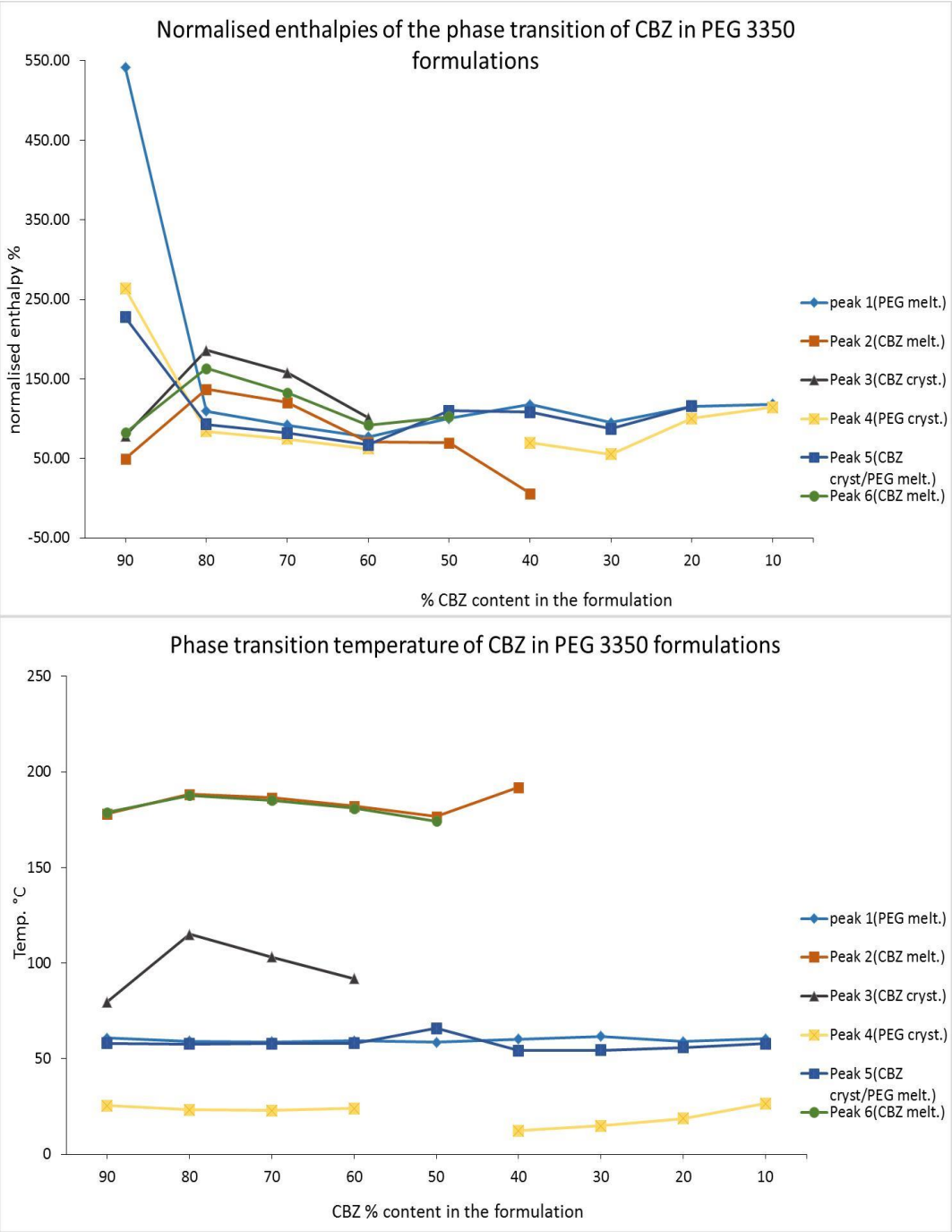

Figure 5.3-5 The melting/ crystallisation peaks of CBZ in PEG 3350 formulations (For the enthalpies in this section, normalised values were calculated based on CBZ or PEG alone depends on the peak)

The formulations with PEG 3350 did show similar behaviour to the PEG 300 formulations, as the PEG concentration increases in the formulation the CBZ melting point decreases. The PEG 3350 did show a melting and crystallisation peak even at

low concentration. At higher PEG ratio formulation, CBZ does not crystallise during cooling or 2nd heating step therefore, no melting peak was observed (20:80 and 10:90 (%w/w) CBZ: PEG 3350). From the graph above, only one sample did not crystallise during cooling and the drug remained in solution until the 2nd heating step, this sample was CBZ: PEG3350 50:50 (%w/w). The melting temperature of PEG and CBZ during the 1st and 2nd heating cycle were the same in all the formulations except for CBZ: PEG 3350 (50:50) peak 5 the temperature was slightly higher than the rest this due to the PEG did not crystallise during cooling and the CBZ crystallise at a slightly higher temperature than what it should be PEG melting.

The enthalpy of the CBZ melting during the 1st and the 2nd heating cycle were the same except for CBZ: PEG 3350 (50:50) was slightly higher during the 2nd heating step. The PEG melting enthalpy also has the same behaviour as the CBZ except for the 50:50 formulation where the enthalpy was higher than expected for PEG and this is due to the crystallisation of CBZ not the PEG melting as discussed before. The PEG enthalpies for crystallisation and melting were very close to each other in the formulations with high CBZ content but when the concentration of CBZ decreased to 40% or under, the melting PEG enthalpy increased due to some or all of the CBZ crystals dissolving in the molten PEG.

5.3.3 CBZ: PEG4000 formulations

The DSC traces for CBZ in PEG 4000 did show similar pattern as the previous PEG used.

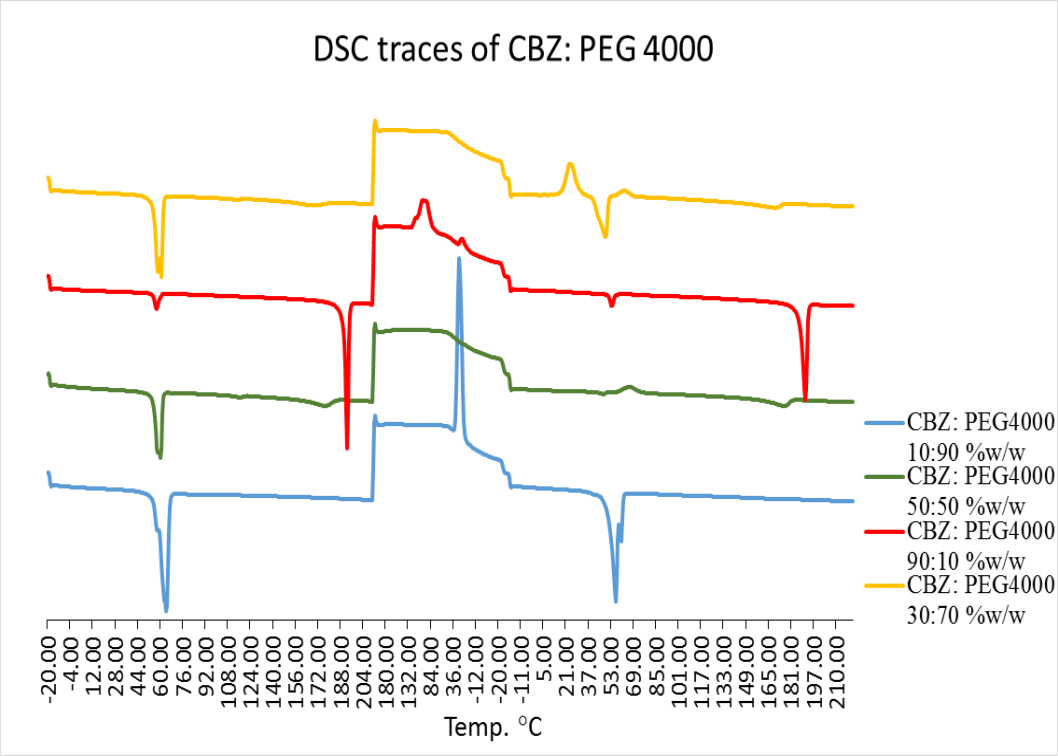

Figure 5.3-6 DSC traces for some of CBZ: PEG 4000

The DSC results show that the formulations containing CBZ: PEG4000 50:50, 40:60 and 30:70 did not show PEG or CBZ crystallisation during cooling and the drug crystals stayed in solution.

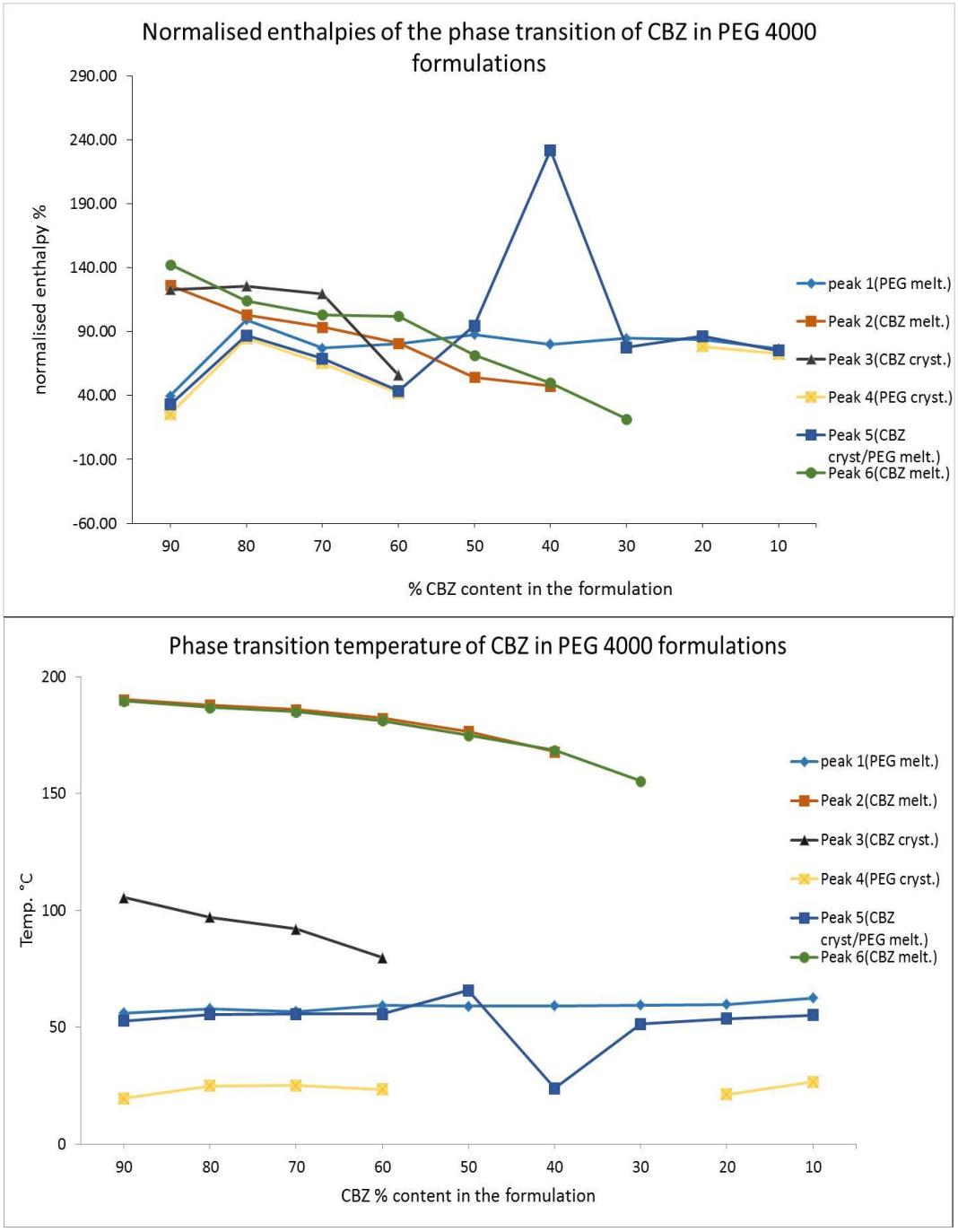

Figure 5.3-7 The melting/ crystallisation peaks and enthalpy of CBZ in PEG4000 formulations

The figure above shows that as the PEG concentration in the formulation increases the melting point of CBZ decreases, the melting point of PEG stayed roughly the same at all concentration. The CBZ crystallisation temperature also decreases with increasing PEG concentration the gap in peak 3 and 4 is due to no crystallisation during cooling at these ratios. For the three formulation where CBZ crystallisation

was observed during the 2nd heating step their crystallisation temperature did vary, the highest crystallisation temperature was for 50:50 (around 60°C) formulation followed by 30:70 (around 50°C) the 40:60 which was around 10°C.

For the enthalpies the melting points of CBZ did follow the same trend as the temperature, the only difference was that the melting enthalpies were slightly higher in the 2nd heating step than the 1st heating step. The enthalpy of CBZ: PEG 4000 (40:60) was higher than the 50:50 formulation or the 30:70, this may be due to the lower crystallization temperature of the CBZ: PEG4000 (40:60) formulation.

5.3.4 CBZ: PEG6000 formulation

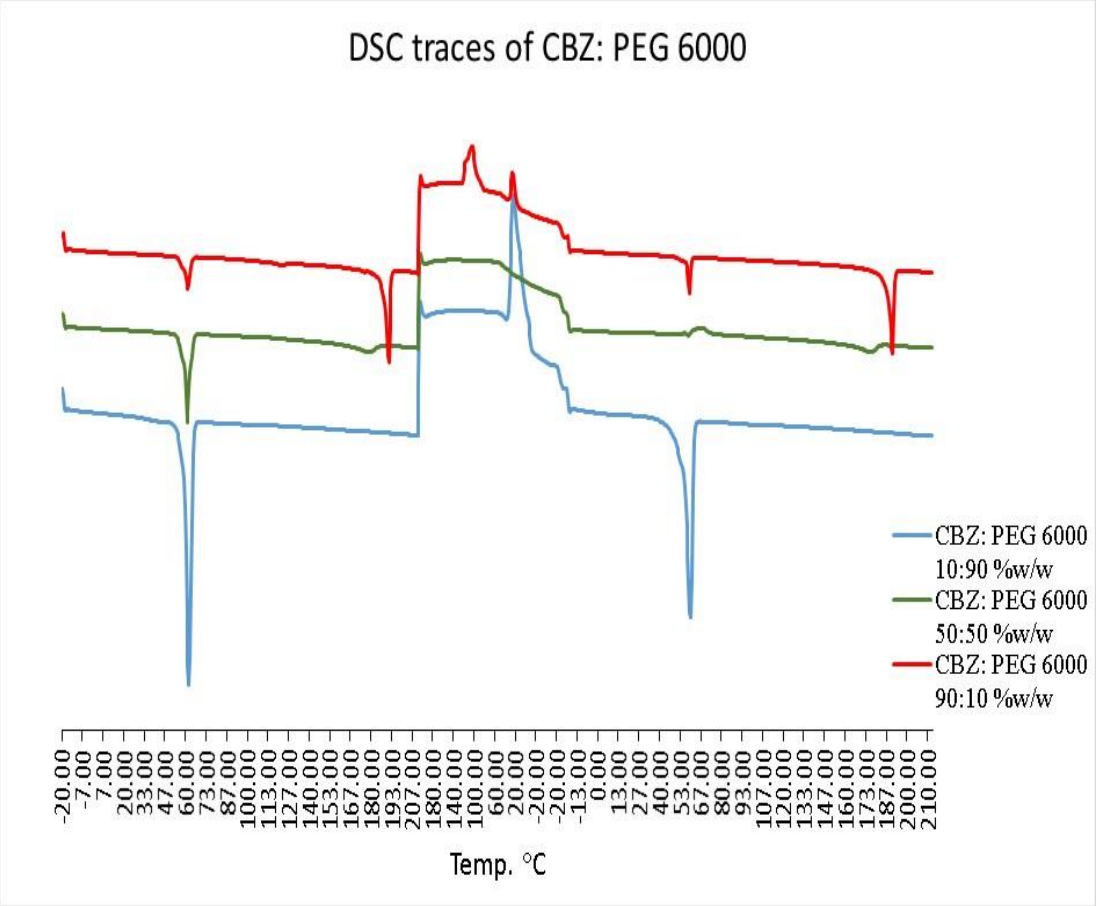

Figure 5.3-8 CBZ: PEG 6000 DSC traces

The DSC traces of the CBZ: PEG 6000 formulations shows that 60: 40, 50:50 and 40:60 formulations did show the CBZ recrystallisation during the 2nd heating step.

At higher PEG concentration (20:80 and 10:90), no CBZ melting and crystallisation peak observed due to the drug dissolving in the molten PEG and stay in solution.

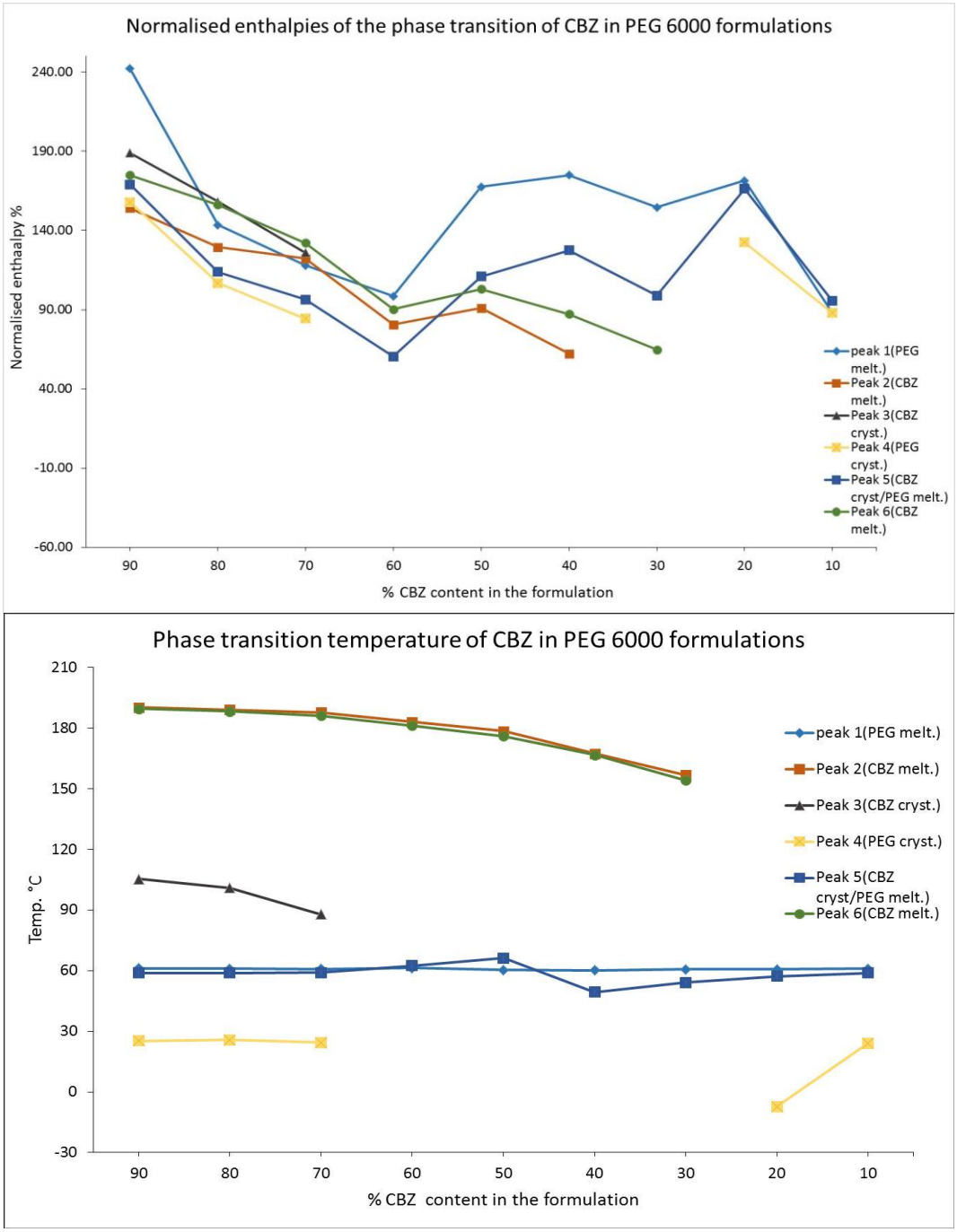

Figure 5.3-9 The melting/ crystallisation peaks of CBZ in PEG6000 formulations

The figure above shows all the results from the DSC and again the results are similar to the other PEG discussed earlier. The PEG melting points during the 1st heating step were very close to each other at all concentrations. For the CBZ melting similar

behaviour as before melting point decreases with decreases CBZ content in the formulation.

The enthalpies of CBZ in the formulations did follow the same trend as the other formulations prepared with other PEG. The PEG melting enthalpies during the 1stnd heating cycle was much higher than the 2nd heating step. The enthalpy of PEG melting decreases as PEG concentration increases until 60:40 formulation then increases again in both cycles. The enthalpy of the CBZ crystallisation during the 2nd heating step in the formulation 60:40, 50:50 and 40:60 was higher than the other formulations but still lower than the 1st heating cycle.

5.4 Discussion

In this chapter CBZ was formulated with multiple PEG molecular weights at different weight ratios then analysed on the DSC using quench cooling method. PEG 300 does not freeze or melt in our study therefore, the enthalpy of the different peaks cannot be normalised according to the weight ratio in the formulations and it was only done for the other PEG formulations.

The CBZ formulations with low molecular weight PEG (PEG 300) showed that at 70, 60, 50, and 40 % w of CBZ in the formulation, the crystallisation from melts will occur during the reheating step and the crystallisation peak temperature increases as the CBZ content decreases. For the formulations with solid PEGs, the formulations with 90, 80, 70 and 60 (except for PEG 6000) % w CBZ did recrystallise during the cooling step. At low CBZ content (30, 20 and 10%w CBZ) in the formulation, the CBZ melting peak (at the first heating cycle) is not observed due to the drug dissolving in PEG and does not come out of the solution during cooling and stays in amorphous state during 2nd heating step. This was also observed by Nair and colleagues where the endothermic peak of CBZ is not evident in the DSC trace (at 60% w CBZ in the formulation) due to the CBZ dissolving in PEG 4000 as the temperature increases (Nair et al., 2002). At higher CBZ content (90, 80 and 70% w/w), the amount of PEG is not sufficient to inhibit CBZ crystallisation from melts (Nair et al., 2002).

In order to stabilise a drug-polymer interaction, a strong hydrogen bond has to be formed between them and this bond will have an impact on the ability of the polymer

to prevent crystal growth from the supercooled liquid drug also, the amount of the polymer in the formulation plays a big role in stabilising this interaction (Trasi and Taylor, 2012). In our study, all the PEG molecular weights used cannot stabilise CBZ amorphous formulation at a percentage weight of PEG lower than 40 (except for PEG 6000). In the samples where CBZ crystallisation from melt occurs during reheating, the crystallisation temperature varied from 40-80°C, depending on the different PEG used and to the percentage of PEG in the formulations. The lower the crystallisation temperature especially for PEG 4000 and 6000, the higher the enthalpy was and this is due to CBZ nuclei quenched in the glass formulation during cooling and upon reheating they crystallise. The formulation having a large number of nuclei will have a lower recrystallisation temperature according to Trasi and Taylor (Trasi and Taylor, 2012) the large number of nuclei will affect the enthalpy hence the increase in enthalpy compared to the other formulations.

In conclusion, at a higher PEG content in the formulation (70% and above), CBZ stays in amorphous form after quench cooling in all molecular weights used. At lower PEG content in the formulation (30% and below), CBZ recrystallises during cooling as PEG cannot inhibit the crystallisation at these formulations. The recrystallisation from melt occurs between 60 to 40% CBZ in the formulation, there is a slight variation in the crystallisation temperature and enthalpy of this crystallisation event using the different PEG molecular weights.

Chapter 6 The effect of the addition of Poloxamer on CBZ: PEG formulations

6.1 Introduction

Poloxamers are synthetic tri-block of copolymers that are known in the market as Pluronics. The polymer based on a hydrophobic centre chain of polypropylene oxide (PPO) and two hydrophilic end chains of polyethylene oxide (PEO)(refer to Figure 6.1-1). Poloxamers have a wide molecular weight range, which can be achieved by varying the PEO or PPO chain lengths. Poloxamer F68 (also known as Poloxamer 188) has 80 PEO chains to 27 PPO chains with an average molecular weight of 8595g/mol.

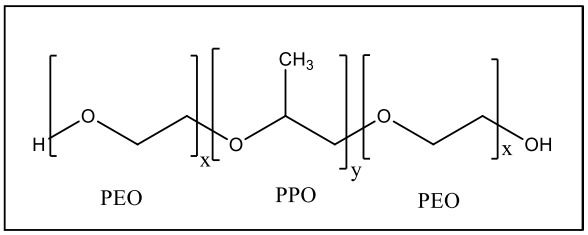

Figure 6.1-1 Poloxamer structure

Poloxamers were used in the pharmaceutical industry as surfactants, wetting agents, dispersants, solubilizing agent and emulsifiers (Patel et al., 2009). The most commonly used Poloxamers in the pharmaceutical industry are P123, P105, L61, L121, F87, F68, and F127 (Pitto-Barry et al., 2014).

Table 6.1-1 Melting Points of the different Poloxamers used in the project

Poloxamer	Appearance	PEO: PPO	Average MW g/mol	Melting Point (°C)
P103	Paste	34: 60	4950	30
P123	Paste	40: 70	5750	31
F68	Solid	80: 27	8595	52
F127	Solid	200: 65	12220	56

Poloxamers were used to enhance the solubility of poorly aqueous soluble drug using solid dispersion method. In a study, Bicalutamide was formulated with F68 at 1:1, 1:3 and 1:5 weight ratios using melt method, the results shows increase in the dissolution rate compared to pure drug. The 1:1 formulation was best performing formulation compared to the formulations with high F68 content. This might be due to the gelling effect of high Poloxamer content in the formulation. (Sancheti et al., 2008) Another study shows that F127 with Quercetin (antioxidant) solid dispersion prepared using evaporation precipitation of nanosuspension method enhances the dissolution of Quercetin. Also, the formulation at 1:1 ratio shows a broad peak in the DSC curve, which indicates that the formulation was amorphous (Kakran et al., 2011). Fenofibrate was formulated with F127 using fusion method in a study made by Karolewicz and colleagues. The study shows, that 16.5% w/w of fenofibrate was needed to form eutectic mixture with F127. Also, the result show enhanced dissolution rate (Karolewicz et al., 2015). Poloxamers was also used to slow the crystallisation growth rate and to inhibit precipitation. In a study, made by Vetter and colleagues show that the addition of F127 to Ibuprofen in ethanol/water mixture, slow the crystal growth rate. The higher the Poloxamer concentration in the mixture, the slower the crystal growth rate is (Vetter et al., 2011).

In another study, made by Guzman and colleagues shows the effect of different excipients on Celecoxib precipitation inhibition. The results show, that F127

inhibits precipitation less than 60 minutes whereas, P103 and P123 inhibit precipitation for longer than 60 minutes. (Guzman et al., 2007)
In this project, Poloxamer F127, P123, P103 and F68 were used to study their effects on stabilising the CBZ recrystallisation event that happens after quench-cooling and to study their effects on the aqueous dissolution of CBZ in PEG formulations.

6.2 Method

6.2.1 Formulation preparation

Formulations of CBZ: PEG: Poloxamer were prepared at 50:40:10 %w/w ratio using the melt method. The PEG used in this chapter was PEG 300:4000 mixture and PEG 6000, where the solid solution was observed. The polymers were weighed in a glass vial and heated on a hot plate until the mixture melts at around 50°C. Then the CBZ was added and mixed thoroughly. The formulations were left to cool in a desiccator. The formulations were studied in the DSC (normal cool and quench cooled method were used), hot stage microscope and Sirius T3 for dissolution (2.2.6 and 2.2.8).

6.2.2 Stability study

The stability of the different formulations at different temperatures (0, 10 and 20°C) was studied using the DSC. The samples were placed in the DSC pan and heated to 210°C at 10°C/min then quench-cooled to -20°C at 30°C/min cooling rate. The pan then reheated to the required temperature and held at this temperature for 1 hour before the temperature was increased again to 210°C at 10°C/min.

6.3 Results

6.3.1 DSC and hot stage microscopy results of the different formulations

The Poloxamers used in this experiment have a low melting point. For the P group the melting points was between 30-32°C and for the F group was between 52-56°C (refer to Table 6.1-1). The melting point of the F group Poloxamer is close to the

melting point of the PEG 300: 4000 (50:50 %w/w) mixture which is around 50°C (refer to Figure 6.3-1) and the melting point of PEG6000 was 65°C **Table 3.3-2**). The freezing point of F127 (37°C) was higher than the PEG 300:4000 (30°C).

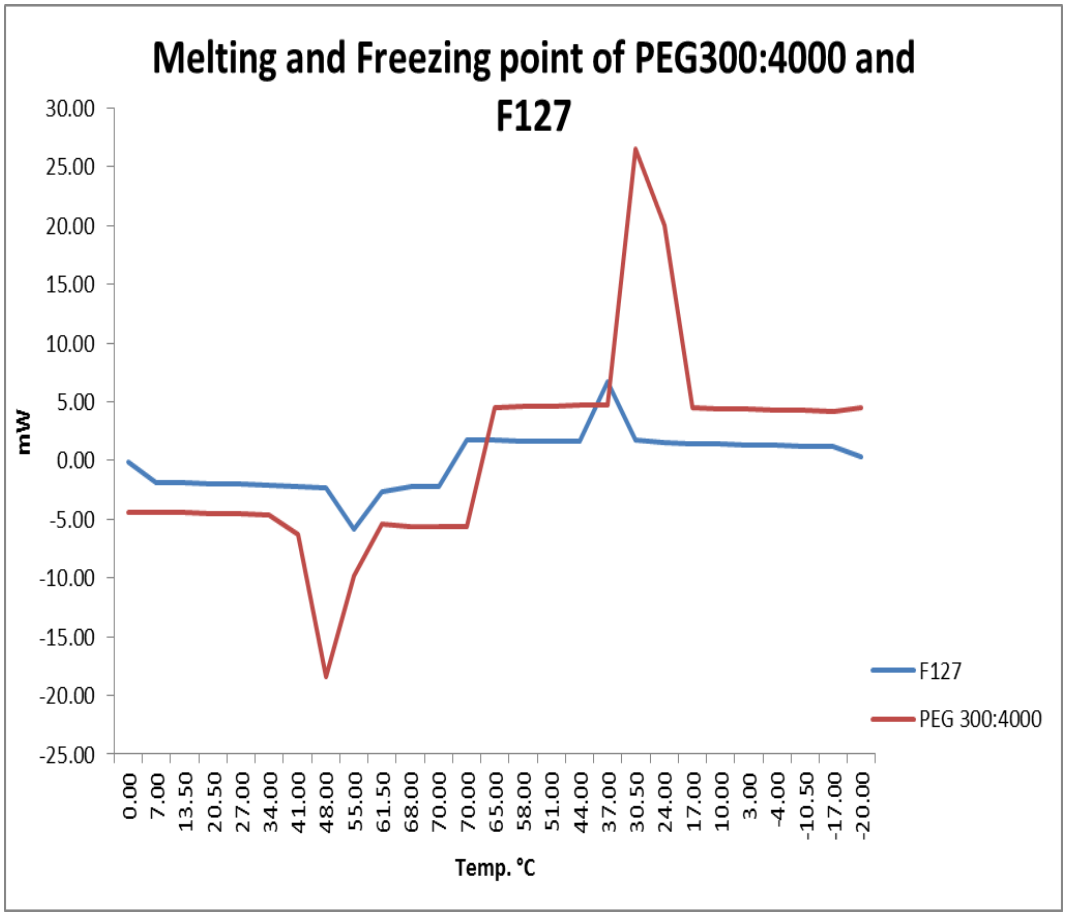

Figure 6.3-1 Melting and freezing point of PEG 300:4000 mixture and F127

The effect of the Poloxamer F127 on the melting / freezing of the PEG blend is shown in the figure and the table below (Figure 6.3-2 and **Table 6.3-1**). One endothermic peak was observed in the DSC curve, which indicates that the Poloxamer and PEG form one phase when they melt, the melting point of PEG blend stayed the same around 50°C. The freezing point of PEG 300: 4000 at 50:50 (%w/w) was around 30°C; the addition of F127 did not change the freezing point of the PEG blend even at high F127 concentration.

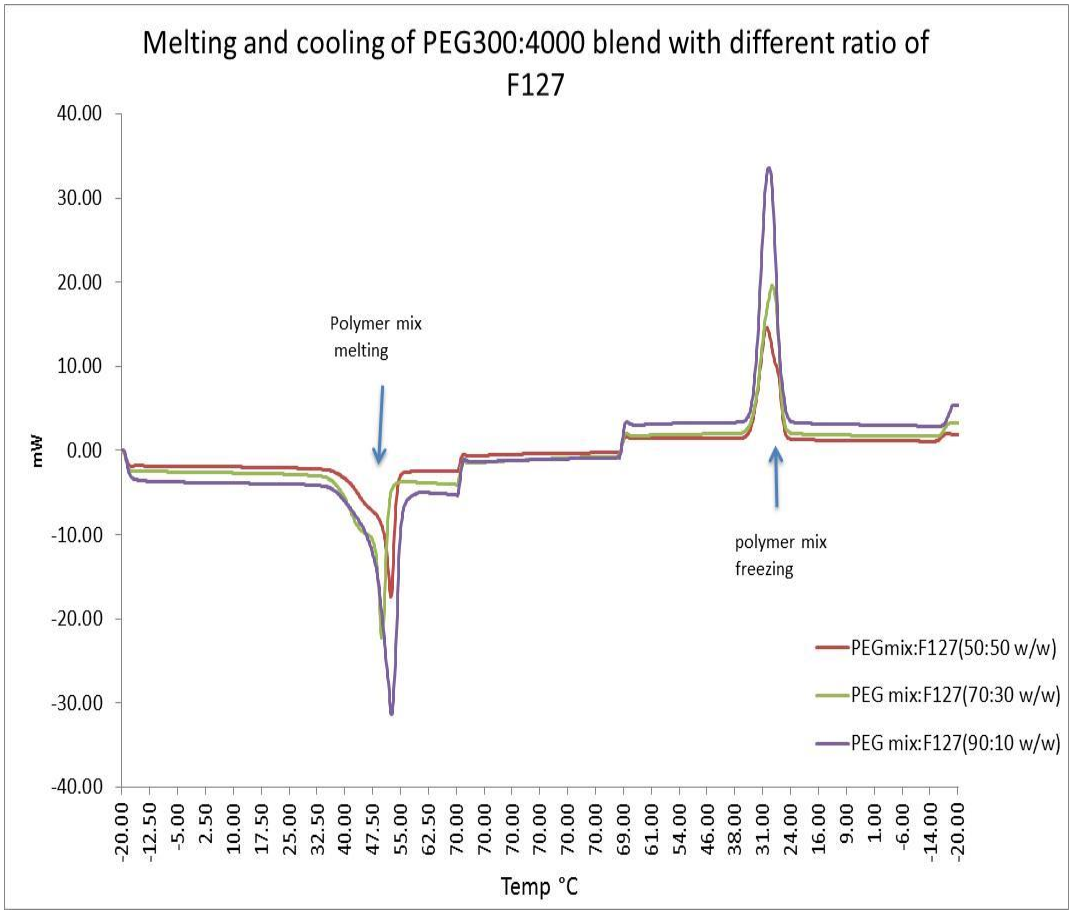

Figure 6.3-2 The effect of F127 concentration on PEG 300: 4000 blend on melting and cooling point

The figure above shows the heating- cooling DSC traces of PEG 300:4000 mixture (50:50 %w/w) blended with F127 at different concentration. The table below shows the melting and freezing point of these formulations.

Table 6.3-1 Melting and freezing point of PEG blend with the different concentration of F127

PEG 300: 4000: F127 (%w/w/w)	Melting point °C	Freezing point °C
45:45:10	51	30
35:35:30	50	29
25:25:50	52	31

The DSC results for the different CBZ formulations shows one melting peak was seen for the formulation containing F127 and F68 Poloxamer at around 50°C with PEG 300:4000 mixture and 60°C with PEG 6000. A small endothermic peak was observed between 20-30°C for the Poloxamer P103 and P123. Altering the cooling rate in the DSC experiments showed a difference in the thermal events associated with crystallisation. In the normal cooling rate at 10°C/min, two peaks appeared during cooling. One starts at around 85°C correspond to CBZ crystallising, and the other peak around 20°C, correspond to the PEG/Poloxamer freezing. (Refer to Figure 6.3-3)

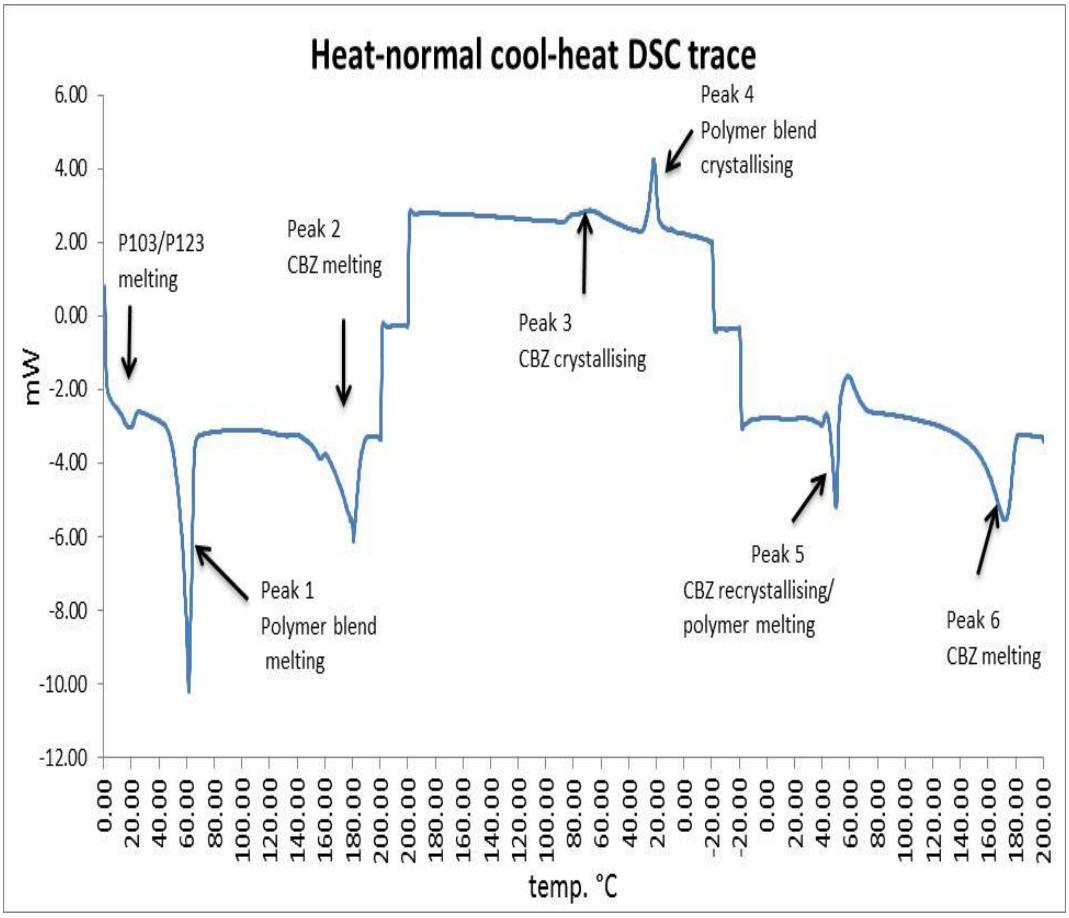

Figure 6.3-3 Heat-normal cool-heat DSC curve

The figure above shows the typical characteristics of a DSC curve of the formulations used. The different CBZ formulations DSC curves aligned with hot stage microscopy figures are discussed later in this section.

For the quench cooled samples, no CBZ crystallisation was seen in some of the samples studied (such as in CBZ: PEG 300: 4000:P103). Some samples show one peak at polymer blend crystallising temperature (such as in CBZ: PEG 300: 4000: F68 formulation) and other samples two peaks were observed one for the CBZ and one for the polymer (refer to Figure 6.3-4).

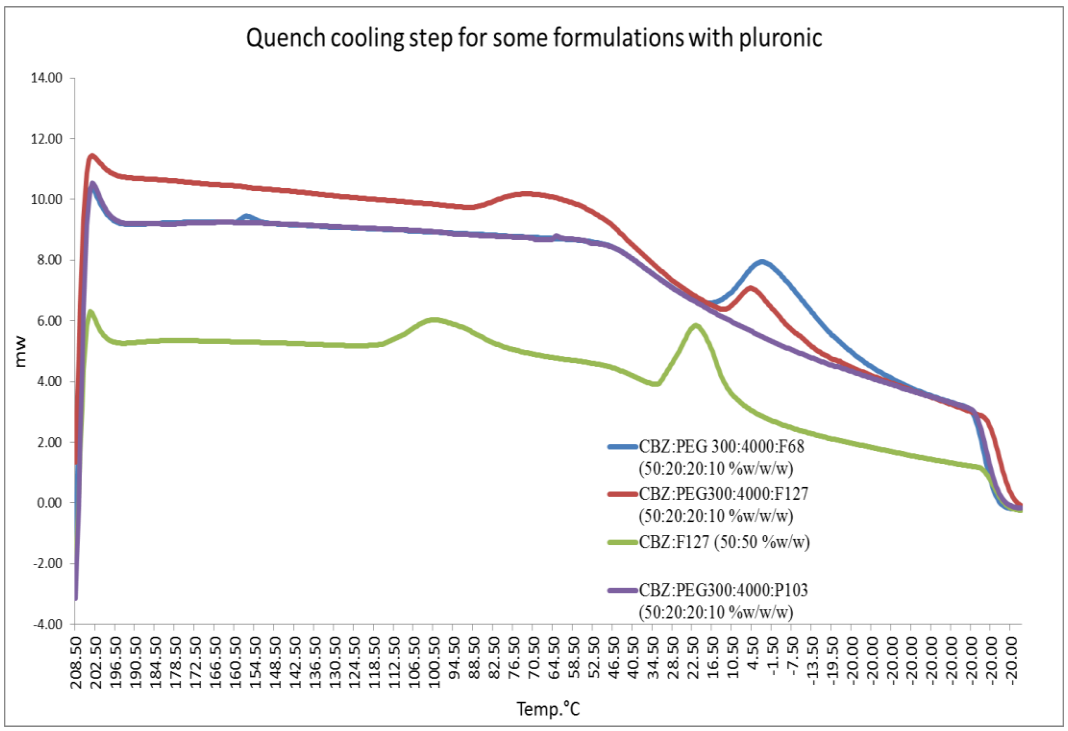

Figure 6.3-4 Quench cooling step for CBZ: PEG 300: 4000: Poloxamer

In some samples where no CBZ crystallisation was observed or a very small exothermic peak was seen during cooling, a peak of polymer melting at 50°C followed at the same temperature by an exothermic peak which is for CBZ crystallisation during the second heating step. Some of the formulations were studied under hot stage microscopy using the same method as the DSC method. The results are shown in the sections below from 6.3.2 to 6.3.4. The data for one formulation is divided into three parts:

Part 1: 1st heating cycle

Part 2: normal cool and 2nd heating cycle

Part 3: quench cool and 2nd heating cycle

The numbers on the figures below corresponds to the hot stage microscopy images aligned with the DSC trace to show exactly the temperature where the event or the images are taking place.

CBZ: F127 was formulated to study the effect of F127 alone on the CBZ crystal behaviour with the heat-cool-heat cycle.

6.3.2 CBZ: F127 (50:50)

6.3.2.1 Part 1: 1st heating cycle

The first heating cycle shows two main peaks: Peak 1 and Peak 2 from Figure 6.3-3. The numbers on the DSC curves are aligned with the microscope images below.

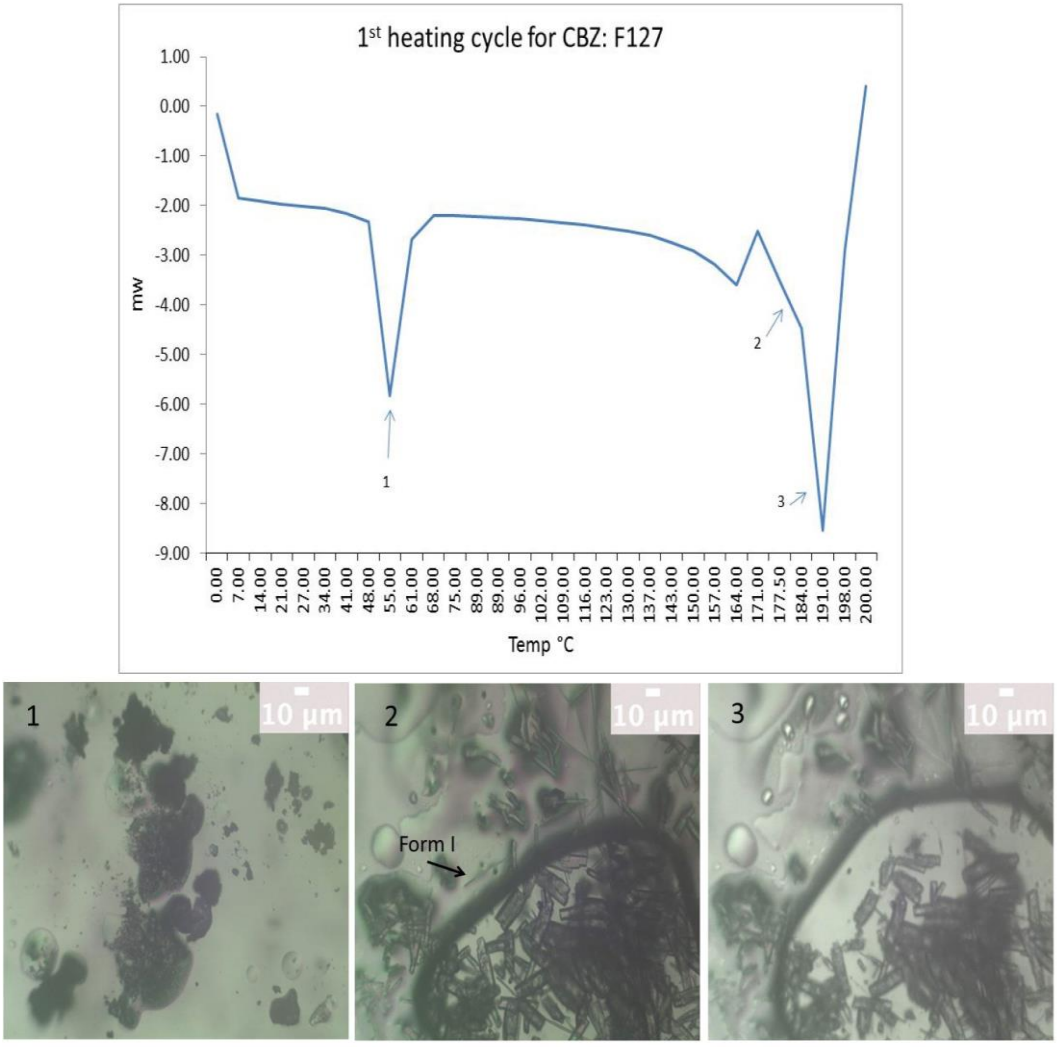

Figure 6.3-5 CBZ: F127 1st heating cycle DSC curve

(Image 1 was taken at 50°C, where F127 in the formulation starts to melt and the CBZ crystals appears to have a rock round shape within the formulation. At 150°C, the drug crystals start to change form from rock shape (form III) to the needle shape (form I). Image 2 was taken at 180°C, where all the crystals have changed form. Image 3 was taken at 187°C, where the CBZ crystals are melting and around 195°C all the CBZ crystals will be in solution.)

The DSC curve of the 1st heating cycle shows three thermal events: melting of the Poloxamer F127 followed by a change of crystal form from CBZ form III to form I then melting of CBZ form I. CBZ has previously shown this pattern in section 4.1.1.

6.3.2.2 Part 2: normal cooling and the 2nd heating step

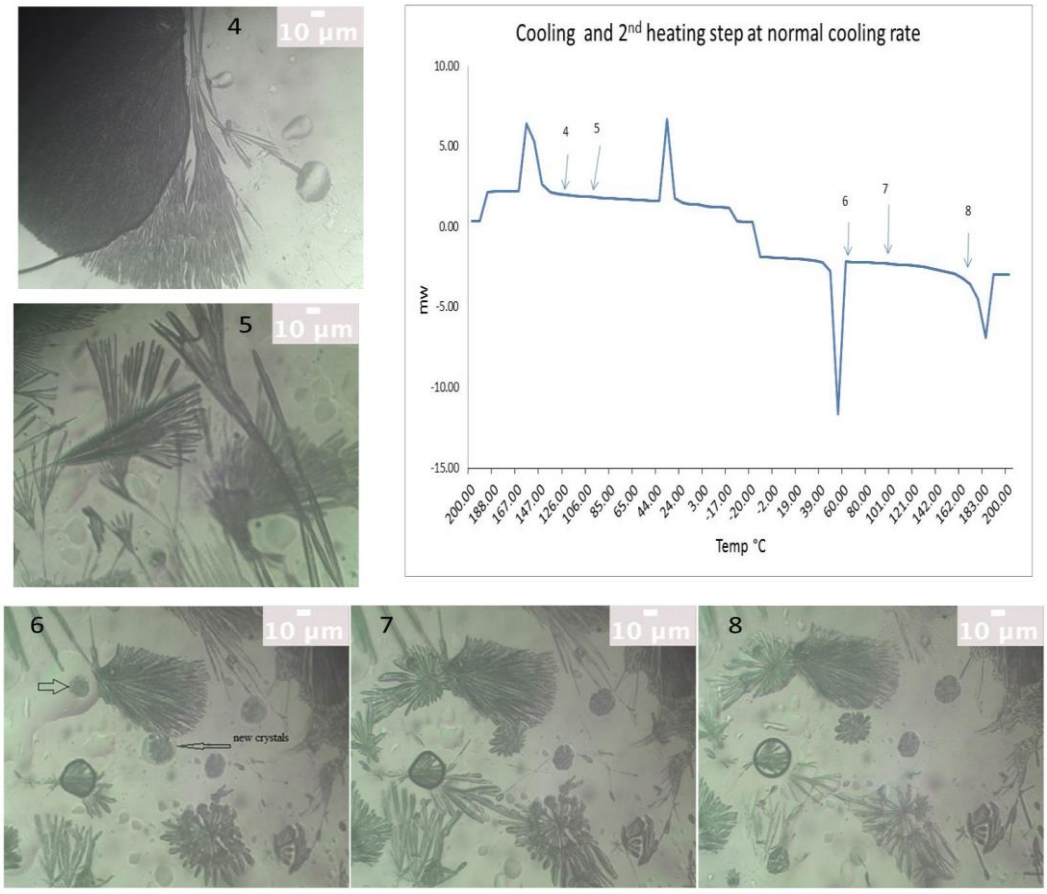

Figure 6.3-6 Normal cooling and 2nd heating step of CBZ: F127

(During the cooling step at 10°C/min, CBZ crystals start to appear at 130°C. The crystals have a very fine; needle shaped as shown in image 4 and then the crystalisation stops at 125°C. As the sample continues to cool new CBZ crystals start to grow at 115°C. Image 5 was taken at 100°C where the newly grown CBZ crystals has a long needle shape which starts from a trapped nucleus and then the CBZ growth stopped. On the reheating cycle, at 60°C, the F127 melts again, and a small CBZ crystals start to grow as shown in image 6. At 100°C, the CBZ crystal

growth stopped (image 7). Picture 8 was taken at 170°C, where the CBZ crystals start to melts.)

During the normal cool rate, two peaks were observed in the DSC curve: one at around 165°C, which is for CBZ crystallisation (Peak 3 in Figure 6.3-3) followed by another peak at 35°C (Peak 4) which corresponds to the F127 crystallising. During the 2nd heating step, two endothermic peaks can be seen which corresponds for F127 and CBZ melting.

The hot stage microscopy data for CBZ: F127 (normal cooled) were slightly different than the DSC data. The crystallisation of CBZ on the hot stage started around 130°C instead of 165°C (on the DSC). Also in the 2nd heating cycle a small crystal growth at 60°C was observed under the microscope was not seen in the DSC curve, which might be due to the F127 melting and the CBZ crystallising at the same time and the enthalpy of F 127 melting was higher than the enthalpy of CBZ crystallising, therefore, the DSC trace did not show this event.

6.3.2.3 Part 3: quench coolling and 2nd heating step

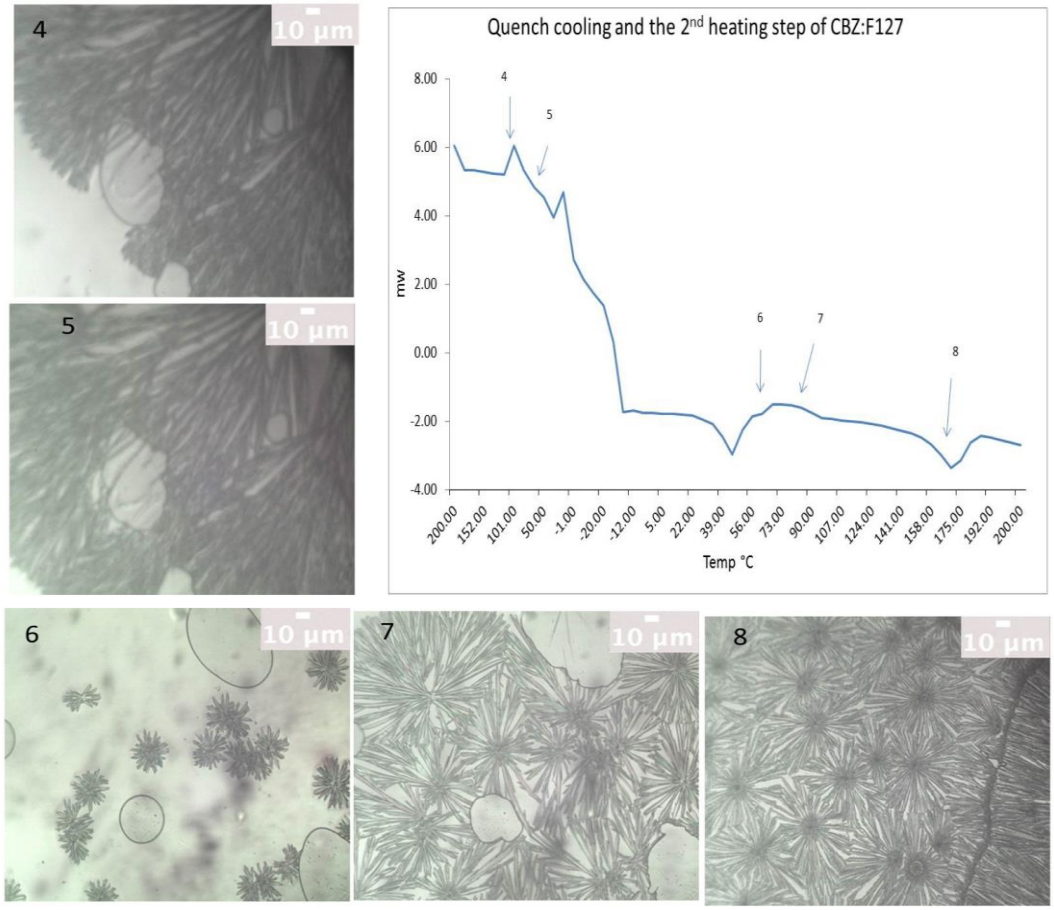

Figure 6.3-7 Quench cooling step and 2nd heating step for CBZ: F127

(During quench cooling step at 30°C/min, very fine branched needle shaped CBZ crystals start to grow at 105°C (image 4 was taken at 100°C). Image 5 was taken at 75°C where the CBZ crystals stopped growing. Image 6 was taken during the 2nd heating cycle, at 60°C the crystals start to grow from the solution where no previous crystallisation was observed. Image 7 was taken at 80°C; the needle shape crystals become bigger. Image 8 shows the CBZ crystals start to melt at 170°C.)

The quench cooling and 2nd heating DSC curve shows two small peaks during cooling which corresponds to CBZ and F127 respectively. During the 2nd heating step, a small endothermic peak at around 45°C indicates F127 melting followed by a hump, which indicates a phase of CBZ crystallisation. Another endothermic peak was observed around 170°C, which corresponds to CBZ melting.

The hot stage microscopy results for the quench cooling of CBZ: F127 were in agreement with the DSC curve. A small CBZ and F127 crystallisation event was observed during cooling and in the 2nd heating step; F127 melts then CBZ crystals starts to grow. The crystals grew from nuclei to form a flower shaped crystals, the CBZ crystals formed exist as form II. The CBZ crystals from the quench cooled sample looked more uniform than the normal cooled ones. Also, more crystals appeared than in the normal cooled sample. In both samples the CBZ crystals had a needle shape crystal and they exist in form II.

6.3.3 CBZ: PEG 300: 4000: F127 (50:20:20:10)

6.3.3.1 Part 1:1st heating cycle

The 1st heating cycle of CBZ: PEG 300: 4000:F127 on the DSC shows two endothermic peaks: one around 50°C which is for the melting of the polymer blend and the 2nd peak for the CBZ melting. The hot stage microscopy images are presented below.

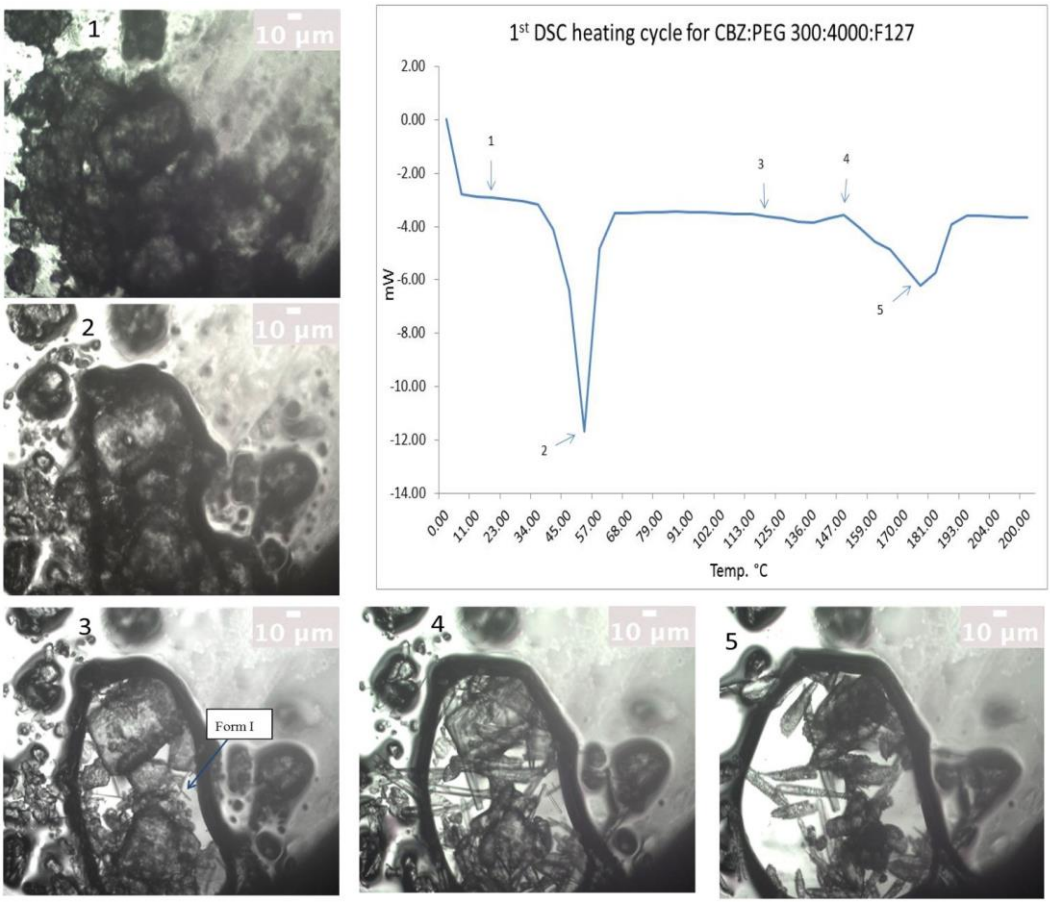

Figure 6.3-8 1st heating cycle for CBZ: PEG 300: 4000:F127

(Image 1 was taken at 20°C and it shows the polymer mix covers the drug particles. Image 2 was taken at 50°C where the polymer mixture starts to melt and the CBZ drug crystals can be seen now. Image 3 was taken at 120°C, CBZ needle shaped crystals start to grow. Image 4 was taken at 150°C where most of the CBZ crystals have changed form to needle shape crystals (form I). Image 5 was taken at 175°C, and it shows that most of the CBZ crystals have melted and at 185°C the drug is in solution.)

6.3.3.2 Part 2: normal cooling and 2nd heating cycle

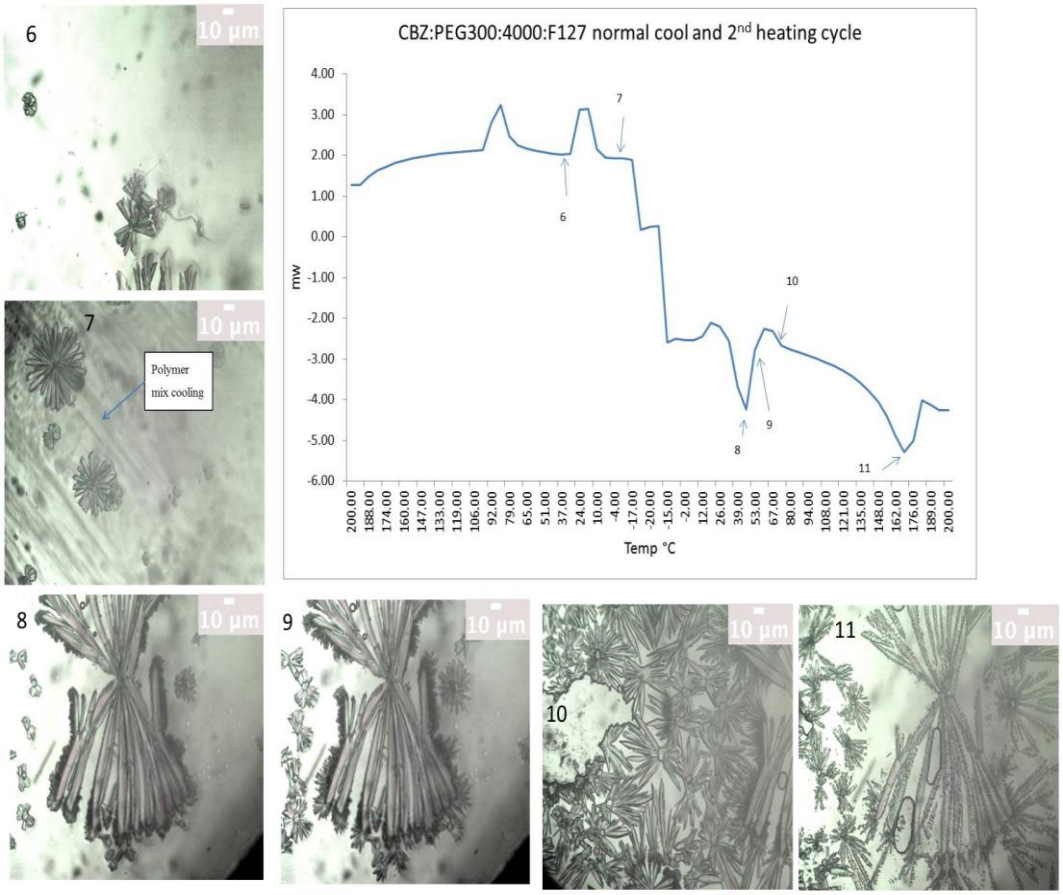

Figure 6.3-9 Normal cooling and 2nd heating cycle for CBZ: PEG 300: 4000: F127 (The sample was cooled at 10°C/min and the first CBZ crystal growth appears at 40°C, image 6 was taken at 30°C. Only a few CBZ crystals appeared during cooling and they did not grow fast, the polymer mixture appears as streaks when cooled. (The arrow in image 7 points to the polymer mixture streaks). When the sample was heated for the 2nd time, at 50°C more crystals did form on top of the older crystals as shown in image 8. Image 9 was taken at 60°C where more CBZ crystals are formed. At 80°C, the crystals stopped growing as shown in image 10. The CBZ crystals start to melt as the temperature exceeded 130°C, image 11 was taken at 170°C where some of the CBZ crystals are in the liquid state.)

The DSC curve shows that during cooling two exothermic peaks one around 85°C corresponds for CBZ crystallising and the other peak at 15°C is for the polymer

mixture crystallising. During 2nd heating step, a small exothermic peak can be seen at around 18°C followed by a melting peak at 46°C then another exothermic peak at 60°C. The hot stage microscopy results shows that CBZ crystals start to form again during the 2nd heating step (image 8 above) in the same time as the polymer mixture is melting then the crystallisation continues until it reaches 80°C where the crystallisation stops.

6.3.3.3 Part 3: Quench cooling and 2nd heating cycle

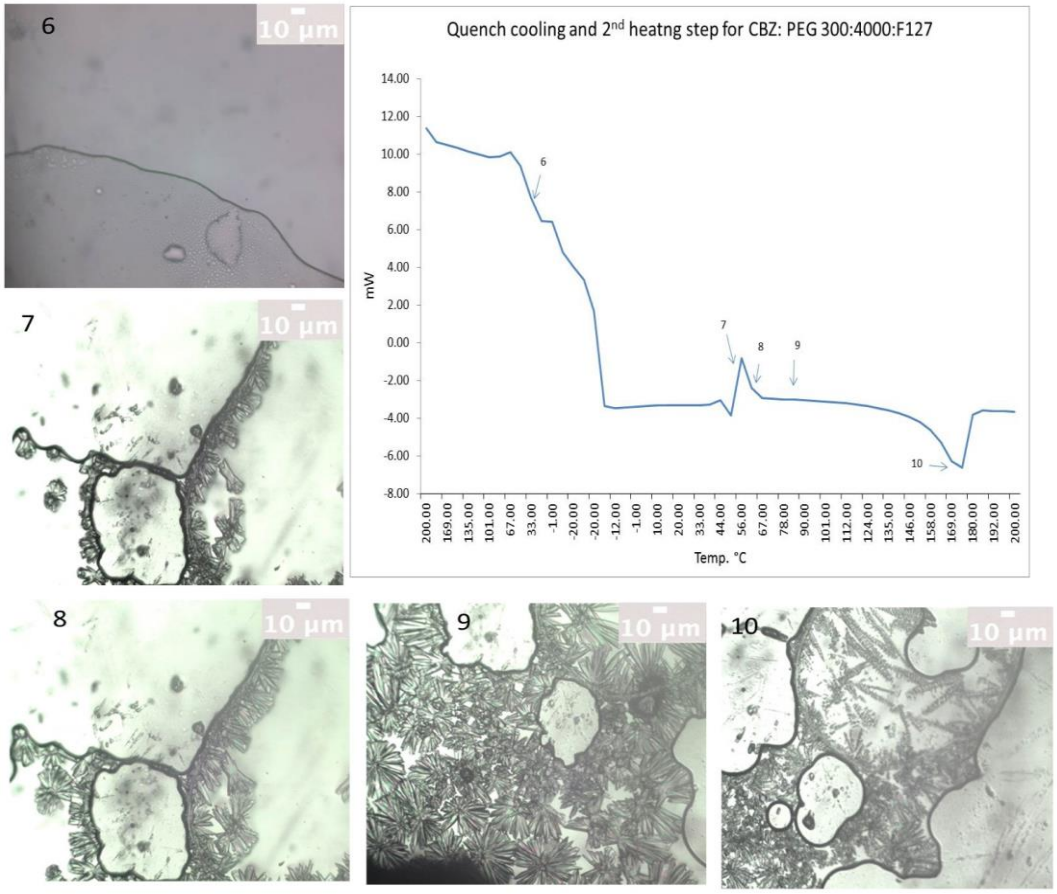

Figure 6.3-10 Quench cooling and 2nd heating cycle for CBZ: PEG 300: 4000:F127 (Image 6 was taken during cooling step at 20°C, no change was observed after the melt. When the sample was heated for the 2nd time, the CBZ crystals start to grow at 50°C as shown in image 7. Image 8 was taken at 60°C, and more CBZ crystals are still growing. At 80°C, the crystals are a mixture of big large needle and very small ones clustered together as image 9 shows. Image 10 was taken at 170°C as some

crystals has melted and some still melting and at 185°C all the CBZ crystals are in the liquid state.

The quench cooling step for CBZ: PEG 300: 4000: F127 show a small exothermic peak at around 50°C. This event was not seen under the hot stage microscope (refer to picture 6 below). During the 2nd heating cycle, the DSC results show a similar pattern as the normal cooled sample but with a smaller endothermic peak for the polymer mixture.

Both samples normal cooled and quenched cooled showed similar thermal behaviour. The difference is when the sample was left to cool slowly some of the CBZ crystallised and when quenched cooled it stayed amorphous / low crystalline. During the 2nd heating step, the crystallization starts at 50°C in both samples.

6.3.4 CBZ:PEG6000:F127(50:40:10)

6.3.4.1 Part 1: 1st heating Cycle

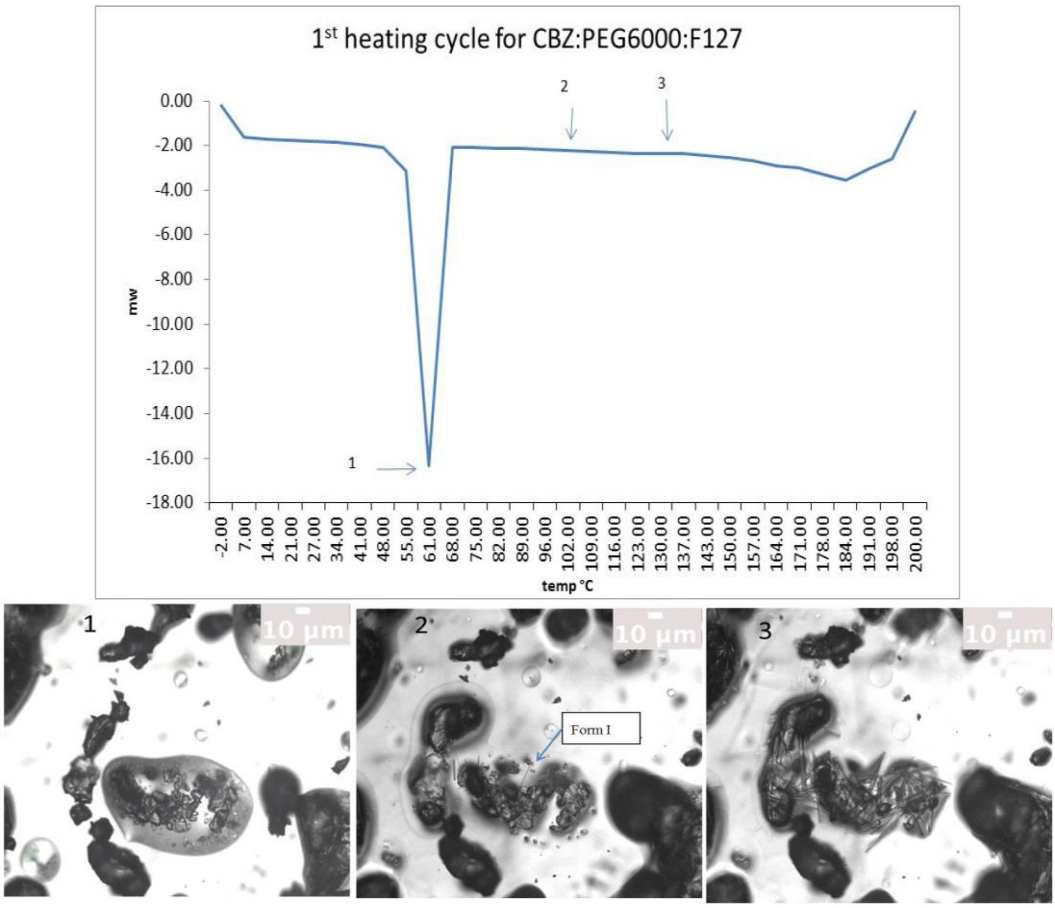

Figure 6.3-11 1st heating cycle of CBZ: PEG6000: F127
(Image 1 was taken at 60°C and shows the PEG 6000 and the Poloxamer F127 are in the liquid state. The CBZ crystals appear as rock shape (form III) in the molten polymer. Image 2 was taken at 100°C, the needle shaped crystals start to grow from the drug crystals. Image 3 was taken at 130°C, almost all the crystals have changed form to needle shape crystals and then at 175°C the CBZ crystals starts to melts).

The 1st part of the DSC cycle of CBZ: PEG 6000: F127 shows that there are two endothermic peaks. One at around 60°C corresponds for the polymer blend melting followed by the CBZ melting peak around 190°C. The hot stage microscopy data shows the typical CBZ thermal behaviour. The CBZ crystals in formulation are

form III due to their rock shape, as the sample was heated it changed form to form I (needle shape) before melting.

6.3.4.2 Part 2: normal cooling and the 2nd heating step

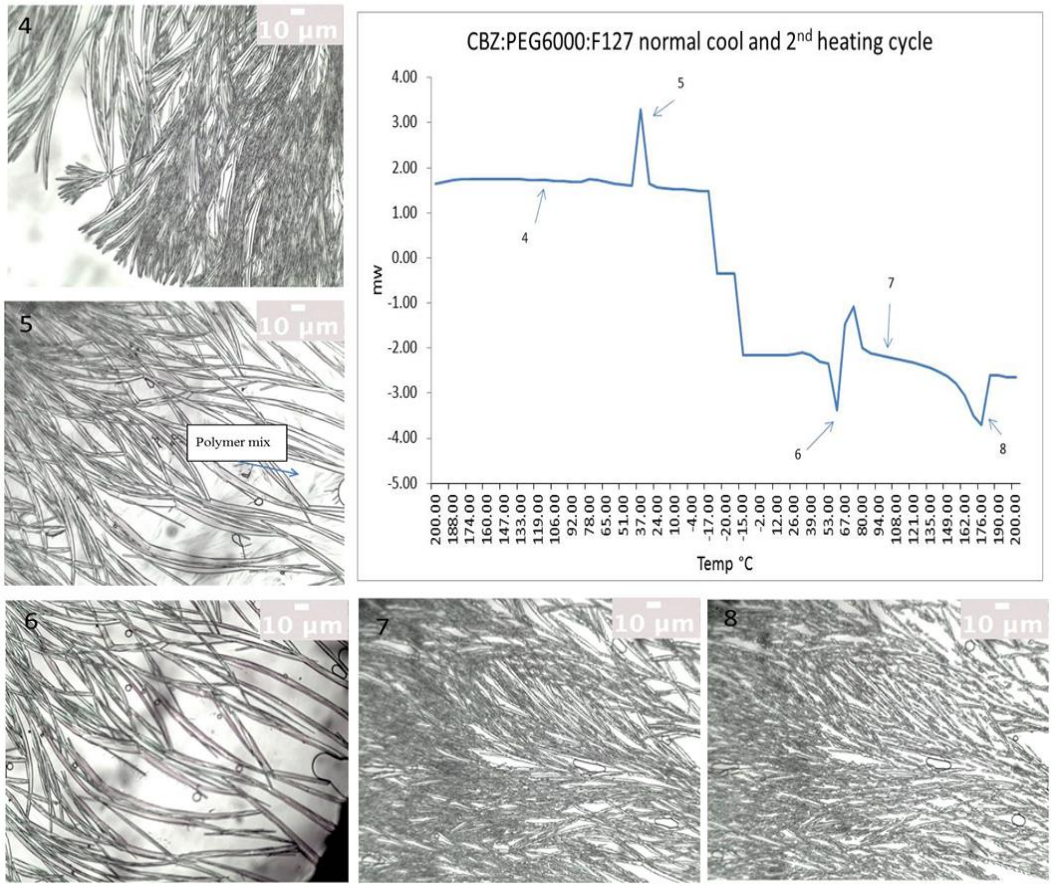

Figure 6.3-12 Normal cooling and 2nd heating cycle for CBZ: PEG6000: F127

(When the sample was cooled, very fine, branched and long needle shape crystals start to grow at 110°C and image 4 was taken at 100°C. Image 5 was taken at 30°C where the PEG6000:F127 solidified and it can be seen as thin striation in the background. Image 6 was taken during the 2nd heating step at 60°C where the PEG6000:F127 mixture starts to melt. At 80°C, a small CBZ crystal growth starts, image 7 was taken at 100°C. At 140°C the CBZ crystals starts to melt. Image 8 was taken at 180°C, the CBZ crystals became smaller and at 195°C all the crystals are in liquid state).

During the normal cooling step and 2nd heating step, the DSC curve shows a very small exothermic peak of CBZ followed by a large exothermic peak corresponds to the polymer blend crystallisation. In the 2nd heating step a melting peak for the polymer blend was seen followed by an exothermic peak, which correspond for CBZ crystallising. These events occurred between 50 and 80°C. CBZ melt around 180°C.

The hot stage microscopy data were in agreement with the DSC curve. A CBZ crystallisation was observed around 100°C followed by polymer freezing around 30°C during the cooling step and during the 2nd heating step, a small CBZ crystals growth was observed as the polymer mixture was melting.

6.3.4.3 Part 3: quench cool and 2nd heating step

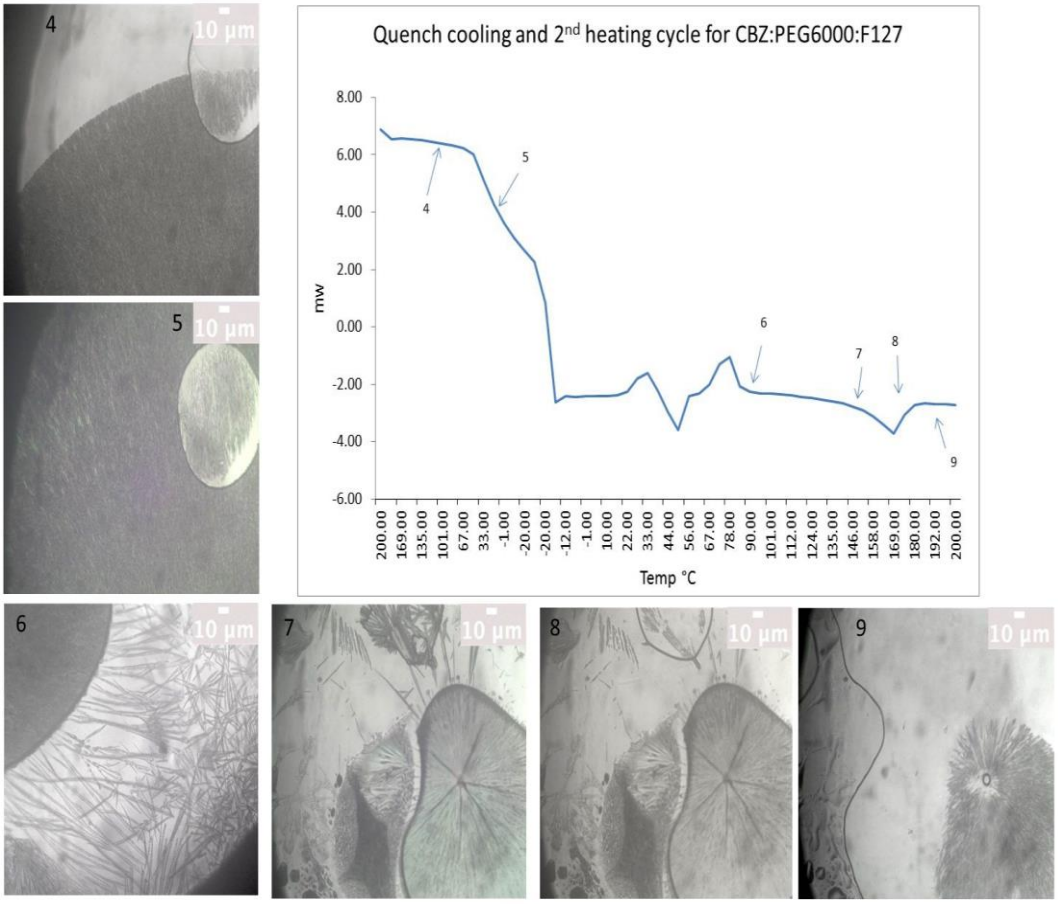

Figure 6.3-13 Quench cooling and 2nd heating step of CBZ: PEG6000: F127

(During the quench cooling step and at 110°C, very fine crystals start to grow very fast. Image 4 was taken at 100°C showing the CBZ crystals growing then the crystals stopped growing at 80°C and stayed the same during the cooling step. Image 5 was taken at 20°C. During the 2nd heating cycle, a few long needle shaped crystals start to grow at 90°C as shown in image 6. At 130°C, the crystals start to melt and image 7 was taken at 150°C. Image 8 was taken at 180°C showing the CBZ crystals are still melting. At 195°C (image 9), a few crystals are still melting until 200°C where all the CBZ crystals did melt).

The DSC curve shows no crystallisation during cooling, then during the 2nd heating step a small exothermic peak was observed followed by melting and another crystallisation. This event corresponds to polymer blend crystallising then melting and CBZ starting to crystallise afterwards.

The hot stage microscopy results showed a different result from the DSC. CBZ crystals started to grow at 110°C and then stopped growing around 80°C and no further growth was observed during the quench cooling. During the 2nd heating step, more CBZ crystals start to appear at 90°C.

The starting materials in all the formulations studied in this section showed the same thermal behaviour: melting of the polymer mix followed by melting of CBZ. The cooling rate did show a difference in crystallisation with the formulations containing PEG. The normal cooling showed crystallisation of both CBZ and polymer blend. Whereas, the quench cooling did show a smaller crystallisation event than the normal cooled sample or no growth as in CBZ: PEG 6000: F127 and CBZ: PEG 300: 4000: P103. A CBZ crystallisation was observed in the formulations containing PEG during the 2nd heating step even when the sample was normal or quench cooled.

6.3.5 Effect of cooling rate on the CBZ: PEG 300:4000: Poloxamer formulations

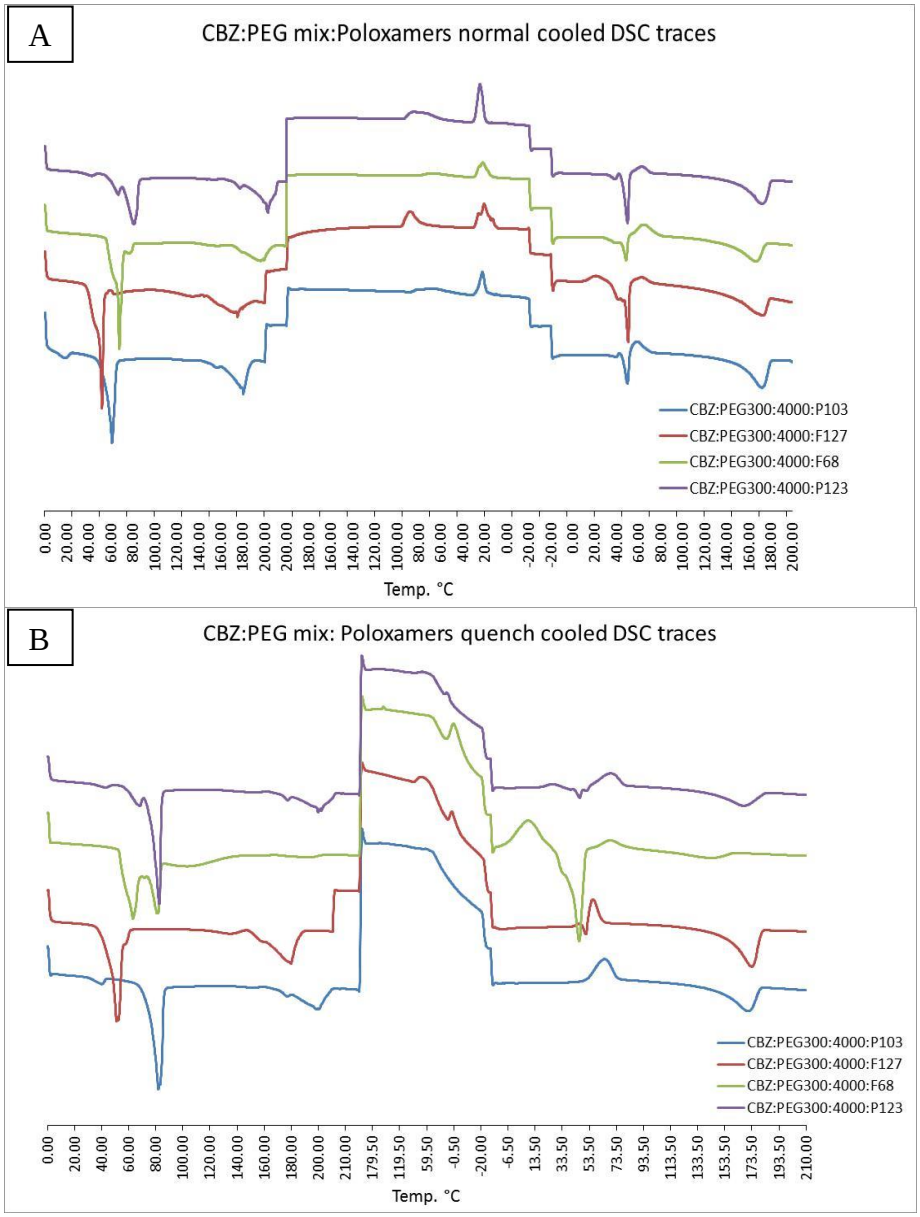

Figure 6.3-14 DSC traces of the different CBZ: PEG mix: Poloxamers formulations normally cooled (A) and quench cooled (B)

The figure above shows the different DSC traces of CBZ: PEG 300: 4000: poloxamer (50:40:10 %w/w/w) formulations at different cooling rate. The results from the normally cooled (10°C/min) DSC samples shows that at the 1st heating step

the polymer mixture did melt at roughly the same temperature around 50°C except for the F127 formulation the melting point was lower, also, the CBZ melting point for P103 and F127 (180°C) was lower than the other formulations (194°C). During the cooling step, all the formulations did show the CBZ crystallisation peak followed by the polymer mixture crystallisation peak. The temperature of CBZ crystallisation was slightly lower than the other formulations. During the 2nd heating step, all the formulations showed the polymer mixture melting at around 50°C followed by CBZ crystallisation peak around 60°C then melting peak at 180°C.

When the samples were quench cooled at 30°C/min, the P103 and P123 formulations shows that the CBZ and polymer mixture crystallisation was inhibited during cooling, the other two formulations did show a very small crystallisation of CBZ and polymer. During the 2nd heating step, P103 formulation did show a large CBZ crystallisation peak. The F68 formulation did show a CBZ/ polymer crystallisation peak at a very low temperature followed by polymer melting peak around 50°C then CBZ crystallisation. This formulation did show the lowest CBZ melting point. P123 and F127 formulation also showed the CBZ crystallisation peak but was smaller than P103 formulation due to small polymer melting peak before the crystallisation event.

6.3.6 Stability results

6.3.6.1 Effect of the Poloxamer on stabilising CBZ recrystallisation

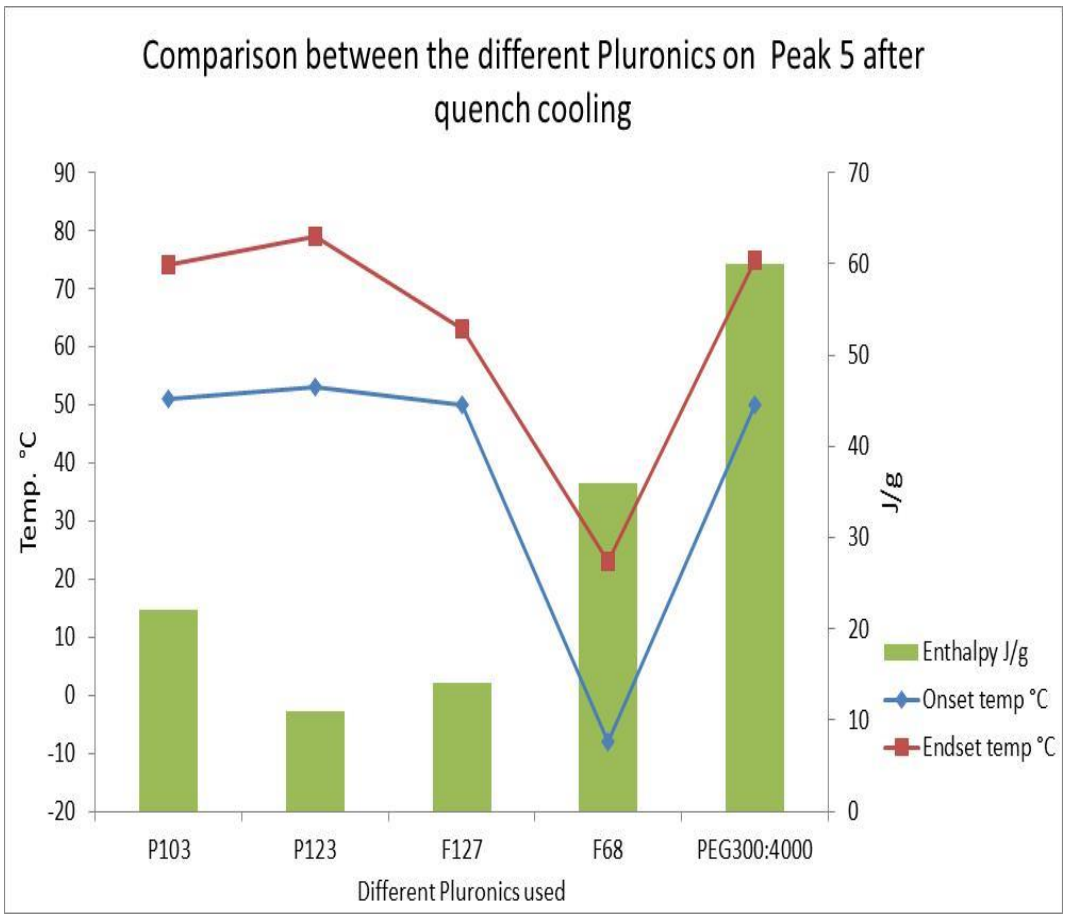

Figure 6.3-15 Effect of the addition of Poloxamer on peak 5.

The effect of the different Poloxamers on the CBZ crystallisation from melt after quench cooling (peak 5 on the DSC trace) was studied on the DSC using CBZ: PEG 300: 4000: Poloxamers formulations at 50:20:20:10 (%w/w/w). The onset temperature, endset temperature and the enthalpy of the peak were measured and presented in Figure 6.3-15. The F68 formulation have induced the crystallisation faster than the other formulation, where the crystallisation started straight after the cooling step and the enthalpy was high which suggest that lots of crystals has been formed. On the other hand, the other formulations had the same onset temperature

as the CBZ: PEG: 300: 4000 but the endset temperature for the formulation with P123 was the highest.

6.3.6.2 Stability of the formulations at different temperature

The stability of the different formulations held isothermally at different temperature was carried out on the DSC. The DSC traces below (Figure 6.3-16) are for CBZ: PEG 300:4000:P103 formulation. They are presented below as an example for the other formulations where the data is presented in Figure 6.3-17 .

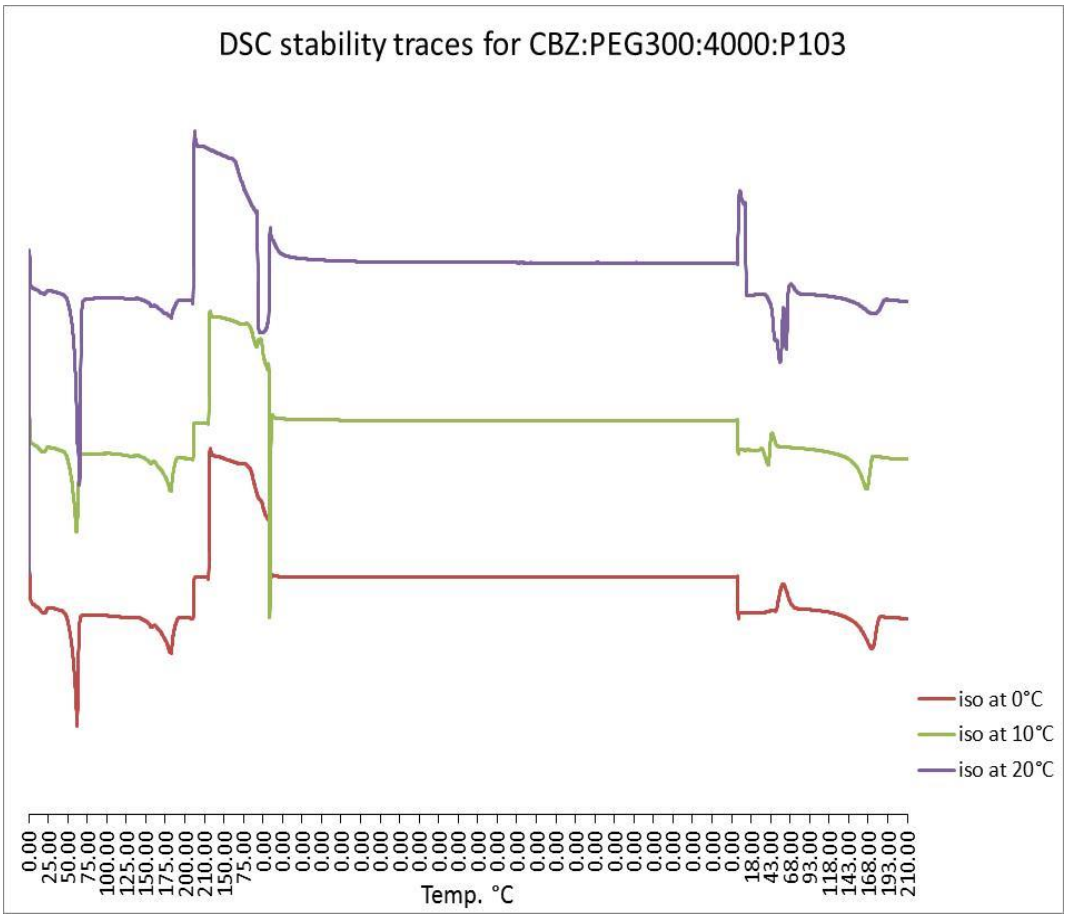

Figure 6.3-16 CBZ:PEG300:P103 stability DSC traces at 0, 10 and 20°C

The DSC stability results for the CBZ: PEG with different Poloxamer are shown in Figure 6.3-17 below. The positive enthalpy of peak 5 (refer to Figure 6.3-3) indicates crystallisation of CBZ and a negative enthalpy indicates melting peak. The stability results show that all the formulations were stable at 0°C and solid CBZ

phase is present above that temperature (except for P123 and F127 formulations were also stable at 10° C).

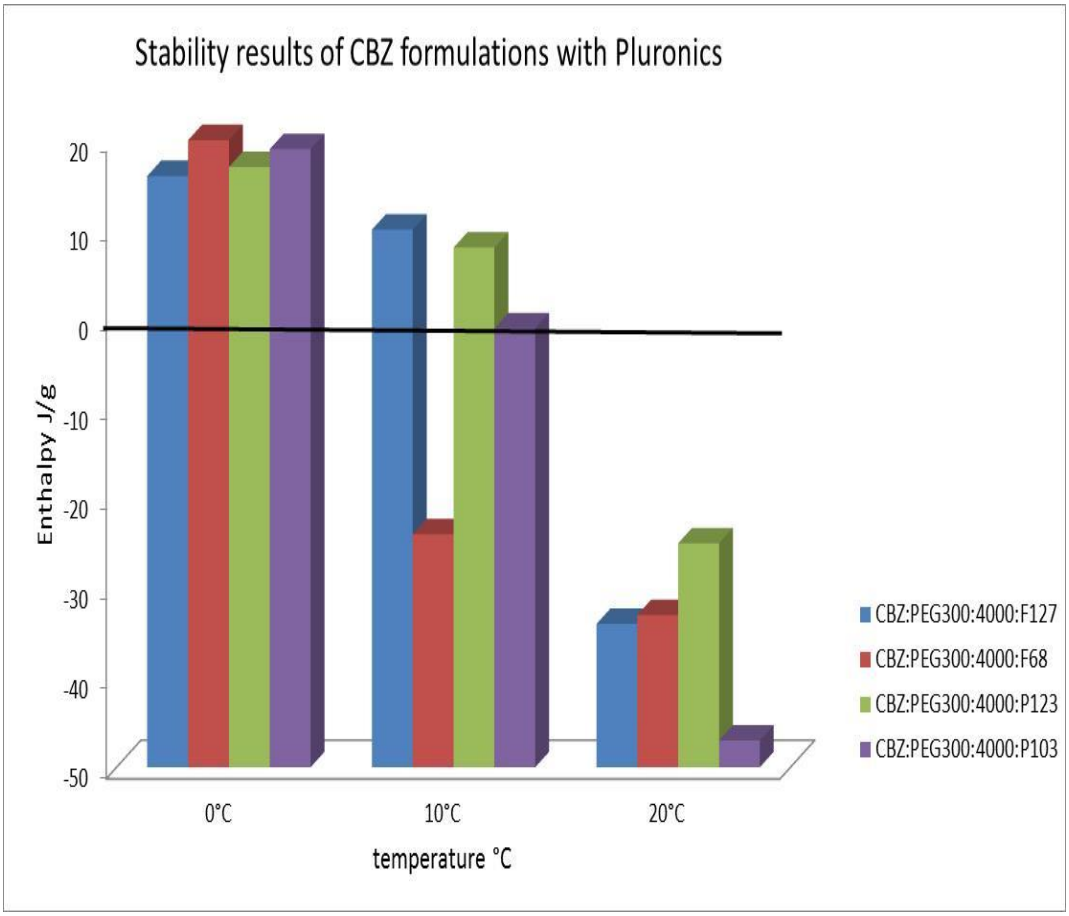

Figure 6.3-17 Stability of the different formulations with Poloxamers over 1 hour at 0, 10 and 20°C

6.3.6.3 The effect of P103 concentration in the formulation on the crystallisation of CBZ

The data above showed that the CBZ solid solution can be formed at high temperature (around 55 °C) in the formulation with P103. The peak on the DSC trace looked well defined, also during the stability study at different temperature, the formulation was found to be stable. Therefore, the effect of P103 concentration on the crystallisation of CBZ from melt was studied using the DSC. Different P103 concentrations were added to the CBZ: PEG 300: PEG4000 (50:25:25) formulation.

The P103 added by % weight keeping the same ratio of CBZ, PEG 300 and 4000 as mentioned above.

All the formulations with the different P103 concentration showed the crystallisation event (Peak 5). The CBZ: P103 at 50:50 %w/w, showed a small exothermic peak during the cooling step, and another one during the reheating step. This is why the peak 5 looks smaller and has lower enthalpy than the other. Some of the DSC traces are shown in Figure 6.3-18. The enthalpy of the formulation with 1% P103 was higher than the 10% because the 1% formulation the crystallisation event was longer.

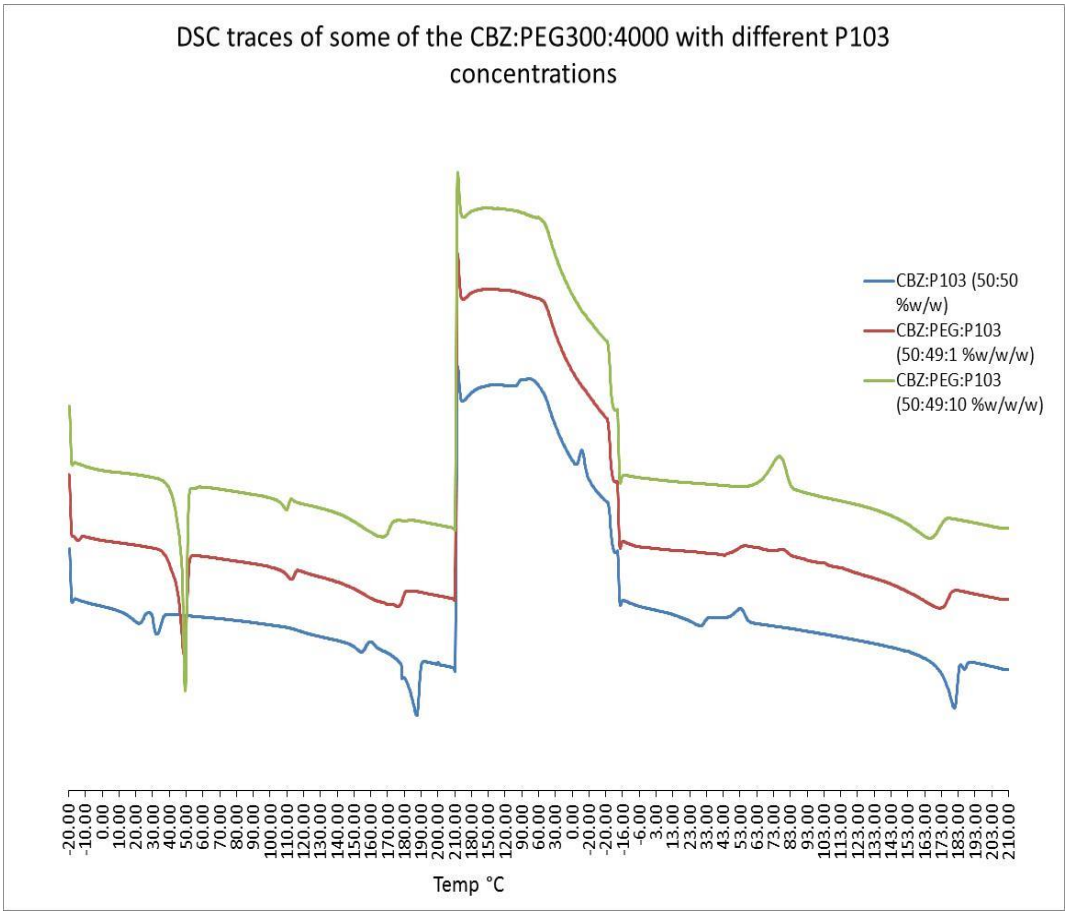

Figure 6.3-18 DSC traces for some of CBZ: PEG 300: 4000 mixtures with P103

The figure below (Figure 6.3-19) shows the onset temperature and endset temperature of the CBZ crystallisation along with the enthalpy of the different formulations containing different concentration of P103 during the 2nd heating step.

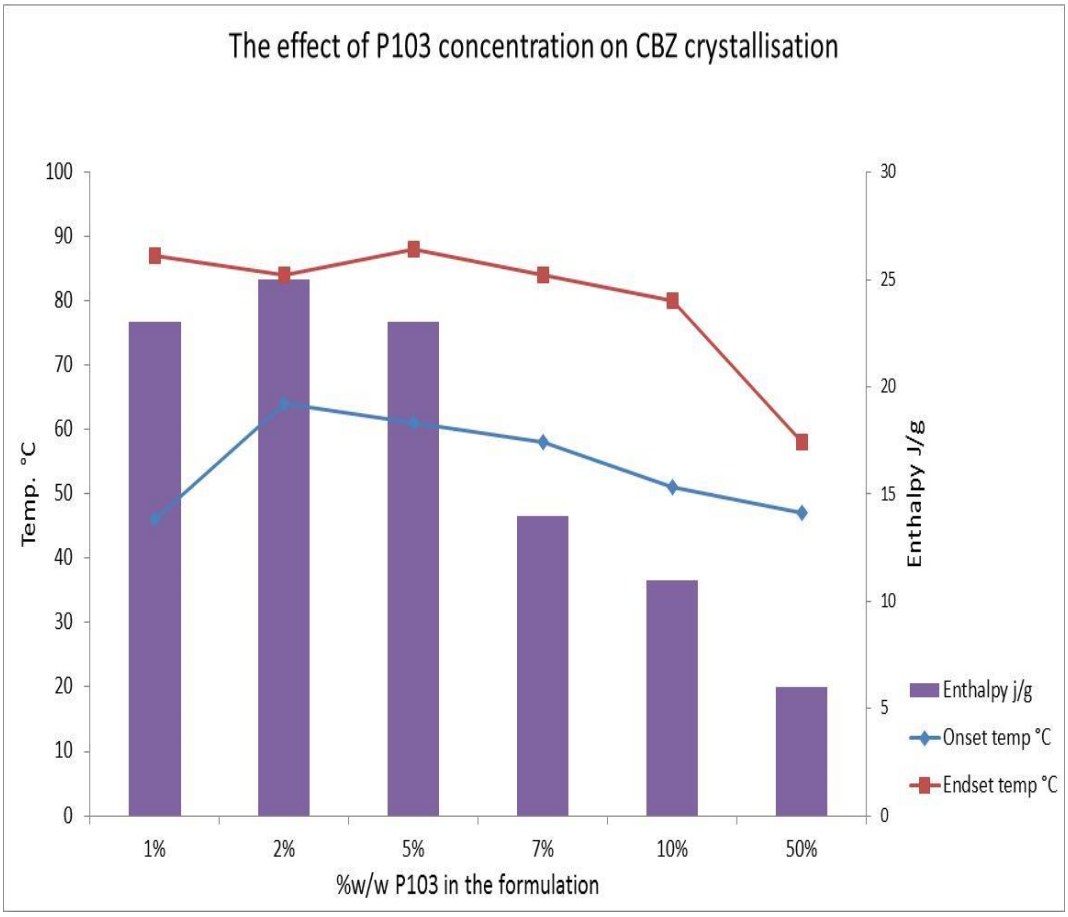

Figure 6.3-19 Comparison between the different formulations with variable P103 concentration

The results show that the P103 alone (with no PEG) cannot totally inhibit the CBZ crystallisation during the cooling step therefore the crystallisation peak was observed during cooling and another one during the 2nd heating step. The different concentration of P103 in the formulations did show a reduction in the enthalpy as the P103 increases in the formulations which indicates that P103 did inhibit the CBZ recrystallisation and the number of nuclei is less in the formulation with 10% P103 than in the 1%.

6.3.7 Dissolution results

The Poloxamer formulations were assessed on the T3 for the dissolution testing. The dissolution was studied at four different pHs (2, 4, 5 and 7) for two hours with 30 minutes at each pH. The dissolution study was carried out as powder dissolution (the formulation was not pressed into disc) as some of the formulations were waxy

and hard to compress into discs therefore the formulation was added to the dissolution media as powder and a reading was taking every 10 seconds. The results were compared to the formulation with PEG alone to show the effect of Poloxamers on the dissolution of CBZ.

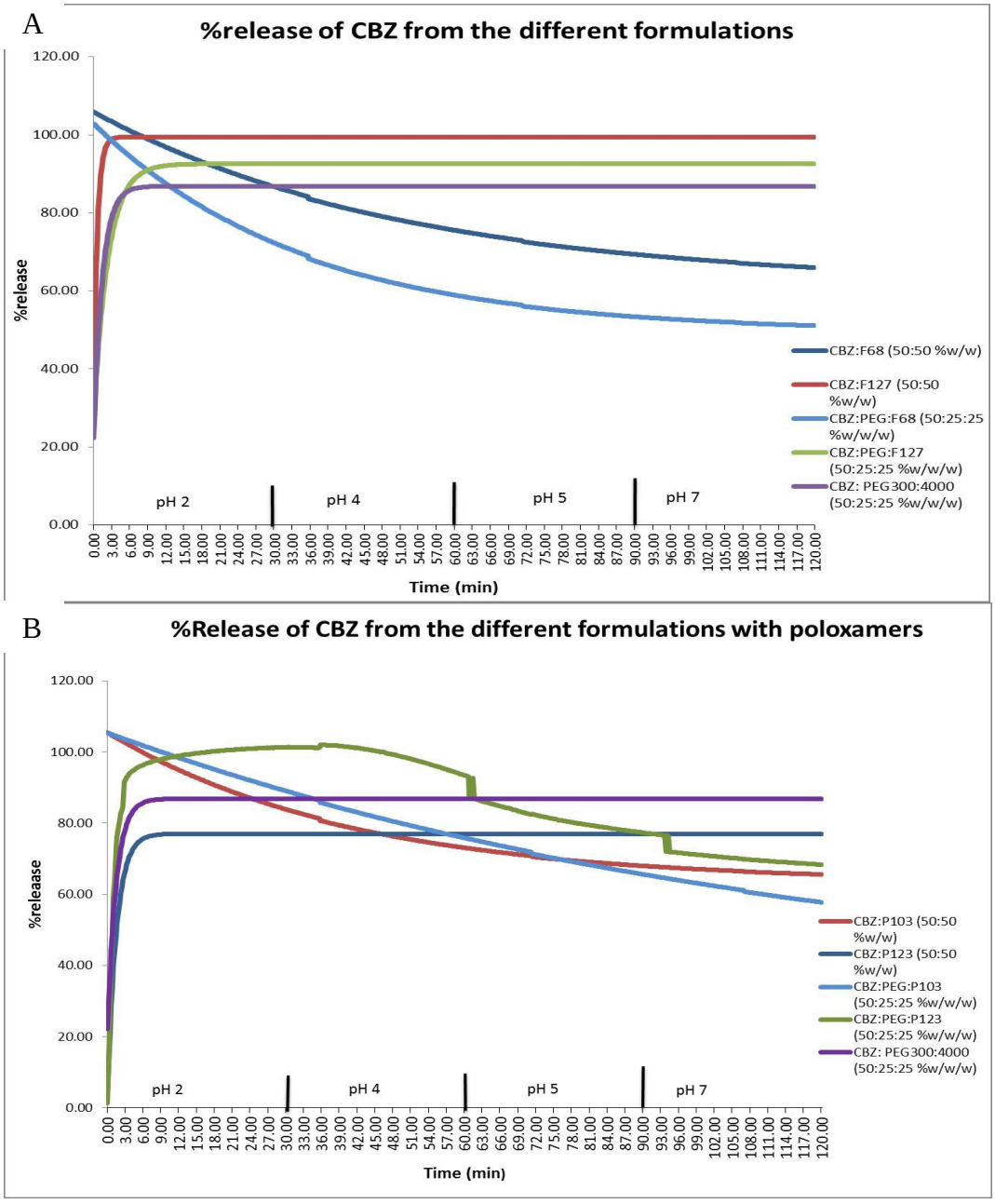

Figure 6.3-20 Release profile of CBZ from the formulation containing either Poloxamers alone or a mixture of PEG 300:4000 /Poloxamers.

(Image A shows the release profile of CBZ from F-poloxamers and image B from P-poloxamers)

The results show that the CBZ formulations with F127 alone and with PEG mixture have a better release profile than the CBZ: PEG 300:4000 formulation. The CBZ: F127 formulation did show a 100% release within 5 minutes and the drug stayed in solution at the different pH used. For the F68 formulations, both formulations did show a 100% release at time 0 minutes which indicates that the polymer act as a spring but then the concentration dropped with time and pH change due to the drug precipitation.

For the formulations with P-Poloxamers, the results show that the release from P103 alone formulation was high at the start of the experiment than decrease due to precipitation. The same phenomenon was seen with the formulation with PEG and P103 but the concentration decrease more in the presence of PEG. For CBZ: P123 formulation the maximum CBZ release was 75% whereas in the formulation with PEG and P123 the release increased to 100% at pH2 which was higher than the release from CBZ: PEG 300:4000 formulation then the concentration starts to decrease with the change of pH this might be due to P123 has a spring and parachute effect on the release of CBZ.

6.3.8 X-ray analysis of the formulations

This section will cover the results from the flat plate x-ray analysis and variable temperature x-ray analysis for some samples.

6.3.8.1 Flat plate X-ray analysis

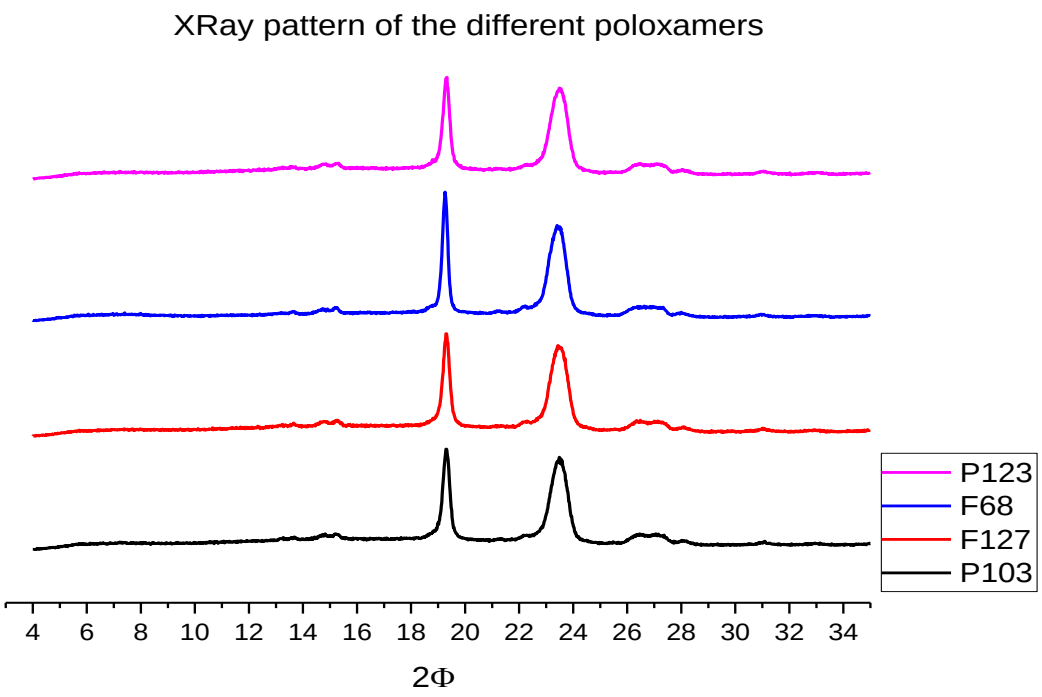

Figure 6.3-21 X-ray pattern of the different poloxamer

The results shows that all the poloxamers have the same pattern and they show two peaks one at 19° and the other at 23°.

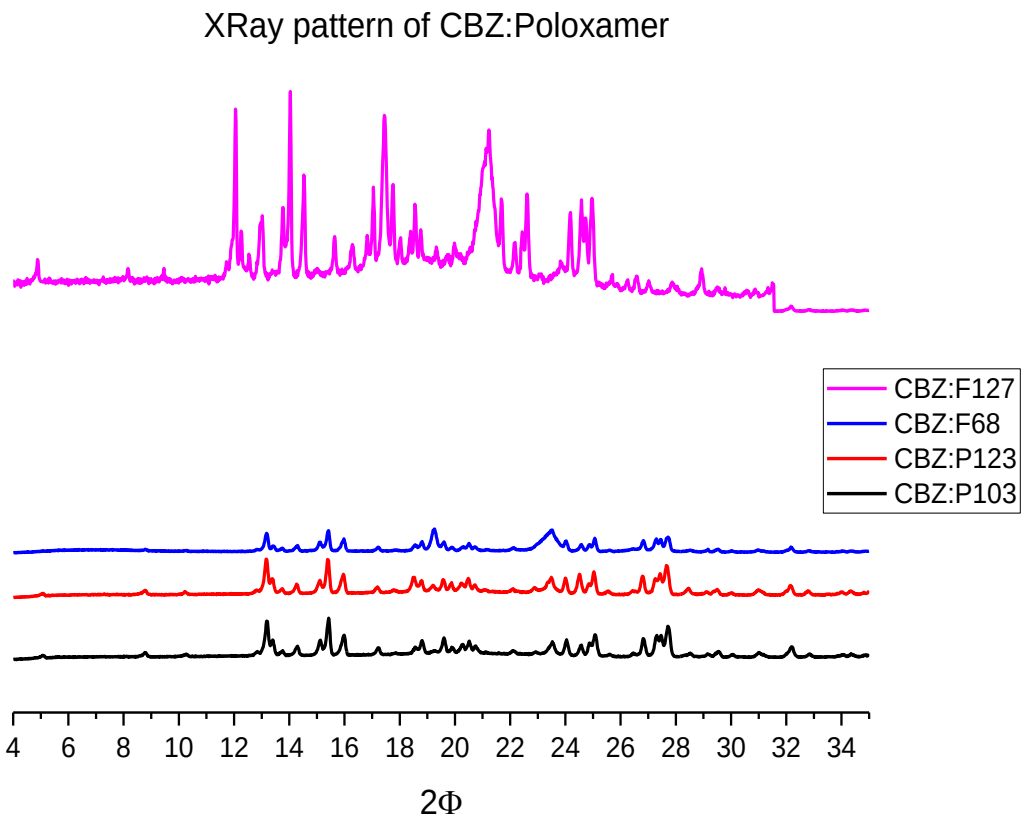

Figure 6.3-22 X-ray pattern for CBZ formulations with the different poloxamers

The formulations used were 50:50 (%w/w CBZ: poloxamers), the results shows that all the samples had a degree of crystallinity. The formulation with F127 was more crystalline compared to the rest, as the intensity of the peaks was higher and the peaks are more defined. The results shows that CBZ crystals in F127 formulation are a mixtures of form II and III (as peaks appeared at 4.5°, 8.5° and 13° which are the distinctive peaks of form II and the three peaks between 15° and 15.8° which correspond to form III), whereas, the crystals in the other formulations stated in the figure above are form II.

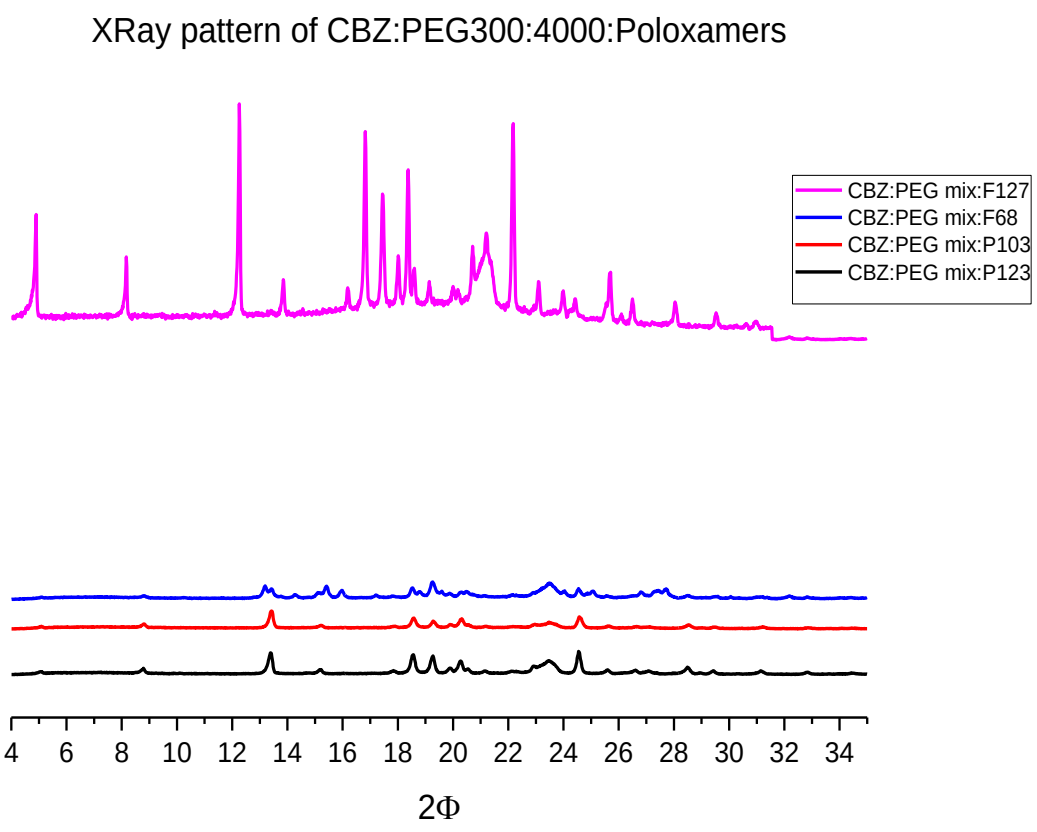

Figure 6.3-23 X-ray pattern for the CBZ formulation with PEG mix and poloxamer

PEG X-ray pattern show two peaks (refer to chapter 8): one at 19° and the other at 24°. The X-ray patterns for the CBZ formulations with PEG 300:4000: poloxamers shows that the CBZ crystals are in form II for the formulations with P103, P123 and F68 and the intensity of the peak was low which indicates that not all of the CBZ crystals are in the crystal form some may still in amorphous form. The formulation with F127 did show a high intensity peaks and the crystals are form II.

6.3.8.2 Variable temperature X-ray analysis

The variable temperature X-ray analysis for the different formulations was carried out and a pattern was collected at different temperature points. The figure below (Figure 6.3-24) shows the different pattern of CBZ: F127 formulations at different temperatures. The CBZ within the formulation at room temperature exist as form II,

then when it was heated to melting state it become amorphous then during cooling, CBZ recrystallised as form II as the patterns show.

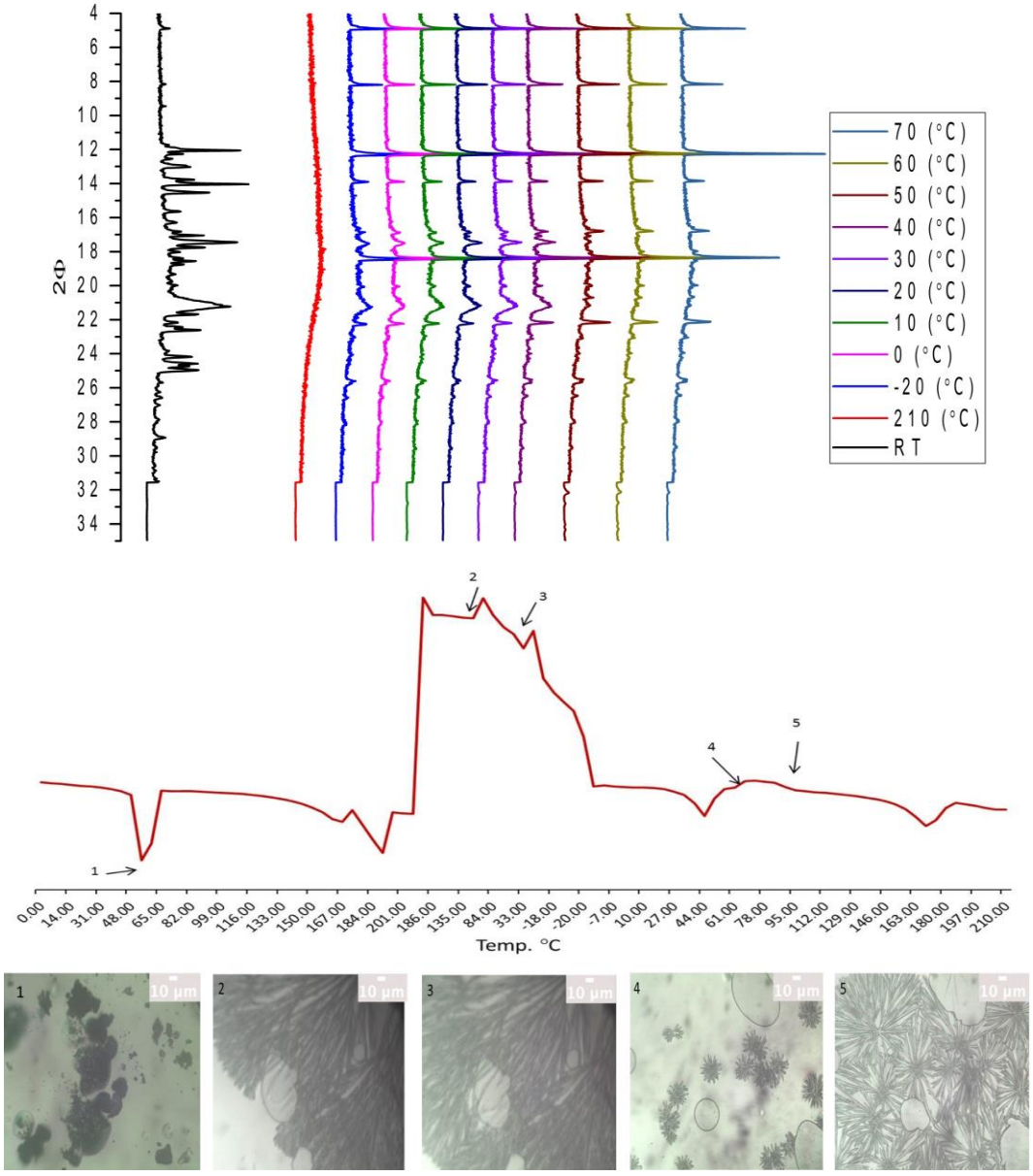

Figure 6.3-24 VT X-ray patterns of CBZ: F127

The results from the DSC and X-ray were consistent and it did show that the drug and the polymer (F127) quickly crystallise from melt during cooling, also, the peaks for the polymer disappears at 50°C where the F127 is in the liquid state.

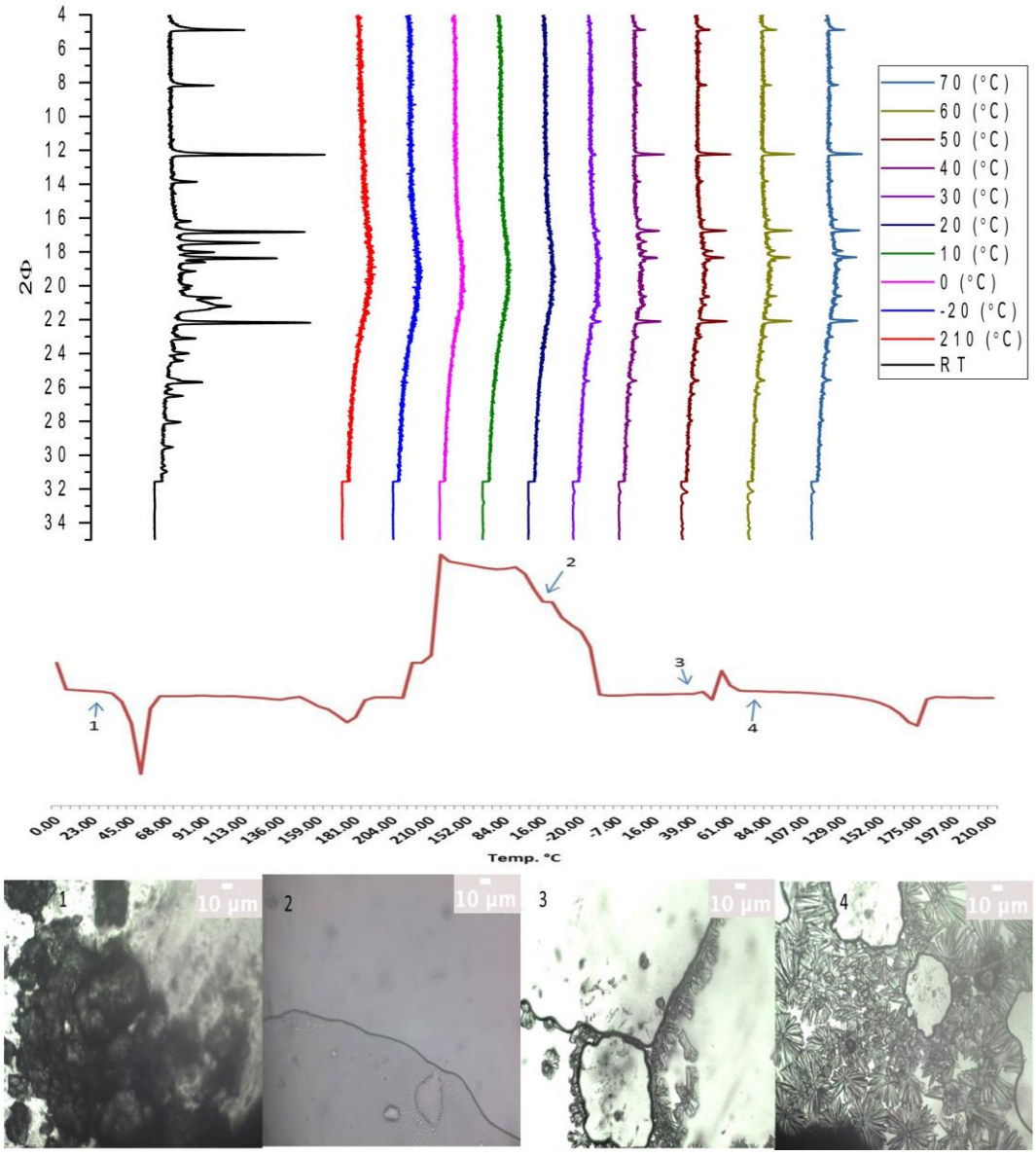

Figure 6.3-25 VT X-ray pattern of CBZ: PEG 300:4000:F127

For the CBZ: PEG 300:4000:F127 formulation the results show that at room temperature the CBZ crystals in the sample exist in form II as the peaks at 4.5, 8.5 and 13° are present. The sample stayed in amorphous state after melting until the temperature reaches 30°C, where crystals start to form and at 40°C the pattern starts to show more peaks and the CBZ crystals exist as form II. The main peaks for the polymer blend can be seen as very small peaks in the pattern at 40°C then disappears at 50°C this is due to the polymer blend melts at this temperature.

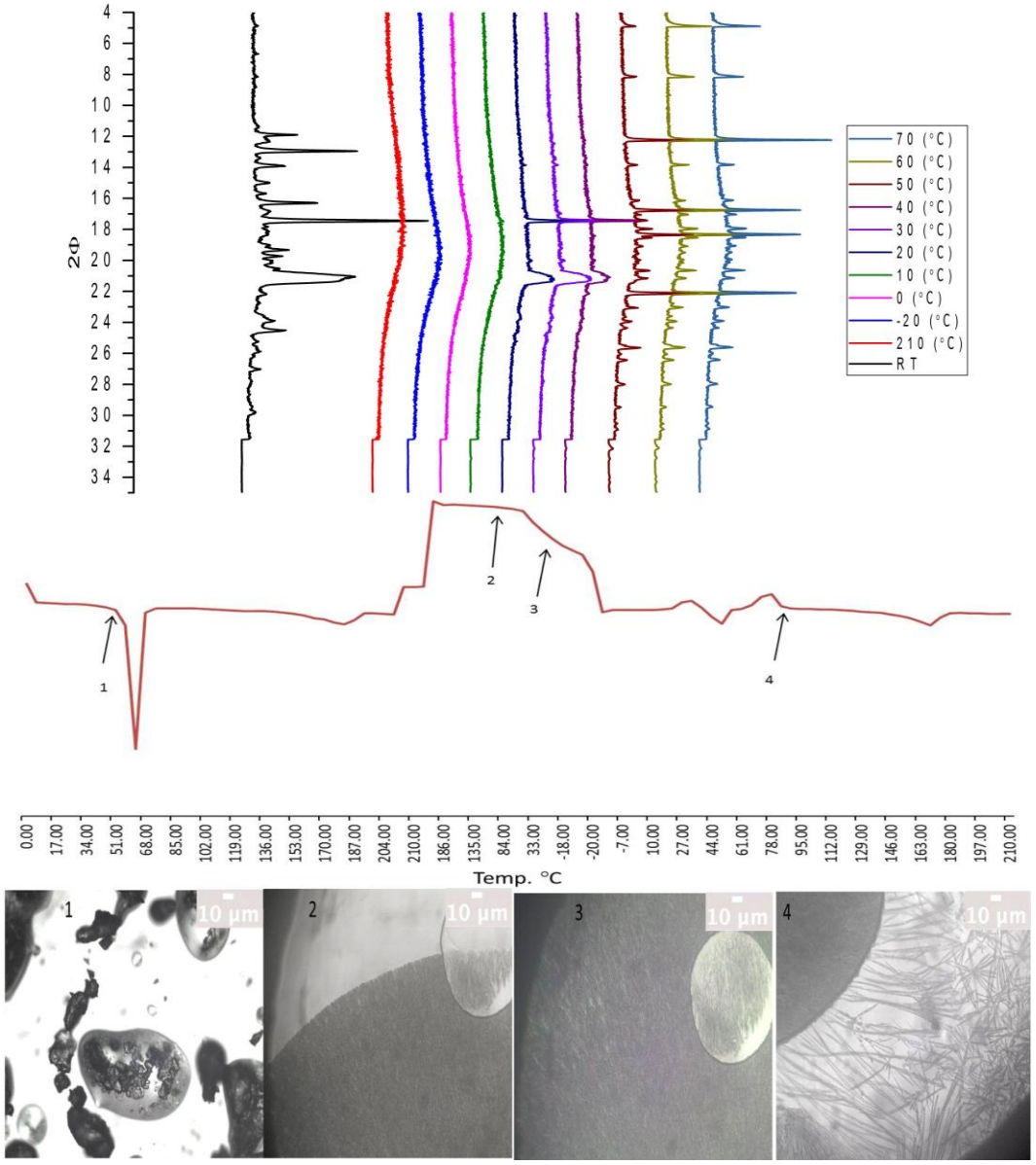

Figure 6.3-26 VT X-ray patterns for CBZ: PEG6000: F127

For the CBZ formulation with PEG6000:F127, the CBZ crystals at room temperature show pattern of form III. After the melt, the polymer blend of PEG 6000 and F127 crystallise at 20°C and the CBZ crystals in the formulation stayed amorphous until the temperature reaches 50°C, where CBZ crystals start to crystals into form II and polymer blend peak disappears dues to melting. The hot stage microscopy results were slightly different than the DSC and the XRPD this is might be due to the method of analyzing the sample which can alter the nucleation or due to the sample preparation where the sample in the DSC and XRPD are in a totally closed environment whereas the sample in the hot plate is more exposed to the atmosphere

and from previous chapter the atmosphere and moisture have a great effect on the crystallisation event of our sample.

6.4 Discussion

According to a study made by Guzman et al (2007), Poloxamers can enhance the solubility of the model drug used Celecoxib and inhibit the precipitation by acting as a parachute. The study showed that F127 inhibits the precipitation after dissolution for less than 60 minutes whereas; P123 and P103 inhibit the precipitation for more than 60 minutes. Based on their study and other literature, our Poloxamers were picked and their effects were studied in our system.

Poloxamers and PEG are compatible with each other and this can be seen from the DSC results of PEG 300:4000 with the F127 and F68 where one endothermic peak when heating and one exothermic peak during cooling were observed. On the other hand the P123 and P103 which melt before the PEG mixture, two peaks can be seen during heating but only one peak during cooling this is due to the Poloxamers not solidify during cooling or due to the Poloxamers not solidifing at the same temperature as the PEG peak.

The cooling rate did have an impact on the CBZ crystallisation from the melt. During the normal cooling rate on the DSC (10°C/min) CBZ recrystallises and the polymer blend solidifies whereas using quench cooling rate (30°C/min) some formulations crystallise during cooling and some not. This phenomenon was also seen in the previous Chapter 4 with the formulation with PEG alone. F127 used alone with CBZ at 50:50 %w/w did not inhibit the CBZ recrystallision from melt at both cooling rates but when it was mixed with the PEG mixture or with PEG 6000, CBZ did not crystallise from melt after quench cooling. A study made by Qian et al (2007) using BMS-347070 with poloxamer F127 at 1:1w/w, the sample was quench cooled from melt and the result showed that when the Poloxamer did crystallise within minutes followed by the drug and this was similar to our results. Also, this study shows a fast nucleation rate and a slow crystal growth rate for the drug with Poloxamer F127 and another study conducted by Vetter et al., (2011), showed that Poloxamer F127 slowed the crystal growth of Ibuprofen in solution, these findings match with our study, in Figure 6.3-15 the effect of the different Poloxamers on the

crystallisation from melt of CBZ:PEG 300:4000 formulation and the results shows that the onset temperature is similar to the formulation with no F127 but the endset was around 20°C lower and the enthalpy of crystallisation was very small compared to the formulation with PEG alone. This indicates that nucleation is going fast but the growth rate is slow.

P103 formulation with CBZ: PEG 300:4000 (at 10% w P103) did show a high CBZ recrystallisation temperature from melt (around 55°C), a different P103 concentration was used to study its effect on the crystallisation temperature and enthalpy. As the results shows (Figure 6.3-18) that P103 alone with CBZ did not inhibit the crystallisation and the results shows that the 2 and 5% P103 shows the highest onset and endset temperature but the enthalpy was large which indicates lots of crystals have been formed whereas the 10% formulation had a high onset and a shorter crystal growth rate and the enthalpy was smaller which indicates that the sample was not fully crystallised and this can be seen from the XRPD pattern of the formulation that the CBZ has a very low signal.

The study made by Guzman and colleagues (Guzman et al., 2007) did show that some excipient work as a spring (form supersaturates) during dissolution and the other work as a parachute (inhibits precipitation) and in his study, Poloxamers P123 and P103 act as Celecoxib precipitation inhibitor for more than 60 mins whereas F127 inhibit precipitation less than 60 mins. In another study by Sancheti et al., 2008 on bicalutamide with Poloxamer F68 shows an enhanced dissolution rate and the 1:1 w/w formulation showed the best performance. In our study, the CBZ dissolution rate in the different Poloxamer or PEG/ Poloxamer blend formulations shows a good performance. The CBZ: F127 formulation shows a 100% release within the first 10 mins whereas the formulation with PEG and F127 shows a 90% release within half an hour and the concentration stayed the same for the rest of the experiment. For the formulations with F68, the CBZ released to 100% within the first few minutes but then the concentration start to drop due to the precipitation and the formulation with the PEG did precipitate faster than the F68 alone. For the formulations with P123 and P103, the best performing formulation was CBZ: PEG 300:4000: P123 where a 100% release was achieved within the first 15 mins then

gradually the concentration drops to 70% after 2 hours. The P103 formulations did show similar behaviour as the F68 formulations. The results in our study does not agree with the data from the Guzman paper, as the P103 should inhibit precipitation for longer than 60 mins but in our case it did not, also F127 supposed to inhibit precipitation for less than 60 min but our sample did not precipitate within the 2 hours experiment. This difference could arise from the different drug behaviour studied also in our study we used 4 different pH whereas the Guzman study they used SGF which is around pH 1.7. In another study, CBZ was prepared as a solid dispersion using melt method with F127 and F68 at different drug/ polymer ratio shows an increase in the dissolution rate of CBZ with all the formulations but they found that F68 was better than F127 as the release was faster and higher from the formulations with F68 due to the more hydrophilic nature of F68 compared to F127 (Medarevic et al., 2015). Our results show that the CBZ from F68 formulations will be released within minutes and faster than the F127 but the concentration dropped due to precipitation. The dissolution results shows that Poloxamers used in this project can affect the CBZ dissolution rate. In some cases PEG did play a role in the enhancement of CBZ release from the formulation (CBZ: PEG 300:4000:P123) in other cases it did not (CBZ: PEG 300:4000:F127). From the X-ray pattern of the different formulations, it was concluded that CBZ exist almost in all formulations as form II except CBZ: F127 which is a mixture between form II and III. The CBZ formulations with F127 showed a higher crystalline peaks compared to the other formulations where the intensity of the peaks were low which indicates that the drug is not fully crystallised and some of the drug remains in an amorphous state which explain the enhanced dissolution rate of CBZ from these formulations compared to pure CBZ. P123 and F127 were better than F68 and P103 in preventing precipitation as the concentration reached a plateau with F127 and in P123 the concentration did decrease slowly.

The variable temperature X-ray data of the formulations with PEG mixture and Poloxamers showed that CBZ exist as form III in the CBZ: F127 and CBZ: PEG 6000: F127 whereas CBZ: PEG 300:4000 exist as form II at room temperature, these results were similar to the results of a study carried out by Medarevic and colleague where they formulated CBZ in F127 and F68 they found that CBZ crystal as exists in

form III in all formulations (Medarevic et al., 2015). After melt only the CBZ crystals in F127 formulation crystallise during cooling as form II. The result shows that PEG 6000:F127 will crystallise from the melt at high temperature (50°C) and from the PEG 300: 4000 at 30°C as form II from both formulations, but the intensity of these peaks were very low compared to the starting materials. This might be due to some of the CBZ still in amorphous form or they are in microcrystalline form as discussed by Chen and his colleagues (Chen et al., 2015) where they obtained a microcrystalline structure of Acetaminophen and Bifonazole after the melt with PEG 3350, F 68 and F127.

In conclusion the best performing formulations in this chapter are the CBZ: PEG 300:4000:P123 and the CBZ: F127. This is due to the low CBZ crystallisation enthalpy from the melt and faster release compared to the other with P123 formulation did sustain the release for longer time than the F127 and acted as a parachute. The CBZ: F127 formulation did show from the XRPD a crystalline pattern but its dissolution profile was very fast.

Chapter 7 CBZ Isothermal studies and the effect of PVP K12 on the formulations

7.1 Introduction

Carbamazepine has a glass-forming ability when quench cooled from melt (Baird et al., 2010). The drug in glassy state or super-cooled liquid after the quench cooling will be in amorphous state. The drug will have a higher energy compared to the crystalline form, which can lead to better solubility. The crystallisation in the amorphous drug requires nucleation and crystal growth. During cooling the molten drug from melt, the drug passes through an appropriate nucleation and growth zone. When the temperature region of the nucleation and crystal growth overlap and the magnitude of these processes are the same, the super-cooled liquid starts to crystallise during cooling. When there is a gap in temperature between the two processes, the super cooled liquid will form a glass. In some cases the glass contains quenched-in nuclei formed during cooling and will crystallise during heating where the temperature is favourable for the crystal growth to start (Trasi and Taylor, 2012).

Two studies made by Trasi and colleague (Trasi and Taylor, 2012) on the effect of the addition of polymers on nucleation and crystal growth of two glass-forming drugs (acetaminophen and flutamide) when quench cooled from melt. The studies show that the addition of 10%w/w of PVP K12 added to the drug reduced the number of nuclei and was effective on inhibiting crystal growth in the study made with acetaminophen. On the other hand, in the study with flutamide PVP had no significant difference on nucleation but was very effective on reducing crystal growth rate. In another study for the same group (Trasi and Taylor, 2015) but accessing the effect of polymers on crystal growth in a supersaturated solution showed that PVP K12 was the best performing in inhibiting primary and secondary nucleation.

The aims of this study are to investigate the effect of the addition of PVP K12 to the CBZ: PEG (50:50) formulation on inhibiting the crystallising from melt after quench

cooling and to stabilise the amorphous solution. This formulation concentration was chosen due the occurrence of CBZ recrystallising from the melt during the reheating step. Also, to investigate the addition of PVP K12 on the dissolution rate of the formulations and on maintaining a parachute effect of the drug.

7.2 Method

7.2.1 DSC Isothermal experiment method

CBZ with different PEG grade (1500, 4000 and 6000) formulations were prepared by the solvent evaporation method at 50:50 %w/w ratios. Then the samples were quench cooled using the DSC and held isothermally at different temperatures such as 30, 20, 10 and 4°C.

The same experiment was repeated by replacing some of the PEG used in the formulations with PVP K-12 at 1, 5, 10 and 20% weight of the PEG and keeping the same ratio of CBZ: polymer 50:50. Hot stage microscopy (for some samples) was performed to visualise the crystal growth when the sample was held isothermally. The sample was quench-cooled on the hot stage then isothermally held at the temperature stated above for 30 minutes.

7.2.2 Variable temperature XRPD

CBZ in PEG 4000 formulations with different PVP concentrations were assessed in the variable temperature XRPD. The formulations were prepared by solvent evaporation then powdered with mortar and pestle. The powder then transferred into a 1 mm borosilicate glass capillary. The scans were collected on a Bruker AXS D8 Advance II, as a continuous coupled 2(theta)/(theta) scan from 4°-35° and a step size of 0.02° and 1s/step. A 0.6mm anti diversion slit was employed with a Cu monochromated source tuned to kα1 x-ray emission. A LynxEYE PSD detector was used operating in 1D mode. Temperature control was achieved using an Oxford Cryosystems 700 plus series cryostream with an error of ± 2°. A scan was carried out at room temperature then the sample was heated to 210°C where a scan was

taken. The sample was cooled with a stream of liquid nitrogen to -20°C followed by a scan. The sample then reheated to the required temperatures (10, 20, 30, 40, 50, 60 and 70°C) where a scan was taken at each temperature. A 15 minutes equilibration time was added when the sample reached the required temperature before a scan was carried out.

7.2.3 Stability on the XRPD

CBZ: PEG 4000 with different PVP content formulations were prepared in large scale (1 g formulation) in glass vials. The samples were heated to 210°C, and then quench cooled in dry ice for 10 minutes before the XRPD analysis. The Samples then transferred to an automated x-y stage 28 well plate with X-ray transparent 7. 5μm Kapton film both under and over the sample to create a sealed environment. The samples appeared as a sticky amorphous paste at low temperature.

The XRPD data was collected on a Bruker D8 Advance II diffractometer (GX002103 - Priscilla). The scan parameters used were 2θ-range from 4° to 35° with a step size of 0.017° and 1s/step. A 1mm anti diversion slit was employed with a Cu monochromated source tuned to kα1 x-ray emission. The operating voltage was 40 kV and Current was 50 mA.

Vantec detector was used operating in 1D mode. The scans were performed at room temperature, which it was around 22°C. Scans were taken on day 0, 1, 3, 7, 10, 13 and 15.

7.2.4 Effect of PVP on the formulations

Formulations were assessed on the FTIR. A small amount of the formulation was placed on the diamond crystal stage. The analysis was performed from 400-4000 cm^{-1} and resolution 16 scans. The dissolution on these formulations were also assessed on the T3, by producing a disc then analysed in GI buffer at pH 2 for 2 hours and take a reading every 30 seconds.

7.3 Results

7.3.1 DSC

The CBZ recrystallisation peak from melt was studied on the DSC by holding the sample isothermally at different temperature. In this section the starting time of the crystallisation was called as 'onset time' and the end of the crystallisation was called as 'endset time'.

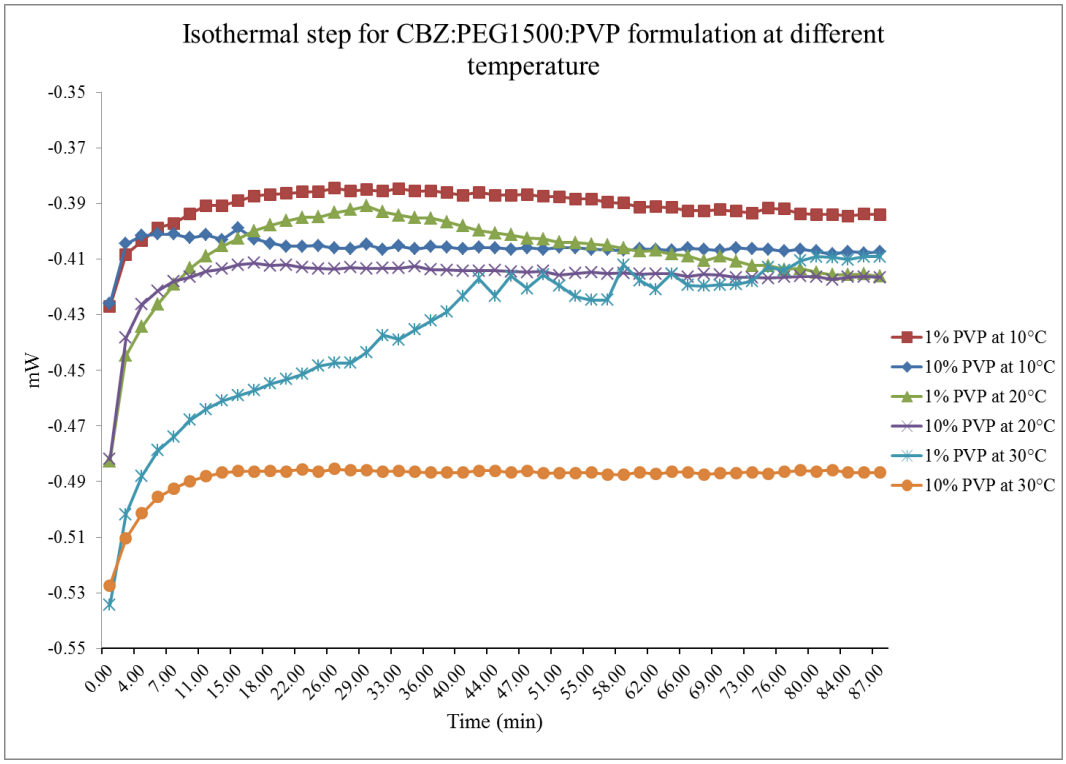

Figure 7.3-1 DSC isothermal step of CBZ: PEG 1500: PVP formulations

The figure above is used as an example to show the isothermal step in each DSC trace. The traces which have crystallisation have a higher mW (milliWatt) compared to the ones that it did not crystallise. The figure above clearly shows that the concentration of the PVP has an effect on decreasing the crystallisation of CBZ from the melt.

7.3.1.1 PEG 1500 based formulation

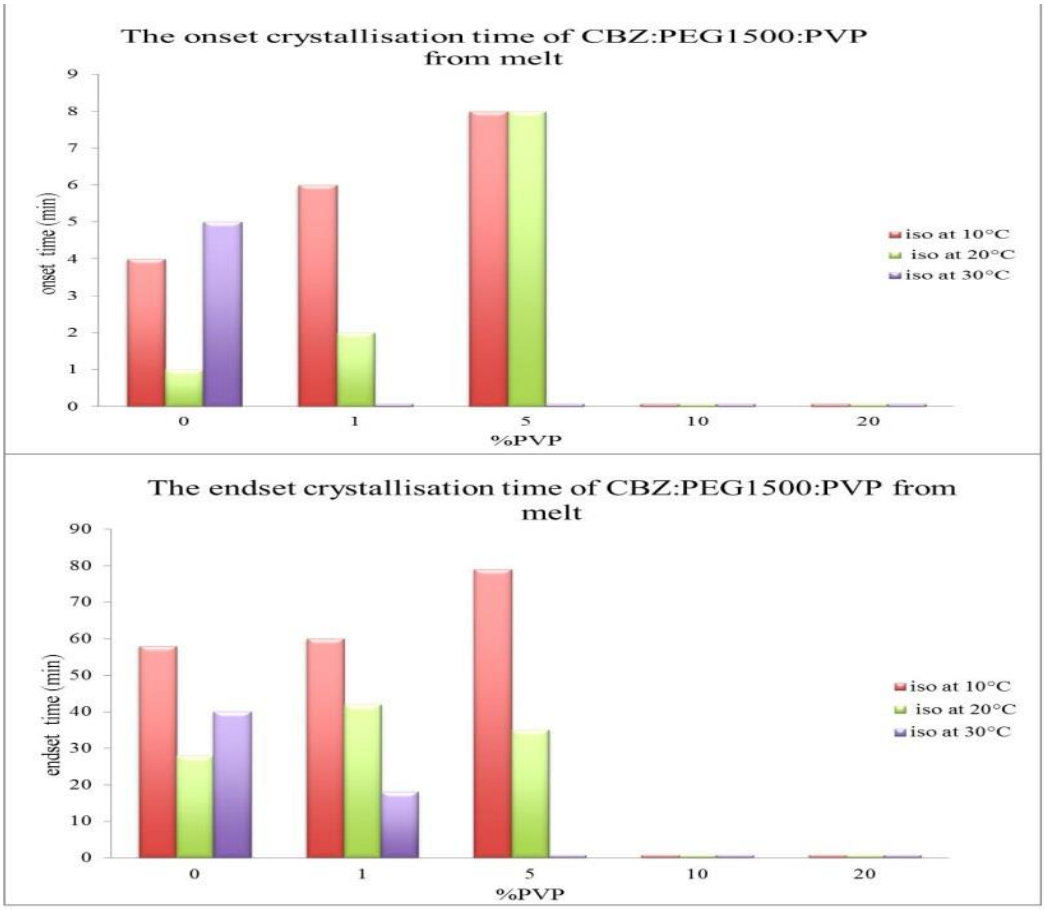

Figure 7.3-2 The crystallisation onset time of the different CBZ in PEG 1500 formulations.

(The graph shows no data for 10%PVP and 20% because they did not crystallise during the experiment time)

The isothermal data from PEG 1500 based formulation shows that the higher amount of PVP in the formulation the longer time it takes for the crystallisation to starts. The lower temperature also affects the crystallisation of the sample. The formulations containing 10 and 20% PVP did inhibit the crystallisation at 10, 20 and 30°C for the duration of the isothermal step which was 2 hours. The onset time for the 5%PVP formulation was the same at 10°C and 20°C but did not crystallise at 30°C.

The endset time of crystallisation decreased as the PVP increased in the formulations. At lower temperature the endset time was higher compared to the

higher temperature. The enthalpy at low temperature was lower than the higher temperature. For example the enthalpy of CBZ: PEG 1500: PVP 1% at 10°C was 5 J/g whereas at 20°C was 10 J/g.

7.3.1.2 PEG 4000 based formulation

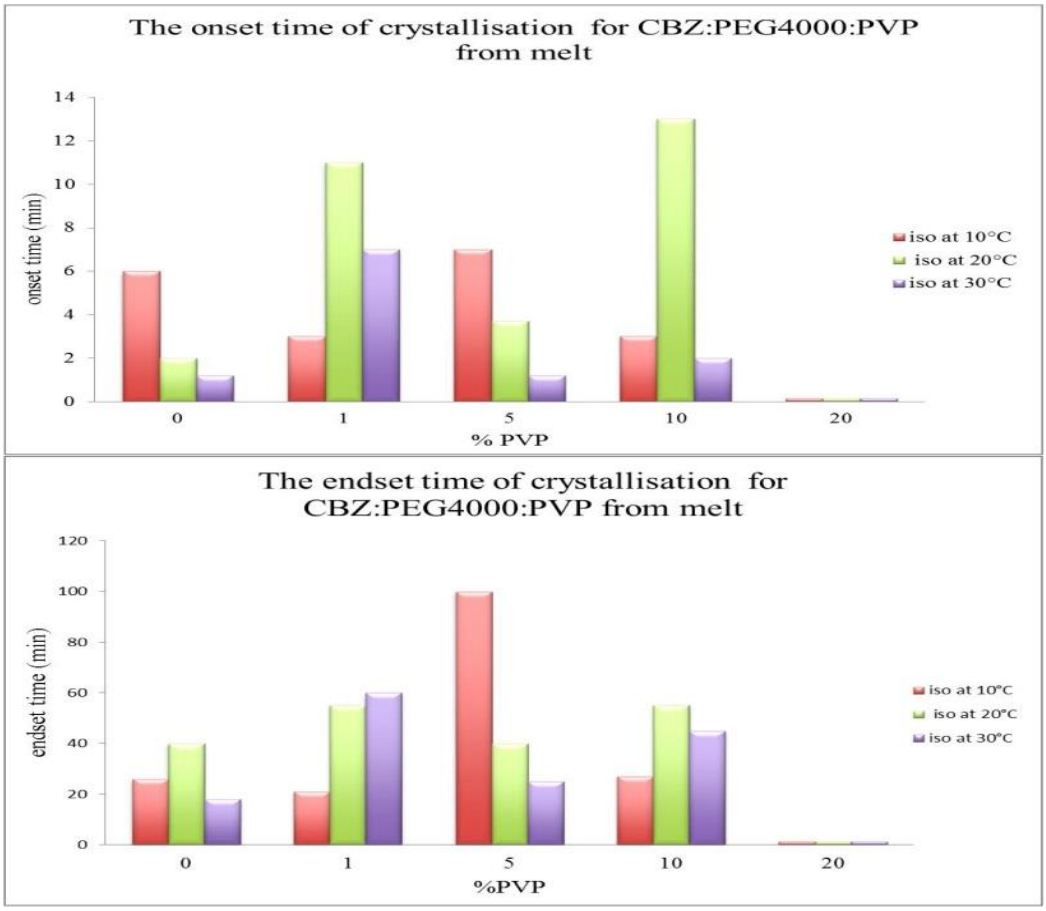

Figure 7.3-3 The crystallisation onset time of the different CBZ in PEG 4000 formulations.

For the PEG 4000 formulations only 20%PVP formulation did not crystallise during the experiment. The lower the temperature, the longer it took for the crystallisation to starts. The results did not follow a trend such as a higher PVP content higher onset time or endset time.

The onset time of the different PVP formulations was higher at the three temperatures used than the PEG alone based formulation. For the endset time, the 5%PVP formulation showed that the lower the temperature, the higher the endset whereas, the 1%PVP formulation did show the opposite.

7.3.1.3 PEG 6000 based formulation

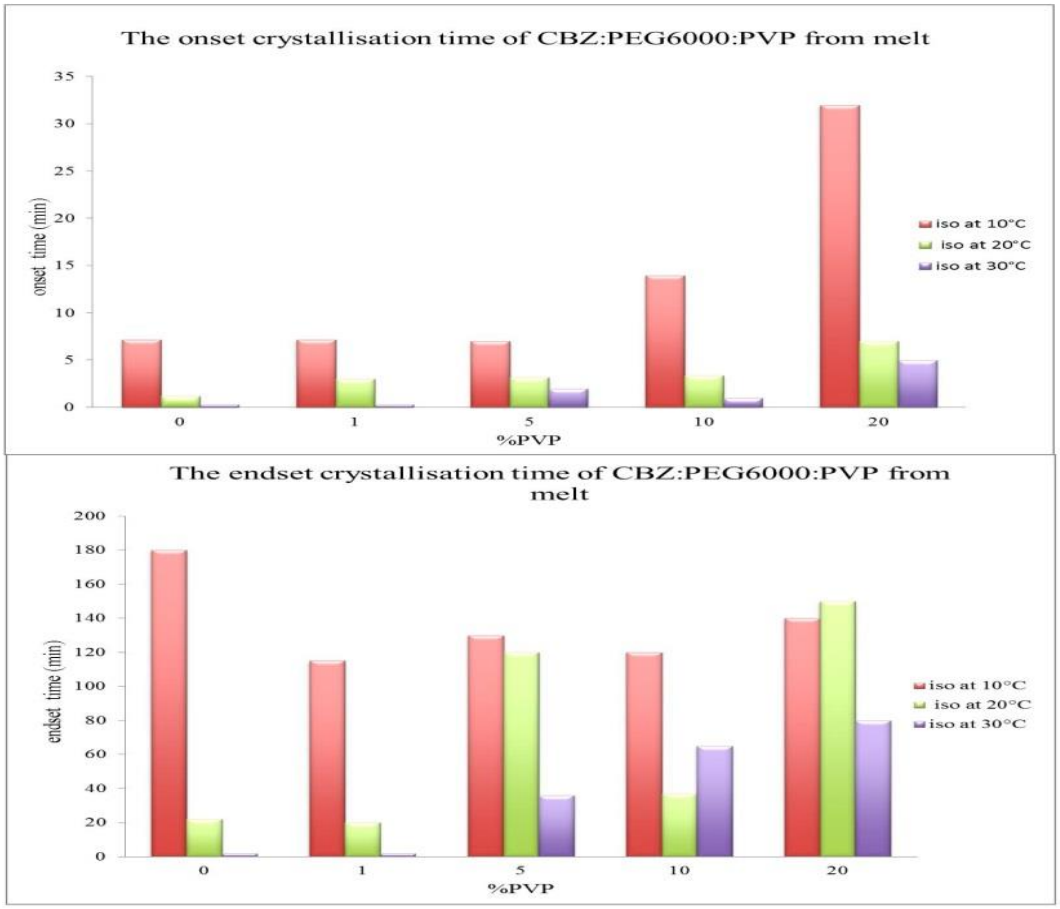

Figure 7.3-4 The crystallisation onset time of the different CBZ in PEG 6000 formulations.

For the PEG 6000 based formulations, when the samples were held isothermally at 20°C, the crystallisation starts immediately in the sample without PVP and after a few minutes in the 20%PVP samples.

The samples were held at 30°C, and some samples crystallised before the isothermal step such as the PEG6000 alone and the 1% PVP. The 5%PVP sample was held

isothermally at 30°C for 1hour a small crystallisation occurs after 2 minutes for 30 minutes and the enthalpy was 2.39 J/g. The 10% PVP formulation did show an immediate crystallisation when held at this temperature whereas, the 20% formulation took around 5 minutes to start crystallising.

In the PEG 6000 formulations, the onset time increased as the PVP concentration increased in the formulations when held at 10 and 20°C. The endset crystallisation time did not follow a trend; the endset time of most of the formulations was higher at low temperature than the higher temperature.

7.3.2 Hot stage microscopy

In this section, the formulations were heated to the melting point then quench cooled. The formulations then heated to the required isothermal temperature and held for 30 minutes then reheated to melting point. The images shown in this section are for the isothermal step onward.

7.3.2.1 CBZ: PEG 1500 isothermally held at 10°C with 5% PVP

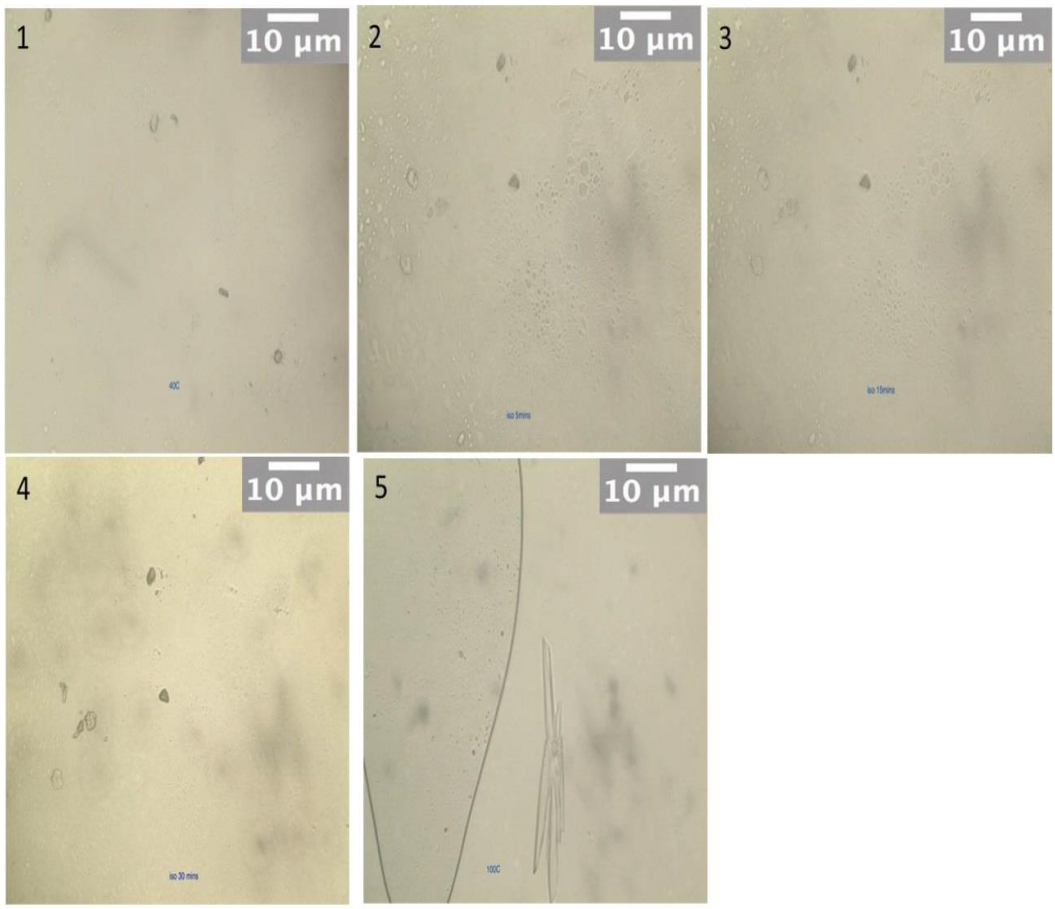

Figure 7.3-5 Hot stage microscopy of CBZ: PEG 1500: PVP (50: 47. 5:2. 5 w/w/w) held isothermally at 10°C

The figure above shows different picture been taken for the sample when held isothermally at 10°C. Picture 1 was taken during cooling step at 40°C where a few crystals were observed. Picture 2 was taken when the sample was held isothermally at 10°C for 5 minutes and no crystal growth was observed. Picture 3 shows no growth after 15 minutes as well as picture 4 which was taken at 30 mins. When the sample was reheated, crystals start to grow at 60°C and Picture 5 was taken at 100°C, where the crystals stopped growing.

The substitution of 5% of the PEG 1500 used with PVP did affect the crystal growth as no crystal growth was seen when the sample was held isothermally at 10°C for 30

minutes. When the sample was reheated to higher temperature the number CBZ crystal was very low compared to the formulation which does not contain PVP.

7.3.2.2 Isothermal hold at 20°C

Two CBZ formulations were investigated under hot stage microscopy held isothermally at 20°C after a quench cooling from melt, one sample with PEG and the other with 5% PVP (CBZ:PEG 6000 (50:50 w/w) and CBZ:PEG 6000:PVP (50:47.5:2.5 w/w/w). At the start of the experiment both samples were amorphous.

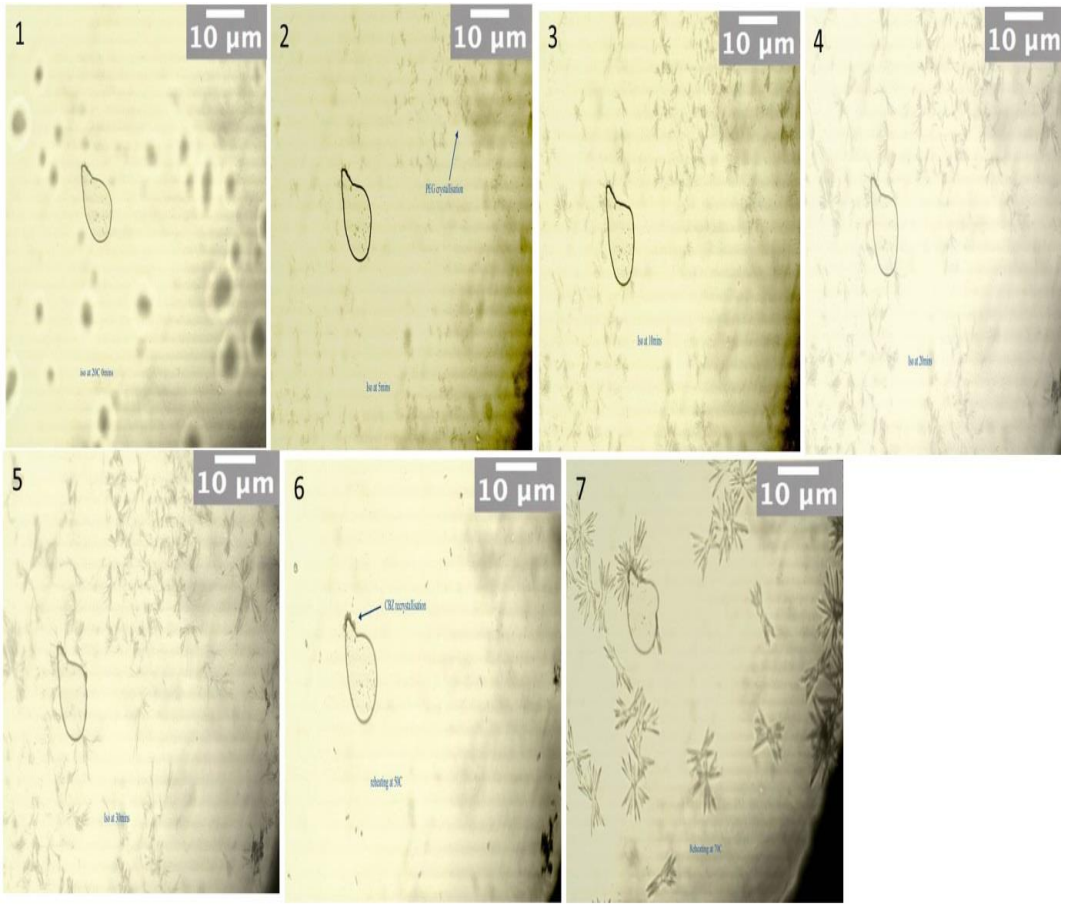

Figure 7.3-6 CBZ: PEG 6000 isothermally held at 20°C

The figure above shows the hot stage microscopy results of CBZ:PEG 6000 isothermally held at 20°C. Picture 1was taken at time 0 mins and no crystals can be seen. Picture 2 was taken at 5 minutes, the PEG starts to crystallise and form spherulites. Picture 3 was taken at 10 minutes and it shows more PEG crystals appearing. Picture 4 was taken at 20 minutes, only PEG crystals can be seen in the

CBZ:PEG sample. Picture 5 was taken at 30 minutes shows more PEG crystals are forming. Picture 6 was taken during the reheating step at 50°C, PEG crystals melts then CBZ nuclei starts to appears. Picture 7 was taken at 100°C shows more CBZ crystals been formed.

The figure below shows the hot stage microscopy of CBZ:PEG 6000:PVP sample with 5% PVP.

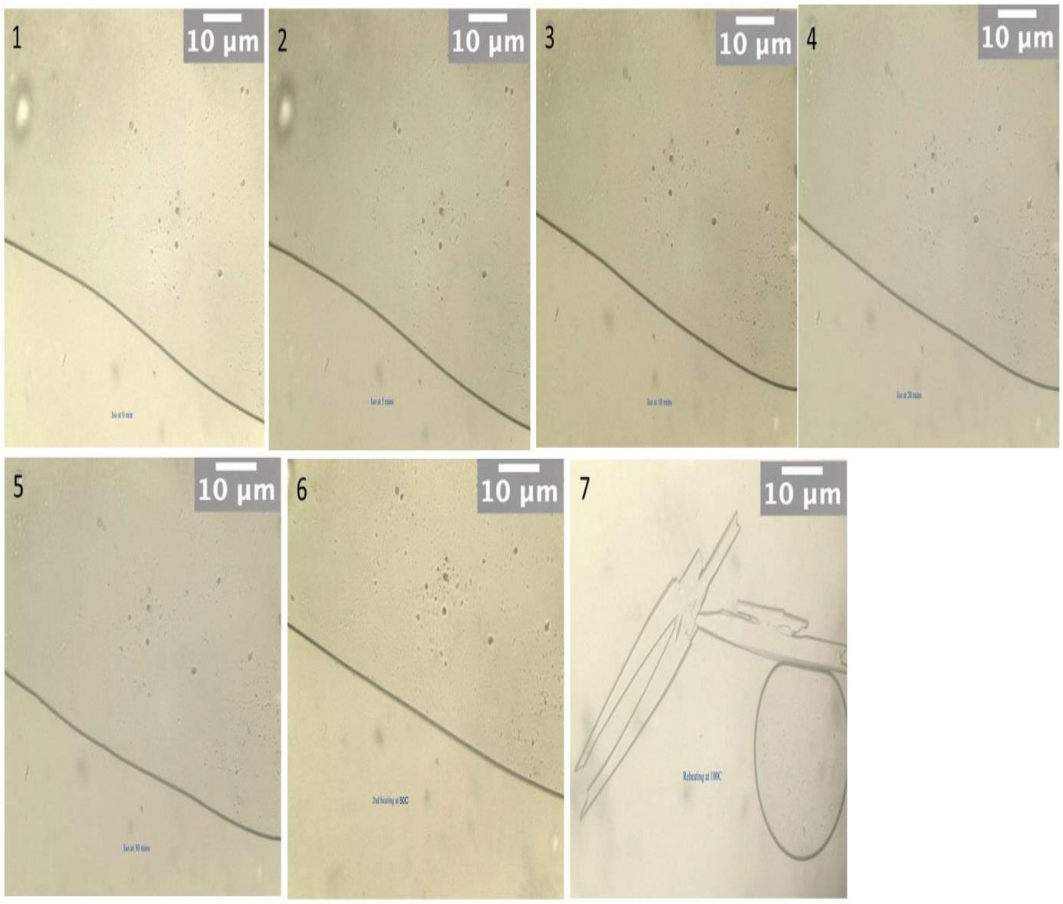

Figure 7.3-7 Hot stage microscopy of CBZ: PEG 6000: PVP isothermally held at 20°C

In the formulation containing PVP, no crystals growth (CBZ or PEG) was observed during the isothermal step (image 1 to 5). When the sample was reheated to 50°C no growth was also observed (image 6). Then when the temperature reaches 80°C a few CBZ nuclei appeared. Image 7 was taken at 100°C where the crystal growth stopped.

7.3.2.3 Isothermal hold at 30°C.

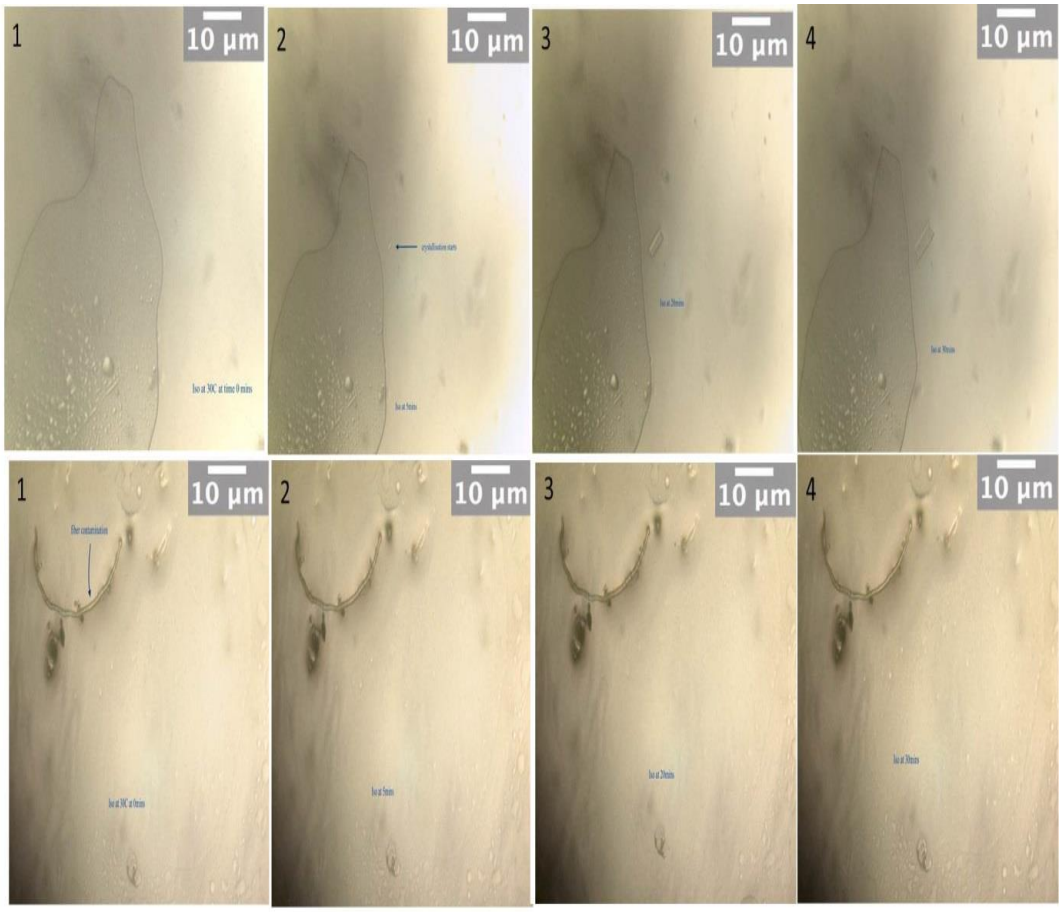

Figure 7.3-8 Isothermal hot stage microscopy of CBZ: PEG 1500 with 1 and 10% PVP

The figure above shows the CBZ: PEG 1500: PVP (50:49.5:0.5 (1%PVP top row) and 50:45:5 w/w/w (10% PVP lower row)) isothermally stored at 30°C after quench cooling. Picture 1 was taken at time 0 minutes and both formulations still amorphous as no crystals can be seen. Picture 2 was taken after 5 minutes, one crystal start to appear in the sample with 1% PVP. Picture 3 was taken at 10 minutes where the crystal in the 1% PVP formulation was growing with time and no growth was observed in the 10%PVP formulation. Picture 4 was taken after 30 minutes, in the 1% PVP formulation the crystal gets bigger and not crystal growth was observed in the 10% PVP formulation. When the both samples were reheated to higher temperature, the 1% PVP formulation showed more crystals been formed,

whereas, in the 10% PVP formulation no growth has been observed even at high temperature.

The results show that when the formulations were held at 30°C, crystallisation can start in the formulation with low PVP content. Although crystallisation has been observed in the 1% PVP formulation but the number of nuclei was very low compared to the formulation without PVP. At 1% PVP, no PEG crystals can be seen during the isothermal step, this is due to PVP inhibited the PEG crystallisation in the formulation.

Samples of CBZ: PEG 6000 and CBZ: PEG 4000 with 20% PVP were carried out under the hot stage microscopy and the results did not show crystallisation when held isothermally at 30°C for 30 minutes.

7.3.3 XRPD

7.3.3.1 Variable temperature XRPD

The PEG 4000 variable temperature XRPD data shows that PEG 4000 has two peaks. One at around 19° it looks as a sharp peak and the second around 24°, which is broad. When PEG was cooled to -20°C from melt at 30°C/min cooling rate it crystallise and the same peaks appears.

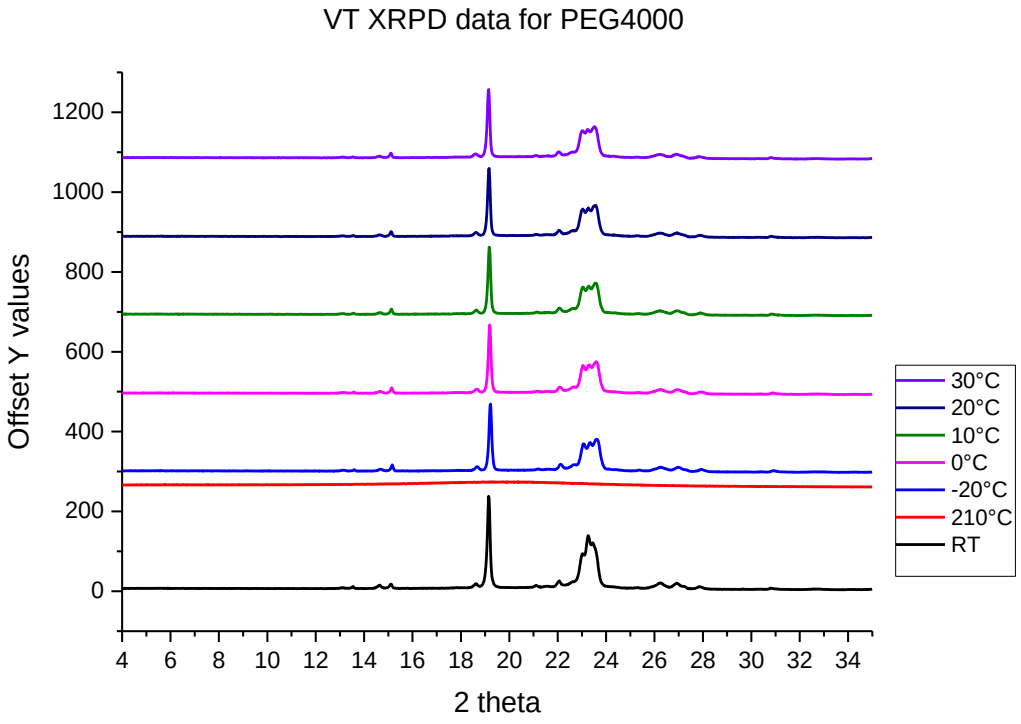

Figure 7.3-9 VT XRPD of PEG 4000

For the CBZ sample alone, the XRPD data shows that the sample at room temperature was CBZ form III. When cooled from the melt, the sample shows a few peaks where they correspond to iminostilbene, which is a CBZ impurity. When the temperature was heated to 100°C, the sample crystallise to CBZ form I.

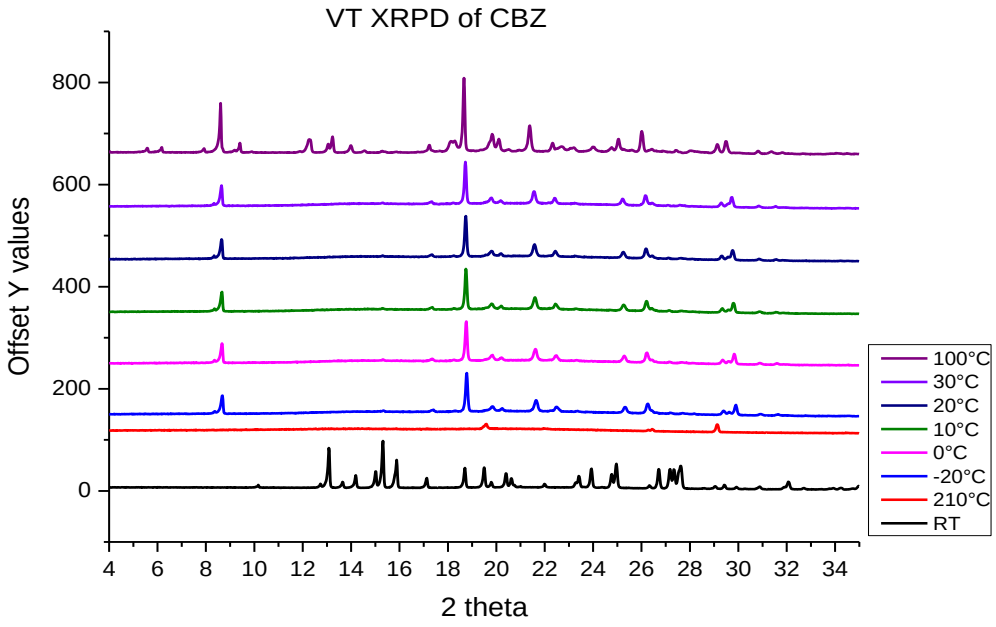

Figure 7.3-10 VT XRPD of CBZ

The graph below shows the XRPD pattern of CBZ at room temperature, after quench cooling at 100°C and the impurity iminostilbene.

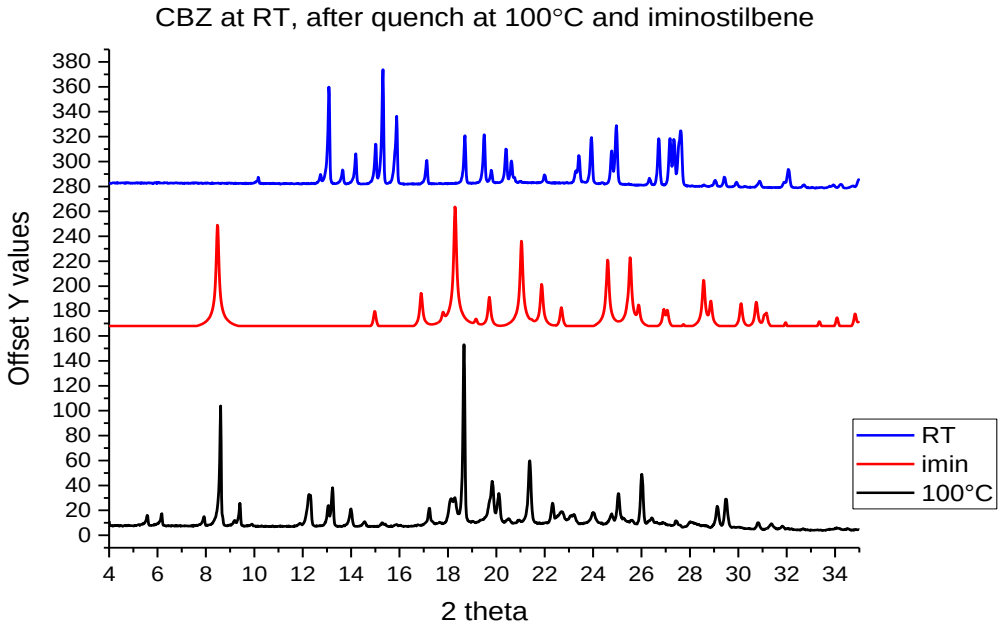

Figure 7.3-11 XRPD pattern of CBZ, CBZ after quench cooling and iminostilbene

Variable temperature XRPD of CBZ: PEG 4000 solid dispersion shows that CBZ crystals in the formulation at room temperature exist as a mixture of form II and III. When the sample was heated to the melting state, it changes to amorphous form. The sample stays in the amorphous form during cooling to -20°C and when reheated to 30°C. The sample starts to crystallise at 40°C into form II. PEG 4000 crystallise at 20°C then the PEG peaks disappears at 60°C, which, indicates that the PEG has melted.

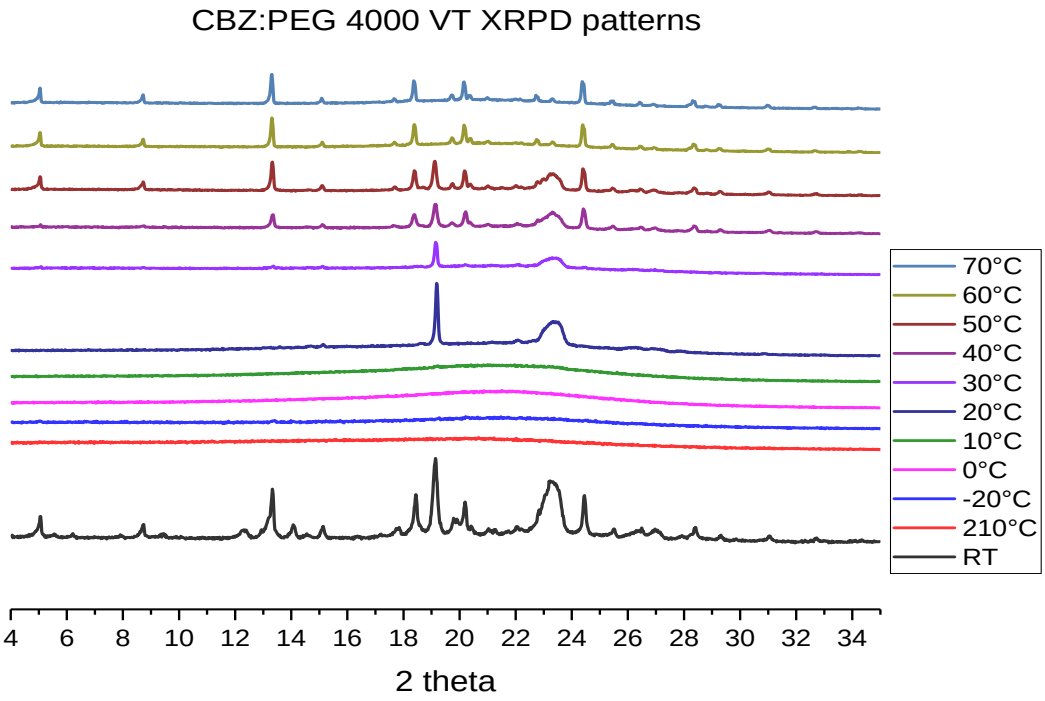

Figure 7.3-12 VT XRPD patterns of CBZ: PEG4000

When 5% PVP was added to the CBZ: PEG 4000 formulation, the CBZ crystals in the formulation at room temperature was form III. After the melt step, the sample stayed amorphous until the temperature reached 50°C. The PEG 4000 in the formulation crystallised at 30°C then melts at 50°C. The PVP did affect the crystallisation of the sample.

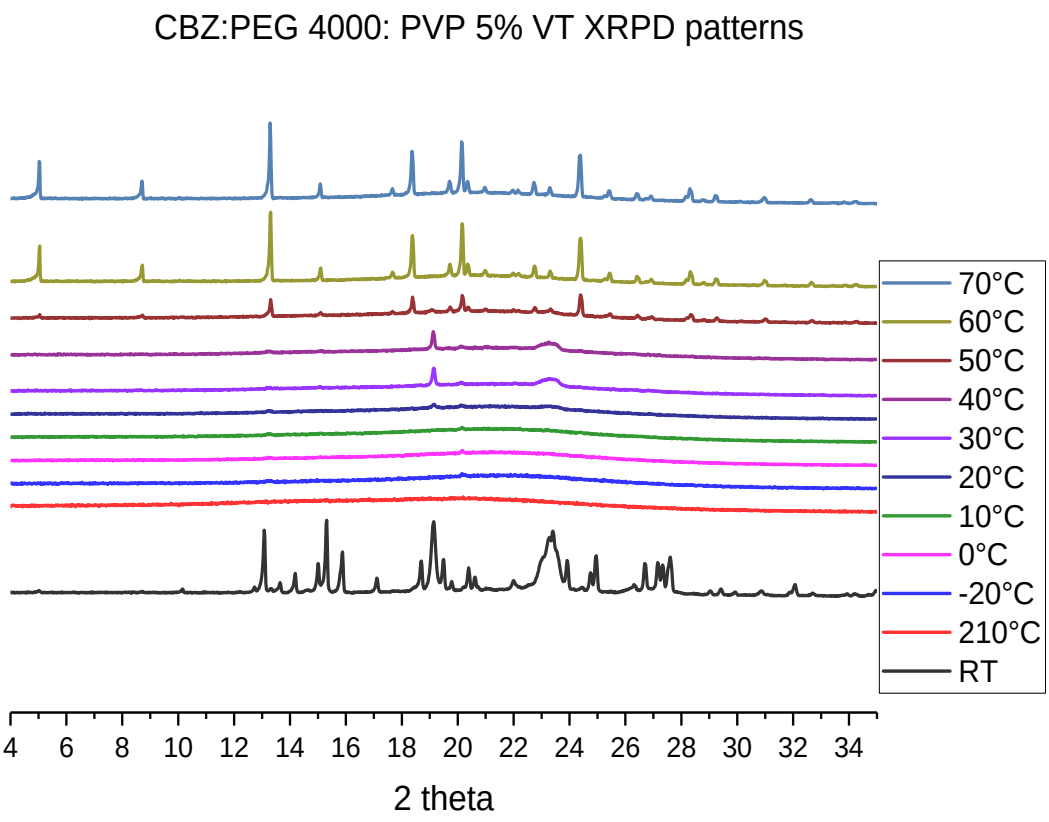

Figure 7.3-13 VT XRPD patterns of CBZ: PEG4000: PVP 5%

The variable temperature XRPD data for CBZ: PEG4000 with 10% PVP shows that the starting material was crystalline and the CBZ crystals were form III. When it is heated then quench cooled, CBZ stayed amorphous until 50°C. At 60°C, crystals start to form and at 70°C CBZ crystals were form II. PEG 4000 in the formulation crystallised at 20°C and melts at 50°C.

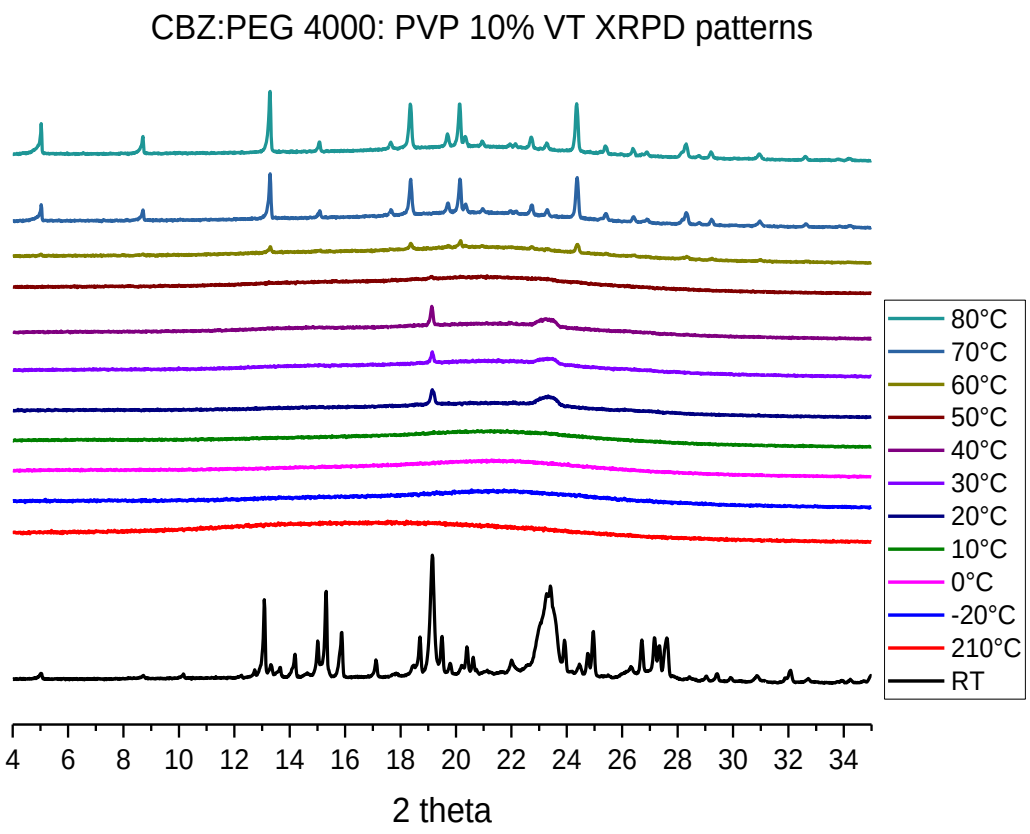

Figure 7.3-14 VT XRPD patterns of CBZ: PEG 4000: PVP 10%

For the CBZ: PEG4000: PVP 20% formulation, the XRPD patterns showed that the CBZ crystals in formulation at room temperature were form II. After the melt the sample stayed amorphous until 50°C, then peaks starts to appear. PEG 4000 in the formulation crystallised at 30°C, then melts at 50°C as no PEG peaks were observed at 50°C.

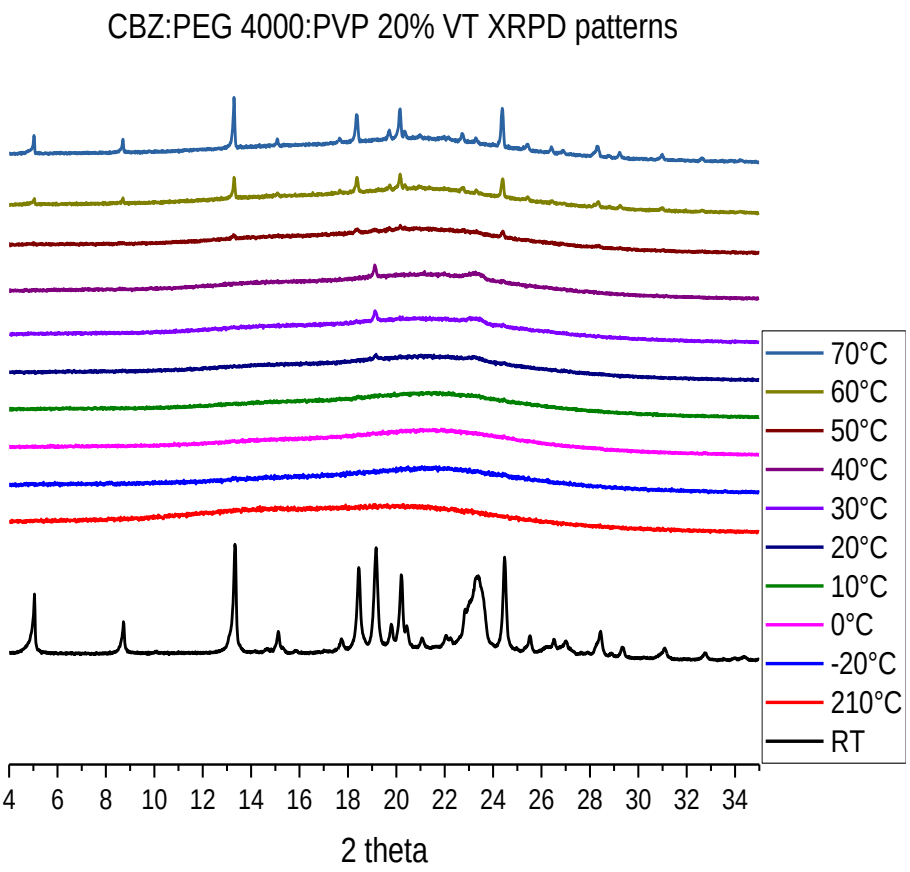

Figure 7.3-15 VT XRPD patterns of CBZ: PEG 4000: PVP20%

7.3.3.2 XRPD stability experiment

The stability experiment was carried out on CBZ: PEG 4000 and with 1%, 5%, 10% and 20% PVP.

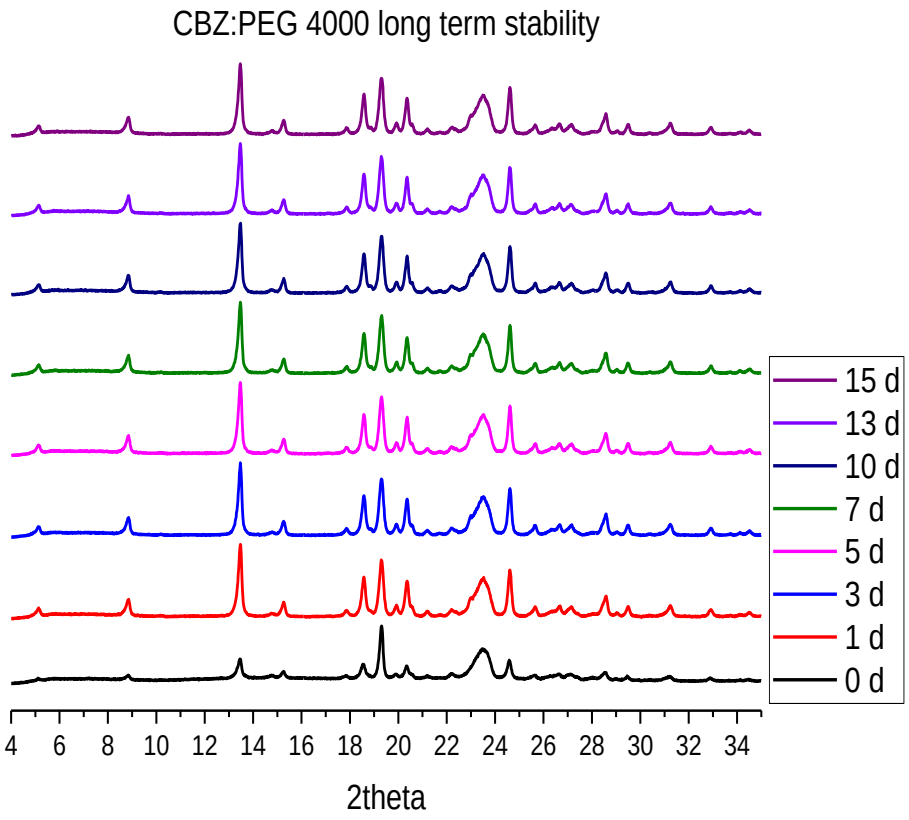

Figure 7.3-16 Stability XRPD pattern of CBZ: PEG 4000

The CBZ: PEG 4000formulation at day 0 showed some crystalline pattern. At day 1, the formulation was crystalline and the CBZ crystals are form II.

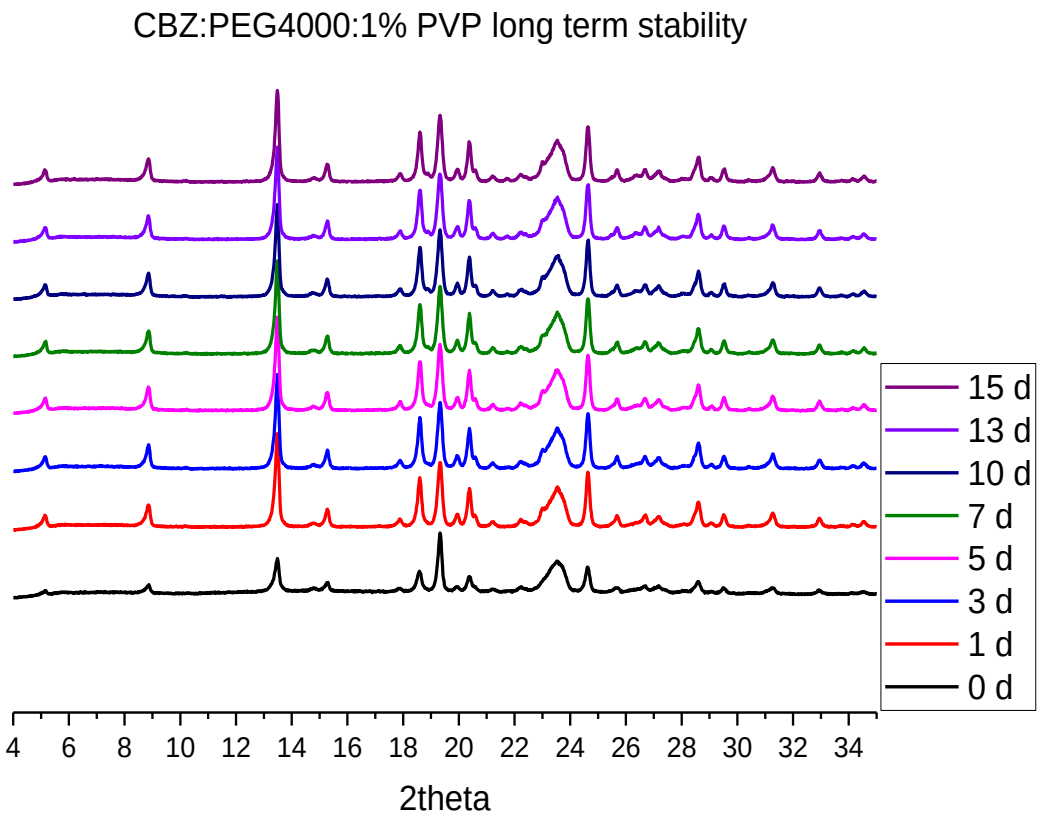

Figure 7.3-17 Stability XRPD patterns of CBZ: PEG 4000: PVP 1%

The substitution of 1% of PEG with PVP did not hugely affect the crystallisation of the formulation. At day 0, the formulation was crystalline.

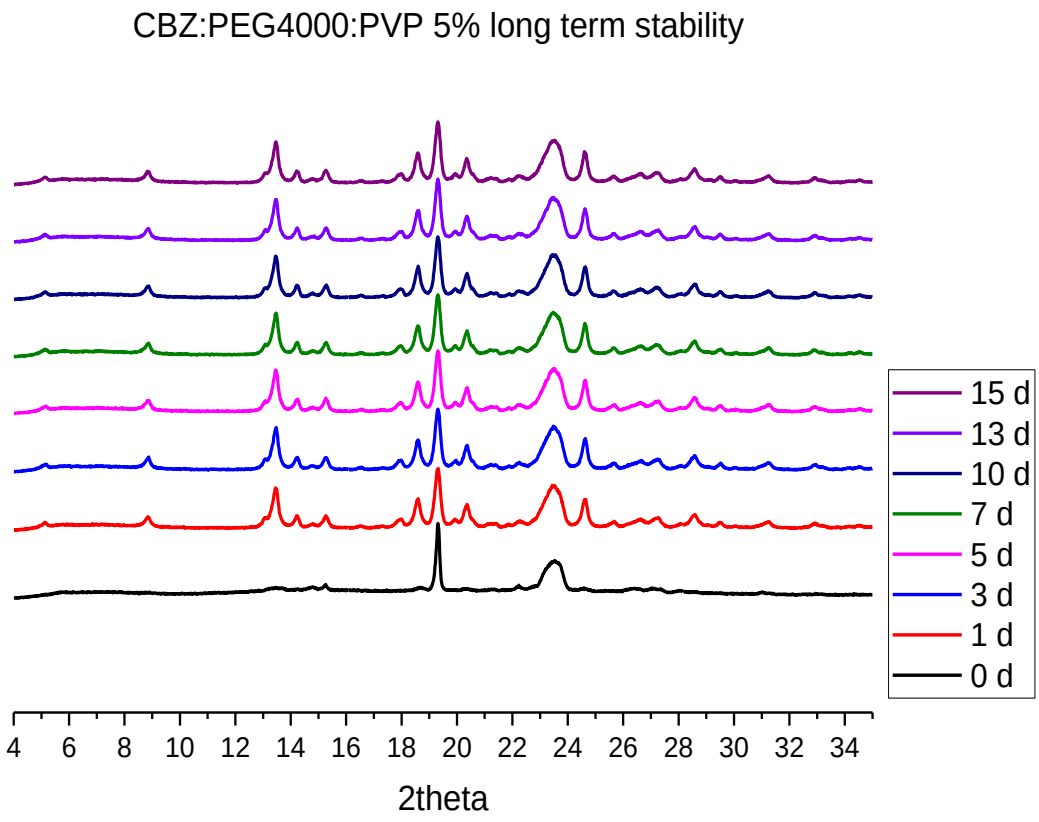

Figure 7.3-18 Stability XRPD patterns of CBZ: PEG 4000: PVP 5%

At 5%PVP, the formulation stayed amorphous at day 0, only PEG 4000 crystallised. At day 1 the formulation was crystalline.

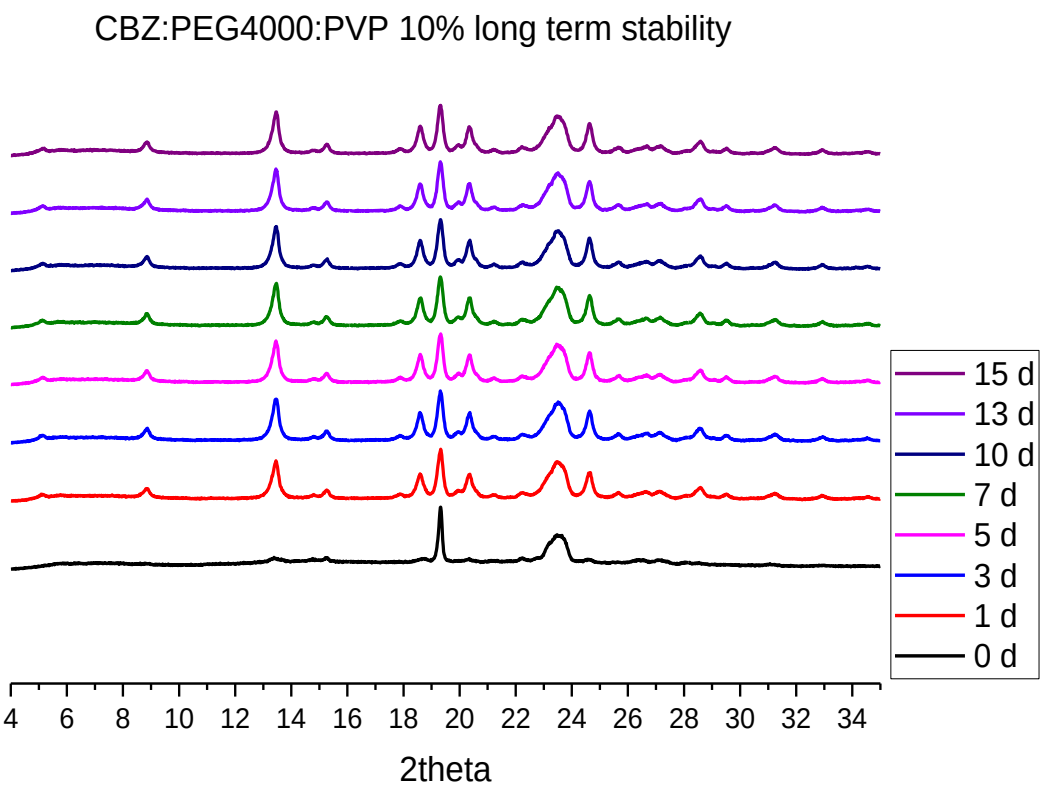

Figure 7.3-19 Stability XRPD patterns of CBZ: PEG 4000: PVP 10%

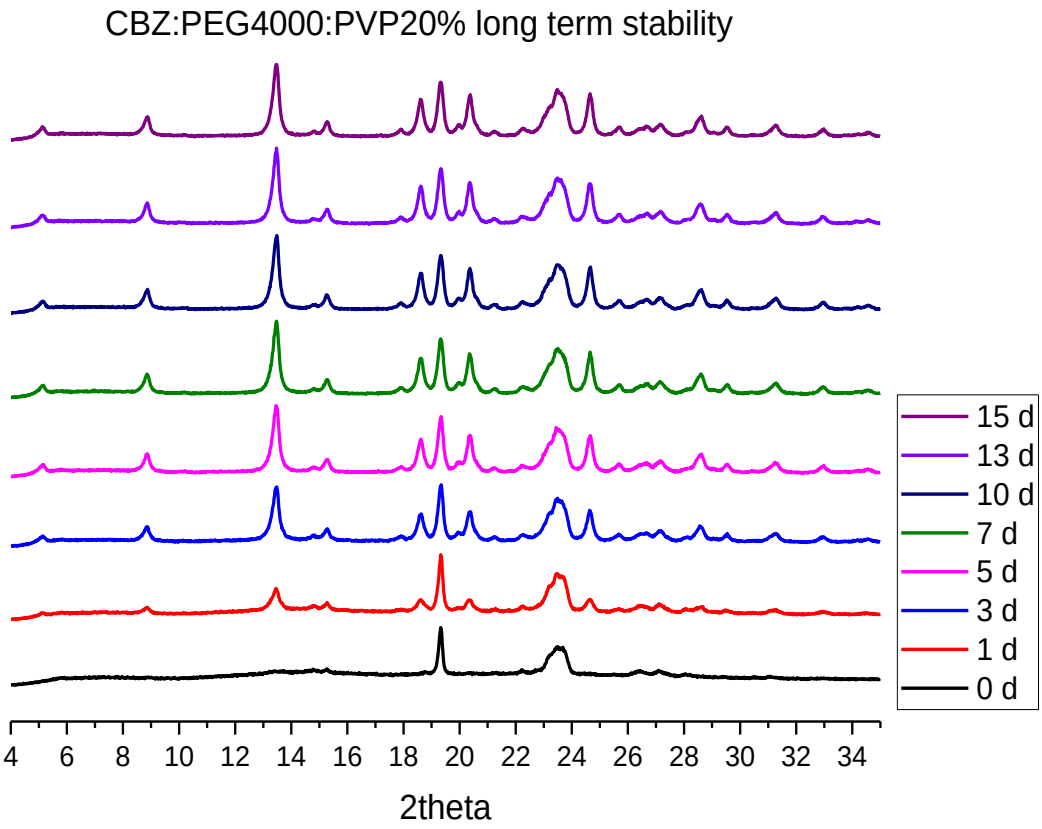

Figure 7.3-20 Stability XRPD patterns of CBZ: PEG 4000: PVP 20%

For the 10% and 20% PVP formulations, the crystallisation starts at day 1 but it takes until day 3 to be fully crystalline as the intensity of some of the peaks was low.

7.3.4 Degree of crystallinity in the amorphous samples

The degree of crystallinity was investigated using XRPD by taking a pattern at room temperature then melted and quench cooled. The sample was reheated to 25°C and held isothermally for 24 hour with a scan been taken every hour. The figures below show some of the X-ray patterns of the CBZ: PEG 4000 and PVP at different concentration at different time points.

7.3.4.1 CBZ: PEG 4000

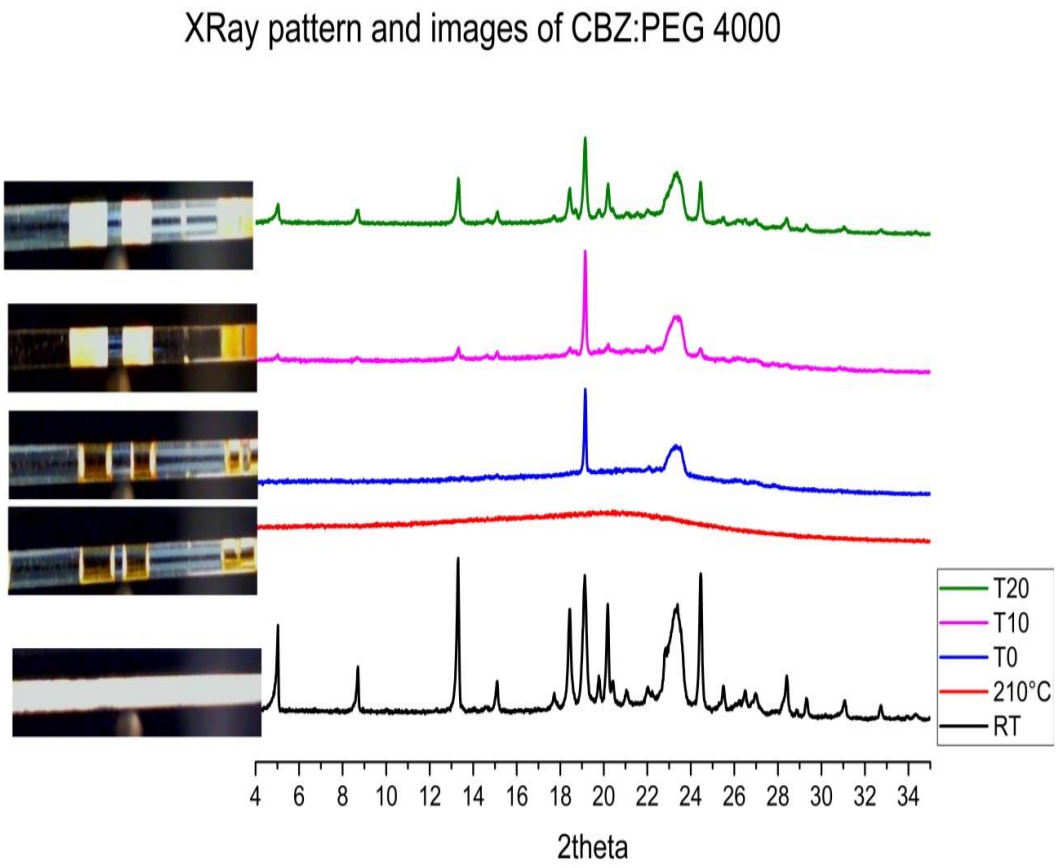

Figure 7.3-21 CBZ: PEG 4000 isothermal X-ray pattern

At room temperature the CBZ crystals within the PEG matrix exists as crystals and it corresponds to form II. At T0, when the sample reaches 25°C, the PEG had already been crystallised and at T10 hours the CBZ crystals starts to form. The peak at 13.5° is the largest peak in the CBZ pattern therefore the % crystallinity (graph) was calculated based on it.

7.3.4.2 CBZ: PEG 4000: PVP 1%

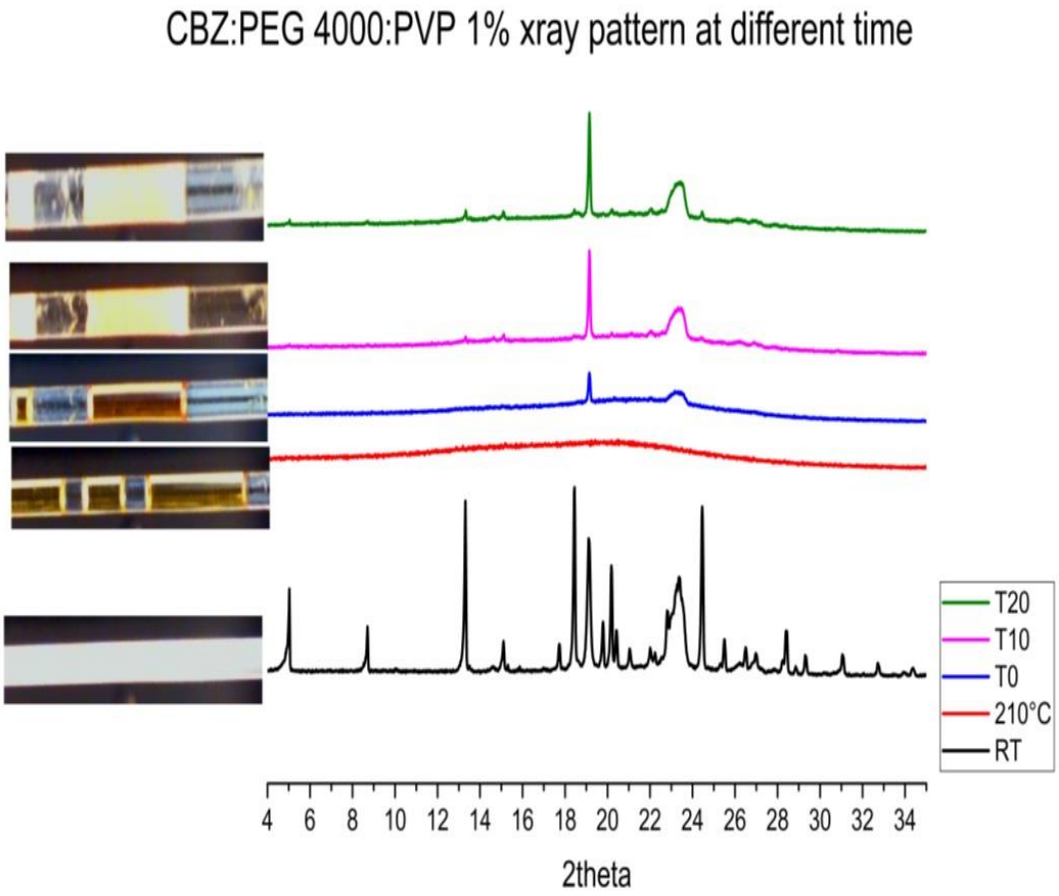

Figure 7.3-22 CBZ: PEG 4000: PVP 1% isothermal X-ray pattern

The figure above shows that the CBZ at room temperature is crystalline and when held isothermally the PEG crystallises at T0 but the intensity of the peak is lower compared to the formulation with no PVP. The addition of 1% PVP to the formulation did inhibit the CBZ crystallisation as it did take longer for the CBZ peaks to appear compared to the formulation with no PVP as shown at T20 hours the CBZ crystalline pattern starts to appear.

7.3.4.3 CBZ: PEG 4000: PVP 5%

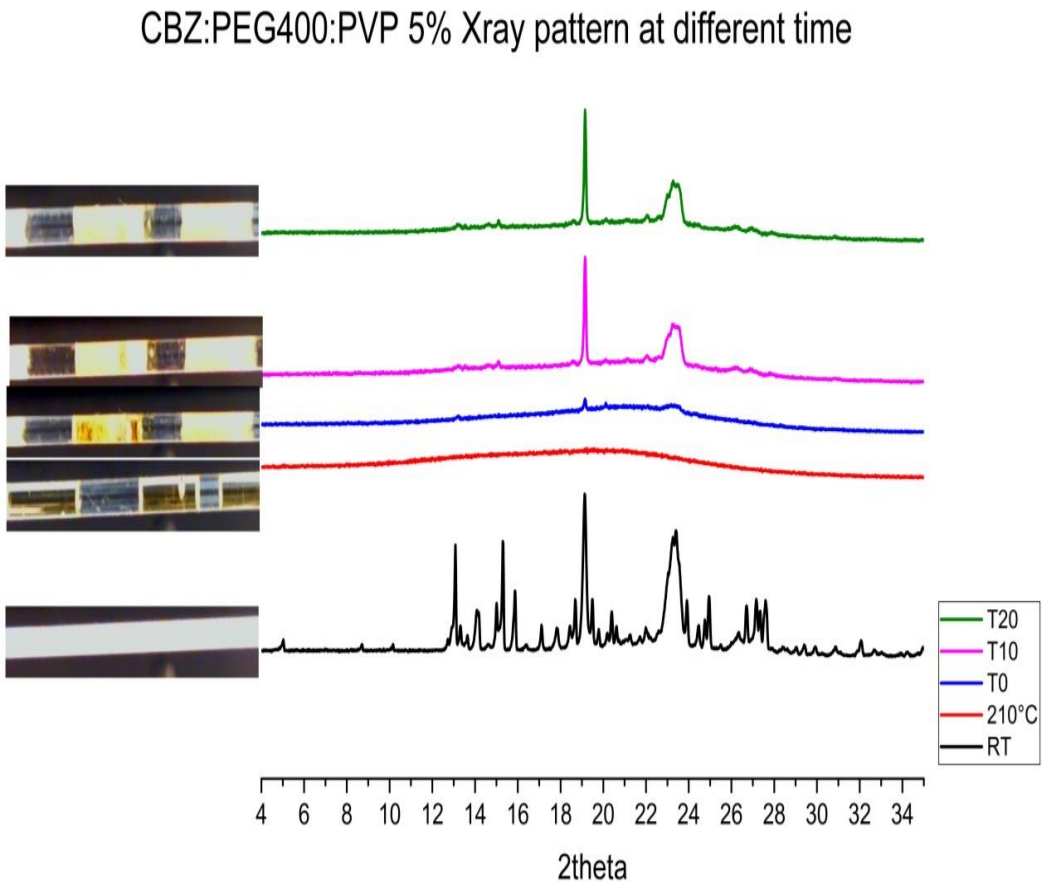

Figure 7.3-23 CBZ: PEG 4000: PVP 5% isothermal X-ray pattern

At 5%PVP in the formulation it did take longer for PEG to fully crystallise and the CBZ crystals takes over a 24 hour to grow and the growth rate was reduced.

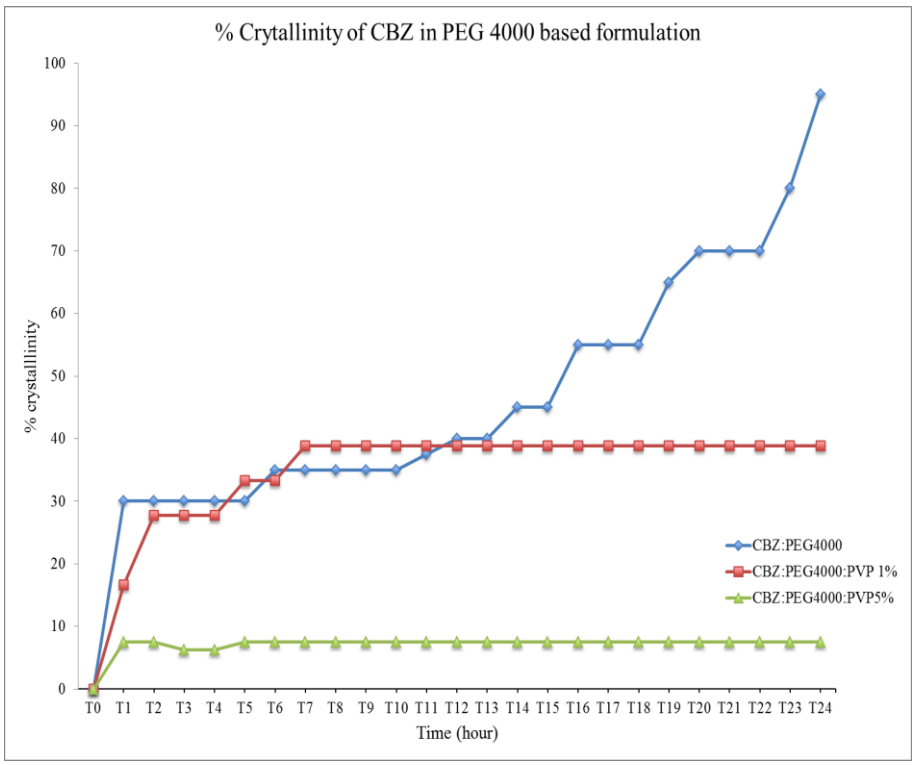

Figure 7.3-24 %Crystallinity of CBZ within PEG4000 formulation

The figure above summarise all the three formulations and compare the % of CBZ crystallinity in the formulation. In the formulation with no PVP the CBZ is 100% crystalline in the formulation after 24 hour from melts whereas when only 1% of PVP added to the PEG less than half of the CBZ are crystalline and the rest are still in amorphous state. At only 5% PVP a very low CBZ crystalline content in the formulation at the beginning of the experiment and it was steady for a long period.

This experiment was repeated with PEG 1500 and PEG 6000 to compare the effect of PEG molecular weight.

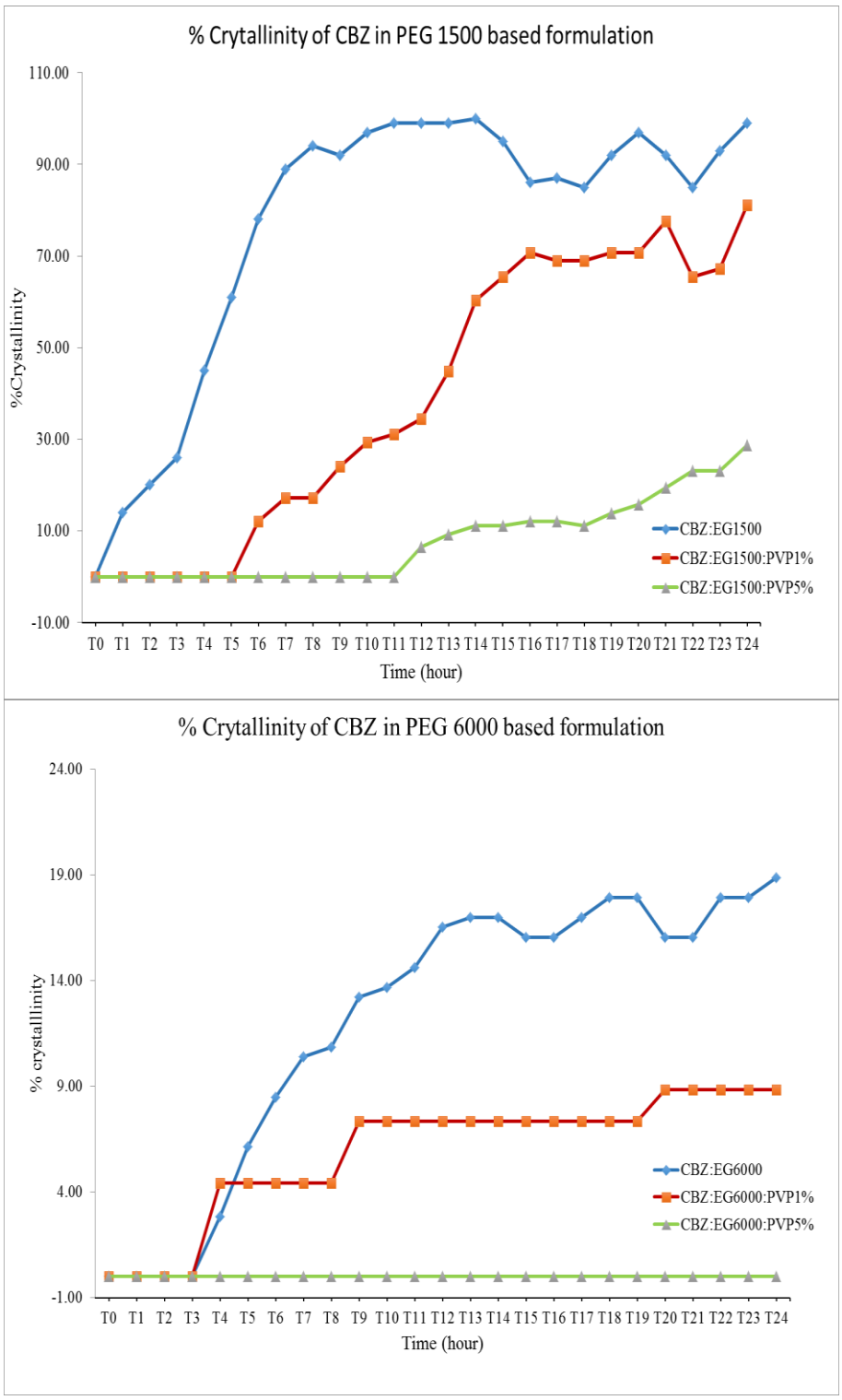

Figure 7.3-25 % Crystallinity of CBZ in PEG 1500 and 6000 formulations

The figure above shows % crystallinity of CBZ in PEG 1500 and PEG 6000 with different PVP concentration in the formulations. In the formulation with PEG 1500

the CBZ fully crystallised within 10 hour and the addition of PVP did inhibit the crystallisation but it did not stop it whereas for the PEG 6000 formulation the % crystallinity was low in the formulation with no PVP and it did increase slowly. In the formulations with PVP the CBZ % crystallinity did decrease and the sample with 5%PVP no CBZ crystal peaks were observed and the PEG peak intensity was lower than the other PEG based formulations. The PEG molecular weight and the PVP concentration play an important role in inhibiting CBZ recrystallisation from the melt.

7.3.5 FTIR

The FTIR spectra of the different formulations was carried out to check if there is a difference a between the different formulations as the PVP concentration increases in the formulations.

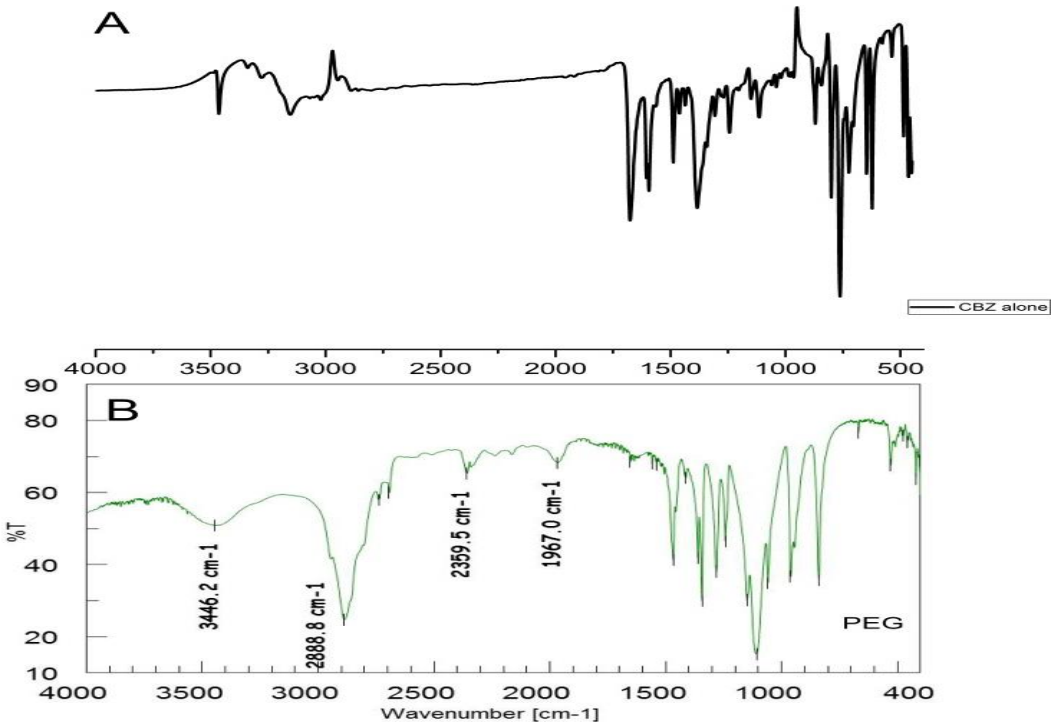

Figure 7.3-26 FTIR spectra of CBZ and PEG alone

(A-CBZ FTIR spectra, B- PEG FTIR spectra)

The Figure 7.3-26 shows that the CBZ has a peak around 3500 cm^{-1} and 3200cm^{-1} corresponds for N-H vibration of CBZ and 1670 cm^{-1} CO-R- vibration. Whereas PEG has a peak around 2800 cm^{-1} corresponds to the C-H stretching of PEG, and the one around 1110 cm^{-1} corresponds to CO ether of the PEG.

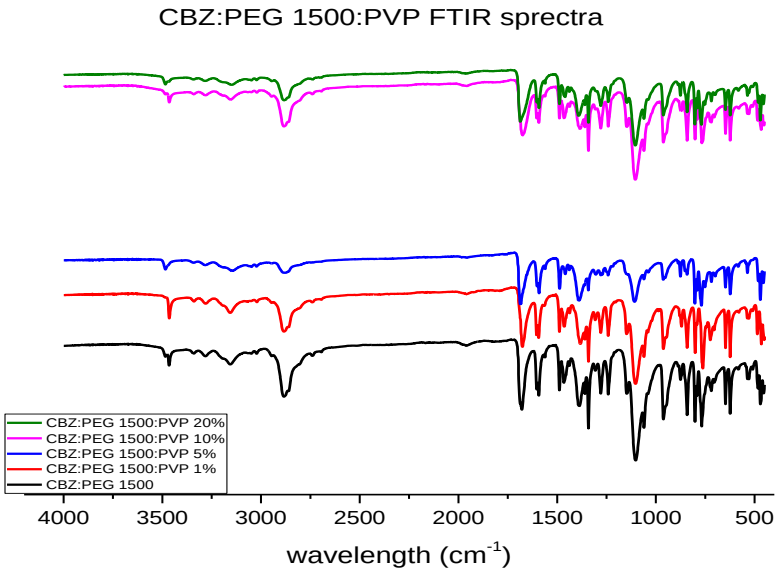

Figure 7.3-27 FTIR spectra of CBZ: PEG 1500: PVP formulations

The figure above shows that the main CBZ peaks are still present and they did not shift on the other hand the PEG peaks they are not present which indicates that the PEG is either interacting with the CBZ or with the PVP by forming hydrogen bonding with them.

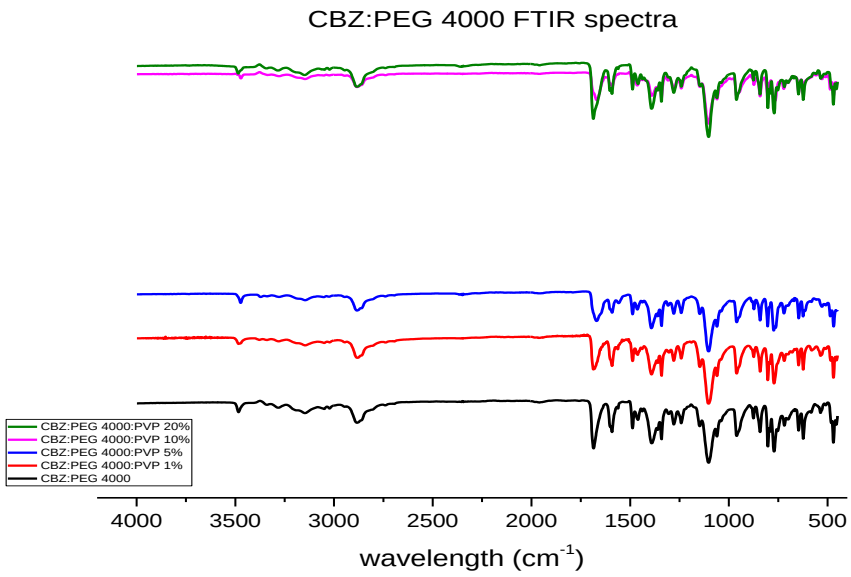

Figure 7.3-28 FTIR spectra of CBZ: PEG 4000: PVP formulations

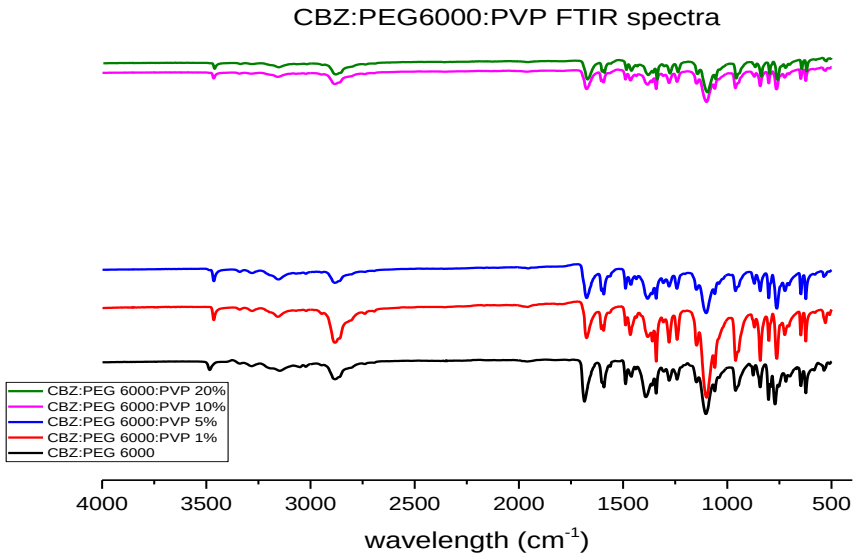

Figure 7.3-29 FTIR spectra of CBZ: PEG 6000: PVP formulations

The results from the PEG 4000 and 6000 are very similar to the PEG 1500; therefore the PEG molecular weight does not affect the CBZ.

7.3.6 Dissolution

The % release of CBZ in the different PEG and PVP formulation was assessed to understand if the concentration of PVP would enhance the dissolution.

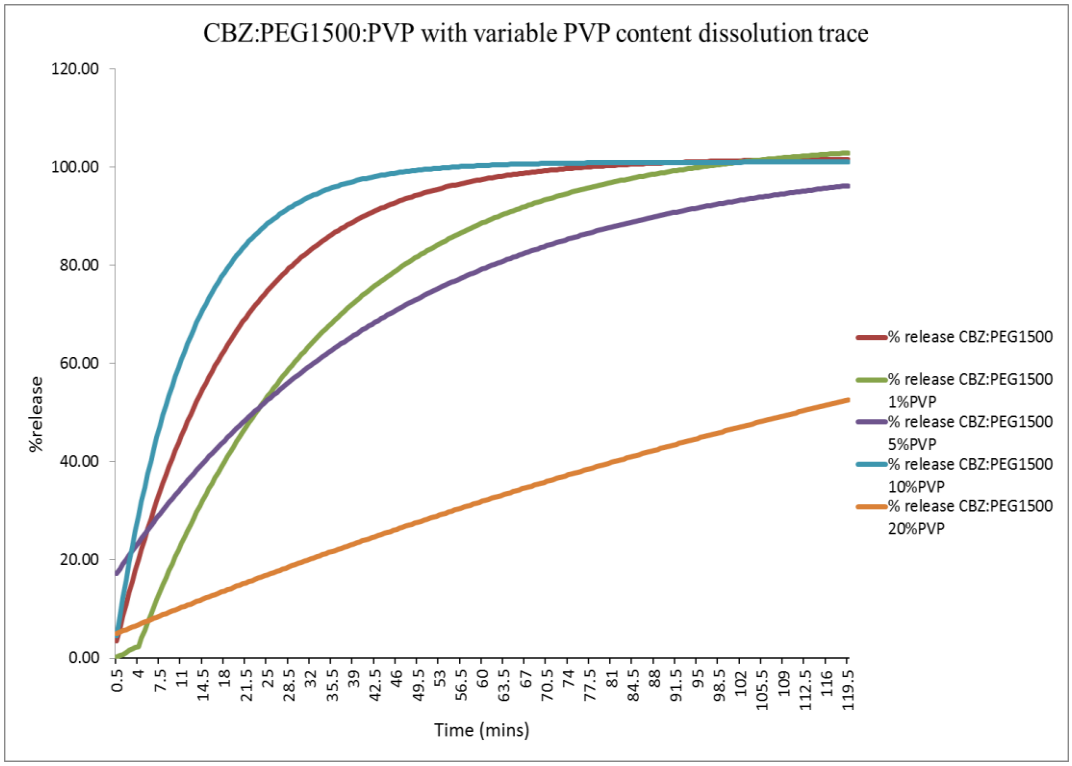

Figure 7.3-30 CBZ % release in PEG 1500 formulation

The CBZ: PEG 1500, CBZ: PEG 1500: PVP 10% and CBZ: PEG 1500: PVP 1% formulations showed a 100% release in less than 1 hour. Whereas the CBZ: PEG 1500: PVP 20% showed the lowest release profile.

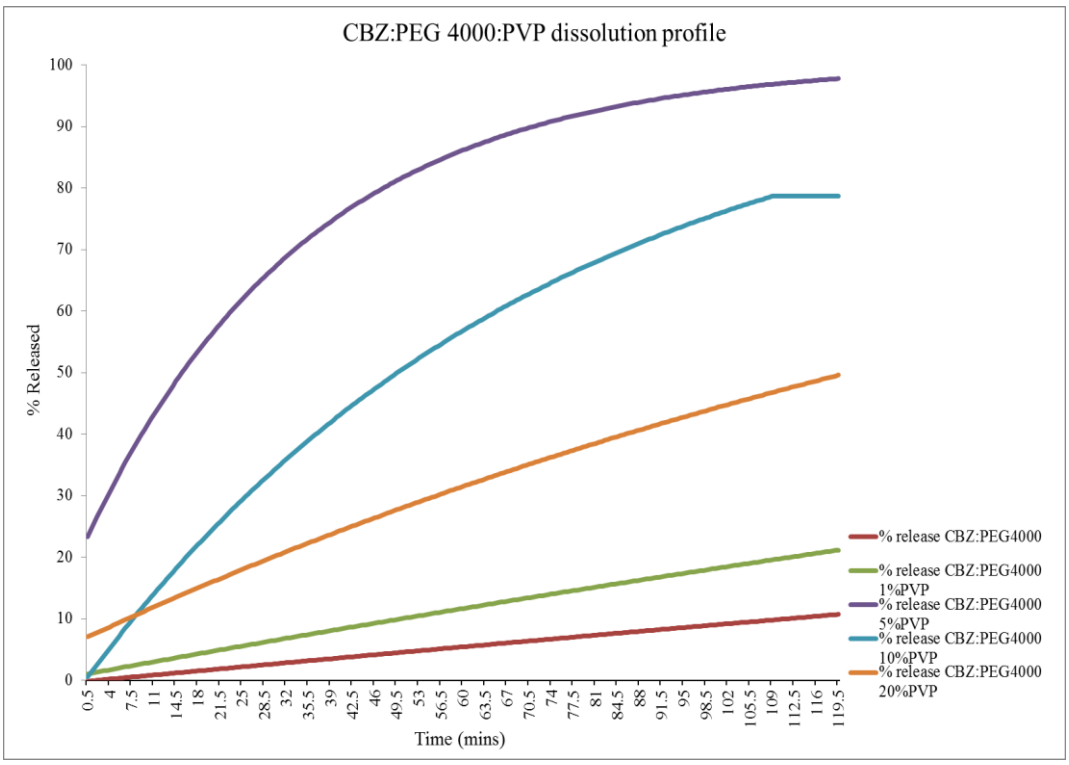

Figure 7.3-31 CBZ % release in PEG 4000 formulation

The % release from PEG 4000 did show different trend than the PEG1500. The 5 and 10% PVP formulations showed the highest release but it did take up to 2 hours to achieve 100% release. The formulations with the PVP showed a better release than the formulation with PEG only.

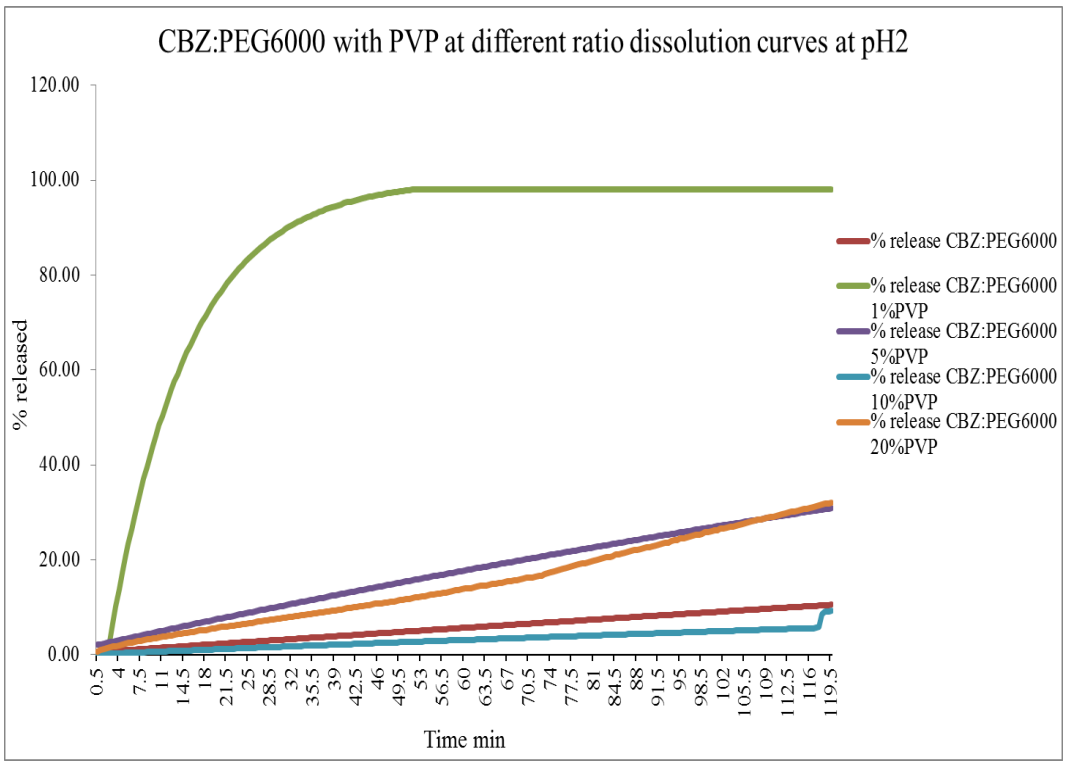

Figure 7.3-32 CBZ % release in PEG 6000 formulation

The 1% PVP formulation with PEG 6000 showed the highest % release, which it was 100% in the first hour. The release profile from 5 and 20% PVP formulations was higher than the release profile from CBZ: PEG 6000 alone and 10%PVP.

The CBZ % release from the different formulations with the different PEG molecular weight did not follow the same trend, which indicates that the lower PEG molecular was better in regard to the release profile. The concentration of PVP in the formulations did not affect the release profile as some formulation with low PVP content had a higher release profile than the high PVP content formulations.

7.4 Discussion

Some pharmaceutical compounds can be trapped in the glassy state when quench cooled from melt and in order to stabilise this amorphous form the drug has to be cooled below its Tg to avoid first order phase transformation to the crystalline from (Baird et al., 2010). Quench cooling method is one of the methods used to trap the drug in the glass form, hence the use of this method in this project. Crystallisation requires nucleation and crystal growth which they are dependent on temperature, molecular mobility and solute concentration. When the liquid is cooled from melt, it passes through a temperature zone where nucleation and growth processes are favourable (Trasi and Taylor, 2012). The temperature zone of nucleation is lower than the temperature region of rapid growth therefore, if the temperature overlap the drug will crystallise during cooling (Trasi and Taylor, 2012) and when they are further apart they stay in the liquid state. The addition of a polymer can inhibit the crystallisation from melt in the drugs with high crystallisation tendency. The amount of the polymer required is based on the crystallisation tendency of the drug (Baird et al., 2010). In the previous chapters PEG and Poloxamers were used to stabilise the glassy amorphous form but it was not quite effective therefore, PVP was used in this chapter. PVP was used in this project as the literature demonstrates that it is a very effective polymer in inhibiting crystal growth and nucleation (Kestur and Taylor., 2010, Trasi and Taylor, 2015). The mechanism of crystallisation inhibition of the polymer is not yet fully understood but several factors are important for the polymer to be able to inhibit the crystallisation such as: formation of hydrogen bonding or ion-diopole between the drug and the polymer (Kestur and Taylor., 2010). Also the polymer has to adsorb to the growing crystal face in order to inhibit crystal growth (Trasi and Taylor, 2015).

The DSC was used as a screening tool for CBZ recrystallisation from melt during isothermal step. The formulation studied did contain 50:50 (w/w drug/ polymer) this is due to the results from previous chapter where CBZ recrystallisation can be well seen in this ratio. The recrystallisation was affected by the %PVP in the formulation and the temperature the sample was held isothermally at. This can be seen in Figure 7.3-1 the higher the isothermal temperature is the higher the crystallisation in the sample with low PVP content. From the PEG 1500 data it

shows that the onset temperature increases as the PVP content in the formulation increases in all temperatures studied. This trend was observed in the formulation with PEG 6000 but not with the PEG 4000, this might be due to the PEG 4000 having two polymeric chains folded and extended chain (refer to 3.1) which will affect the interaction with both PVP and CBZ. For the endset crystallisation in the PEG 1500 formulations, it did increases with increases in the PVP in the formulations held at 10°C but lower for the 30°C (in the 1% PVP formulation) this is due to the faster rate of growth. As discussed above that PVP concentration in the formulation had an impact on inhibiting crystallisation but it did not reduce the nucleation rate this phenomena was also seen in the study made by Trasi and colleague where they found that if a polymer does inhibit crystal growth it might not reduce crystal nucleation rate and this is due to the drug-polymer hydrogen bonding interaction (Trasi and Taylor, 2012).

The hot stage microscopy results were in agreement with the DSC results as the formulation with no PVP did show a high number of crystals formed and when PVP was added the number of crystals did reduce to only a few crystals or none in some formulations. The temperature did affect the crystal growth as at 20°C the crystals were larger than the 10°C.

The variable temperature XRPD is a very useful tool in our project as from the DSC an exothermic peak cannot all the time being identified as PEG or CBZ. Therefore, the variable temperature XRPD it did assure what happens at each temperature point studied. As the results showed that PEG does recrystallise from the melt as soon as it is cooled to -20°C and CBZ alone when quench cooled and reheated an impurity can be seen but when CBZ used in the formulation, the impurity peaks do not appear and this is due to the PEG preventing the drug from degrading. The figures for the different CBZ: PEG4000: PVP formulations show that as the PVP concentration increases in the formulation the higher the CBZ recrystallisation temperature.

The XRPD long term stability study was carried out on a flat plate and the samples were held in the room temperature inside the XRPD instrument. The data was also consistent with the previous section as the PVP content increases in the formulation the crystallisation is inhibited for longer period. CBZ is a very hygroscopic

substance as well as PVP and PEG and this experiment was done in an open plate where the samples were exposed to humidity and atmosphere which would have affected the results.

The % crystallinity experiment results did show that PEG alone does not inhibit the CBZ crystallisation and the molecular weight of PEG has an impact on the crystallisation as PEG 6000 showed only 20% crystallisation after 24 hours whereas PEG 1500 achieve 100% crystallisation after 6 hours. The formulation containing PVP were in agreement with the study made by Trasi and Taylor where PVP K12 did inhibit the crystal growth of acetaminophen at 10%w/w from the melt (Trasi and Taylor, 2012 and 2015). Our study shows that the higher the PVP concentration in the formulation the less CBZ crystallisation in the 24 hours. In the PEG 4000 based formulation the % crystallisation drops from 100 to 10% using only 5% PVP and in the PEG 6000 no CBZ crystallisation was observed at 5%PVP.

The FTIR results shows that the main peaks of CBZ are present in all the formulations (around 3500 and 3200 cm^{-1}) these peaks were in agreement with the results from Varma and Begum study (Varma and Begum, 2012). The CBZ peaks did not shift when the PEG and PVP were added which indicated that the drug did not interact with the polymers (Varma and Begum, 2012). There is a difference in the shift of the asymmetric stretching vibration of the N-H bonds which can differentiate between the different polymorphic forms and in our study it looks like the CBZ exist as form I as the peak was around 3486 cm^{-1} (Kipouros et al., 2006).

The dissolution results did show that the PVP containing formulations had a better release than the PEG alone except for PEG 1500. There was no trend in the CBZ release from the different formulations but the formulations containing 20% PVP did show less release than the other PVP formulations. As the higher PVP concentration increases in the formulations, less crystal growth was observed in the solid state but this not the case in aqueous solution this is due the effectiveness of a polymer as a crystal growth inhibitor depends on its structure and the degree of hydrophobic interaction between the drug and the polymer (Ilevbare et al., 2013) also, a study showed that the moderately hydrophobic polymers such as PVP/VA are better than PVP at inhibiting crystal growth of Felodipine in solution (Schram et al., 2015). At

higher PVP content, CBZ is able to crystallise or change form to less soluble hydrate form and have a lower release than the other formulations.

Chapter 8 Design of experiment (DoE) of CBZ in PEG 300:4000

8.1 Introduction

It became apparent that not all CBZ: PEG mixtures showed similar characteristics in terms of the low temperature recrystallisation after melt (Figure 5.3-1): some samples showed a large re-crystallisation peak (for example CBZ: PEG 4000 50:50 %w/w), while others showed none at all (for example CBZ: PEG 4000 80:20 %w/w). In addition to this, the temperatures at which the re-crystallisation peak could be observed and the energy generated varied. It appeared as if the low temperature recystallisation had a formulation 'sweet spot', so the statistical software Minitab was used to identify where the crystallisation after melt 'rich area' could be found. This was done by using the Design of Experiment model in Minitab to produce a contour plot. DoE is a statistical approach that permits the variation of different factors simultaneously that can influence the output results it is also been used to estimate the best operating conditions of a system. The aim of this chapter is to produce a contour plot of CBZ in different PEG mixtures where the important factor of the DoE can be identified and at which percentage of CBZ to PEG the recrystallisation event will occur and at which temperature.

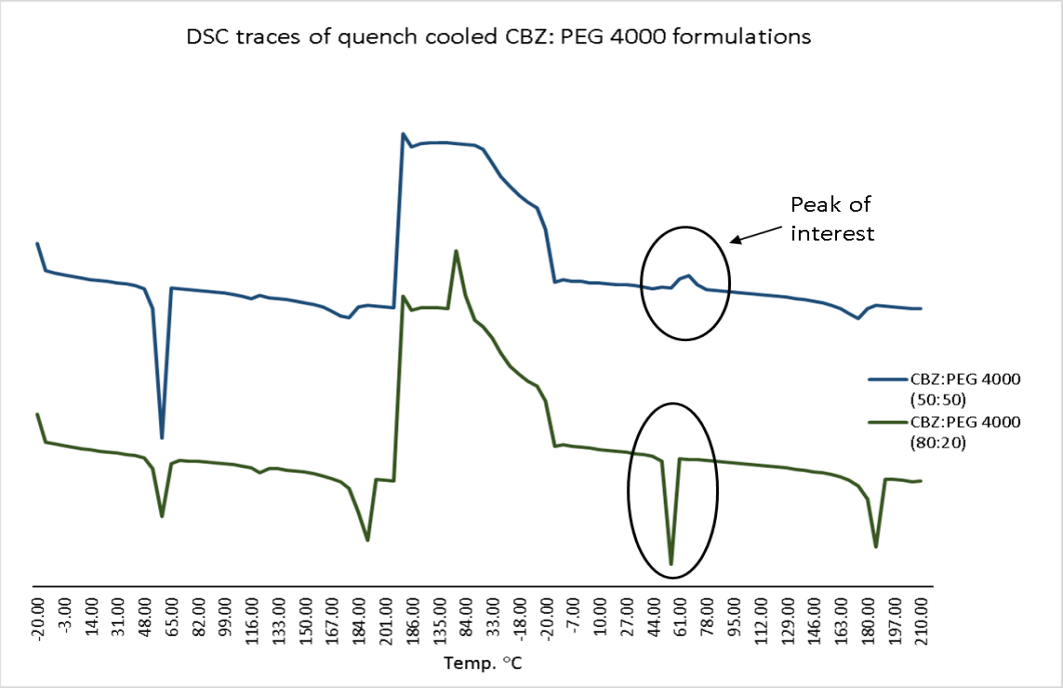

Figure 8.1-1DSC traces of CBZ: PEG 4000

Figure 8.1-1 shows two DSC traces for two CBZ: PEG 4000 formulations. The 50: 50 (%w/w) formulation (blue trace) shows the recrystallisation event (the highlighted area) and the 80:20 formulation (green trace) did show a melting peak at the same temperature due to the formulation crystallising during cooling.

8.2 Method

Minitab model used:

The Minitab model used in this project was a simplex centroid with a total of 10 points (refer to figure below Figure 8.2-1). The output of the model gave the different compositions of the formulations required to be tested, then the formulations were prepared using solvent evaporation technique (refer to section 2.2.2.4). After the solvent was evaporated, the formulations were stored at room temperature in a desiccator containing silica beads and analysed using the DSC the next day. The DSC method used was the quench-cooled 2.2.4.1.2

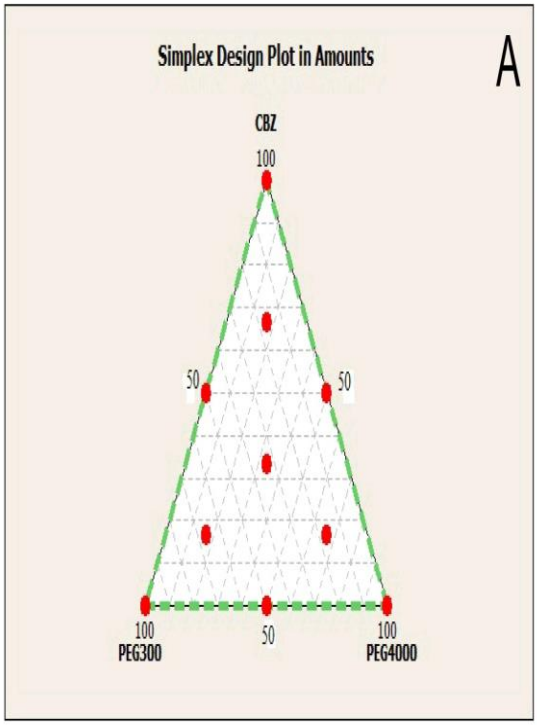

Worksheet 4 ***

B

	C1	C2	C3	C4	C5	C6	C7	C8	C9
	StdOrder	RunOrder	PtType	Blocks	cbz	peg300	peg4000	response J/g	
1	7	1	0	1	33.333	33.333	33.333		
2	8	2	-1	1	66.667	16.667	16.667		
3	3	3	1	1	0.000	0.000	100.000		
4	2	4	1	1	0.000	100.000	0.000		
5	6	5	2	1	0.000	50.000	50.000		
6	10	6	-1	1	16.667	16.667	66.667		
7	5	7	2	1	50.000	0.000	50.000		
8	1	8	1	1	100.000	0.000	0.000		
9	9	9	-1	1	16.667	66.667	16.667		
10	4	10	2	1	50.000	50.000	0.000		
11									
12									

Figure 8.2-1 Minitab design plot

(A) Minitab model used in the project, (B) Minitab output of the different weight composition of the samples.

8.3 Results

8.3.7 CBZ: PEG 300:4000

The DSC of the Minitab suggestion formulation composition was carried out and the results shows that some of the formulations did show a crystallisation event after quench cooling and other did not as shown in Figure 8.3-1. An onset temperature and enthalpy contour plots were produced on the Minitab and, in the response column for the onset temperature contour plot a value of 0 was put for the samples where a PEG melting peak or no CBZ crystallisation peak was observed in the second heating step at peak of interest (Figure 8.1-1), this to show only where is the most likely the crystallisation event will occur and to show only the onset temperature of crystallisation peak.

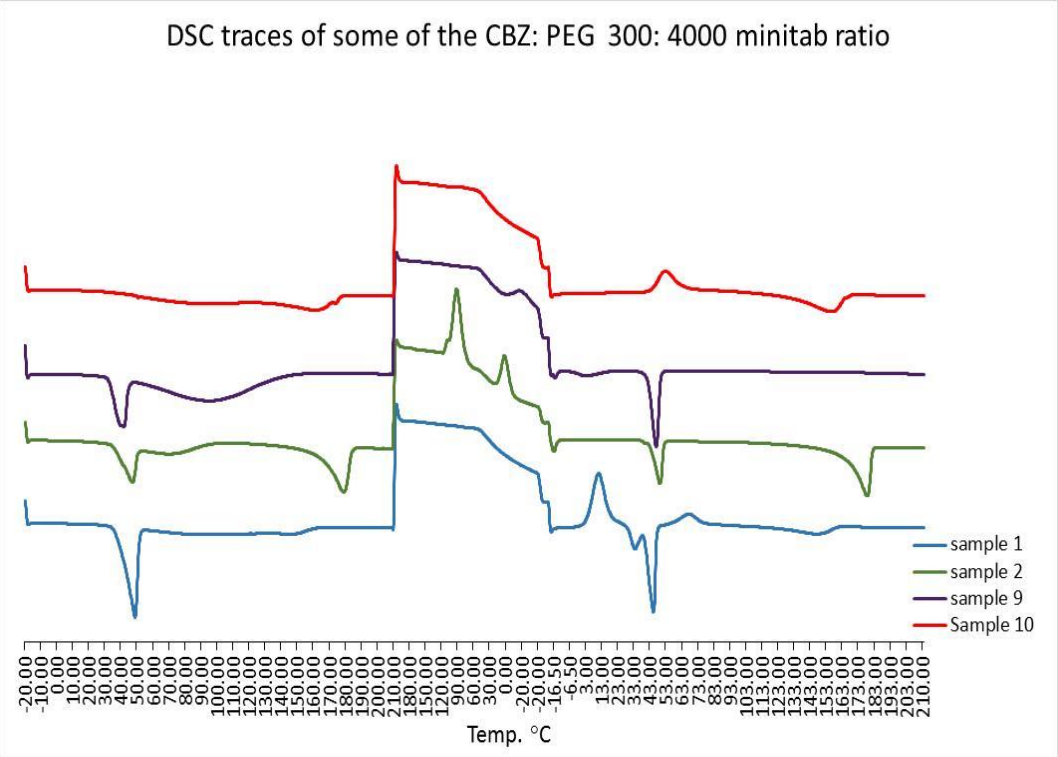

Figure 8.3-1 DSC traces of some of the Minitab samples with PEG 300:4000

The figure above shows some the DSC traces of the Minitab suggestion composition formulations. The traces show that thermal events changes according to the composition of the formulations. Some formulations did show a CBZ melting peak, some show a CBZ dissolution peak into the hot PEG during the 1st heating cycle. Some formulations PEG and CBZ did crystallise during cooling some only PEG and some none of them, same for the 2nd heating step where some formulation CBZ recrystallisation was observed the other a melting peak.

The two contour plots for CBZ: PEG 300: 4000 are presented in the figure below

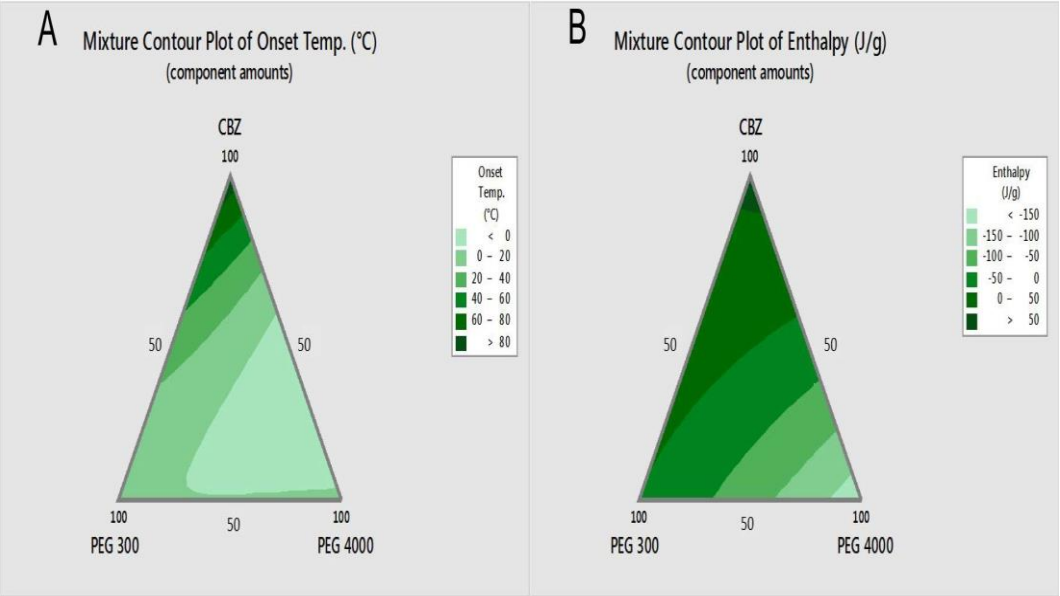

Figure 8.3-2 The contour plot of CBZ onset crystallisation temperature and enthalpy in PEG 300:4000 formulations

The CBZ crystallisation temperature contour plot above shows that the onset crystallisation temperature changes widely with the change in the composition ratio. Minitab output suggest that the more CBZ in the formulation, the more likely the crystallisation event to happen and the higher the onset temperature. Also, it shows that the formulation with a ratio of PEG 300 more than the PEG 4000, the crystallisation event will occurs at a temperature higher than the formulations with higher PEG 4000 ratio.

The enthalpy results were presented as J/g of CBZ. The Minitab contour plot for the enthalpy of peak 5 in the CBZ: PEG 300: 4000 formulations show that the higher the CBZ content in the formulation the more likely for the crystallisation event to happen and the larger the enthalpy will be. Also, the PEG ratios have a role in the occurrence of the event, as the contour plot shows that the higher the PEG 300 ratio in the formulation the higher the crystallisation enthalpy.

8.3.8 CBZ: PEG200:4000

A lower PEG molecular weight was used instead of PEG 300 to study if the crystallisation event will differ with change in PEG molecular weight. From the DSC traces of the different formulations the contour plots were constructed on Minitab software and the results are shown in figure (Figure 8.3-4) and the Figure 8.3-3 below show the different thermal behaviour of two formulations of CBZ with PEG 200: 4000.

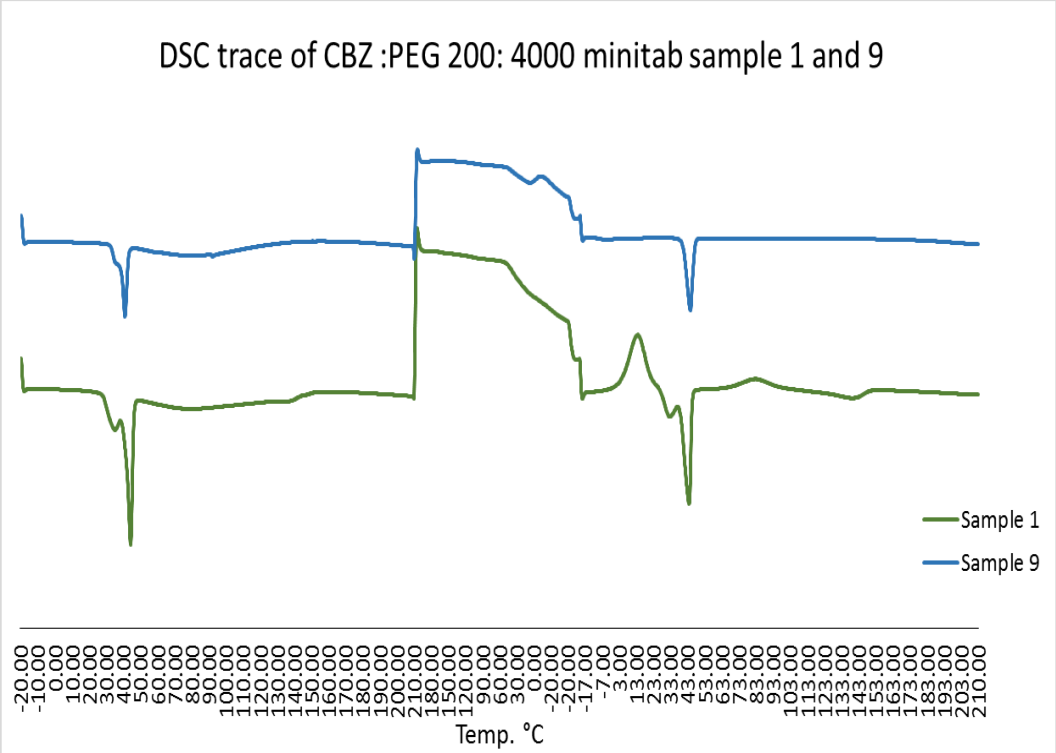

Figure 8.3-3 DSC traces for some of the CBZ: PEG 200:4000

The DSC traces did show the same thermal behavior as the formulations of CBZ with PEG 300:4000. For sample 9 where PEG 200 content ratio is high compared to the CBZ and PEG 4000 in the formulation, the DSC trace show a PEG peak melting followed with a broad melting/ dissolving CBZ peak. A small PEG crystallisation peak was observed during cooling which melts during the reheating cycle. The DSC trace for sample 1 shows similar pattern during the 1st heating cycle but no crystallisation during cooling, and during the 2nd heating step, a PEG crystallisation peak followed by PEG melting then another crystallisation peak which correspond to CBZ crystallising.

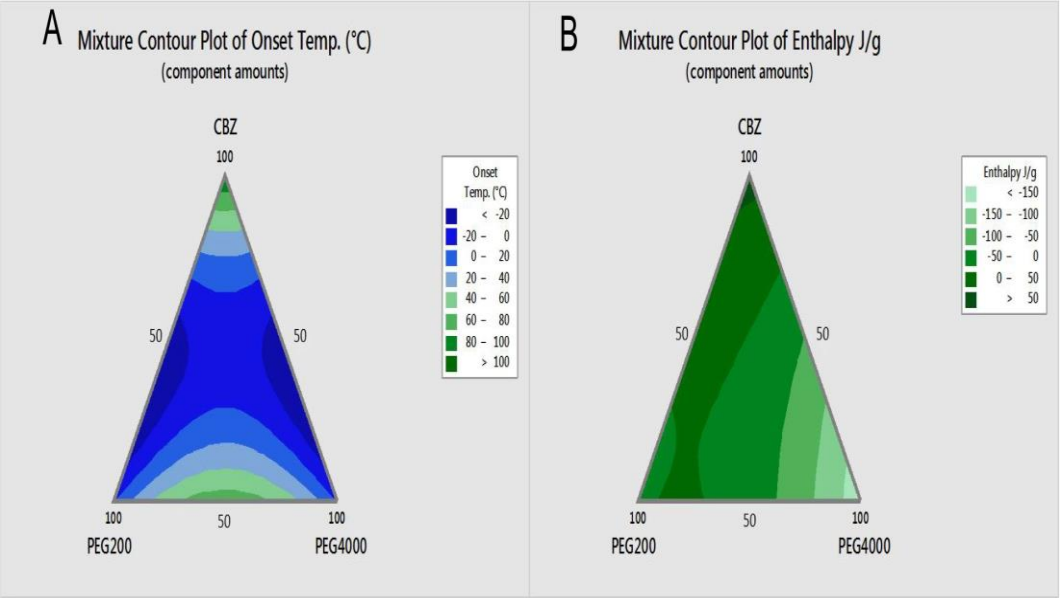

Figure 8.3-4 The contour plot of CBZ onset crystallisation temperature and enthalpy in PEG 200:4000 formulations

The contour plot of the peak 5 (peak of interest) enthalpy in the CBZ: PEG200:4000 formulations shows that the sweet spot for CBZ recrystallisation during the 2nd heating step is when the CBZ content in the formulations is higher than the PEG mixture where high enthalpy is expected according to the plot. Also, the higher the PEG 200 content ratio to PEG 4000, the higher the enthalpy of the peak. The formulations with no PEG 200 or a very low content ratio the enthalpy will be negative which means a melting peak instead of crystallisation peak. If we superimpose the two plots together, it can be concluded that in order to observe a recrystallisation peak at high temperature (above 50°C) the CBZ content ratio in the formulations should be higher than the PEG mixture. Whereas if the CBZ content was lower than the PEG mixture and the PEG mixture contains more PEG 200 than 4000 the crystallisation peak will occur at a very low temperature.

8.3.9 CBZ: PEG 300:6000

To investigate the effect of a higher PEG molecular weight on the recrystallisation event, PEG 6000 was used instead of PEG 4000 and the same Minitab model was used. The figure below shows some of the DSC traces of CBZ: PEG 300:6000. The thermal behaviour of the formulations was similar to the 2 models stated before.

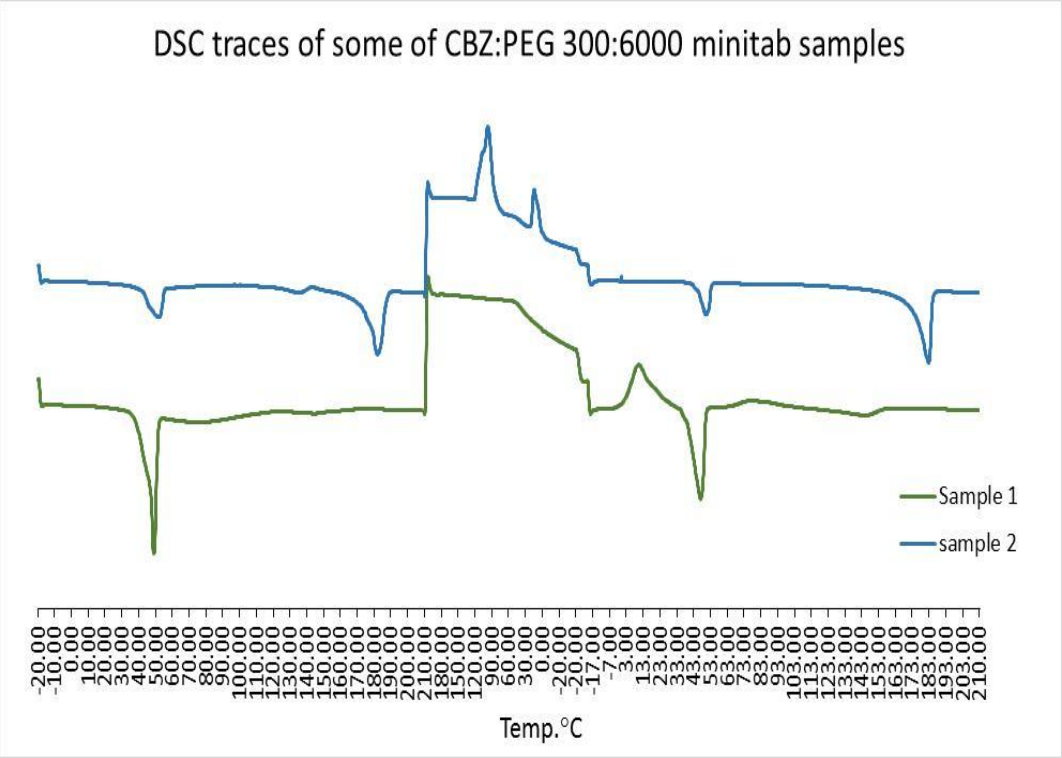

Figure 8.3-5 DSC traces for some of CBZ: PEG 300: 6000 formulations.

The figure below shows the contour plot of the CBZ recrystallisation temperature and the enthalpy of the peak from Minitab software.

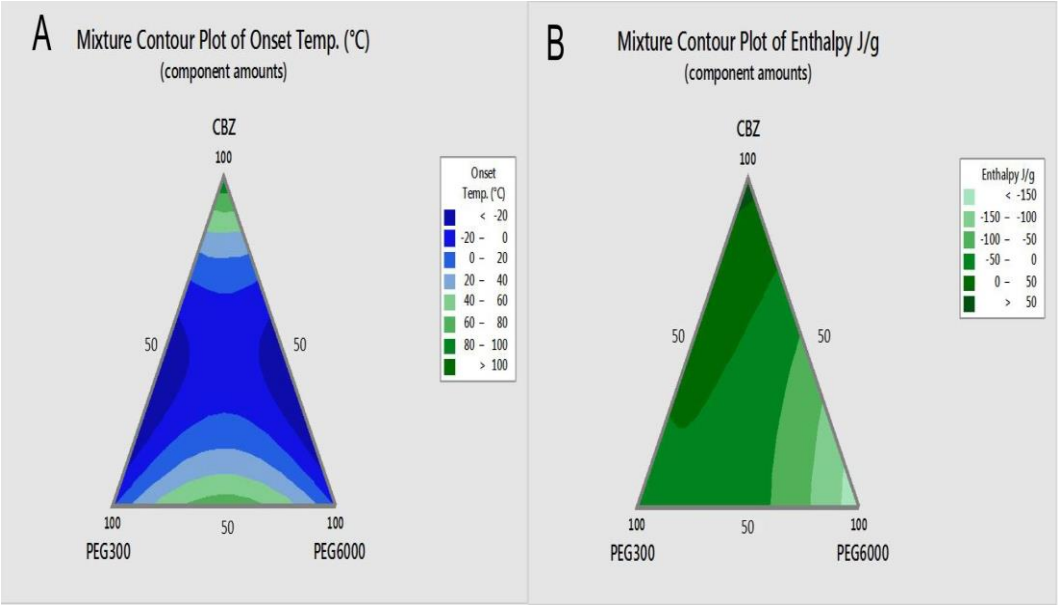

Figure 8.3-6 The contour plot of CBZ onset crystallisation temperature and enthalpy in PEG 300:6000 formulations

The Minitab contour plot for CBZ onset crystallisation temperature in CBZ: PEG 300: 6000 formulations show very similar results as the CBZ: PEG200: 4000 mixture. For the enthalpy contour plot the results shows that in order to see a recrystallisation peak the formulation should have a high CBZ content also the higher the PEG 300 content compared to PEG 6000 the more likely the event will occur.

8.4 Discussion

Two different PEG molecular weights (200 and 6000) were used to see if the molecular weight of PEG has an effect on the crystallisation event studied in CBZ:PEG 300:4000. The results shows that in the three different models the more CBZ content in the formulation the more likely for the recrystallisation event to happens at a high temperature. When comparing the PEG 200: 4000 model to the PEG 300:4000 model, the CBZ crystallisation occurs at a wider range of PEG 300: 4000 mixture compared to the other model where the PEG mixture range was limited to low PEG 4000 content in the mixture. There is a minimum CBZ content in the formulation to be able to see the crystallisation event and in the 300:4000 model around 35-40% but with the PEG 200 it can be lower if the PEG 200 content was very high compared to PEG 4000 (such as 90:10 PEG 200:4000) but the peak will occur at a very low temperature. For the PEG 300:6000 model the range where the crystallisation event occurs is smaller than the other models.

The results from the Minitab contour plot suggest that the three models used has similar pattern where a high CBZ content is required for the crystallisation event to happen at a high temperature. Also, it shows that the liquid PEG is an important component in the mixture because the crystallisation will occur in the formulations with high liquid PEG (300 or 200) compared to the solid PEG (4000 or 6000), this is due to the degree of fluidity and mobility liquid PEG give to the formulation which aid the crystallisation and nucleation process.

These models gave us the ability to choose a temperature range and composition to study in regards to CBZ recrystallisation from the melt.

Chapter 9 CBZ solid dispersion fluorescence studies

9.1 Background about fluorescence spectroscopy

Fluorescence spectroscopy is a technique used to measure the intensity of photons emitted from a molecule after the molecule has been excited with a source of light. Fluorescence spectroscopy can be used as both qualitative and quantitative methods; it is a very sensitive and selective method. Fluorescence occurs when a fluorophore within a molecule is excited from the lowest vibrational level of the ground electronic state into a higher vibrational state within a higher electronic state by absorbing an incident photon and cannot return to the ground state except by emitting a photon. The emission usually occurs when the molecules in the excited state relaxes by dissipation of the energy through vibrational transitions and photon emission (see Figure 9.1-1) to the ground electronic state. Thus fluorescence signals occur at longer wavelengths than absorbance. The energies and relative intensities of the fluorescence signals give information about structure and environments of the fluorophores (Royer, et al., 1995).

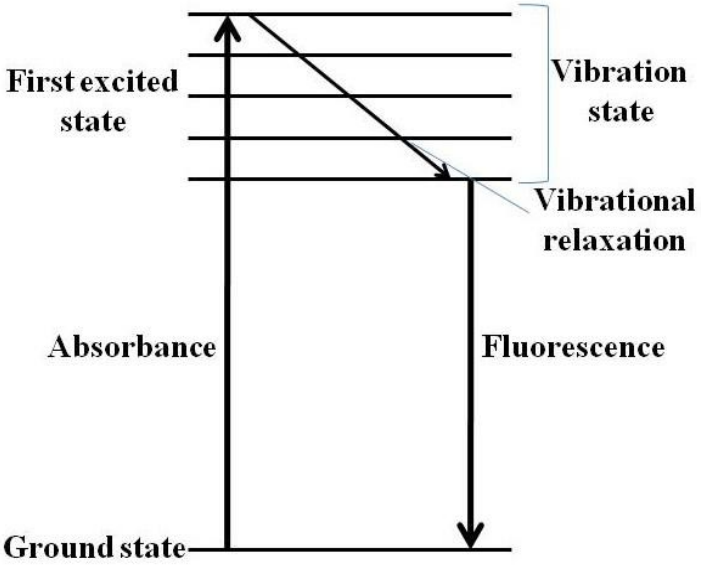

Figure 9.1-1 Energy transfer in fluorescence system
(Sauer et al., 2011)

9.2 Introduction

Carbamazepine quench-cooled formulations did show a change in colour to a yellow colour compared to the starting materials; this is might be due to some impurities or decomposition at high temperature. When they were placed under a UV light for a few seconds they started to glow blue. A photoluminescence was a possibility as well as fluorescence. A study by Escandar et al (2004), stated that carbamazepine does not fluoresce either in solution nor supported on a variety of surfaces and a significant emission signals was observed when the sample was supported on a nylon matrix. The quench-cooled formulation did absorb the UV light and glow blue which put fluorescence as an option. The fluorescence of CBZ, CBZ solid dispersion and CBZ formulation quench cooled were studied using the fluorescence spectrophotometer in solid state and different solutions such as water and methanol.

9.3 Method

The fluorescence of carbamazepine and the different solid dispersions (CBZ: PEG 300: 4000 (50:25:25) solvent evaporation and quench cooled) was measured using the fluorescence spectrophotometer in solid state, dissolved in methanol and in water.

For the solid-state samples, the cuvette was filled with the powder then scanned. An excitation spectrum was collected at 360nm and the emission spectrum was collected at 417nm at 5nm slit width, the scan range from 300-500nm and the integration time used 1nm/sec. The emission and excitation wavelengths were chosen based on Brittain (2003) and the 3D map (Figure 9.3-1) obtained from the fluorescence spectrophotometer for CBZ was in agreement with these values.

For the methanol and water samples, a small amount of the powder sample (~50 mg) was dissolved in 3 ml of the specific solvent then filtered into the cuvette. The filtrate were then analysed at the same excitation and emissions wavelengths as stated above.

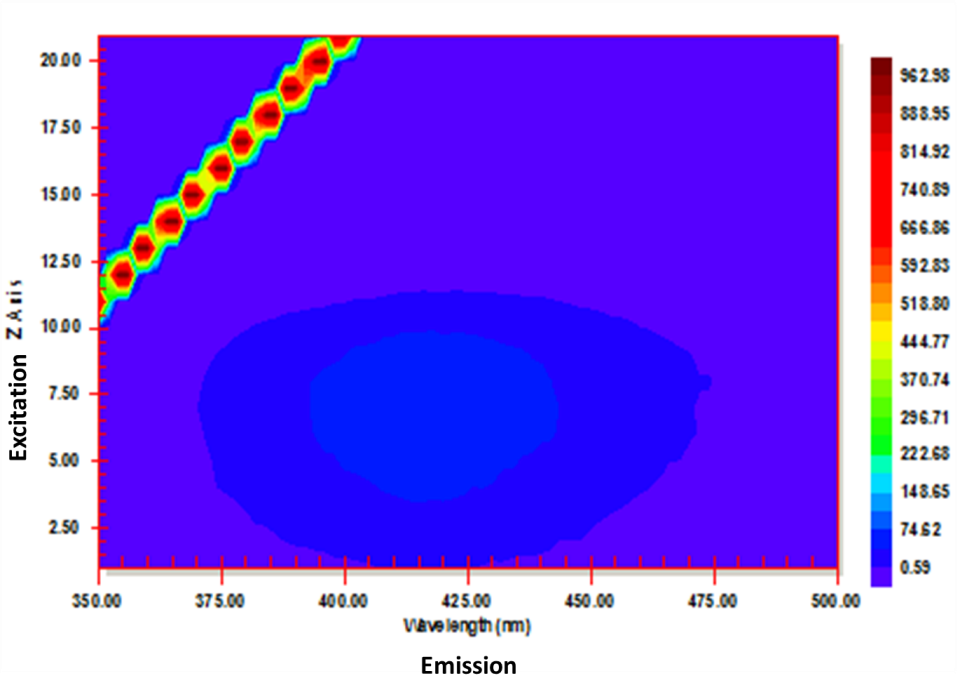

Figure 9.3-1 Fluorescence 3D map of CBZ emission against excitation wavelength

The above 3D map shows that the CBZ emit at around 417-420nm when excited at 360nm. The Z-axis on the graph is the fluorescence intensity.

9.4 Results

9.4.1 Solid-state fluorescence results

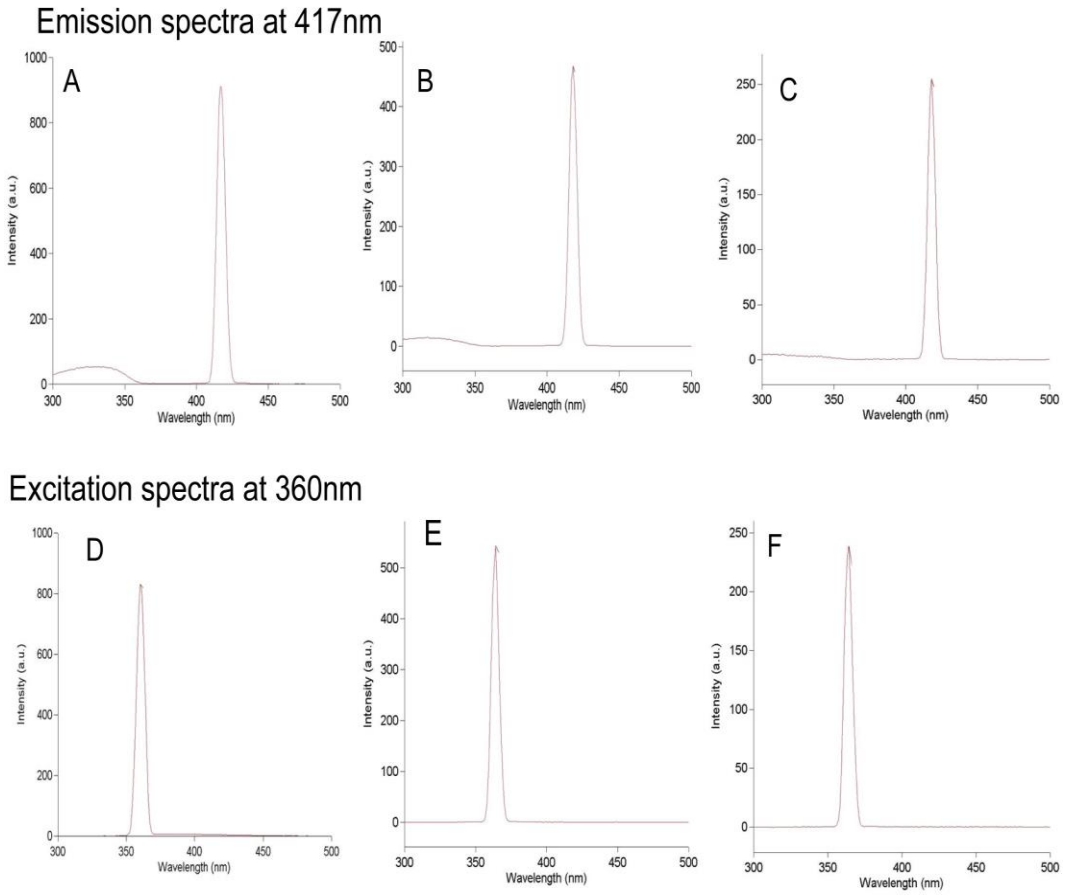

Figure 9.4-1 Fluorescence spectra of CBZ in the different formulations in solid state

(A- emission spectra of CBZ alone, B- emission spectra of CBZ: PEG300:4000 (50:25:25) solvent evaporation formulation, C- emission spectra of CBZ: PEG300:4000 (50:25:25) quench cooled formulation, D- excitation spectra of CBZ alone, E- excitation spectra of CBZ: PEG300:4000 (50:25:25) solvent evaporation formulation, F- excitation spectra of CBZ: PEG300:4000 (50:25:25) quench cooled formulation)

CBZ in solid state shows significant fluorescence according to a study made by Brittain (Brittain, 2003), and this phenomena was observed with the different CBZ formulations stated above (Figure 9.4-1) at solid state. The intensity of fluorescence peak for the quench-cooled formulation was lower than the drug alone and the solvent evaporation formulation.

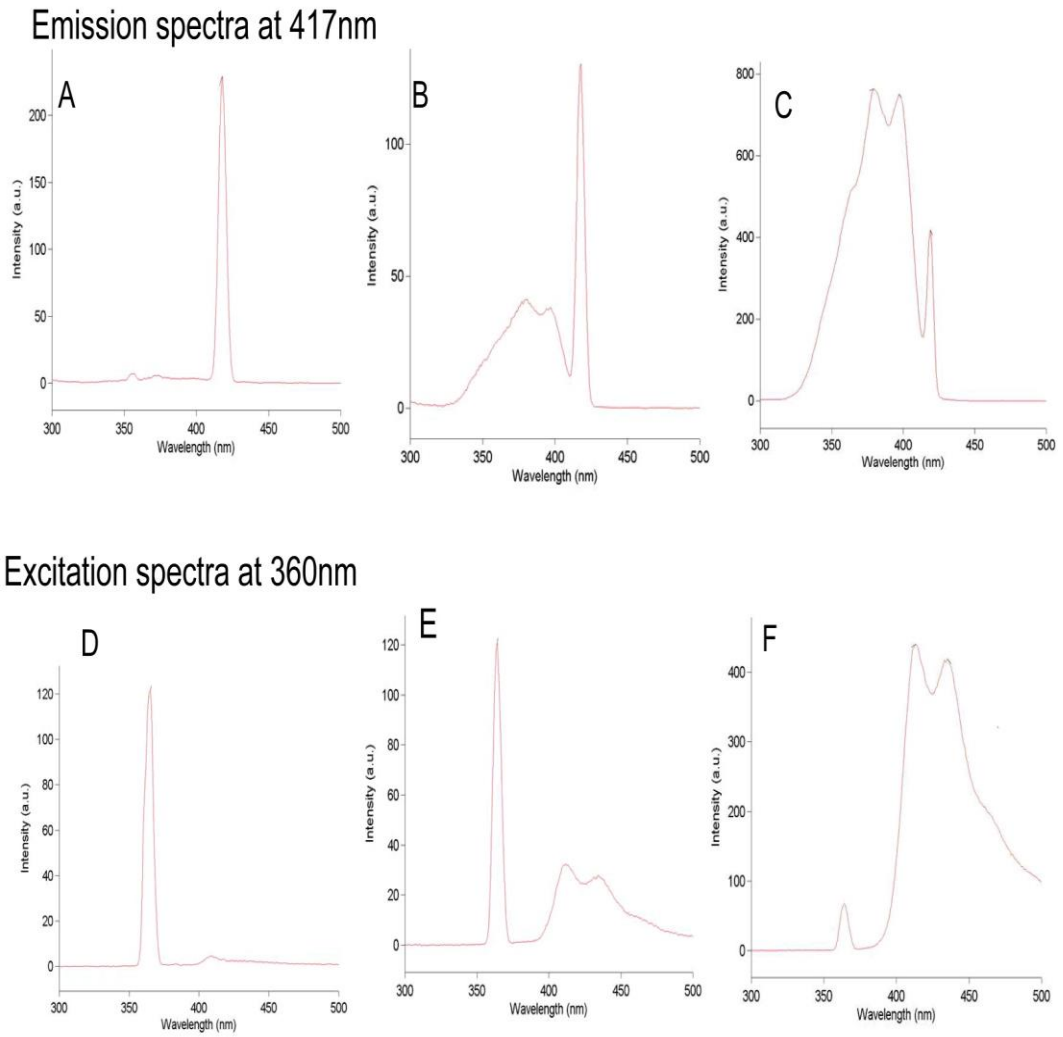

Figure 9.4-2 Fluorescence spectra of CBZ in the different formulations dissolved in methanol

(A- emission spectra of CBZ alone, B- emission spectra of CBZ: PEG300:4000 (50:25:25) solvent evaporation formulation, C- emission spectra of CBZ: PEG300:4000 (50:25:25) quench cooled formulation, D- excitation spectra of CBZ alone, E- excitation spectra of CBZ: PEG300:4000 (50:25:25) solvent evaporation formulation, F- excitation spectra of CBZ: PEG300:4000 (50:25:25) quench cooled formulation)

When the samples were dissolved in methanol, fluorescence spectra were collected despite the literature statement that CBZ does not exhibit fluorescence in the dissolved form (Brittain, 2003). For the solvent evaporation and quench-cooled samples a broad peak appears after the excitation peak and before the emission peak this may be due to light scattering.

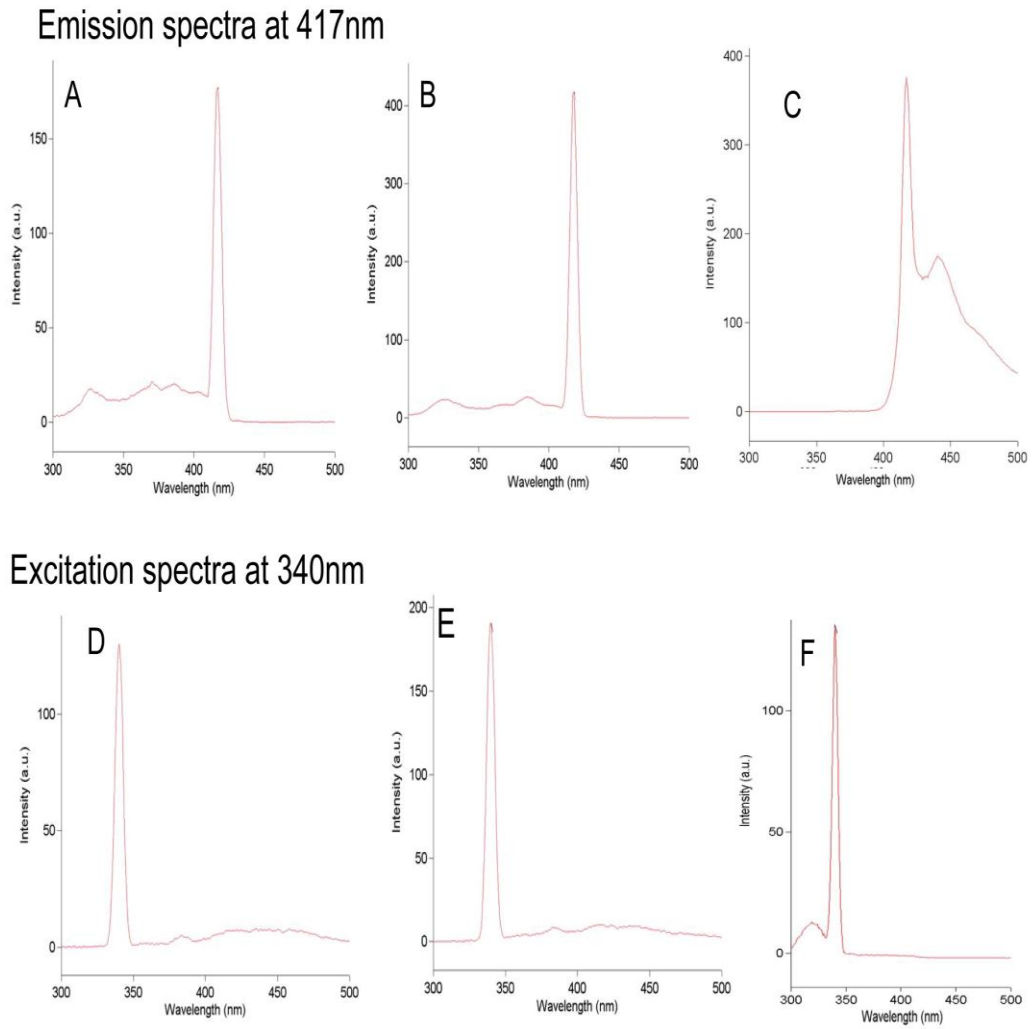

Figure 9.4-3 Fluorescence spectra of CBZ in the different formulations dissolved in water

(A- emission spectra of CBZ alone, B- emission spectra of CBZ: PEG300:4000 (50:25:25) solvent evaporation formulation, C- emission spectra of CBZ: PEG300:4000 (50:25:25) quench cooled formulation, D- excitation spectra of CBZ alone, E- excitation spectra of CBZ: PEG300:4000 (50:25:25) solvent evaporation formulation, F- excitation spectra of CBZ: PEG300:4000 (50:25:25) quench cooled formulation)

For the samples dissolved in water, the excitation wavelength was lower than the one in the solid state and solvent evaporation, it was 340nm. Light scattering was seen in the spectra of quench cooled formulation only.

9.5 Discussion

Carbamazepine form III shows a fluorescence activity in solid state. The dihydrate also, show a fluorescence activity in the solid state with 3.15 times higher intensity than the anhydrous form (Brittain, 2004).

The solid-state fluorescence results show that all the samples have some fluorescence activity. The solvent evaporation solid dispersion fluorescence intensity was half of the pure drug and this is due to the CBZ drug within the formulation is mixed with the PEG. For the quench-cooled samples, the intensity was much lower than the pure drug and the solvent evaporation. The results suggest that the CBZ within the quench-cooled formulation are not dihydrate as the fluorescence intensity should be higher or the solid form has been disrupted by the formulation.

The emission wavelength of the formulations in water was shifted down to 340nm and this maybe due to the CBZ is in solution or have a different form which is lower in energy than the anhydrous (Brittain, 2003). The fluorescence spectra of the quench-cooled formulation in water have an unresolved peak due to the conversion of the anhydrous CBZ to CBZ dihydrate in situ or due to the scattering of light.

Chapter 10 Karl Fischer chapter

10.1 Introduction

To understand the crystal form of the CBZ in PEG systems it became important to understand if the dihydrate form of CBZ was present in the formulations (Qiu et al., 2016). It should also be noted that in its dihydrate state CBZ is reported to show higher fluorescence (Brittain, 2003). In order to examine this possibility the water content of PEG systems (both anhydrous and hydrated) as well as CBZ-PEG samples generated as part of this work were assayed by Karl Fischer. Coulometric Karl Fischer (KF) is an analytical technique used to determine the water content in solids, liquids and gases samples (Schöffski et al., 2006). The aim of this chapter is determine the water content in the different formulations to identify if there is enough water for CBZ dihydrate to form.

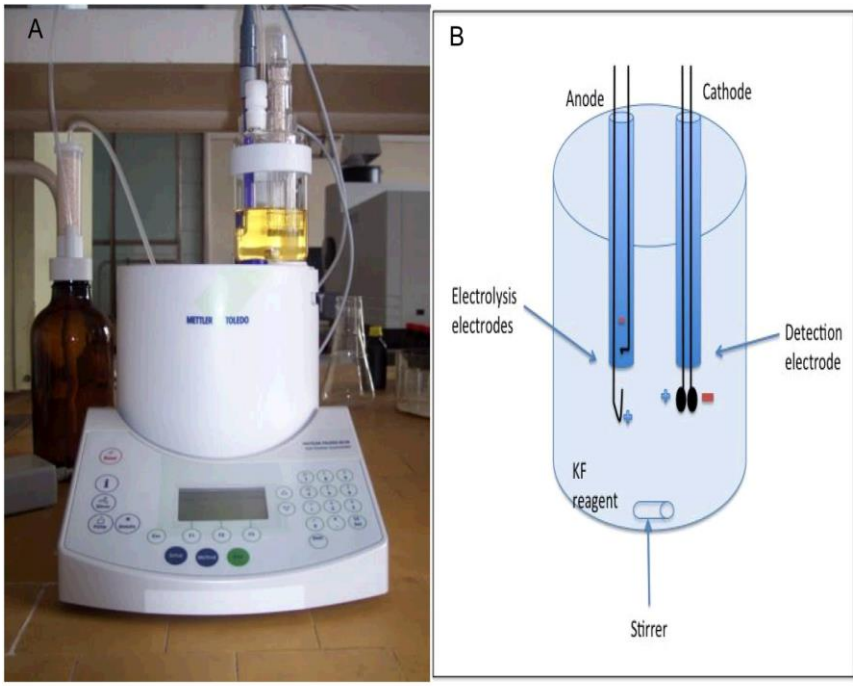

Figure 10.1-1 Karl Fischer instrument.

Figure A, shows the Karl Fischer instrument used in the project. Figure B, shows the inside of the Karl Fischer titration cell where the iodine is generated and the current is recorded.

The reagent in titration cell of the coulometric KF contains iodide (I^-), sulphur dioxide (SO_4) and imidazole (as a base) dissolved in methanol. The water content in the samples was determined based on the amount of iodine-generated electrochemically during titration by anodic oxidation from Iodide, which is contained in the coulometric reagent. The iodine (I) will be formed at the anode and the hydrogen from the cathode. The amount of consumed electric charge for this transformation of iodide to iodine is used to calculate the consumption of Iodine, hence the water content in the sample.

The formation of iodine by anodic oxidation:

$$2\,I^- \rightarrow I_2 + 2e^-$$

Equation 10-1

The reaction of KF titration is as follow:

$$ROH + SO_2 + 3RN + I_2 + H_2O \rightarrow (RN)SO_4R + 2(RNH)I$$

Equation 10-2

RN: base, ROH: methanol or ethanol

The end point of the titration is determined by the presence of free iodine in the solution as all the water in the sample has reacted with the iodine. The presence of free iodine affects the voltage at the detection electrode which drops dramatically and is used to indicate the end of the titration. Karl Fischer experiment was used in this project to quantify the water content in the different formulations especially for the quench-cooled formulations where the XRPD data suggest that the CBZ in the formulation have converted to a dihydrate form.

10.2 Method

PEG samples (300 and 4000) were deliberately dried or hydrated as follow: For the hydrated samples, the samples were placed for 24 hours in a glass petri dish in a sealed desiccator (with no desiccant material) above an open glass beaker of water (to produce an atmosphere saturated with water). For the dried samples, they were placed for 24 hours in a petri dish in a desiccator with silica beads underneath. The desiccators were stored on the bench at 18°C and the relative humidity in the desiccator containing the hydrated samples was between 80-90% and 10-15% for the dried samples.

Karl Fischer titration was used to determine the amount of water in the PEG 300, 4000, different formulations and in the quench-cooled samples. The samples were added to the reagent vessel as solids. The samples were weighed (around 10 mg of solid sample was added to the vessel) then placed directly in the Karl Fischer titration cell, where the water content of the samples was determined (each sample was repeated three times).

The sample parameters used on the Karl Fischer were:

-Speed: 35%

-Mix time: 10 seconds

- Source of drift: online (based on last measured value of standby)

10.3 Results

The water content of the different samples is noted below in **Table 10.3-1**

Table 10.3-1 Percentage water content in the different PEG and formulations

Sample	% Water content
PEG 4000 dried	0.0155
PEG 300 dried	0.034
PEG 300 hydrated	26.83
PEG 4000 hydrated	5.06
CBZ as received	0.0831
CBZ: PEG 300: 4000 Solid dispersion	0.29
PEG 4000 as received	0.50
PEG 300 as received	0.079
PEG 300:4000 mix (50:50)	1.87
Quench cooled CBZ: PEG 300: 4000(50:25:25) at 4°C stored for 24 hours	11.14
Quench cooled CBZ: PEG 300: 4000(50:25:25) at 25°C stored for 24 hours	1.18

The hydrated and dried results show that PEG 300 is more hygroscopic than the PEG 4000, the results are in agreement with the literature as liquid PEG is more hygroscopic than solid PEG (Clariant, 2007). The PEG 300 did absorb water (300 times more than the sample as received) when exposed to a saturated RH environment. At 80% RH PEG 300 is able to absorb water up to 45% (m/m) and at 50% RH it will absorb up to 18% (m/m) at 23°C, whereas, PEG 4000 can absorb water up to 20% (m/m) at 80% RH and 1%(m/m) at 50% RH. (Clariant, 2007) The

PEG 4000 and PEG 300 did lose some water when dried compared to the water content for the samples direct from the container. The water content in the PEG 300: 4000 mixture was higher than PEG 300 and PEG 4000 alone from the container. This might be due to the water from the atmosphere been absorbed by PEG during the preparation of the mixture as the mixture were prepared in an open glass petri dish during the weighing and melting the mixture.

The solid dispersion was prepared with (50:25:25) CBZ: PEG 300: 4000

For a 1 g solid dispersion contains 500mg of CBZ and 2.9 mg of H_2O (0.29 % from the table above)

CBZ molecular weight = 236g/mol

Number of moles of CBZ= 500/236= 2.12 mmoles.

CBZ dihydrate has the molecular formula CBZ: 2 H_2O (1:2)

Therefore, for around 2 mmoles of CBZ, 4 mmoles of H_2O is needed to form the dihydrate.

The mass of water needed in the system= 4*18 =72 mg of water = 7.2 %

The data suggest that the water content in the PEG 300 and 4000 as received used to prepare the CBZ: PEG mix formulation does not contain enough water to form the CBZ dihydrate. The mixture of PEG 300: 4000 (50:50 %w/w) contains a significant percentage water content but still not enough to form all the CBZ in the formulation as a dihydrate form in the solid dispersion. In the quench cooled sample stored at 4°C, the water content was higher than 7.2% the amount of water needed to form CBZ dihydrate which suggest that the sample stored at 4°C absorbed water during storage and can convert to the dihydrate form.

Chapter 11 HPLC and forced degradation study for CBZ

HPLC is a technique used to separate the individual components of a mixture. This process involves mass transfer of a sample through a polar mobile phase and non-polar stationary phase. In order to study the effect of the high temperature (210°C) on the quench cooled CBZ formulation, a HPLC study along with degradation of CBZ study were carried out to find out if CBZ will degrade and what it will degrade to. The aim of this chapter is to develop a HPLC method to analyse and quantify any degradation product of CBZ may arise during the quench cooling from the melt process.

11.1 Method

11.1.1 HPLC method

A linear gradient HPLC method was developed for identifying if there are some degradants of CBZ in the quench cooled formulations. The mobile phase used was acetate buffer at pH 5.2 (mobile phase A) and methanol (mobile phase B). The mobile phase composition at the start of the run was 95% A then it decrease to 5% in 30 minutes. A 15 minutes equilibration time at the initial mobile phase ratio was added. The flow rate used was 1.00ml/min and the detection wavelengths used were 214 and 285nm. The HPLC method was developed based on a HPLC method developed by Mowafy and colleagues (Mowafy et al., 2011). A stock solution of 1mg/ml of CBZ or CBZ formulations were dissolved in methanol then aliquots were taken from the stock and diluted to the required concentration with the mobile phase.

The column used was Luna C18 column, 15cm x 4.6 cm, 5μm.

11.1.2 Forced degradation for CBZ

A 1mg/ml CBZ in methanol stock solution was prepared. Then the required aliquots were taken from the stock to prepare a 100μg CBZ in 1.5M HCl, 1.5M NaOH, 3% H_2O_2 and in mobile phase stored at 80°C. The degradation solutions were stored for 2 days at 55°C.

11.2 Results

In the literature more than one wavelength was used to detect CBZ using HPLC. A wavelength of 285 nm was used by Mowafy and colleagues to quantify CBZ in plasma whereas, a 214 nm was used by Zhang and colleagues (Zhang et al., 2011) to study the impurities of CBZ, hence the use of the two wavelengths mentioned above in this project. The HPLC method developed proved to be accurate and reproducible at both wavelengths used. The calibration series used from 1 to 50 ppm was linear with R^2 value of 0.99. The results were produced with three replicates at each point with %deviation of 0.6%.

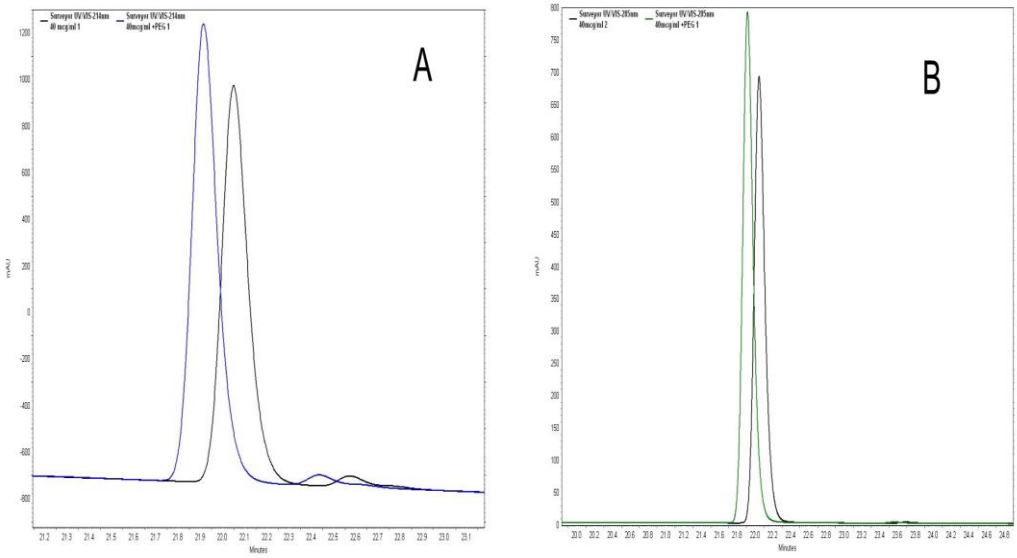

Figure 11.2-1 HPLC chromatogram

(HPLC chromatogram of CBZ at 40ppm: (A) at 214 nm, black trace for CBZ without PEG, blue trace for CBZ with PEG and (B) at 285nm, black trace for CBZ without PEG and green trace for CBZ with PEG)

The CBZ peak with PEG elute at 6 seconds before the CBZ with no PEG, CBZ elute at 22 minutes whereas with PEG will elute at 21.9 minutes and these results were consistent at both wavelengths used.

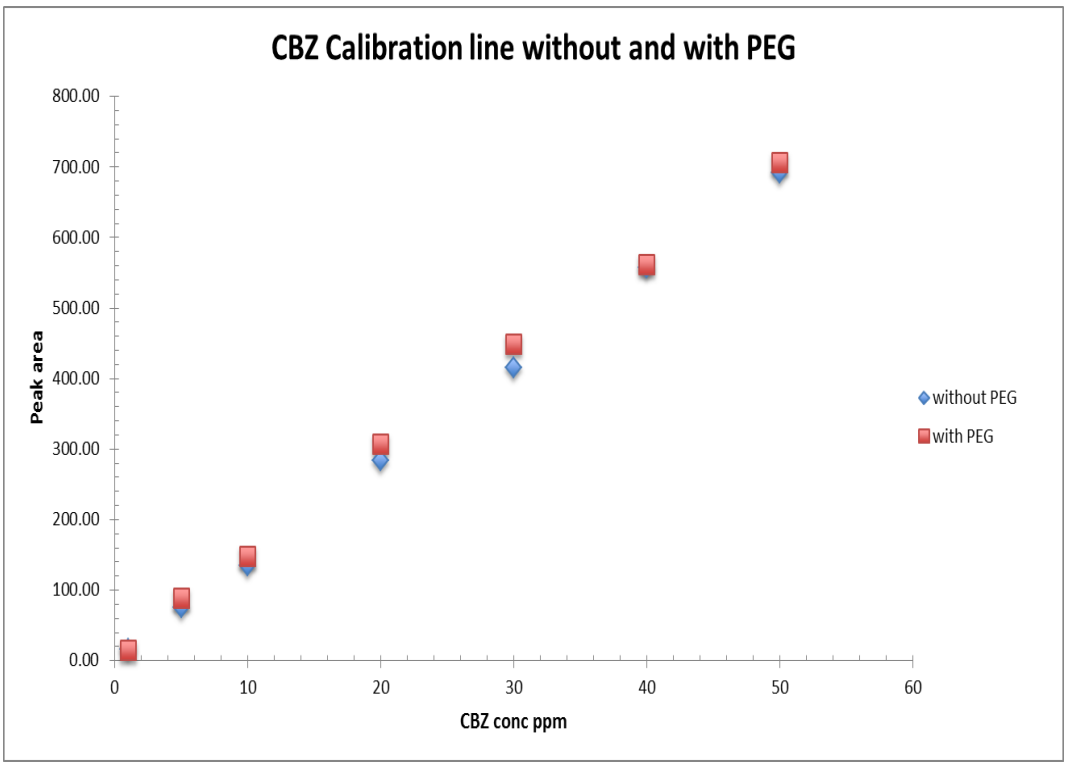

Figure 11.2-2 HPLC Calibration graph of CBZ in presence and absence of PEG

The calibration line of CBZ with and without PEG shows that the presence of PEG in the formulation did not interfere with peak area. CBZ has known impurities and they are stated in the literature and in the pharmacopoeia (BP, volume I, 2017, accessed online), three of these impurities were analysed in the HPLC using the same HPLC method stated above to identify if the solid dispersion contains any of them, and the results are as follow:-

Table 11.2-1 The retention time of CBZ and its impurities

Drug	Retention time (minutes)
CBZ	22.0
Impurity A	22.9
Iminodibenzyl	27.0
Iminostilbene	29.0

The HPLC results of the solid dispersions prepared with melt, solvent method, quench cooled stability samples at 4 and 25°C did not show any impurities as the figure below shows (

Figure 11.2-3).

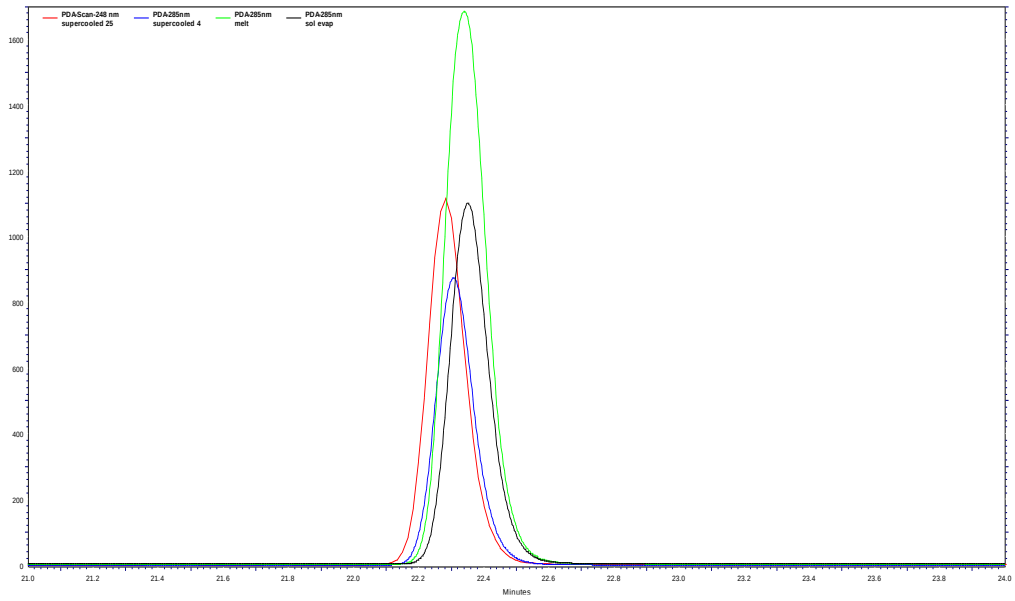

Figure 11.2-3 HPLC chromatogram of the different CBZ formulation
(Light green chromatogram: for the formulation prepared by melt method, red chromatogram for quench cooled sample stored at 25°C, blue chromatogram: quench cooled sample stored at 4°C and the black chromatogram for formulation prepared by solvent method)

A fluorescence detector was used with the HPLC to identify which of the samples show fluorescence peak and the results shows that a fluorescence peak was only observed with the quenched cooled sample and the intensity of the peak of the sample stored at 4°C was higher than the sample stored at 25°C.

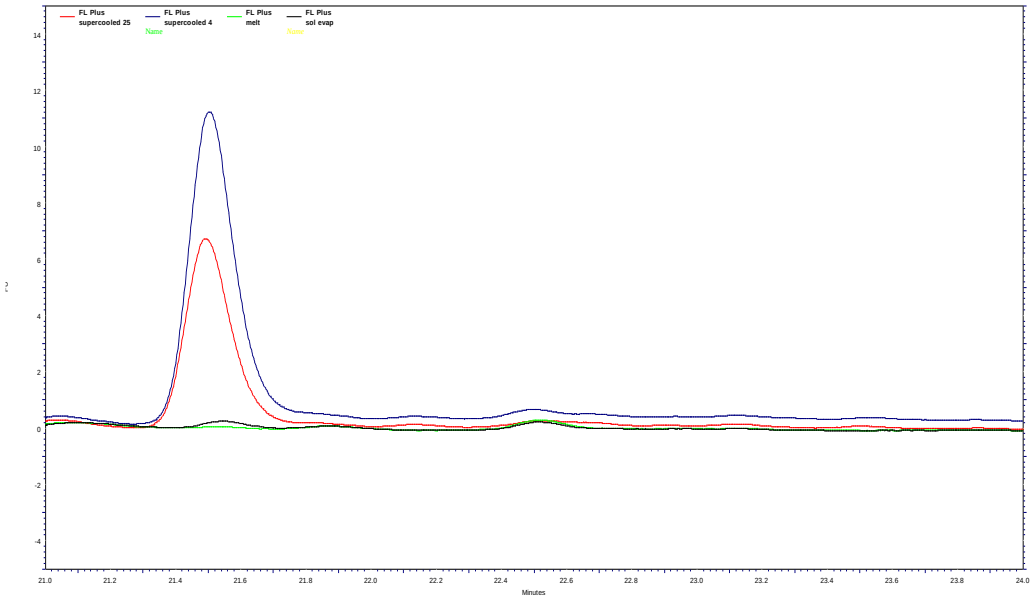

Figure 11.2-4 Fluorescence HPLC chromatogram

(HPLC fluorescence of CBZ solid dispersion prepared by: melt method (green trace), solvent evaporation (black trace), quench cooled stored at 4°C (blue trace) and quench cooled stored at 25°C (red trace)).

A forced degradation study was carried out to see if the high temperature used to prepare the quench cooled sample will affect the CBZ in the formulation. CBZ forced degradation was carried out in in base, peroxide, acid and heat and the traces are shown in the figure below.

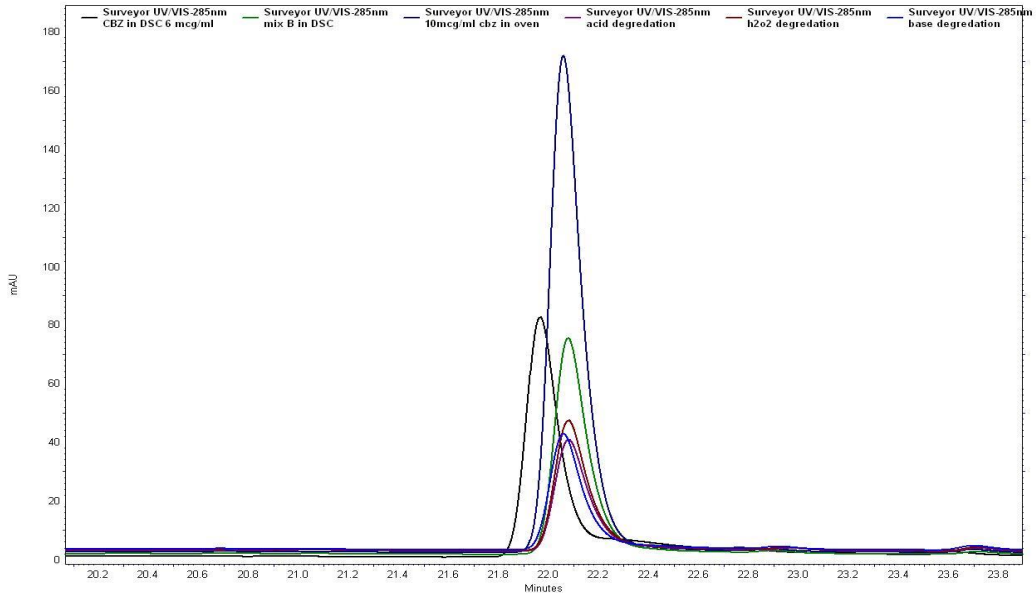

Figure 11.2-5 CBZ forced degradation chromatograms

(CBZ at 6 µg/ml concentration heated in the DSC to 210°C (black trace), CBZ: PEG 300: 4000 (50:25:25) heated in the DSC to 210°C (green trace), 10 µg/ml CBZ in the oven at 55°C for 2 days (navy trace), CBZ in HCl stored at 55°C for 2 days (purple trace), CBZ in H_2O_2 stored at 55°C for 2 days (red trace), CBZ in NaOH stored at 55°C for 2 days (blue trace).

The forced degradation HPLC results did not show any degradation peaks in all the samples studied and the results were in agreement with a study made by Rao and colleague (Rao and Belorkar., 2010).

11.3 Conclusion

The gradient HPLC method developed in this project was accurate and the presence of PEG in the formulation did slightly interfere with CBZ retention time (CBZ will elute 6 seconds before the retention time without PEG). The fluorescence was only seen in the quench cooled samples which may be due to the way of the preparation of the formulation. The forced degradation study did not show any degradation peak which indicates that CBZ is stable at high temperature and in harsh environment such as acidic and basic environment.

Chapter 12 Preparation and characterisation of nifedipine solid dispersion in PEG

12.1 Introduction

Nifedipine (Nif) drug is a calcium channel blocker which is used to treat different range of cardiovascular disorder (Law et al., 1992). Nif is a class II drug which means that it aqueous solubility is low but has a high permeability; this could affect the drug administration orally as its bioavailability will be low (Law et al., 1992). The drug appears as a yellow crystalline powder, it is a light sensitive drug. The drug has a molecular weight of 346.3g/mol and melting point 171 °C to 175 °C. (BP, volume I&II, 2014 online accessed). The aim of this chapter was to prepare nifedipine solid dispersion in PEG and to find a formulation where we can enhance its physical stability.

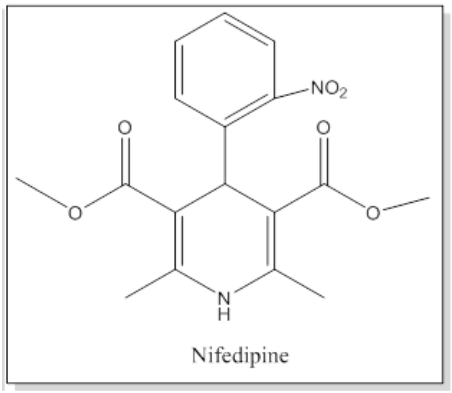

Figure 12.1-1 Nifedipine chemical structure

12.2 Method

The Nifedipine physical mixtures with PEG 300 were prepared in the same way as the CBZ solid dispersion. The solid dispersions were prepared with PEG 300: 4000 mixtures using the ratios mentioned in **Table 2.2-2**. The formulations were assessed on the DSC using the two heating-cooling profiles (refer to 2.2.4.1), also some of the formulations were assessed on the hot stage microscopy and Sirius T3 for dissolution.

12.3 Results

12.3.1 Nifedipine DSC traces

Nifedipine DSC traces along with the hot stage microscopy images are presented in the figure below. The figure shows that Nif alone does not crystallise during cooling and stays in amorphous form as no peak was observed during cooling. During the 2nd heating step, an exothermic peak around 100°C was observed in both thermal profile DSC traces but the peak was sharper in the normal cooled samples. This also was observed in the hot stage microscopy images as the quench cooled sample had fewer crystals than the normal cooled sample.

The DSC traces of Nif: PEG 300 formulations

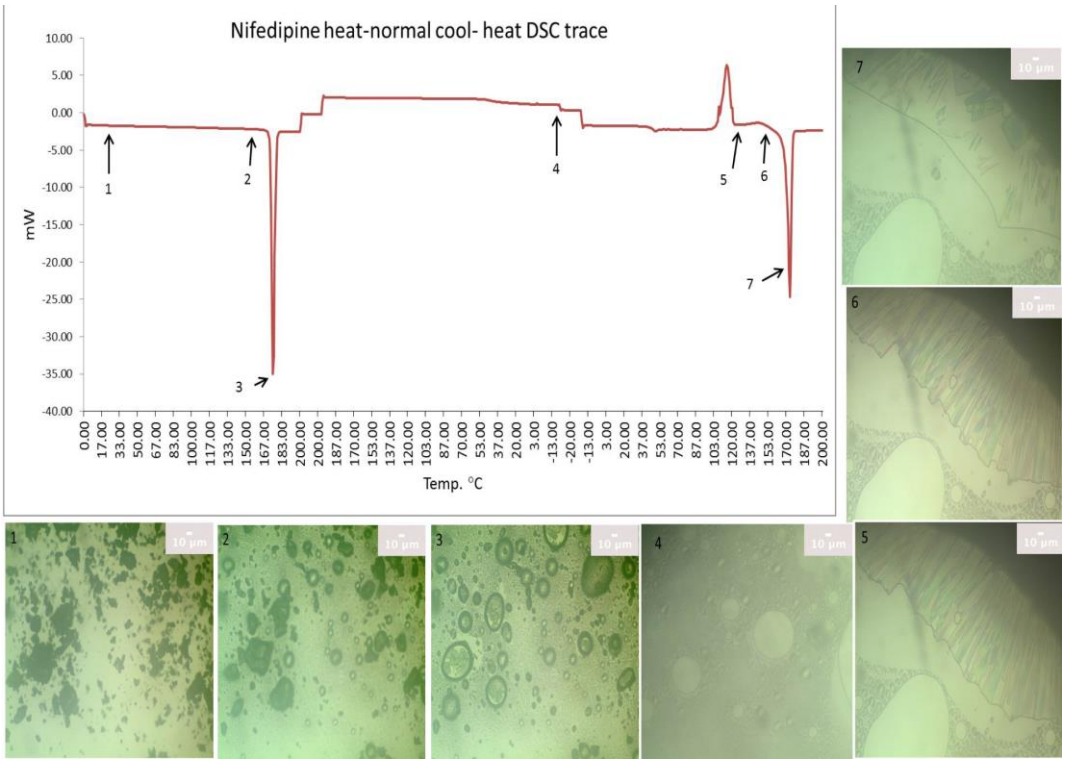

Figure 12.3-1 Heat - normal cool – heat DSC and hot stage microscopy of Nif

The figure above shows the DSC trace of Nif normally cooled along with the hot stage microscopy images taken at x10 objective. Nif at room temperature appears to be as fine small crystals, these crystals start to melt at around 160°C. At 170°C, most of the drug crystals are in the molten state as image 3 shows and at 177°C all

the crystals are in the molten state. During cooling no crystal growth was observed and image 4 shows that the drug was still in the amorphous state. During the 2nd heating step, at 100°C long crystals starts to appears and image 5 was taken at 120°C where the crystallisation event stopped. Image 6 was taken at 150°C where the crystals started to melts and image 7 shows that at 165°C most of the drug crystals are in liquid state.

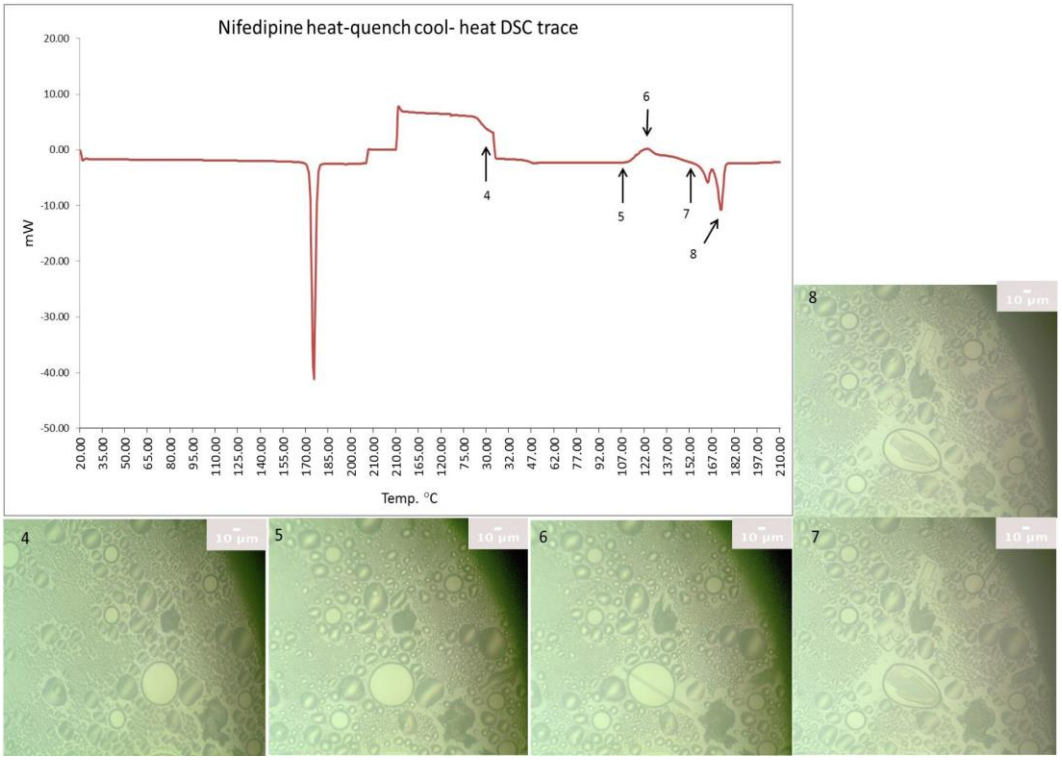

Figure 12.3-2 Heat – quench cool - heat DSC trace and hot stage microscopy of Nif

Nifedpine after quench cooling stays in amorphous state until the sample was reheated to 100°C where crystals start to appear. The crystals appeared were small in size compared to the normal cooled samples. These crystals behaved similar to the normal cooled sample.

12.3.2 Nif : PEG 300 formulations

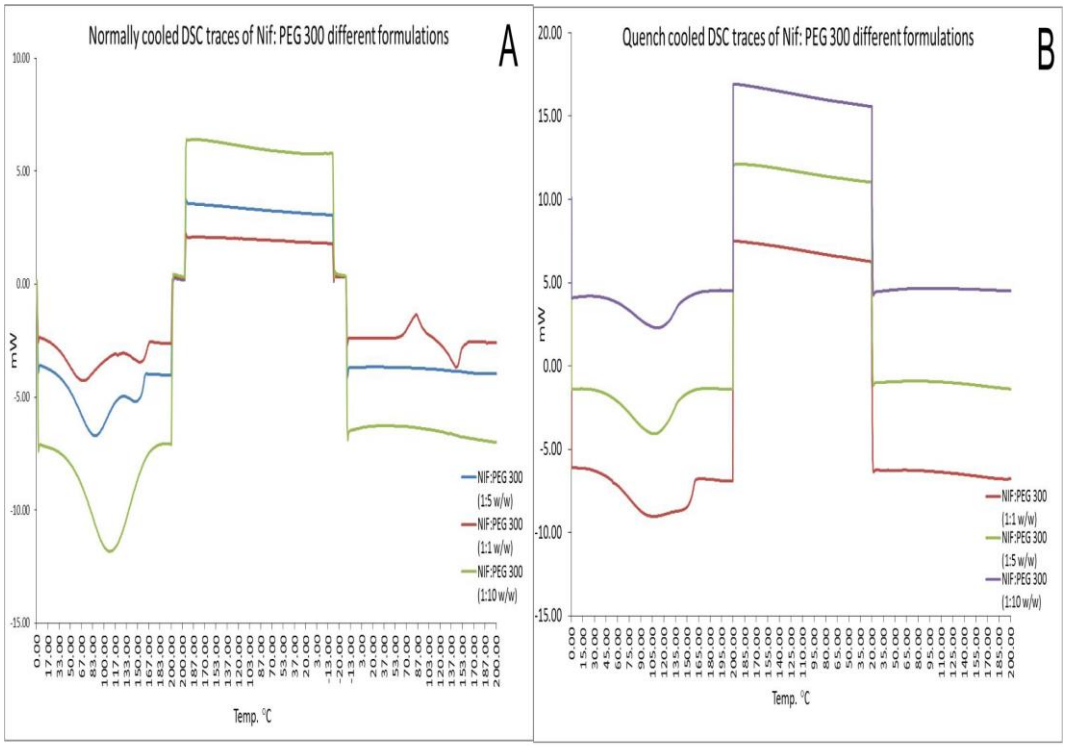

Figure 12.3-3 DSC traces of Nif: PEG 300 formulations

Nifedipine was formulated as solid dispersion with PEG 300 at different weight ratio and two thermal profiles were used on the DSC.

The DSC traces shows that in all formulations the sharp endothermic peak of Nif at around 175°C disappeared and replaced by a broad peak which indicates that the drug is dissolving in the PEG 300. After cooling, all the formulations stayed in amorphous state at both thermal profiles used except the 1:1 w/w (normally cooled formulation) where the crystallisation event from the melt occurred. The crystallisation temperature was lower than the Nif alone (around 75°C) and the Nif in the formulation melted at around 150°C which is lower than the Nif melting point.

12.3.3 Nif :PEG 300: 4000 formulations

The different Nifedipine formulations with mixture of PEG300 with PEG 4000 were analysed on the DSC and the results showed (refer to the figure below) that two endothermic peaks appeared in the 1st heating cycle one for the PEG mixture melting

and the other for Nif melting. The Nif melting temperature in the formulations was less than the Nif alone. During cooling no crystal growth appears in both thermal profiles used. During the 2nd heating step, only two formulations (mix A and B Nif: PEG 300: 4000 50: 37.5: 12.5and 50:25:25 %w/w/w) did crystallise at both thermal profile used. The formulation which contains more liquid PEG did crystallise at lower temperature (95°C for normal cooled and 80°C for quench cooled) than the other formulation (104°C and 100°C respectively).

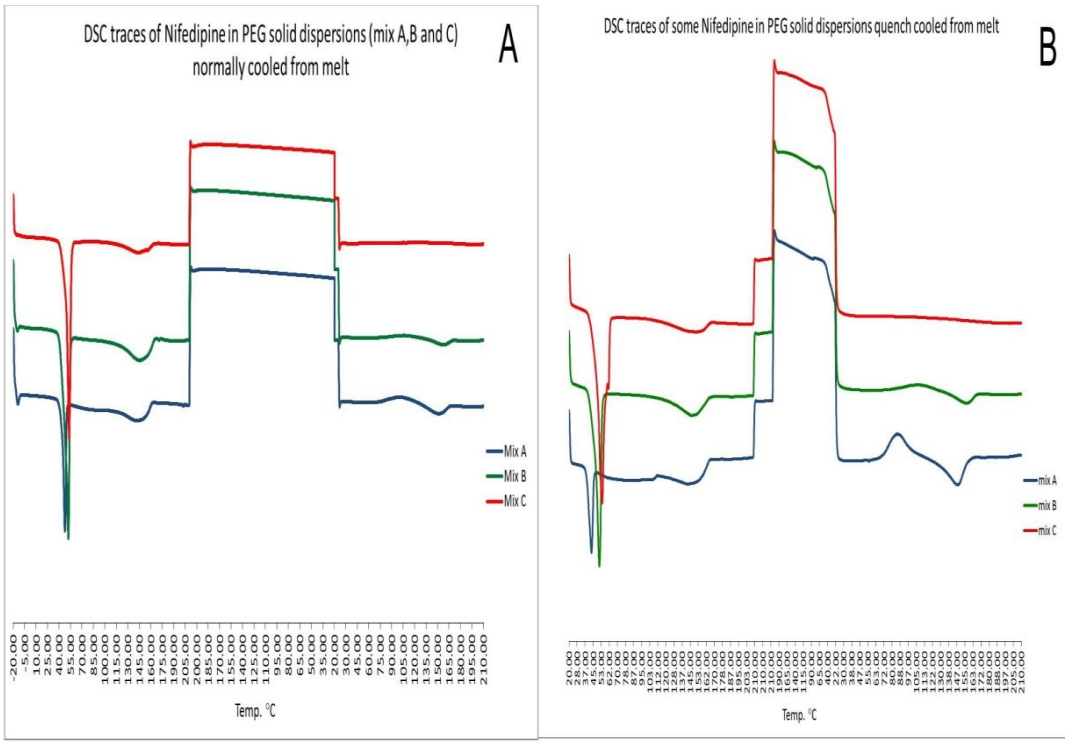

Figure 12.3-4 Nif: PEG 300:4000 at 1:1 w/w drug: PEG mixture formulations

For the other formulations were the PEG ratio to drug was high in formulations, the DSC traces (refer to figure below) show the PEG melting peak followed by a broad peak which correspond to the drug dissolving in PEG. after cooling in both thermal profiles only PEG crystallise and melt in the 2nd heating step, no Nif crystallisation was observed. This suggset that the drug stay in amorphous form in the PEG mixture.

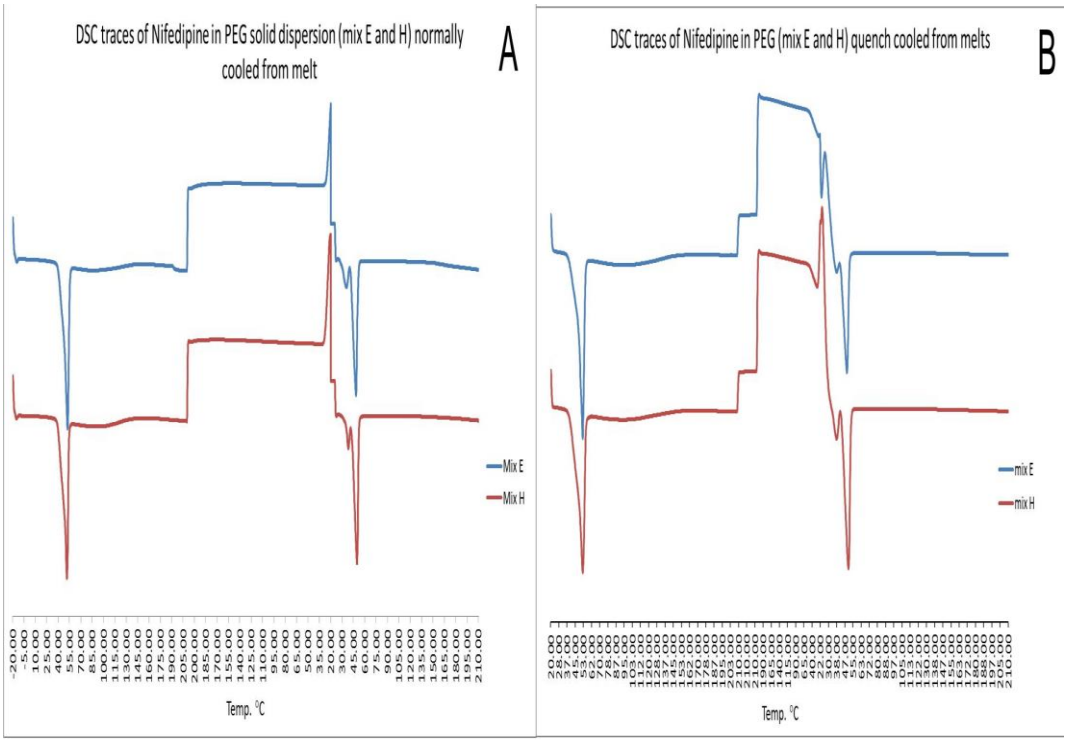

Figure 12.3-5 DSC traces of Nif: PEG 300: 4000 different formulations

12.3.4 Nifedipine dissolution studies

The dissolution of nifedipine was carried out on Sirius T3 at four different pH. The results are presented in the figure below

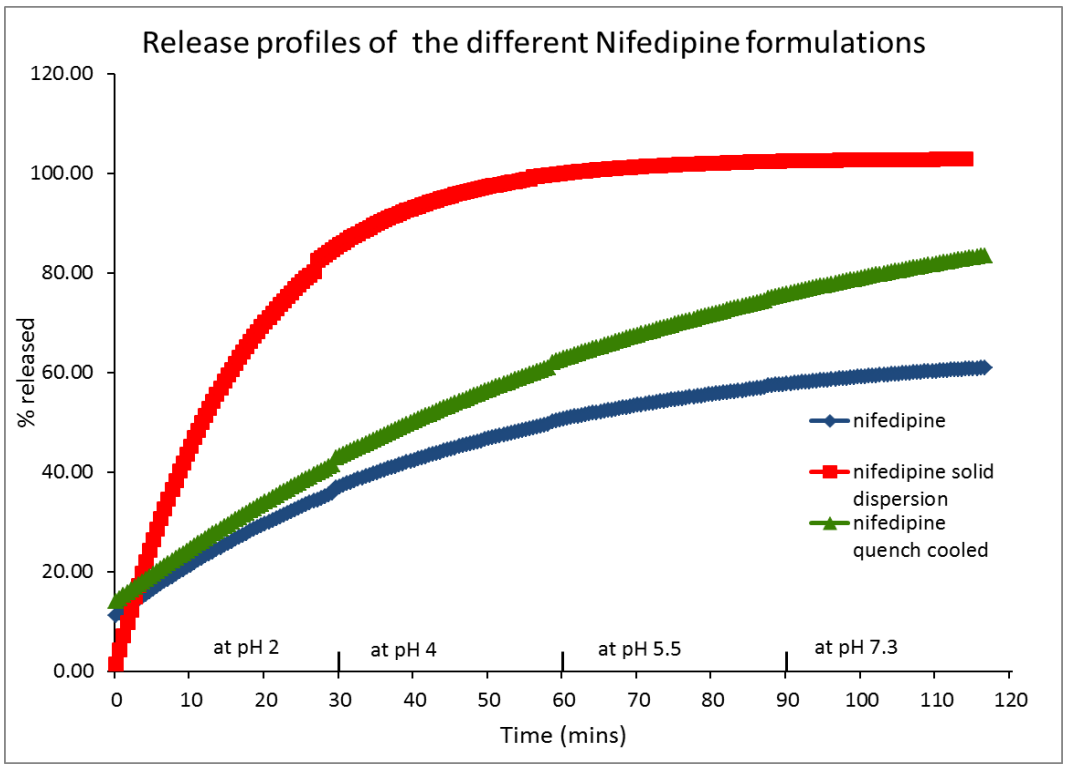

Figure 12.3-6 Dissolution profile of Nif formulations

The figure above shows the dissolution profile of Nif drug alone, Nif: PEG 300: 4000 (50:25:25 %w/w/w mix B) and mix B dissolution profile after quench cooling. An enhanced release was observed with the Nif solid dispersion where at 60 mins a 100% release was achieved whereas the quench cooled sample the maximum release was 80% which still higher than the drug alone (the high release at T0 minutes is due to some free drug in the vial).

12.4 Discussion

Nifedipine solid dispersions were prepared using different methods and polymers in the literature (such as PEG, Pluronic F68 and PVP these solid dispersions were prepared by melt method, solvent evaporation and qench cooled from melt (law et al., 1992, Vippagunta et al., 2002 and Yuan et al., 2013). In this project Nif solid dispersion with PEG 300 and PEG 300:4000 blend were prepared using melt method and quench cooled method in order to obtain a solid solution of Nif. The quench cooled DSC trace of Nif alone was in agreement with the work carried out by Aso and colleagues (Aso et al., 2000) where Nif recrystallisation was observed from melt after quench cooling at around 110°C followed by the melting peak. At higher PEG mixture ratio to drug the endothermic peak of Nif at 177°C disappears and replaced by a broad peak and no crystallisation was observed during 2nd heating step indicates that the drug stay in amorphous state and it is miscible with the PEG mixture. This phenomenon was also seen in a study made by Cilurzo where Nif in HPMC stayed in amorphous state after quench cooling when the Nif content was lower than 30/70 w/w Nif/HPMC (Cilurzo et al., 2002).

The Nif dissolution profile was remarkably enhanced when PEG mixture was used in the formulation at 50:50 w/w (Nif: PEG mixture), this was expected as solid dispersion enhance the dissolution of the drug also in a study made by Law and colleague using PEG 4000 in the Nif formulations the dissolution profiles did enhance sharply (Law et al., 1992). The dissolution profile of the same formulation mentioned above when quench cooled showed less Nif release than the physical mixture formulation these results were slightly different than the results from a study made by Forster and colleagues were the dissolution profile of quench cooled Nif: PVP (1:1 w/w) was higher than the physical mixture (Forster et al., 2001) this is due to the drug in amorphous state and has a higher energy which make it more soluble.

In order to understand the Nif interaction with the PEG more studies should be done such as XRPD were we can identify if the formulations were amorphous or crystalline also a stability studies on these formulations and more dissolutions studies would be ideal to see how Nif behave in the formulation.

Chapter 13 Experiments with other drugs

13.1 Introduction

In order to understand if the exothermic crystallisation event after cooling from melt is specific to CBZ or can be applied to wide range of drugs, an experiment was carried out by choosing some drugs and mixing them with PEG 300:4000 at 50:50 w/w ratio (drug: PEG mix). The drugs were chosen as they belongs to BCS class II and some of them have different polymorphic forms as CBZ. The PEG 300:4000 mixture was chosen as a well-defined peak was observed with CBZ.

The aim of this chapter was to prepare each of the different drugs mentioned in this chapter in PEG300: 4000 (50:50 w/w) to find which drug will be in amorphous state when cooled from melt and the effect of the PEG mixture on these formulations.

13.2 Method

A number of drugs were used in this experiment: acid drugs (Naproxen and Indomethacin), basic drugs (Carvedilol and Itraconazole) and neutral drugs (Probucol and Fenofibrate). These drugs were used to compare the effect of quench cooling from melt on them with CBZ. The drug solid dispersion was prepared PEG300: 4000 at the ratio of 50:25:25 %w/w/w (drug: PEG 300: 4000) using melt method described in section 2.2.2.2. Each formulation have a different melting point, therefore the formulations were not heated to a fixed temperature instead the formulations were heated to the liquid state depends on the melting point of the drug then quench cooled. The solid dispersions were analysed using DSC, HSM and dissolution on Sirius T3 for some of them.

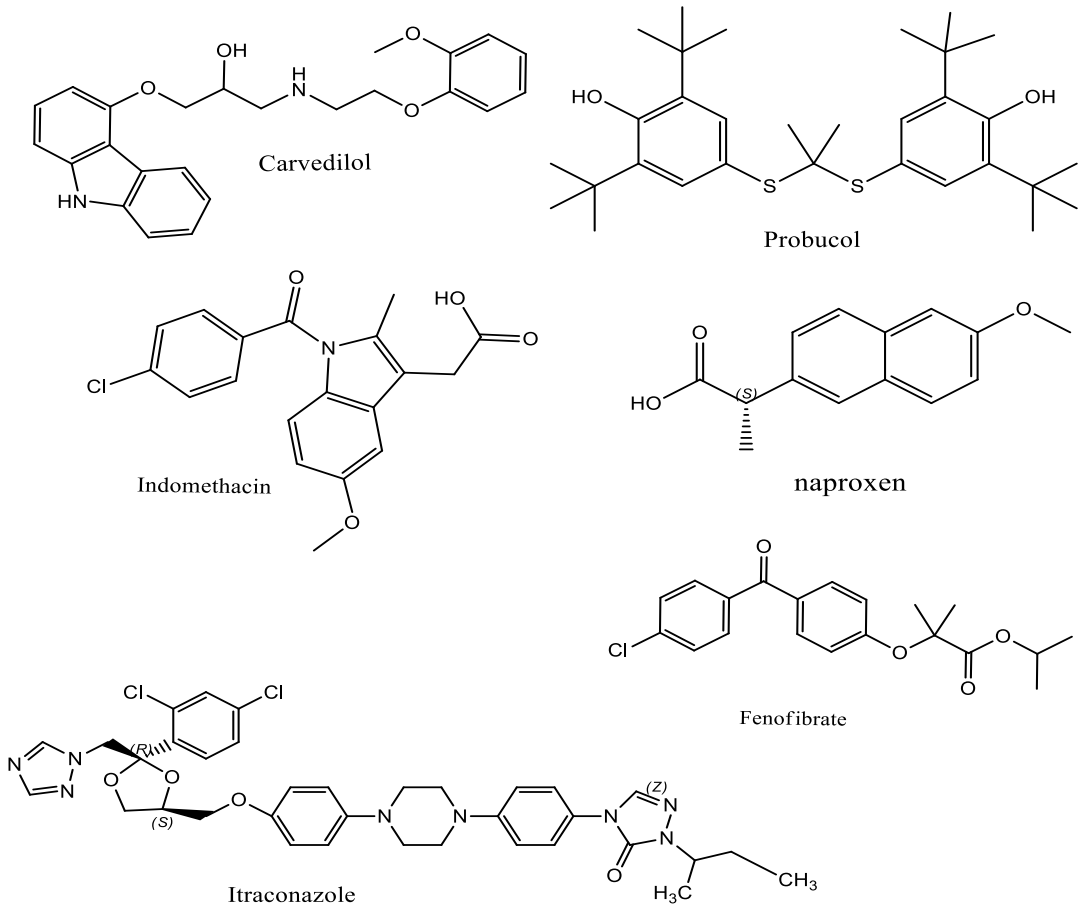

Figure 13.2-1 Chemical structure of the drugs used

Table 13.2-1 pKa and uses of the different drugs used

Drug	pKa	uses
Naproxen	4.2	Non steroidal anti inflammatory drug
Indomethacin	4.5	Non steroidal anti inflammatory drug
Carvedilol	7.8	Used for high blood pressure
Probucol	neutral	Lower level of cholesterol in blood
Fenofibrate	neutral	Decrease serum triglycerides
Itraconazole	3.7	Anti fungal

13.3 Results

The melting point of each drug was determined using the DSC, and the data was recorded in the table below:

Table 13.3-1 Melting point of the drugs

Drug	Melting Point °C
Probucol	129
Carvedilol	120
Indomethacin	164
Itraconazole	170
Naproxen	154
Fenofibrate	83

13.3.1 Normal cooling DSC results

The effect of the cooling rate on the crystallisation from melt of these drugs was studied by using 10°C/min cooling rate. Almost all drugs used alone or formulated with PEG 300:4000 mixture did not show crystallisation during cooling (refer to figures below) except Naproxen. Naproxen alone did show a large crystallisation peak during cooling step but show a smaller peak in the PEG formulation.

Fenofibrate in PEG formulation show a crystallisation during cooling at 20°C then melts at 50°C which indicates that PEG has crystallised during cooling. Probucol formulation was the only sample to show an exothermic peak during the 2nd heating stage starts at 0°C with peak temperature around 15°C which melts at around 50°C.

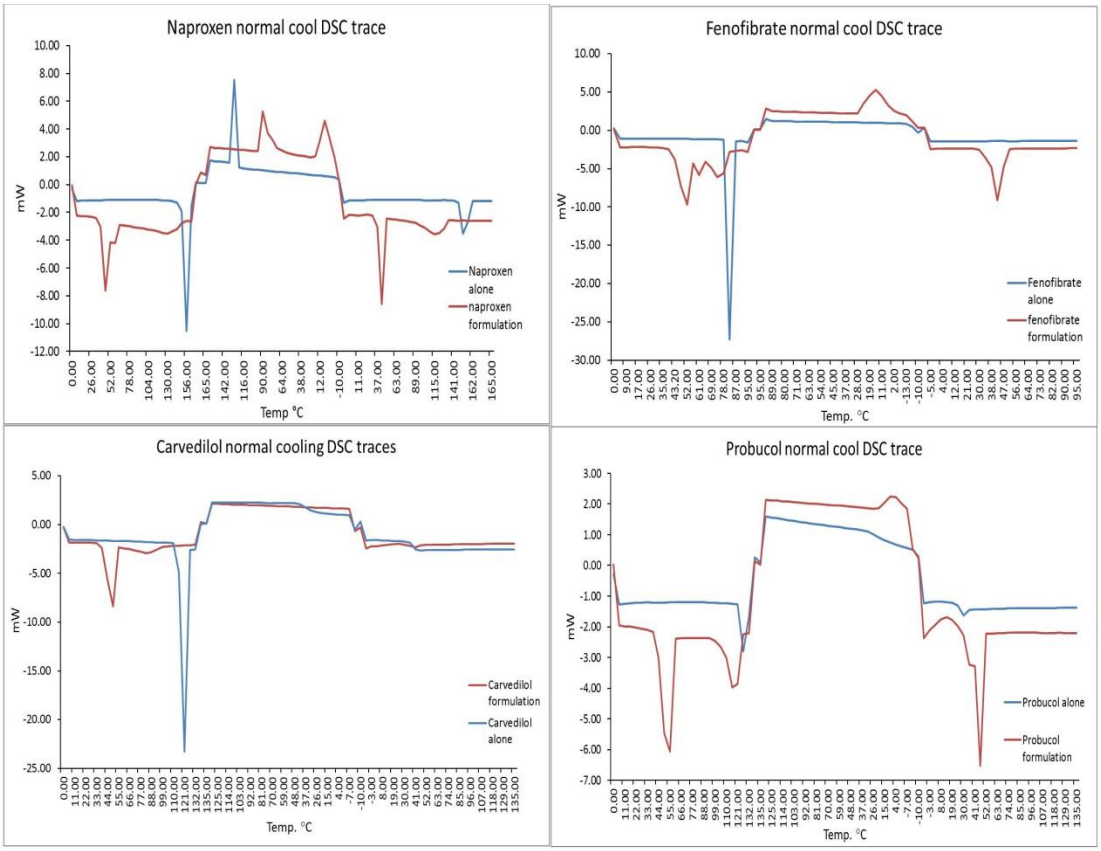

Figure 13.3-1 DSC traces of some drugs and their formulations normally cooled from melt

13.3.2 Quench cooling DSC results

During the quench cooling step, naproxen drug showed a large crystallisation peak during cooling and a smaller one when formulated with PEG as shown in the figure below. Probucol and Fenofibrate DSC trace was similar to the one normally cooled. The DSC trace of Carvedilol in PEG formulation showed an exothermic peak during reheating step which melts at 50°C. The rest of the drug used did not show any crystallisation peak alone or with PEG. This result suggests that the drug stays in amorphous form during cooling.

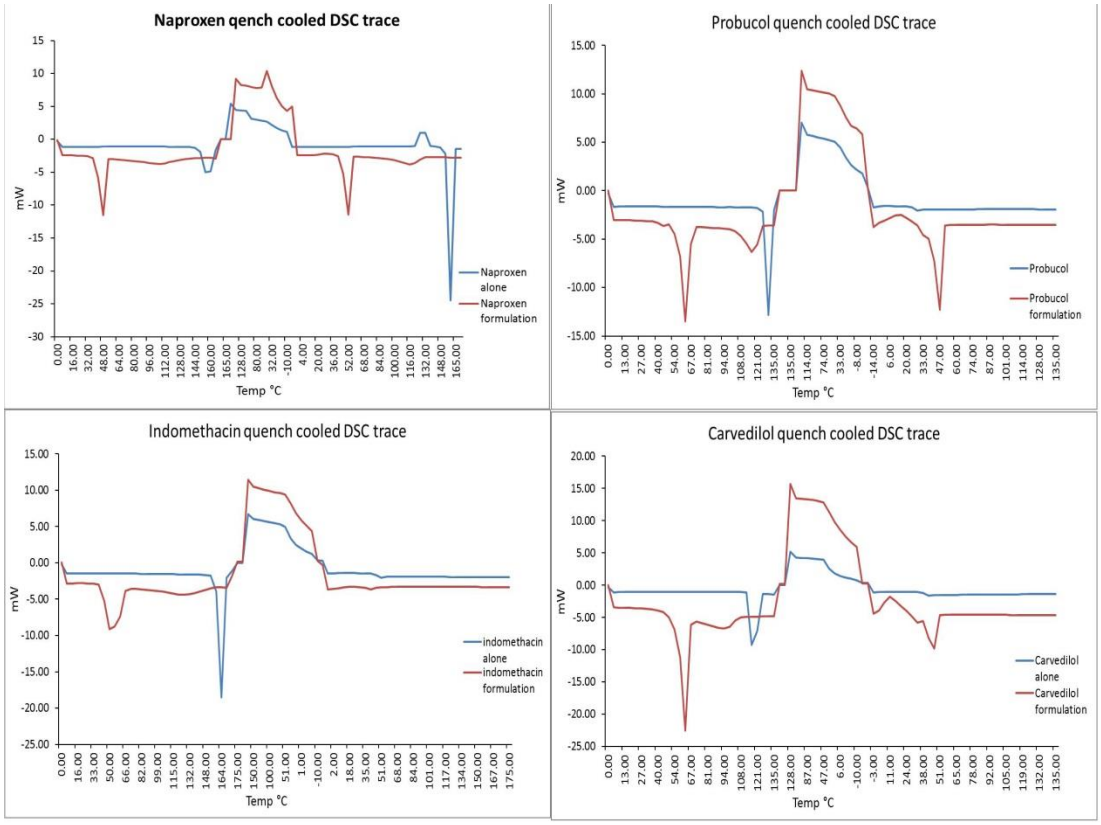

Figure 13.3-2 Naproxen alone and in PEG formulation quench cooled DSC trace

Itroconazole and Indomethacin did not show any crystallisation peak in drug alone or within the formulation during the second heating step whereas Probucol and Carvedilol did not show any crystallisation peak in the drug alone trace but in the formulation traces of both drugs an exothermic peak was observed starting at around 0°C to 40°C followed by a melting peak at 50°C.

13.3.3 Hot stage microscopy

Carvedilol, probucol and indomethacin were investigated under the hot stage microscopy.

13.3.3.1 Carvedilol

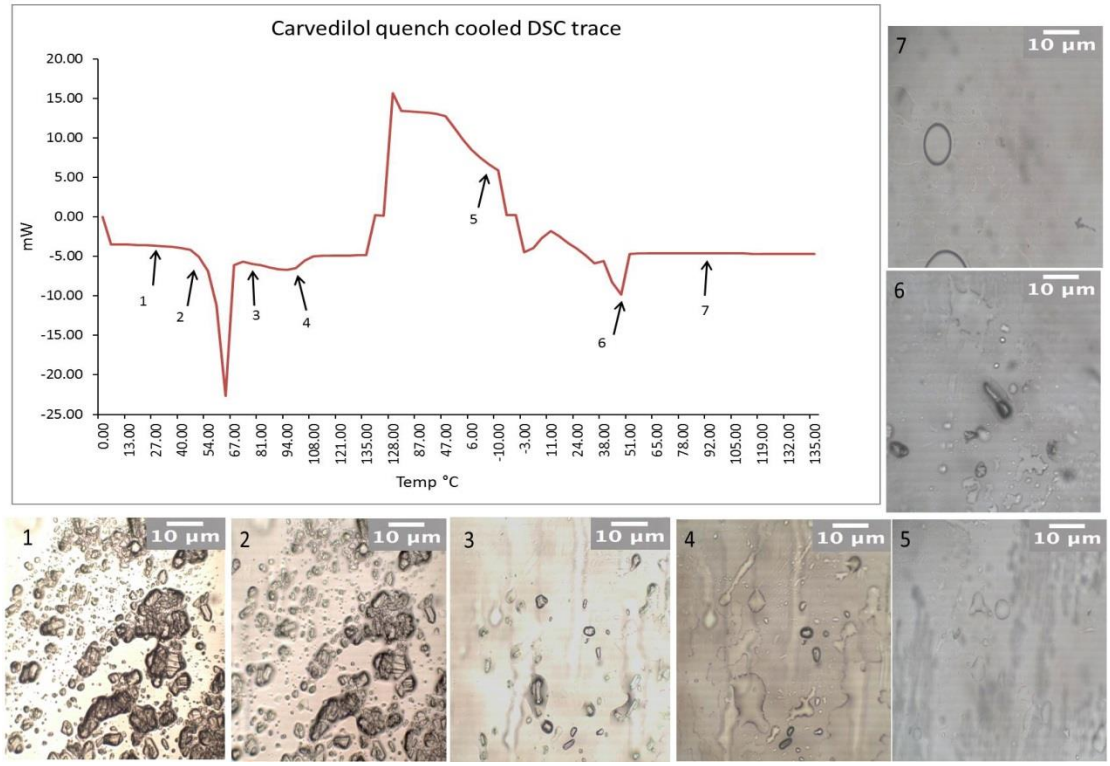

Figure 13.3-3 Carvedilol hot stage microscopy images

The figure above shows the hot stage microscopy events of Carvedilol solid dispersion using quench cooled method. Picture 1 was taken at 25°C, the drug crystals can be seen in the PEG matrix. At 50°C, PEG starts to melts (picture 2). At 85°C, most of the drug crystals have been dissolved in the PEG (picture 3). Picture 4 was taken at 100°C where most of the drug is in liquid state. During quench cooling, no crystal growth was observed as in picture 5 which was taken at -10°C.

During the 2nd heating step, a few crystals growth appears then starts to melts, Picture 6 was taken at 50°C before the crystals melts. Picture 7 was taken at 90°C and it shows that the drug is in the liquid state.

13.3.3.2 Probucol

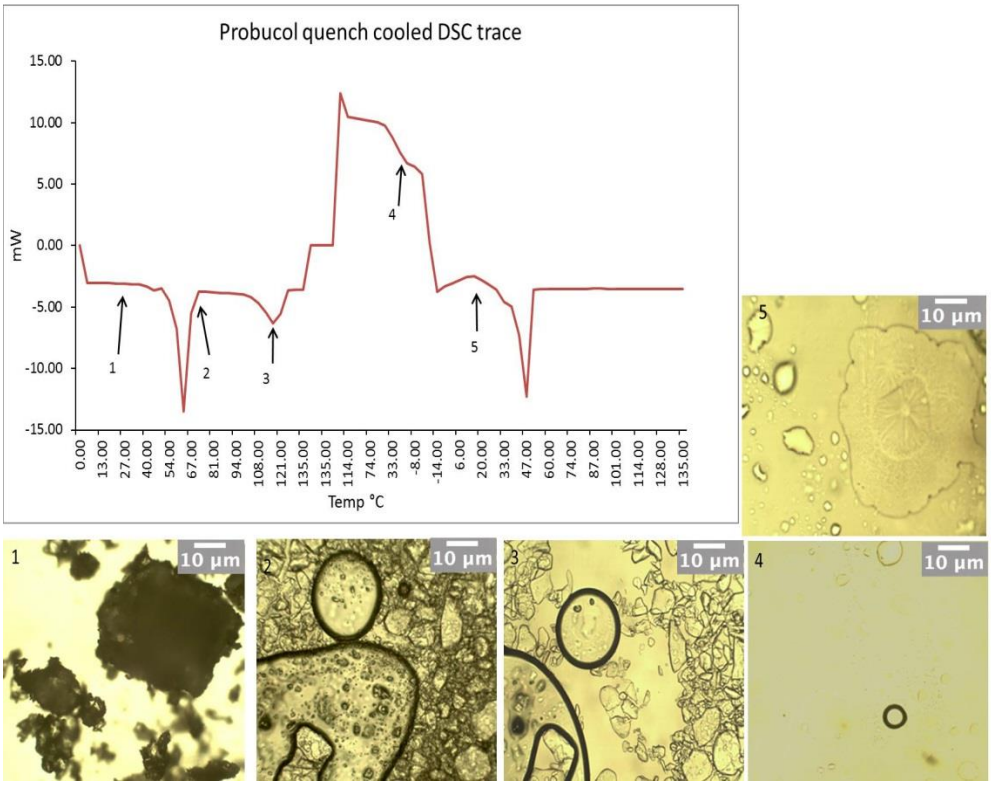

Figure 13.3-4 Probucol hot stage microscopy images

The probucol formulation at 20°C (Picture 1), shows that the drug is incorporated with the PEG. Picture 2 was taken at 70°C and the drug crystals can be seen as the PEG has melted. Picture 3 was taken at 120°C, where the drug crystals continue to dissolve in molten PEG as the temperature increases. After quench cooling no crystal growth was observed as shown in Picture 4 which was taken at 20°C. During the reheating step, a crystal growth appears at 20°C (picture 5) which has a spherulite shape then quickly melts at 50°C.

13.3.3.3 Indomethacin

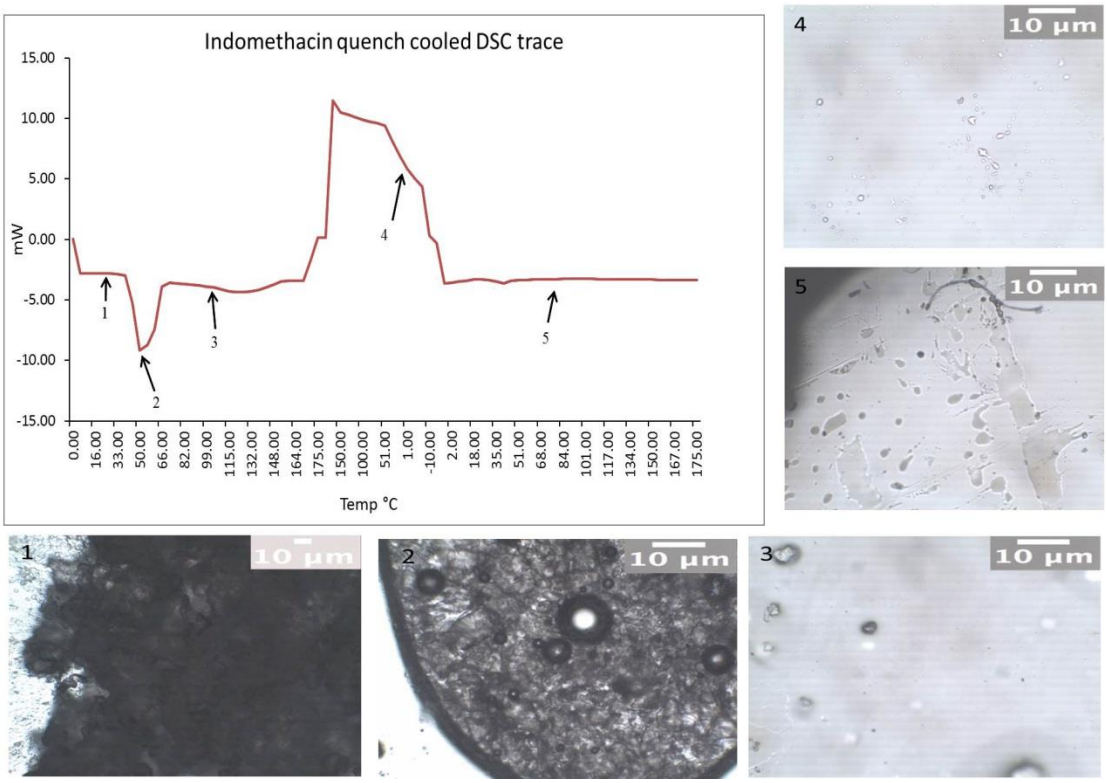

Figure 13.3-5 Indomethacin hot stage microscopy images

The figure above shows the hot stage microscopy results of indomethacin formulations and in Picture, at 25°C the drug cannot be seen as it is incorporated in the PEG mixture. Picture 2 was taken at 55°C, where the PEG melts and the drug crystals can be seen. At 100°C, almost all crystals are in the liquid state as shown in Picture 3. During cooling and 2nd heating step no crystal growth was observed (Picture 4 and 5 were taken at 0°C and 80°C respectively).

13.3.4 Dissolution studies

The dissolution of some of the formulations was assessed on the Sirius T3. The dissolution was performed at four different pH for 30 minutes at each pH. The quench cooled sample was quenched cooled in the DSC then transferred to the T3 vial.

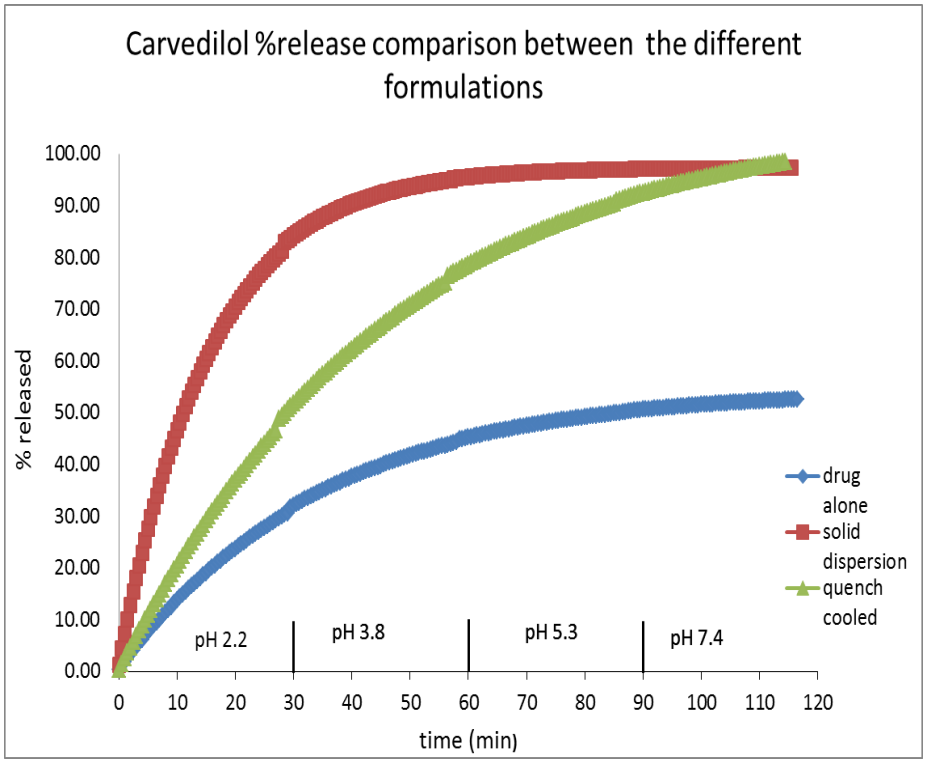

Figure 13.3-6 Carvedilol drug and the different solid dispersion solubility traces.

The solubility of Probucol drug on the Sirius T3 was not achieved due to the drug insolubility.

13.4 Discussion

In this chapter the effect of cooling rate on crystallisation from melt was studied on a range of drugs to compare it with the CBZ results studied in previous chapters. The normal cooling rate DSC traces did show that the only drug that crystallise from melt was Naproxen alone and in formulation. The crystallisation event of Naproxen alone during cooling was much higher than in the PEG formulation which suggests that drug and the PEG are to some degree miscible together. Also, the melting point of Naproxen is lower in the formulation than alone which suggest that the drug and the PEG are interacting together. The normal cooling DSC trace for Carvedilol were in agreement with the literature (Gallo et al., 2016) as Carvidelol did not show any recrystallisation from melt during cooling or reheating (alone or as a formulation), hence the drug stayed in the amorphous form. PEG did recrystallise during cooling in Fenofibrate formulation and during reheating step in Probucol formulation and all the other formulations stayed amorphous after melt.

The quench cooled DSC results were similar to the normal cooled one, only naproxen alone and in formulation did crystallise during cooling. Itraconazole drug recrystallise from melt as a spherulite into three different polymorphic forms at around 100°C (Zhang et al., 2016), whereas in our study no crystallisation from melt was observed and the drug stayed in amorphous form. Probucol and Carvedilol formulations did show a recrystallisation event during reheating after quench cooling around 15°C then melts between 45-50°C. The hot stage microscopy results for these formulations shows that the crystals formed in Probucol formulation has a spherulite morphology which is similar to PEG crystallising whereas for Carvedilol, a small rod shaped crystals appeared. It is hard to properly identify these crystals as they melting at the PEG melting temperature, another technique to identify them such as X-ray could be beneficial in identifying these crystals.

The dissolution profile of Carvedilol was carried out on the Sirius T3 and as the results shows in Figure 13.3-6 the Carvedilol solid dispersion did show a fast release whereas the quench cooled sample did achieve a 100% release but it did take more than 90 mins.

Chapter 14 Conclusion and future work

14.1 Conclusion

Physical stability of an amorphous solid dispersion presents a challenge to the pharmaceutical industry as it can a have significant influence on the bioavailability of their product. Therefore, from the point of view of the formulation development of amorphous solid dispersions, it is essential to gain a comprehensive understanding of the physical stability in order to better predict and control the physical stability. This project was focused on preparing a solid dispersion using a model drug which has more than one polymorphic form and to test the effect of the use of polymer blend and different concentration in stabilising the amorphous form of the drug. Also, to test the percentage drug release in the different formulations prepared. The model drug used in this project was CBZ to prepare a solid solution with PEG mixtures. The PEG was chosen due to the CRUK formulation unit use PEG as the carrier in the formulation they prepare.

The thermal behaviour of PEG mixtures was studied using the DSC and it was found that the degree of crystallinity of the higher molecular weight PEG can be changed by mixing it with PEG 300 as only 10% w/w PEG300 can decrease the crystallinity of PEG 2000 by 10% and reduce the crystallisation temperature and melting point. Therefore, by mixing PEG 300 with other PEG we can work on a wide range of melting and freezing point and we can adjust the degree of crystallinity of the blend we want.

CBZ was formulated with the different PEG 300: PEG mixtures at different concentration to find a suitable formulation. PEG 300 forms a stable nanosuspension with CBZ this was observed in our study as the hot stage microscopy images of CBZ: PEG 300 (50:50% w/w) shows a reduced CBZ crystal size after melt. The higher the PEG 300 content in the formulation the more CBZ is soluble in the PEG and the formulation stayed amorphous after cooling. In the formulation with PEG mixture, the fast cooling rate had a great impact on the stability of the CBZ amorphous form. There was a trend in most formulations where the PEG mixture concentration should be above 50% in order for the PEG to stabilise the solid

solution from melt. The CBZ recrystallisation from the solid solution is affected by the storage temperature as when the temperature reaches 30°C the CBZ recrystallise from melt during the isothermal step. CBZ: PEG 300:6000 (50: 12.5:37.5 %w/w/w) showed the highest crystallisation temperature at around 100°C which is good for stability and the CBZ: PEG 300:35000 (50:37.5:12.5 %w/w/w) showed the lowest % crystallisation which indicates that the CBZ did not fully crystallise in this formulation and some still in amorphous form. The dissolution profile showed a 100% release within the 2 hours study from the formulations with PEG4000, 6000, and 35000 with PEG 6000 was the fastest release but when PEG 300 mixed with PEG 4000 or PEG 6000 the release decreases. The addition of PEG 300 to the formulation had a plasticizing effect on the CBZ and the other PEG used but it did not help the dissolution of the CBZ. CBZ when cooled from some degradation will occur but when PEG was added no degradation was observed and the VT XRPD data did confirm that.

The PEG mixtures did not fully stabilise the CBZ solid solution therefore it was decided to use Poloxamers as they have been used in pharmaceutical industry in enhancing solubility of poorly soluble drug when prepared as a solid dispersion (Guzman.et al., 2007), their ability in reducing crystal growth and inhibiting precipitation. The results show that the quench cooling rate is really important in order to achieve an amorphous sample. F127 alone or with PEG mixtures was not able to totally inhibit the CBZ crystallisation during cooling but it was the best performing Poloxamer in crystal inhibition as the onset and endset temperature of the crystallisation was the smallest and the enthalpy of the peak was the smallest compared to the other formulations this was also have been seen in the literature by Qian and colleagues where F127 had a fast nucleation but slow crystal growth (Qian et al., 2007). P103 concentration has an effect on CBZ recrystallisation from melt as the higher the P103 concentration the smaller the difference between the onset and endset temperature is and the enthalpy of the peak is small which indicate that only a small quantity of CBZ did recrystallise and the rest stayed amorphous. The dissolution study did show an increase in dissolution of CBZ from some formulations such as CBZ: F127, CBZ: PEG300:4000: F127, CBZ: P123 and CBZ: PEG 300: 4000: P123. The F68 and P103 based formulations did show a very fast

release within a few minutes followed by a drop in concentration which indicate that the CBZ is precipitating from these formulations. CBZ: PEG 300: 4000: P123 formulation did show a 100% release within the first 30 minutes at pH2 and when the pH changed the concentration started to decrease indicating a precipitation and pH dependent formulation. The dissolution results did show that P103 did not inhibit precipitation of the drug after dissolution as Guzman paper did show. The XRPD data did show that the CBZ in the CBZ: F127 formulation is crystalline and the CBZ exist as form II whereas the other formulations (F68, P123 and P103) had a low crystalline pattern and the main CBZ peaks are not observed which indicates that there is an interaction between the CBZ and the different Poloxamers. The same results were achieved when PEG mixture is added to the formulations.

PVP was also used to study its effect on stabilising the CBZ solid solution as PVP shows a good crystal growth inhibition and nucleation rate (Trasi and Taylor, 2012). PVP K12 was mixed with PEG 1500, 4000 or 6000 at different concentrations. PVP was able to stabilise the CBZ solid solution stored at 30°C. The PEG molecular weight and the PVP concentration both played a role in the crystallisation inhibition. PEG 1500 with PVP 10 and 20% did inhibit the crystallisation in all temperature used and it was better performing than the PEG 4000 and 6000 this is due to the PEG 1500 is less crystalline which help stabilise the formulations. The VT XRPD results for the CBZ: PEG4000: PVP did show that the concentration of PVP in the formulation affects the degree of crystallinity of CBZ as well as the crystallisation temperature (Tc). The higher the PVP concentration the higher the Tc but there was no difference between the 10 and 20% in the Tc only in the degree of crystallinity. The % of crystallinity experiment shows the PEG molecular weight also important in stabilising the amorphous form as PEG 6000 showed the lowest % crystallinity and the CBZ: PEG6000: PVP5% did not crystallise at room temperature for 24 hours. The dissolution profiles showed a better release than the pure drug.

In conclusion, some drugs can form an amorphous form when quench cooled but their stability will be low and they are prone to recrystallisation. CBZ is one of these drugs and it is possible to stabilise it by solid dispersion with PEG and some

PVP. PEG will enhance its solubility and PVP will delay the crystal growth in solid state.

The recommended CBZ formulation would be the CBZ: PEG 6000 (50:50 %w/w), which showed a rapid dissolution profile with low crystalline content. When PVP was added to that formulation, CBZ: PEG 6000: PVP (50:45:5), there was no crystal growth and the CBZ stayed in amorphous state after quench cooling, however the comparative dissolution profile was not studied.

This work has examined the creation, measurement and stabilisation of an amorphous form of CBZ as solid solution and CBZ solid dispersion. Based upon these studies the following steps mentioned in figure Figure 14.1-1 can be taken to develop a new drug formulation using solid dispersion technique.

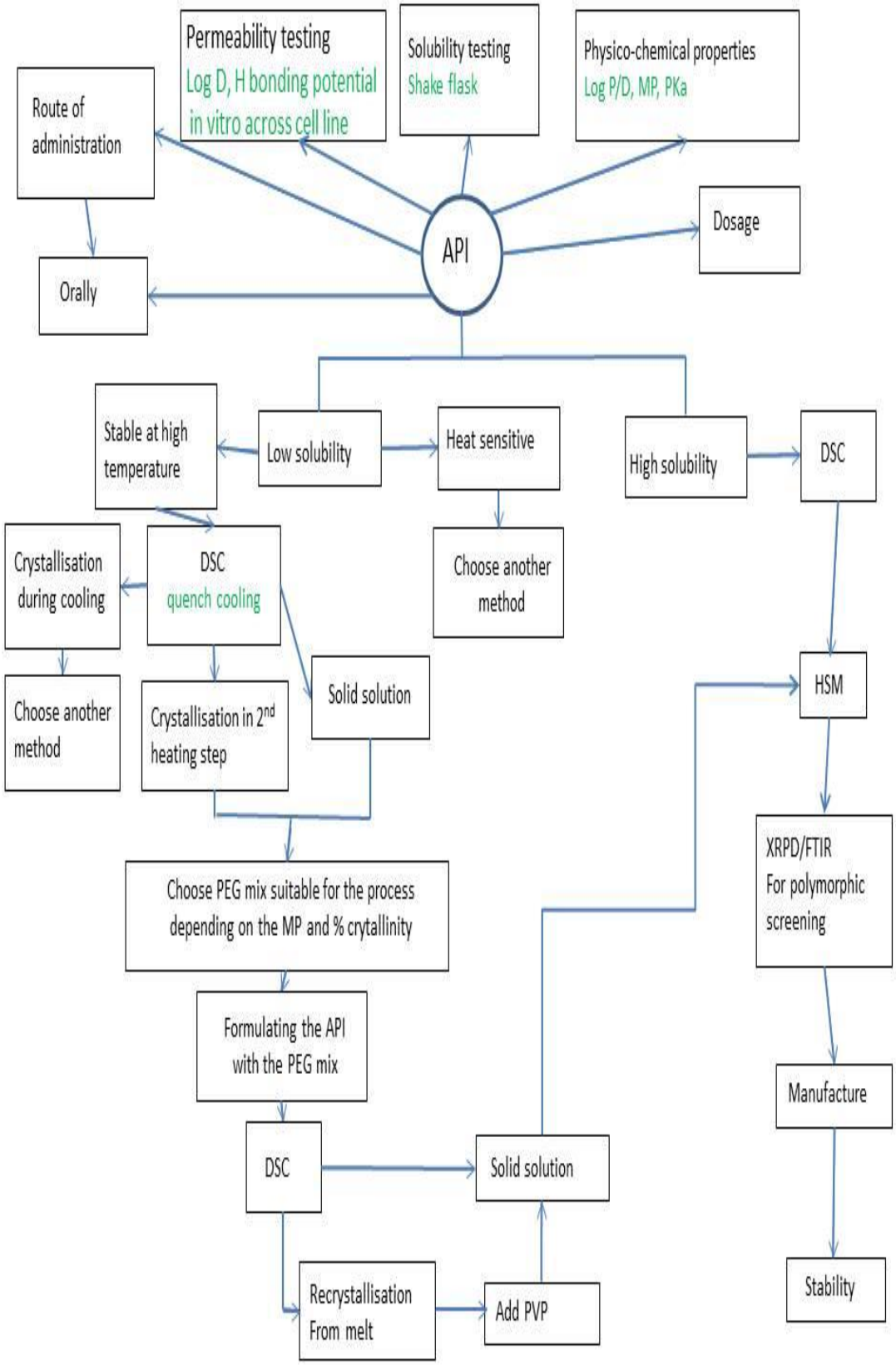

Figure 14.1-1 Road map for a new drug solid dispersion formulation

14.2 Future work

The results collected from this project did show the effect of the different polymer mix and the polymer concentration on the stability of the CBZ solid solution. However, as there were still several results from the project need more investigation to understand the broader image in stabilising the solid solution; the continuation related to this project might be needed. The recommended future work is listed as follows:

- Isothermally held formulations with the different Poloxamer under a hot stage microscopy would be beneficial in order to understand the nucleation and crystal growth rate of the CBZ with the polymer matrix. Also, the dissolution behaviour of the different formulation at one pH at a time could give us an idea why some formulations are precipitating.
- To increase the stability study on the formulations with PVP that showed a promising stability.
- To identify the best performing formulation in term of stability of the solid solution and to produce it at a larger scale and might be filled in a capsule for further stability studies.
- Use Terahertz spectroscopy to study the molecular mobility of the formulations.

References

Abu-Diak, O. A., Jones, D. S., & Andrews, G. P. (2011). An investigation into the dissolution properties of celecoxib melt extrudates: Understanding the role of polymer type and concentration in stabilizing supersaturated drug concentrations. *Molecular Pharmaceutics*, *8*(4), 1362–1371.

Agyemang-yeboah, F., & Oppong, S. Y. (2013). 3 . Caffeine : The wonder compound , chemistry and properties. *Topical Series in Health Science 1*, *661*(2), 27–37.

Alam, A. (2013). Formulation of solid dispersion and surface solid dispersion of nifedipine: A comparative study. *African Journal of Pharmacy and Pharmacology*, *7*(25), 1707–1718.

Ali, W., Badawi, A. A., Mahdy, M. A., & El-Nahas, H. (2013). FORMULATION AND EVALUATION OF CARBAMAZEPINE SOLID DISPERSIONS WITH POLYETHYLENE GLYCOL 6000 AND THEIR INCORPORATION INTO TABLETS. *International Journal of Basic and Applied Chemical Sciences*, *3*(3), 11–20.

Ali, W., Badawi, A. A., Mahdy, M. A., & El-nahas, H. M. (2013). Formulation and Evaluation of Carbamazepine 200mg Immediate Release Tablets using Polyethylene Glycol 6000. *Int J Pharm Pharm Sci*, *5*(1), 114–119.

Allen, L. V., Levinson, R. S., & De Martono, D. (1977). Dissolution rates of hydrocortisone and prednisone utilizing sugar solid dispersion systems in tablet form. *Journal of Pharmaceutical Sciences*, *67*(7), 979–981.

Almeida, a, Possemiers, S., Boone, M. N., De Beer, T., Quinten, T., Van Hoorebeke, L., Vervaet, C. (2011). Ethylene vinyl acetate as matrix for oral sustained release dosage forms produced via hot-melt extrusion. *European Journal of Pharmaceutics and Biopharmaceutics : Official Journal of Arbeitsgemeinschaft Für Pharmazeutische Verfahrenstechnik e.V*, *77*(2), 297–305.

Amidon, G. L., Lennernas, H., Shah, V. P., & Crison, J. R. (1995). A theoretical basis for a biopharmaceutic drug classification: the correlation of in vitro drug product dissolution and in vivo bioavailability. *Pharmaceutical Research*, *12*(3), 413–420.

Alonzo, D. E., Raina, S., Zhou, D., Gao, Y., Zhang, G. G. Z., & Taylor, L. S. (2012). Characterizing the impact of hydroxypropylmethyl cellulose on the growth and nucleation kinetics of felodipine from supersaturated solutions. *Crystal Growth and Design*, *12*(3), 1538–1547.

Alonzo, D. E., Zhang, G. G. Z., Zhou, D., Gao, Y., & Taylor, L. S. (2010). Understanding the behavior of amorphous pharmaceutical systems during dissolution. *Pharmaceutical Research*, *27*(4), 608–618.

Al-Zein, H., Riad, L. E & Abd-Elbary, A. (1999) Effect of Packaging and Storage on the Stability of Carbamazepine Tablets, Drug Development and Industrial Pharmacy, 25:2, 223-227,

Andrews, G. P., Abudiak, O. a., & Jones, D. S. (2009). Physicochemical characterization of hot melt extruded bicalutamide- polyvinylpyrrolidone solid dispersions. *Journal of Pharmaceutical Sciences*, *99*(3), 1322–1335.

Akers, M. J., Strother, C. S., & Walden, M. R. (2014). Sterile Formulation. Fermentation and Biochemical Engineering Handbook (Third Edition). Elsevier Inc.

Aparecida, M., Pinto, L., Ambrozini, B., Paula, A., Ferreira, G., Tadeu, É., & Cavalheiro, G. (2014). Thermoanalytical studies of carbamazepine: hydration/ dehydration, thermal decomposition, and solid phase transitions. *Brazilian Journal of Pharmaceutical Sciences*, *50*(4), 877–884.

Arlin, J., Johnston, A., Miller, G., Kennedy, A., Price, S., & Florence, A. (2010). A predicted dimer-based polymorph of 10,11-dihydrocarbamazepine (Form IV). *CrystEngComm*, *12*(739821), 64–66.

Arlin, J.-B., Price, L. S., Price, S. L., & Florence, A. J. (2011). A strategy for producing predicted polymorphs: catemeric carbamazepine form V. *Chemical Communications (Cambridge, England)*, *47*, 7074–7076.

Arora, K. K., Thakral, S., & Suryanarayanan, R. (2013). Instability in theophylline and carbamazepine hydrate tablets: Cocrystal formation due to release of lattice water. *Pharmaceutical Research*, *30*(7), 1779–1789.

Ashland. (2013). PVP/VA polyvinylpyrrolidone/Vinyl Acetate copolymers Intermediates.

Aso, Y.; Yoshioka, S.; Kojima, S. (2000). Relationship between the crystallization rates of amorphous nifedipine, phenobarbital, and flopropine, and their molecular mobilty as mesured by their enthalpy relaxation and (1)H NMR relaxation times. *Journal of Pharmaceutical Sciences*, *89*(3), 408–416.

Baird, J. A., Van Eerdenbrugh, B., & Taylor, L. S. (2010). A classification system to assess the crystallization tendency of organic molecules from undercooled melts. *Journal of Pharmaceutical Sciences*, *99*(9), 3787–3806.

Barmpalexis, P., Koutsidis, I., Karavas, E., Louka, D., Papadimitriou, S. a, & Bikiaris, D. N. (2013). Development of PVP/PEG mixtures as appropriate carriers for the preparation of drug solid dispersions by melt mixing technique and optimization of dissolution using artificial neural networks. *European Journal of Pharmaceutics and Biopharmaceutics : Official Journal of Arbeitsgemeinschaft Für Pharmazeutische Verfahrenstechnik e.V*, *85*(3), 1219–1231.

Basf. (2004). Technical Bulletin Pluronic ® Block Copolymer NF Grades (Poloxamer NF Grades), 1–2.

Bauer, J., Spanton, S., Henry, R., Quick, J., Dziki, W., Porter, W., & Morris, J. (2001). Ritonavir : An Extraordinary Example of Conformational Polymorphism. *Pharmaceutical Research*, *18*(6), 859–866.

Beyssac, E., & Lavigne, J. (2005). Dissolution study of active pharmaceutical ingredients using the flow through apparatus Usp 4. *Dissolution Technologies*, *12*(May), 23–25.

Biswal, S., Sahoo, J., & Murthy, P. N. (2009). Physicochemical Properties of Solid Dispersions of Gliclazide in Polyvinylpyrrolidone K90. *AAPS PharmSciTech*, *10*(2), 329–334.

Biswal, S., Sahoo, J., Murthy, P. N., Giradkar, R. P., & Avari, J. G. (2008). Enhancement of Dissolution Rate of Gliclazide Using Solid Dispersions with Polyethylene Glycol 6000. *AAPS PharmSciTech*, *9*(2), 563–570.

Bley, H., Fussnegger, B., & Bodmeier, R. (2010). Characterization and stability of solid dispersions based on PEG / polymer blends. *International Journal of Pharmaceutics*, *390*(2), 165–173.

Bobe, K. R., Subrahmanya, C. R., Suresh, S., Gaikwad, D. T., Patil, M. D., Khade, T. S., Gaikwad, U. T. (2011). Formulation and evaluation of solid dispersion of atorvatstatin with various carriers. *International Journal of Comprehensive Pharmacy*, *02*(01), 1–6.

Bodratti, A. M., & Alexandridis, P. (2018). Formulation of Poloxamers for Drug Delivery. *Journal of Functional Biomaterials*, *9*(11), 1–24.

Box, K., Comer, J. E., Gravestock, T., & Stuart, M. (2009). New Ideas about the Solubility of Drugs. Chemistry and Biodiversity, 6, 1767–1788.

Breitenbach, J. (2002). Melt extrusion: from process to drug delivery technology. *European Journal of Pharmaceutics and Biopharmaceutics : Official Journal of Arbeitsgemeinschaft Für Pharmazeutische Verfahrenstechnik e.V*, *54*(2), 107–117.

Brittain, H. G. (2003). Fluorescence Studies of the Transformation of Carbamazepine Anhydrate Form III to its Dihydrate Phase. *Journal of Pharmaceutical Sciences*, *93*(2), 375–383.

Brough, C., & Williams, R. O. (2013). Amorphous solid dispersions and nano-crystal technologies for poorly water-soluble drug delivery. *International Journal of Pharmaceutics*, *453*(1), 157–166.

Bruce, C., Fegely, K. A., Rajabi-Siahboomi, A. R., & McGinity, J. W. (2007). Crystal growth formation in melt extrudates. *International Journal of Pharmaceutics*, *341*(1–2), 162–172.

Buanz, A. B. M., Parkinson, G. N., & Gaisford, S. (2011). Characterization of carbamazepine-nicatinamide cocrystal polymorphs with rapid heating DSC and XRPD. *Crystal Growth and Design*, *11*(4), 1177–1181.

Butler, J. M., & Dressman, J. B. (2010). The developability classification system: Application of biopharmaceutics concepts to formulation development. *Journal of Pharmaceutical Sciences*, *99*(12), 4940–4954.

Campbell, K., Craig, D. Q. M., & McNally, T. (2008). Poly(ethylene glycol) layered silicate nanocomposites for retarded drug release prepared by hot-melt extrusion. *International Journal of Pharmaceutics*, *363*(1–2), 126–131.

Caon, T., Konig, R. A., da Cruz, A. C. C., Cardoso, S. G., Campos, C. E. M., Cuffini, S. L., … Simões, C. M. O. (2013). Development and physicochemical

characterization of saquinavir mesylate solid dispersions using Gelucire 44/14 or PEG 4000 as carrier. *Archives of Pharmacal Research*, *36*(9), 1113–1125.

Charkoftaki, G., Dokoumetzidis, A., Valsami, G., & Macheras, P. (2011). Supersaturated dissolution data and their interpretation: The TPGS-carbamazepine model case. *Journal of Pharmacy and Pharmacology*, *63*(3), 352–361.

Chen, Z., Liu, Z., & Qian, F. (2015). Crystallization of bifonazole and acetaminophen within the matrix of semicrystalline, PEO-PPO-PEO triblock copolymers. *Molecular Pharmaceutics*, *12*(2), 590–599.

Chiou, W. I. N. L., & Riegelmant, S. (1971). Pharmaceutical sciences Pharmaceutical Applications of Solid. *Journal of Pharmaceutical Sciences*, *60*(9), 1281–1302.

Chiou, W. L., & Niazi, S. (1976). Pharmaceutical Applications of Solid Dispersion Systems: Dissolution of Griseofulvin–Succinic Acid Eutectic Mixture. *Journal of Pharmaceutical Sciences*, *65*(8), 1212–1214.

Cilurzo, F., Minghetti, P., Casiraghi, A., & Montanari, L. (2002). Characterization of nifedipine solid dispersions. *International Journal of Pharmaceutics*, *242*, 313–317.

Clariant,2007. Your universally applicable Polymer Functional Chemicals Division. Accessed on 21/8/2017

Craig, D. Q. M., & Newton, J. M. (1991). Characterisation of polyethylene glycols using differential scanning calorimetry. *International Journal of Pharmaceutics*, *74*(1), 33–41.

Craig, D. Q. M. (2002). The mechanisms of drug release from solid dispersions in water-soluble polymers. *International Journal of Pharmaceutics*, *231*(2), 131–144.

Crowley, M. M., Schroeder, B., Fredersdorf, A., Obara, S., Talarico, M., Kucera, S., & McGinity, J. W. (2004). Physicochemical properties and mechanism of drug release from ethyl cellulose matrix tablets prepared by direct compression and hot-melt extrusion. *International Journal of Pharmaceutics*, *269*(2), 509–522.

Date, a. a., Jain, A., Khachane, P., & Nagarsenker, M. S. (2010). Organic solvent-free approach to single step fabrication of Eudragit nanoparticles using Labrasol. *Pharmazie*, *65*, 733–736.

Delori, A., Maclure, P., Bhardwaj, R. M., Johnston, A., Florence, A. J., Sutcliffe, O. B., & Oswald, I. D. H. (2014). Drug solid solutions – a method for tuning phase transformations. *CrystEngComm*, *16*, 5827.

Desai, K. G. H., & Park, H. J. (2004). Solubility studies on valdecoxib in the presence of carriers, cosolvents, and surfactants. *Drug Development Research*, *62*(May), 41–48.

Dewan, I., Hossain, A., & Islam, S. M. A. (2012). Formulation and Evaluation of Solid Dispersions of Carvedilol , a Poorly Water Soluble Drug By Using Different Polymers. *International Journal of Research in Pharmacy and Chemistry*, *2*(3), 585–593.

Djuris, J., Nikolakakis, I., Ibric, S., Djuric, Z., & Kachrimanis, K. (2013). Preparation of carbamazepine-Soluplus solid dispersions by hot-melt extrusion, and prediction of drug-polymer miscibility by thermodynamic model fitting. *European Journal of Pharmaceutics and Biopharmaceutics : Official Journal of Arbeitsgemeinschaft Für Pharmazeutische Verfahrenstechnik e.V*, *84*(1), 228–237.

Docoslis, A., Huszarik, K. L., Papageorgiou, G. Z., Bikiaris, D., Stergiou, D., & Georgarakis, E. (2007). Characterization of the distribution, polymorphism, and stability of nimodipine in its solid dispersions in polyethylene glycol by micro-Raman spectroscopy and powder X-ray diffraction. *The AAPS Journal*, *9*(3), E361-70.

Douroumis, D., & Fahr, A. (2006). Stable carbamazepine colloidal systems using the cosolvent technique. *European Journal of Pharmaceutical Sciences*, *30*(5), 367–374.

Douroumis, D., Fahr, A., Siepmann, J., & Snowden, M. (2013). *Drug Delivery Strategies for Poorly Water-Soluble Drugs*. West Sussex: Wiley.

Dow Company, L. (2011). CARBOWAX ™ Polyethylene Glycols. *DOw Company, USA*.

Edwards, A. D., Shekunov, B. Y., Kordikowski, A., Forbes, R. T., & York, P. (2001). Crystallization of pure anhydrous polymorphs of carbamazepine by solution enhanced dispersion with supercritical fluids (SEDS^{TM}). *Journal of Pharmaceutical Sciences*, *90*(8), 1115–1124.

Einfal, T., Planinšek, O., & Hrovat, K. (2013). Methods of amorphization and investigation of the amorphous state. *Acta Pharmaceutica*, *63*(3), 305–334.

El-zein, H., Riad, L., & El-bary, A. A. (1998). Enhancement of carbamazepine dissolution : in vitro and in vivo evaluation. *International Journal of Pharmaceutics*, *168*, 209–220.

Escandar, G. M., Gómez, D. G., Mansilla, a. E., De La Peña, a. M., & Goicoechea, H. C. (2004). Determination of carbamazepine in serum and pharmaceutical preparations using immobilization on a nylon support and fluorescence detection. *Analytica Chimica Acta*, *506*, 161–170.

Haaf, F., Sanner, A., & Straub, F. (1985). Polymers of N-Vinylpyrro;idpne:synthesis, characterization and uses. *Polymer Journal*, *17*(1), 143–152.

Han, S., Kim, C., & Kwon, D. (1995). Thermal degradation of poly(ethyleneglycol). Polymer Degradation and Stability, 47, 203–208.

Feucht, C., & Patel, D. R. (2011). Principles of pharmacology. *Pediatric Clinics of North America*, *58*(1), 11–9, ix.

Florence, A. J., Leech, C. K., Shankland, N., Shankland, K., & Johnston, A. (2006). Control and prediction of packing motifs: A rare occurrence of carbamazepine in a catemeric configuration. *CrystEngComm*, *8*(10), 746–747.

Florence, A.T., Attwood, D. (2011). Physicochemical principal of pharmacy, 5th edn, Pharmaceutical Press, London.

Ford, J. L. (2014). Hydrophilic Matrix Tablets for Oral Controlled Release. In AAPS PharmSciTech (Vol. 16, pp. 17–52).

Forster, a, Hempenstall, J., Tucker, I., & Rades, T. (2001). Selection of excipients for melt extrusion with two poorly water-soluble drugs by solubility parameter calculation and thermal analysis. *International Journal of Pharmaceutics*, *226*(1–2), 147–161.

Frackowiak Danuta, The Jablonski diagram, Journal of Photochemistry and Photobiology B: Biology,Volume 2, Issue 3, 1988,Page 399.

Fule, R. A., Meer, T. S., Sav, A. R., & Amin, P. D. (2013). Artemether-Soluplus Hot-Melt Extrudate Solid Dispersion Systems for Solubility and Dissolution Rate Enhancement with Amorphous State Characteristics. *Journal of Pharmaceutics*, 1–15.

Gallo, R. C., Ferreira, A. P. G., Castro, R. E. A., & Cavalheiro, E. T. G. (2016). Studying the thermal decomposition of carvedilol by coupled TG-FTIR. *Journal of Thermal Analysis and Calorimetry*, *123*(3), 2307–2312.

Ghebremeskel, A. N., Vemavarapu, C., & Lodaya, M. (2007). Use of surfactants as plasticizers in preparing solid dispersions of poorly soluble API: Selection of polymer-surfactant combinations using solubility parameters and testing the processability. *International Journal of Pharmaceutics*, *328*, 119–129.

Ginés, J. M., Arias, M. J., Rabasco, A. M., Novák, C., Ruiz-Conde, A., & Sánchez-Soto, P. J. (1996). Thermal characterization of polyethylene glycols applied in the pharmaceutical technology using differential scanning calorimetry and hot stage microscopy. *Journal of Thermal Analysis*, *46*(1), 291–304.

Ginés, J. M., Arias, M. J., Rabasco, A. M., & Sánchez-Soto, P. J. (1993). Thermal study of the polyethyleneglycol 6000-triamterene system. *Journal of Thermal Analysis*, *40*(2), 453–462.

Greco, K., & Bogner, R. (2010). Crystallization of amorphous indomethacin during dissolution: Effect of processing and annealing. *Molecular Pharmaceutics*.

Grzesiak, A. L., Lang, M., Kim, K., & Matzger, A. J. (2003). Comparison of the Four Anhydrous Polymorphs of Carbamazepine and the Crystal Structure of Form I. *Journal of Pharmaceutical Sciences*, *92*(11), 2260–2271.

Guinet, Y., Paccou, L., Danède, F., Willart, J. F., Derollez, P., & Hédoux, A. (2016). Comparison of amorphous states prepared by melt-quenching and cryomilling polymorphs of carbamazepine. *International Journal of Pharmaceutics*, *509*(1–2), 305–313.

Guzmán, H. R., Tawa, M., Zhang, Z., Ratanabanangkoon, P., Shaw, P., Gardner, C. R., Remenar, J. F. (2007). Combined use of crystalline salt forms and precipitation inhibitors to improve oral absorption of celecoxib from solid oral formulations. *Journal of Pharmaceutical Sciences*, *96*(10), 2686–2702.

Halliwell, R. A., Bhardwaj, R. M., Brown, C. J., Briggs, N. E. B., Dunn, J., Robertson, J., Florence, A. J. (2017). Spray Drying as a Reliable Route to Produce Metastable Carbamazepine Form IV. *Journal of Pharmaceutical Sciences*, *106*(7), 1874–1880.

Han, S., Kim, C., & Kwon, D. (1994). Thermal degradation of poly(ethyleneglycol). *Polymer Degradation and Stability*, *47*(2), 203–208.

Hardikar, S., Bhosale, A., Vanave, S., & Kamathe, B. (2017). Short Communication PREPARATION AND EVALUATION OF CO-CRYSTALS OF CARBAMAZEPINE WITH GLUCOMANNAN, *9*(10), 9–11.

Herzberger, J., Niederer, K., Pohlit, H., Seiwert, J., Worm, M., Wurm, F. R., & Frey, H. (2015). Polymerization of Ethylene Oxide , Propylene Oxide , and Other Alkylene Oxides : Synthesis , Novel Polymer Architectures , and Bioconjugation. Chemical Reviews, 116, 2170–2243.

Hou, P., Ni, J., Cao, S., Lei, H., Cai, Z., Zhang, T., Tan, Q. (2013). Preparation and Evaluation of Solid Dispersions of A New Antitumor Compound Based on Early-Stage Preparation Discovery Concept. *AAPS PharmSciTech*, *14*(2), 629–638.

Huang, Y., & Dai, W.-G. (2014). Fundamental aspects of solid dispersion technology for poorly soluble drugs. *Acta Pharmaceutica Sinica B*, *4*(1), 18–25.

Ilevbare, G. A., Liu, H. Y., Edgar, K. J., & Taylor, L. S. (2013). Impact of Polymers on Crystal Growth Rate of Structurally Diverse Compounds from Aqueous Solution. *Molecular Pharmaceutics*, *10*(6), 2381–2393.

Ilevbare, G. A., Liu, H., Edgar, K. J., & Taylor, L. S. (2012). Effect of binary additive combinations on solution crystal growth of the poorly water-soluble drug, ritonavir. *Crystal Growth and Design*, *12*(12), 6050–6060.

Ilevbare, G. A., Liu, H., Edgar, K. J., & Taylor, L. S. (2012). Understanding Polymer Properties Important for Crystal Growth Inhibition - Impact of Chemically Diverse Polymers on Solution Crystal Growth of Ritonavir. *Crystal Growth & Design*, *12*(6), 3133–3143.

Iski, E. V, Johnston, B. F., Florence, A. J., Urquhart, A. J., & Sykes, E. C. H. (2010). Surface-Mediated Two-Dimensional Growth ofthe Pharmaceutical Carbamazepine. *ACSnano*, *4*(9), 5061–5068.

Ismail Ashraf A., van de Voort Frederick R, Sedman Jacqueline, Techniques and Instrumentation in Analytical Chemistry, Volume 18, 1997, Pages 93-139.

Isp. (2012). Polyvinylpyrrolidone Polymers. *Performance-Enhancing Products*.

Janssens, S., De Armas, H. N., Roberts, C. J., & Den Mooter, G. Van. (2008). Characterization of ternary solid dispersions of itraconazole, PEG 6000, and HPMC 2910 E5. *Journal of Pharmaceutical Sciences*, *97*(6), 2110–2120.

Jensen, L. G., Skautrup, F. B., Müllertz, A., Abrahamsson, B., Rades, T., & Priemel, P. A. (2017). Amorphous is not always better—A dissolution study on solid state forms of carbamazepine. *International Journal of Pharmaceutics*, *522*(1–2), 74–79.

Joe, J. H., Lee, W. M., Park, Y.-J., Joe, K. H., Oh, D. H., Seo, Y. G., Choi, H.-G. (2010). Effect of the solid-dispersion method on the solubility and crystalline property of tacrolimus. *International Journal of Pharmaceutics*, *395*(1–2), 161–166.

Johnston, A., Johnston, B. F., Kennedy, A. R., & Florence, A. J. (2008). Targeted crystallisation of novel carbamazepine solvates based on a retrospective Random Forest classification. *CrystEngComm*, *10*(1), 23–25.

Joshi, M. (2013). Role of Eudragit in targeted drug delivery. *International Journal of Current Pharmaceutical Research*, *5*(2), 58–62.

Joshi, B. V , Patil, V. B.,& Pokharkar, V. B. (2002) Compatibility Studies Between Carbamazepine and Tablet Excipients Using Thermal and Non-thermal Methods, Drug Development and Industrial Pharmacy, 28:6, 687-694,

Jung, J. Y., Yoo, S. D., Lee, S. H., Kim, K. H., Yoon, D. S., & Lee, K. H. (1999). Enhanced solubility and dissolution rate of itraconazole by a solid dispersion technique. *International Journal of Pharmaceutics*, *187*(2), 209–218. Retrieved from

Kadam, Y., Yerramilli, U., & Bahadur, A. (2009). Solubilization of poorly water-soluble drug carbamezapine in Pluronic®micelles: Effect of molecular characteristics, temperature and added salt on the solubilizing capacity. *Colloids and Surfaces B: Biointerfaces*, *72*(1), 141–147.

Kakran, M., Sahoo, N. G., & Li, L. (2011). Dissolution enhancement of quercetin through nanofabrication, complexation, and solid dispersion. *Colloids and*

Surfaces B: Biointerfaces, *88*, 121–130. Kalivoda, A., Fischbach, M., & Kleinebudde, P. (2012). Application of mixtures of polymeric carriers for dissolution enhancement of oxeglitazar using hot-melt extrusion. *International Journal of Pharmaceutics*, *439*(1–2), 145–156.

Kalivoda, A., Fischbach, M., & Kleinebudde, P. (2012). Application of mixtures of polymeric carriers for dissolution enhancement of oxeglitazar using hot-melt extrusion. *International Journal of Pharmaceutics*, *439*(1–2), 145–156.

Kang Naewon, Jangmi, L., Choi, J. N., Mao, C., & Hee Lee, E. (2015). Cryomilling-induced solid dispersion of poor glass forming/poorly water-soluble mefenamic acid with polyvinylpyrrolidone K12. *Drug Development and Industrial Pharmacy*, *41*(6), 978–988.

Kansara, H., Panola, R., & Mishra, A. (2015). Techniques used to Enhance Bioavailability of BCS Class II Drugs: A Review, *7*(1), 82–93.

Kapsi, S. G., & Ayres, J. W. (2001). Processing factors in development of solid solution formulation of itraconazole for enhancement of drug dissolution and bioavailability. *International Journal of Pharmaceutics*, *229*, 193–203.

Karolewicz, B., Gajda, M., Pluta, J., & Górniak, A. (2015). Dissolution study and thermal analysis of fenofibrate–Pluronic F127 solid dispersions. *Journal of Thermal Analysis and Calorimetry*, *125*, 751–757.

Keller, H. E. (2003). Proper Alignment of the Microscope. In *METHODS IN CELL BIOLOGY* (Vol. 72, pp. 45–55).

Kestur, U. S., & Taylor, L. S. (2010). Role of polymer chemistry in influencing crystal growth rates from amorphous felodipine. *CrystEngComm*, *12*(8), 2288–2295.

Khan, S. H., Hussain, I., Rasool, G., & Mubarak, N. (2013). Physicochemical characterization of solid dispersion of artemether with polyethylene glycol-6000. *Journal of Pharmaceutical and Cosmetic Sciences*, *1*(3), 24–32.

Khan, S., Batchelor, H., Hanson, P., Perrie, Y., & Mohammed, A. R. (2011). Physicochemical characterisation, drug polymer dissolution and in vitro evaluation of phenacetin and phenylbutazone solid dispersions with polyethylene glycol 8000. *Journal of Pharmaceutical Sciences*, *100*(10), 4281–4294.

Kim, E. J., Chun, M. K., Jang, J. S., Lee, I. H., Lee, K. R., & Choi, H. K. (2006). Preparation of a solid dispersion of felodipine using a solvent wetting method. *European Journal of Pharmaceutics and Biopharmaceutics*, *64*, 200–205.

Kipouros, K., Kachrimanis, K., Nikolakakis, I., Tserki, V., & Malamataris, S. (2006). Simultaneous quantification of carbamazepine crystal forms in ternary mixtures (I, III, and IV) by diffuse reflectance FTIR spectroscopy (DRIFTS) and multivariate calibration. *Journal of Pharmaceutical Sciences*, *95*(11), 2419–2431.

Klug, Harold P.; Alexander, Leroy E., X-Ray Diffraction Procedures: For Polycrystalline and Amorphous Materials, 2nd Edition, pp. 992, Wiley, May 1974.

Knopp, M. M., Olesen, N. E., Holm, P., Langguth, P., Holm, R., & Rades, T. (2015). Influence of Polymer Molecular Weight on Drug-Polymer Solubility: A Comparison between Experimentally Determined Solubility in PVP and Prediction Derived from Solubility in Monomer. *Journal of Pharmaceutical Sciences*, *104*(9), 2905–2912.

Kobayashi, Y., Ito, S., Itai, S., & Yamamoto, K. (2000). Physicochemical properties and bioavailability of carbamazepine polymorphs and dihydrate. *International Journal of Pharmaceutics*, *193*, 137–146.

Koester, L. S., Bertuol, J. B., Groch, K. R., Xavier, C. R., Moellerke, R., Mayorga, P., Bassani, V. L. (2004). Bioavailability of carbamazepine:β-cyclodextrin complex in beagle dogs from hydroxypropylmethylcellulose matrix tablets. *European Journal of Pharmaceutical Sciences*, *22*, 201–207.

Konno, H., Handa, T., Alonzo, D. E., & Taylor, L. S. (2008). Effect of polymer type on the dissolution profile of amorphous solid dispersions containing felodipine. *European Journal of Pharmaceutics and Biopharmaceutics : Official Journal of Arbeitsgemeinschaft Für Pharmazeutische Verfahrenstechnik e.V*, *70*(2), 493–499.

Laitinen, R., Priemel, P. A., Surwase, S., Graeser, K., Clare, J., Grohganz, H., & Rades, T. (2014). Amorphous Solid Dispersions. *Advances in Delivery Science and Technology*, 35–44.

Lakshman, J. P., Cao, Y., Kowalski, J., & Serajuddin, A. T. M. (2008). Application of Melt Extrusion in the Development of a Physically and Chemically Stable High-Energy Amorphous Solid Dispersion of a Poorly Water-Soluble Drug. *Molecular Pharmaceutics*, *5*(6), 994–1002.

Lauer, M. E., Grassmann, O., Siam, M., Tardio, J., Jacob, L., Page, S., Alsenz, J. (2011). Atomic force microscopy-based screening of drug-excipient miscibility and stability of solid dispersions. *Pharmaceutical Research*, *28*(3), 572–584.

Law, D., Wang, W., Schmitt, E. A., & Long, M. A. (2001). Prediction of Poly(Ethylene)Glycol-drug eutectic compositions using an index based on the van ' t Hoff equation. *Phamceutical Research*, *19*(3), 315–321.

Law, S. L., Lo, W. Y., Lin, F. M., & Chaing, C. H. (1992). Dissolution and absorption of nifedipine in polyethylene glycol solid dispersion containing phosphatidylcholine. *International Journal of Pharmaceutics*, *84*(2), 161–166.

Lehmkemper, K., Kyerematen, S. O., Degenhardt, M., & Sadowski, G. (2017). Influence of Low-Molecular-Weight Excipients on the Phase Behavior of PVPVA64 Amorphous Solid Dispersions. *Pharmaceutical Research*, *35*(1).

Leuner, C., & Dressman, J. (2000). Improving drug solubility for oral delivery using solid dispersions. *European Journal of Pharmaceutics and Biopharmaceutics : Official Journal of Arbeitsgemeinschaft Für Pharmazeutische Verfahrenstechnik e.V*, *50*(1), 47–60.

Li, Y., Chow, P. S., Tan, R. B. H., & Black, S. N. (2008). Effect of water activity on the transformation between hydrate and anhydrate of carbamazepine. *Organic Process Research and Development*, *12*(2), 264–270.

Lim, A. W., Löbmann, K., Grohganz, H., Rades, T., & Chieng, N. (2016). Investigation of physical properties and stability of indomethacin-cimetidine and naproxen-cimetidine co-amorphous systems prepared by quench cooling, coprecipitation and ball milling. *Journal of Pharmacy and Pharmacology*, *68*(1), 36–45.

Lin, C., & Cham, T. (1996). journal of Effect of particle size on the available surface area of nifedipine from nifedipine-polyethylene glycol 6000 solid dispersions. *International Journal of Pharmaceutics*, *127*, 261–272.

Lingam, M., & Venkateswarlu, V. (2001). Enhancement of Solubility and Dissolution Rate of Poorly Water Soluble Drug using Cosolvency and Solid Dispersion Techniques. *International Journal of Pharmaceutical Sciences and Nanotechnology*, *1*(4), 349–356.

Litvinov, V. M., Guns, S., Adriaensens, P., Scholtens, B. J. R., Quaedflieg, M. P., Carleer, R., & Mooter, G. Van Den. (2012). Solid State Solubility of Miconazole in Poly [(ethylene glycol)- g - vinyl alcohol] Using Hot-Melt Extrusion. *Molecular Pharmaceutics*.

Liu, J., Cao, F., Zhang, C., & Ping, Q. (2013). Use of polymer combinations in the preparation of solid dispersions of a thermally unstable drug by hot-melt extrusion. *Acta Pharmaceutica Sinica B*, *3*(4), 263–272.

Liu, X., Lu, M., Guo, Z., Huang, L., Feng, X., & Wu, C. (2012). Improving the chemical stability of amorphous solid dispersion with cocrystal technique by hot melt extrusion. *Pharmaceutical Research*, *29*(3), 806–817.

Loftsson, T., Vogensen, S. B., Desbos, C., & Jansook, P. (2008). Carvedilol: Solubilization and Cyclodextrin Complexation: A Technical Note. *AAPS PharmSciTech*, *9*(2), 425–430.

Lopes Jesus, a J., Nunes, S. C. C., Ramos Silva, M., Matos Beja, a, & Redinha, J. S. (2010). Erythritol: crystal growth from the melt. *International Journal of Pharmaceutics*, *388*(1–2), 129–135.

Lyons, J. G., Hallinan, M., Kennedy, J. E., Devine, D. M., Geever, L. M., Blackie, P., & Higginbotham, C. L. (2007). Preparation of monolithic matrices for oral drug delivery using a supercritical fluid assisted hot melt extrusion process. *International Journal of Pharmaceutics*, *329*(1–2), 62–71.

Ma, H., Choi, D. S., Zhang, Y. E., Tian, H., Shah, N., & Chokshi, H. P. (2013). Evaluation on the drug-polymer mixing status in amorphous solid dispersions at the early stage formulation and process development. *Journal of Pharmaceutical Innovation*, *8*(3), 163–174.

Mahlin, D., & Bergström, C. A. S. (2013). Early drug development predictions of glass-forming ability and physical stability of drugs. *European Journal of Pharmaceutical Sciences*, *49*(2), 323–332.

Majumdar, R., Alexander, K. S., & Riga, A. T. (2010). Physical characterization of polyethylene glycols by thermal analytical technique and the effect of humidity and molecular weight. *Die Pharmazie*, *65*, 343–347.

Marsac, P. J., Konno, H., & Taylor, L. S. (2006). A comparison of the physical stability of amorphous felodipine and nifedipine systems. *Pharmaceutical Research*, *23*(10), 2306–2316.

Martïnez, L. M., Videa, M., Sosa, N. G., Ramïrez, J. H., & Castro, S. (2016). Long-term stability of new co-amorphous drug binary systems: Study of glass transitions as a function of composition and shelf time. Molecules, 21(12).

Maulvi, F. a., Dalwadi, S. J., Thakkar, V. T., Soni, T. G., Gohel, M. C., & Gandhi, T. R. (2011). Improvement of dissolution rate of aceclofenac by solid dispersion technique. *Powder Technology*, *207*(1–3), 47–54.

Medarević, D. P., Kachrimanis, K., Mitrić, M., Djuriš, J., Djurić, Z., & Ibrić, S. (2015). Dissolution rate enhancement and physicochemical characterization of carbamazepine-poloxamer solid dispersions. *Pharmaceutical Development and Technology*, *7450*, 1–9.

Miyazawa, T., Fukushima, K., & Ideguchi, Y. (1962). Molecular vibrations and structure of high polymers. III. Polarized infrared spectra, normal vibrations, and helical conformation of polyethylene glycol. *The Journal of Chemical Physics*, *37*(12), 2764–2776.

Moes, J. J., Koolen, S. L. W., Huitema, a D. R., Schellens, J. H. M., Beijnen, J. H., & Nuijen, B. (2011). Pharmaceutical development and preliminary clinical testing of an oral solid dispersion formulation of docetaxel (ModraDoc001). *International Journal of Pharmaceutics*, *420*(2), 244–250.

Mohamed, M., Talari, M. K., Tripathy, M., & Majeed, A. A. (2012). Pharmaceutical Applications of Crospovidone : a Review . *International Journal of Drug Formulation and Research*, *3*(1), 13–28.

Moneghini, M., Kikic, I., Voinovich, D., Perissutti, B., & Filipović-Grcić, J. (2001). Processing of carbamazepine-PEG 4000 solid dispersions with supercritical carbon dioxide: preparation, characterisation, and in vitro dissolution. *International Journal of Pharmaceutics*, *222*(1), 129–138.

Mowafy, H. A., Alanazi, F. K., & El Maghraby, G. M. (2011). Development and validation of an HPLC-UV method for the quantification of carbamazepine in rabbit plasma. *Saudi Pharmaceutical Journal*, *20*(1), 29–34.

Murphy, D., Rodríguez-Cintrón, F., Langevin, B., Kelly, R. C., & Rodríguez-Hornedo, N. (2002). Solution-mediated phase transformation of anhydrous to dihydrate carbamazepine and the effect of lattice disorder. *International Journal of Pharmaceutics*, *246*(1–2), 121–134.

Naima, Z., Siro, T., & Chantal, C. (2001). Interactions between carbamazepine and polyethylene glycol (PEG) 6000 : characterisations of the physical , solid dispersed and eutectic mixtures. *European Journal of Pharmaceutical Sciences : Official Journal of the European Federation for Pharmaceutical Sciences*, *12*, 395–404.

Nair, R., Gonen, S., & Hoag, S. W. (2002). Influence of polyethylene glycol and povidone on the polymorphic transformation and solubility of carbamazepine. *International Journal of Pharmaceutics*, *240*, 11–22.

Nagesh, C., Shankaraiah, M., Attimarad, S., Patil, A., & Kumar, V. (2013). Improving the Solubility and Dissolution of Ritonavir By Solid Dispersion. *Journal of Pharmaceutical and Scientific Innovation*, *2*(4), 30–35.

Nghiem, L. D., Schafer, A. I., & Elimelech, M. (2005). Pharmaceutical retention mechanisms by nanofiltration membranes. *Environmental Science and Technology*, *39*(19), 7698–7705.

Nidhi, K., Indrajeet, S., Khushboo, M., Gauri, K., & Sen, D. J. (2011). Hydrotropy: A promising tool for solubility enhancement: A review. *International Journal of Drug Development and Research*, *3*(2), 26–33.

Nikam, V. K., Kotade, K. B., Gaware, V. M., & Dolas, R. T. (2011). Eudragit a versatile Polymer: a Review. *Pharmacologyonline*, *1*, 152–164.

Nikghalb, L. A., Singh, G., Singh, G., & Kahkeshan, K. F. (2012). Solid Dispersion : Methods and Polymers to increase the solubility of poorly soluble drugs. *Applied Pharmaceutical Science*, *2*(10), 170–175.

Nokhodchi, A., Al-Hamidi, H., Antonijevic, M. D., Owusu-Ware, S., & Kaialy, W. (2015). Dissolution and solid state behaviours of carbamazepine-gluconolactone

solid dispersion powders: The potential use of gluconolactone as dissolution enhancer. *Chemical Engineering Research and Design*, *100*, 452–466.

Noyes, arthur A., & Whitney, willis R. (1897). THE RATE OF SOLUTION OF SOLID SUBSTANCES IN THEIR OWN SOLUTIONS. By. Journal of the American Chemical Society, 19(12), 930–934.

Oberoi, L. M., Alexander, K. S., & Riga, A. T. (2004). Evaluation of an index based on van't Hoff equation to predict peg-drug eutectic composition. *Journal of Thermal Analysis and Calorimetry*, *78*(1), 83–89.

O'Brien, L. E., Timmins, P., Williams, A. C., & York, P. (2004). Use of in situ FT-Raman spectroscopy to study the kinetics of the transformation of carbamazepine polymorphs. *Journal of Pharmaceutical and Biomedical Analysis*, *36*, 335–340.

Okonogi, S., & Puttipipatkhachorn, S. (2006). Dissolution Improvement of High Drug-loaded Solid Dispersion. *AAPS PharmSciTech*, *7*(2).

O'Mahony, M. A., Maher, A., Croker, D. M., Rasmuson, Å. C., & Hodnett, B. K. (2012). Examining solution and solid state composition for the solution-mediated polymorphic transformation of carbamazepine and piracetam. *Crystal Growth and Design*, *12*(4), 1925–1932.

Overhoff, K. a., Moreno, A., Miller, D. a., Johnston, K. P., & Williams, R. O. (2007). Solid dispersions of itraconazole and enteric polymers made by ultra-rapid freezing. *International Journal of Pharmaceutics*, *336*, 122–132.

Pagire, S. K., Jadav, N., Vangala, V. R., Whiteside, B., & Paradkar, A. (2017). Thermodynamic Investigation of Carbamazepine-Saccharin Co-Crystal Polymorphs. *Journal of Pharmaceutical Sciences*, *106*(8), 2009–2014.

Papadimitriou, S. a, Barmpalexis, P., Karavas, E., & Bikiaris, D. N. (2012). Optimizing the ability of PVP/PEG mixtures to be used as appropriate carriers for the preparation of drug solid dispersions by melt mixing technique using artificial neural networks: I. *European Journal of Pharmaceutics and Biopharmaceutics : Official Journal of Arbeitsgemeinschaft Für Pharmazeutische Verfahrenstechnik e.V*, *82*(1), 175–186.

Papadimitriou, S., & Bikiaris, D. (2009). Dissolution rate enhancement of the poorly water-soluble drug Tibolone using PVP, SiO2, and their nanocomposites as

appropriate drug carriers. *Drug Development and Industrial Pharmacy*, *35*(9), 1128–1138.

Patel, D. D., & Anderson, B. D. (2015). Adsorption of Polyvinylpyrrolidone and its Impact on Maintenance of Aqueous Supersaturation of Indomethacin via Crystal Growth Inhibition. *Journal of Pharmaceutical Sciences*, *104*(9), 2923–2933.

Patel, H. R., Patel, R. P., & Patel, M. M. (2009). Poloxamers: A pharmaceutical excipients with therapeutic behaviors. *International Journal of PharmTech Research*, *1*(2), 299–303.

Patil, H., Tiwari, R. V, & Repka, M. A. (2015). Hot-Melt Extrusion : from Theory to Application in Pharmaceutical Formulation. AAPS PharmSciTech, 17(1), 20–42.

Patterson, J. E., James, M. B., Forster, A. H., Lancaster, R. W., Butler, J. M., & Rades, T. (2005). The influence of thermal and mechanical preparative techniques on the amorphous state of four poorly soluble compounds. *Journal of Pharmaceutical Sciences*, *94*(9), 1998–2012.

Patterson, J. E., James, M. B., Forster, A. H., Lancaster, R. W., Butler, J. M., & Rades, T. (2007). Preparation of glass solutions of three poorly water soluble drugs by spray drying, melt extrusion and ball milling. *International Journal of Pharmaceutics*, *336*(1), 22–34.

Paus, R., Ji, Y., Vahle, L., & Sadowski, G. (2015). Predicting the Solubility Advantage of Amorphous Pharmaceuticals: A Novel Thermodynamic Approach. *Molecular Pharmaceutics*, *12*(8), 2823–2833.

Perissutti, B., Michael, J., Podczeck, F., & Rubessa, F. (2001). Preparation of extruded carbamazepine and PEG 4000 as a potential rapid release dosage form. *European Journal of Pharmaceutics and Biopharmaceutics : Official Journal of Arbeitsgemeinschaft Für Pharmazeutische Verfahrenstechnik e.V*, *53*, 125–132.

Perissutti, B., Rubessa, F., Moneghini, M., & Voinovich, D. (2002). Formulation design of carbamazepine fast-release tablets prepared by melt granulation technique. *International Journal of Pharmaceutics*, *256*(1–2), 53–63.

PerkinElmer. (2000). An Introduction to fluorescence spectroscopy. *PerkinElmer, Inc.*, 1–36.

Piccinni, P., Tian, Y., McNaughton, A., Fraser, J., Brown, S., Jones, D. S., Andrews, G. P. (2016). Solubility parameter-based screening methods for early-stage formulation development of itraconazole amorphous solid dispersions. *Journal of Pharmacy and Pharmacology*, *68*(5), 705–720.

Pielichowski, K., & Flejtuch, K. (2002). Differential scanning calorimetry studies on poly(ethylene glycol) with different molecular weights for thermal energy storage materials. *Polymers for Advanced Technologies*, *13*, 690–696.

Pitto-barry, A., Barry, N. P. E., & Barry, N. P. E. (2014). Pluronic® block-copolymers in medicine: from chemical and biological versatility to rationalisation and clinical advances. *Polymer Chemistry*, *5*(10), 3291–3297.

Pouton, C. W. (2006). Formulation of poorly water-soluble drugs for oral administration: physicochemical and physiological issues and the lipid formulation classification system. *European Journal of Pharmaceutical Sciences : Official Journal of the European Federation for Pharmaceutical Sciences*, *29*(3–4), 278–287.

Preetham, a C., & Satish, C. S. (2011). Formulation of a Poorly Water-Soluble Drug Sirolimus in Solid Dispersions to Improve Dissolution. *Journal of Dispersion Science and Technology*, *32*(May), 778–783.

Prentice, A. G., & Glasmacher, A. (2005). Making sense of itraconazole pharmacokinetics. Journal of Antimicrobial Chemotherapy, 56(S1), 17–22.

Price Sarah L. , Leslie Maurice, Welch Gareth W. A. , Habgood Matthew, Price Louise S., K. P. G. and D. G. M. (2010). Modelling organic crystal structures using distributed multipole and polarizability-based model intermolecular potentials. *Physical Chemistry Chemical Physics : PCCP*, *12*, 8466–8477.

Price JC, Polyethylene glycol, in: A. Wade, P.J. Weller (Eds.),Handbook of Pharmaceutical Excipients, American Pharmaceutical Association/The Pharmaceutical Press, Washington, DC/London, 1994; pp. 355-61.

Prodduturi, S., Urman, K. L., Otaigbe, J. U., & Repka, M. A. (2007). Stabilization of Hot-Melt Extrusion Formulations Containing Solid Solutions Using Polymer Blends. *AAPS PharmSciTech*, *8*(2), article 50.

Prudic, A., Ji, Y., Luebbert, C., & Sadowski, G. (2015). Influence of humidity on the phase behavior of API/polymer formulations. *European Journal of Pharmaceutics and Biopharmaceutics*, *94*, 352–362.

Prudic, A., Ji, Y., & Sadowski, G. (2014). Thermodynamic phase behavior of API/polymer solid dispersions. *Molecular Pharmaceutics*, *11*(7), 2294–2304.

Prudic, A., Kleetz, T., Korf, M., Ji, Y., & Sadowski, G. (2014). Influence of copolymer composition on the phase behavior of solid dispersions. *Molecular Pharmaceutics*, *11*(11), 4189–4198.

Qi, S., Belton, P., Nollenberger, K., Clayden, N., Reading, M., & Craig, D. Q. M. (2010). Characterisation and Prediction of Phase Separation in Hot-Melt Extruded Solid Dispersions: A Thermal, Microscopic and NMR Relaxometry Study. *Pharmaceutical Research*, *27*(9), 1869–1883.

Qi, S., Gryczke, A., Belton, P., & Craig, D. Q. M. (2008). Characterisation of solid dispersions of paracetamol and EUDRAGIT E prepared by hot-melt extrusion using thermal, microthermal and spectroscopic analysis. *International Journal of Pharmaceutics*, *354*(1–2), 158–167.

Qian, F., Tao, J., Desikan, S., Hussain, M., & Smith, R. L. (2007). Mechanistic investigation of Pluronic based nano-crystalline drug-polymer solid dispersions. *Pharmaceutical Research*, *24*(8), 1551–1560.

Qiu, S., Lai, J., Guo, M., Wang, K., Lai, X., Desai, U., Li, M. (2016). Role of polymers in solution and tablet-based carbamazepine cocrystal formulations. *CrystEngComm*, *18*(15), 2664–2678.

Qiu, S., & Li, M. (2015). Effects of coformers on phase transformation and release profiles of carbamazepine cocrystals in hydroxypropyl methylcellulose based matrix tablets. *International Journal of Pharmaceutics*, *479*(1), 118–128.

Rao, K.S. & Belorkar, N. (2010). Development and validation of a specific stability indicating liquid chromatographic method for carbamazepine in bulk and pharmaceutical dosage forms. J Adv Pharm Res. 1. 36-47.

Rowe, R. C., Sheskey, P. J., & Quinn, M. E. (Eds.). (2009). *Handbook of Pharmaceutical Excipients* (6th ed.). London: Pharmaceutical Press.

Royer, C. a. (1995). Fluorescence spectroscopy. *Methods in Molecular Biology (Clifton, N.J.)*, *40*, 65–89.

Rumondor, A. C. F., & Taylor, L. S. (2010). Application of Partial Least-Squares (PLS) modeling in quantifying drug crystallinity in amorphous solid dispersions. *International Journal of Pharmaceutics*, *398*(1–2), 155–160.

Rustichelli, C., Gamberini, G., Ferioli, V., & Gamberini, M. C. (2000). Solid-state study of polymorphic drugs : carbamazepine. *Journal of Pharmaceutical and Biomedical Analysis*, *23*, 41–54.

Saerens, L., Dierickx, L., Lenain, B., Vervaet, C., Remon, J. P., & De Beer, T. (2011). Raman spectroscopy for the in-line polymer-drug quantification and solid state characterization during a pharmaceutical hot-melt extrusion process. *European Journal of Pharmaceutics and Biopharmaceutics : Official Journal of Arbeitsgemeinschaft Für Pharmazeutische Verfahrenstechnik e.V*, *77*(1), 158–163.

Salameh, A. K., & Taylor, L. S. (2006). Physical stability of crystal hydrates and their anhydrates in the presence of excipients. *Journal of Pharmaceutical Sciences*, *95*(2), 446–461.

Sancheti, P. P., Vyas, V. M., Shah, M., Karekar, P., & Pore, Y. V. (2008). Development and characterization of bicalutamide-poloxamer F68 solid dispersion systems. *Pharmazie*, *63*, 571–575.

Saravanan, R., Gupta, V. K., Narayanan, V., Stephen, a., Codex, F. C., Of, T., & Chem, J. (2013). a Simple and Effective Method for Preparation and Characterization of Zinc Oxide. *Journal of Molecular Liquids*, *11*(2), 7932.

Sarode, A. L., Sandhu, H., Shah, N., Malick, W., & Zia, H. (2012). Hot melt extrusion (HME) for amorphous solid dispersions: Predictive tools for processing and impact of drug-polymer interactions on supersaturation. *European Journal of Pharmaceutical Sciences : Official Journal of the European Federation for Pharmaceutical Sciences*, *48*(3), 371–384.

Sauer, M., Hofkens, J. and Enderlein, J. (2011) Front Matter, in Handbook of Fluorescence Spectroscopy and Imaging: From Single Molecules to Ensembles, Wiley-VCH Verlag GmbH & Co. KGaA, Weinheim, Germany.

Savjani, K. T., Gajjar, A. K., & Savjani, J. K. (2012). Drug Solubility: Importance and Enhancement Techniques. *ISRN Pharmaceutics*, *2012*(100), 1–10.

Schöffski, K., & Strohm, D. (2006). Karl Fischer Moisture Determination. In *Encyclopedia of Analytical Chemistry* (pp. 1–13).

Schram, C. J., Taylor, L. S., & Beaudoin, S. P. (2015). Influence of Polymers on the Crystal Growth Rate of Felodipine: Correlating Adsorbed Polymer Surface Coverage to Solution Crystal Growth Inhibition. *Langmuir*, *31*(41), 11279–11287.

Sekiguchi, K., & Obi, N. (1961). Studies on Absorption of Eutectic Mixture. I. A Comparison of the Behavior of Eutectic Mixture of Sulfathiazole and that of Ordinary Sulfathiazole in Man. *Chemical & Pharmaceutical Bulletin*, *9*(11), 866–872. Retrieved from

Semjonov, K., Salm, M., Lipiäinen, T., Kogermann, K., Lust, A., Laidmäe, I., Heinämäki, J. (2018). Interdependence of particle properties and bulk powder behavior of indomethacin in quench-cooled molten two-phase solid dispersions. *International Journal of Pharmaceutics*, *541*(1–2), 188–197.

Sethia, S., & Squillante, E. (2004). Solid dispersion of carbamazepine in PVP K30 by conventional solvent evaporation and supercritical methods. *International Journal of Pharmaceutics*, *272*, 1–10.

Sevelius, H., Runkel, R., Segre, E., & Bloomfield, S. (1980). Bioavailability of naproxen sodium and its relationship to clinical analgesic effects. *British Journal of Clinical Pharmacology*, *10*(3), 259–263.

Shah, B., Kakumanu, V. K., & Bansal, A. K. (2006). Analytical techniques for quantification of amorphous/crystalline phases in pharmaceutical solids. *Journal of Pharmaceutical Sciences*, *95*(8), 1641–1665.

Shah, J. C., Chen, J. R., & Chow, D. (1995). Preformulation study of etoposide : II . Increased solubility and dissolution rate by solid-solid dispersions. International Journal of Pharmaceutics, 113, 103–111.

Shah, J., Vasanti, S., Anroop, B., & Vyas, H. (2008). Enhancement of dissolution rate of valdecoxib by solid dispersions technique with PVP K 30 & PEG 4000: Preparation and in vitro evaluation. *Journal of Inclusion Phenomena and Macrocyclic Chemistry*, *63*, 69–75.

Shah, S., Maddineni, S., Lu, J., & Repka, M. a. (2013). Melt extrusion with poorly soluble drugs. *International Journal of Pharmaceutics*, *453*(1), 233–252.

Sharma, A., & Jain, C. P. (2010). Preparation and characterization of solid dispersions of carvedilol with PVP K30. *Research in Pharmacieutical Sciences*, *5*(1), 49–56.

Shavi, G. V., Kumar, A. R., Usha, Y. N., Armugam, K., Ranjan, O. P., Ginjupalli, K., Udupa, N. (2010). Enhanced dissolution and bioavailability of gliclazide using solid dispersion techniques. *International Journal of Drug Delivery*, *2*(1), 49–57.

Shin, S., Oh, I., Lee, Y., Choi, H., & Choi, J. (1998). Enhanced dissolution of furosemide by coprecipitating or cogrinding with crospovidone. *International Journal of Pharmaceutics*, *175*, 17–24.

Shinde, V. R., Shelake, M. R., Shetty, S. S., Chavan-patil, A. B., Pore, Y. V, & Late, S. G. (2008). Enhanced solubility and dissolution rate of lamotrigine by inclusion complexation and solid dispersion technique. *Journal of Pharmacy and Pharmacology*, *60*, 1121–1129.

Singhal, D., & Curatolo, W. (2004). Drug polymorphism and dosage form design: a practical perspective. *Advanced Drug Delivery Reviews*, *56*(3), 335–347.

Sinha, S., Ali, M., Baboota, S., Ahuja, A., Kumar, A., & Ali, J. (2010). Solid Dispersion as an Approach for Bioavailability Enhancement of Poorly Water-Soluble Drug Ritonavir. *American Association of Pharmaceutical Scientists*, *11*(2), 518–527.

Six, K., Verreck, G., Peeters, J., Brewster, M., & Van Den Mooter, G. (2004). Increased Physical Stability and Improved Dissolution Properties of Itraconazole, a Class II Drug, by Solid Dispersions that Combine Fast- and Slow-Dissolving Polymers. *Journal of Pharmaceutical Sciences*, *93*(1), 124–131.

Smith, B. T. (2016). Remington education: physical pharmacy, Pharmaceutical Press, London, P32-34.

Sotthivirat, S., McKelvey, C., Moser, J., Rege, B., Xu, W., & Zhang, D. (2013). Development of amorphous solid dispersion formulations of a poorly water-soluble drug, MK-0364. *International Journal of Pharmaceutics*, *452*(1–2), 73–81.

Sridhar, I., Doshi, A., Joshi, B., Wankhede, V., & Doshi, J. (2013). Solid Dispersions : an Approach to Enhance Solubility of poorly Water Soluble Drug. *Scientific and Innovation Research*, *2*(3), 685–694.

Srirambhatla, V. K., Guo, R., Price, S. L., & Florence, A. J. (2016). Isomorphous template induced crystallisation: A robust method for the targeted crystallisation of computationally predicted metastable polymorphs. *Chemical Communications*, *52*(46), 7384–7386.

State, S., & Pharmaceutical, O. F. (2007). Solid State of Pharmaceutical Compounds, 1–30.

Strachan, C. J., Pratiwi, D., Gordon, K. C., & Rades, T. (2004). Quantitative analysis of polymorphic mixtures of carbamazepine by Raman spectroscopy and principal components analysis. *Journal of Raman Spectroscopy*, *35*, 347–352.

Swidan, S. A., Ghonaim, H. M., Ghorab, M. M., & Samy, A. M. (2013). Design , Formulation and Evaluation of Piroxicam Capsules Prepared by Solid Dispersion Technique. *British Journal of Pharmaceutical Research*, *3*(1), 108–134.

Tachibana, T., & Nakamura, A. (1965). A Methode for Preparing an Aqueous Colloidal Dispersion of Organic Materials by Using Water-Soluble Polymers : Dispersion of fl-Carotene by Polyvinylpyrrolidone. *Kolloid-Z.u.Z.Polymere*, *203*(2), 130–133.

Tantishaiyakul, V., Kaewnopparat, N., & Ingkatawornwong, S. (1999). Properties of solid dispersions of piroxicam in polyvinylpyrrolidone. *International Journal of Pharmaceutics*, *181*, 143–151.

Tian, F., Sandler, N., Aaltonen, J., Lang, C., Saville, D. J., Gordon, K. C., Rades, T. (2007). Influence of polymorphic form, morphology, and excipient interactions on the dissolution of carbamazepine compacts. *Journal of Pharmaceutical Sciences*, *96*(3), 584–594.

Tian, F., Saville, D. J., Gordon, K. C., Strachan, C. J., Zeitler, J. A., Sandler, N., & Rades, T. (2007). The influence of various excipients on the conversion kinetics of carbamazepine polymorphs in aqueous suspension. *Journal of Pharmacy and Pharmacology*, *59*(2), 193–201.

Tiwari, S. B., & Rajabi-Siahboomi, A. R. (2008). Modulation of drug release from hydrophilic matrices. *Pharm Tech Europe*, *20*(September), 24–32.

Trasi, N. S., Abbou Oucherif, K., Litster, J. D., & Taylor, L. S. (2015). Evaluating the influence of polymers on nucleation and growth in supersaturated solutions of acetaminophen. *CrystEngComm*, *17*(6), 1242–1248.

Trasi, N. S., & Taylor, L. S. (2012). Effect of additives on crystal growth and nucleation of amorphous flutamide. *Crystal Growth and Design*, *12*(6), 3221–3230.

Trasi, N. S., & Taylor, L. S. (2012). Effect of polymers on nucleation and crystal growth of amorphous acetaminophen. *CrystEngComm*, *14*(16), 5188–5197.

Urbanetz, N. A. (2006). Stabilization of solid dispersions of nimodipine and polyethylene glycol 2000. *European Journal of Pharmaceutical Sciences : Official Journal of the European Federation for Pharmaceutical Sciences*, *28*(1–2), 67–76.

Urbanetz, N. A., & Lippold, B. C. (2005). Solid dispersions of nimodipine and polyethylene glycol 2000: Dissolution properties and physico-chemical characterisation. *European Journal of Pharmaceutics and Biopharmaceutics*, *59*, 107–118.

Van Den Mooter, G. (2012). The use of amorphous solid dispersions: A formulation strategy to overcome poor solubility and dissolution rate. *Drug Discovery Today: Technologies*, *9*(2), e79–e85.

Varma, M. M., Begum, S. K. R., Mohan, V. M., & S.K., R. B. (2012). Formulation, Physicochemical Evaluation, and Dissolution Studies of Carbamazepine Solid Dispersions. *International Journal of Pharmaceutical Sciences and Nanotechnology*, *5*(3), 1790–1807.

Vartapetyan, R. S., Khozina, E. V., Chalykh, A. E., Skirda, V. D., Feldstein, M. M., Kärger, J., & Geschke, D. (2003). Molecular Mobility in a Poly(ethylene glycol)-Poly(vinyl pyrrolidone) Blends: Study by the Pulsed Gradient NMR Techniques. *Colloid Journal of the Russian Academy of Sciences: Kolloidnyi Zhurnal*, *65*(6), 684–690.

Vasa, D. M., Dalal, N., Katz, J. M., Roopwani, R., Nevrekar, A., Patel, H., Wildfong, P. L. D. (2014). Physical characterization of drug:Polymer dispersion behavior

in polyethylene glycol 4000 solid dispersions using a suite of complementary analytical techniques. *Journal of Pharmaceutical Sciences*, *103*(9), 2911–2923.

Verma, S., & Rudraraju, V. S. (2014). A Systematic Approach to Design and Prepare Solid Dispersions of Poorly Water-Soluble Drug. *AAPS PharmSciTech*, *15*(3), 641–657.

Vetter, T., Mazzotti, M., & Brozio, J. (2011). Slowing the Growth Rate of Iburpofen Crystals Using the Polymeric Additive Pluronic F127. *Crystal Growth & Design*, 3813–3821.

Vippagunta, S. R., Brittain, H. G., & Grant, D. J. W. (2001). Crystalline solids. *Advanced Drug Delivery Reviews*, *48*, 3–26.

Vippagunta, S. R., Maul, K. A., Tallavajhala, S., & Grant, D. J. W. (2002). Solid-state characterization of nifedipine solid dispersions. *International Journal of Pharmaceutics*, *236*(1–2), 111–123.

Wei, T., Zheng, B., Yi, H., Gao, Y., & Guo, W. (2014). Thermal analysis and non-isothermal kinetics of poly(ethylene glycol) with different molecular weight. *Polymer Engineering and Science*, *54*(12), 2872–2876.

Widjaja, E., Kanaujia, P., Lau, G., Ng, W. K., Garland, M., Saal, C., Tan, R. B. H. (2011). Detection of trace crystallinity in an amorphous system using Raman microscopy and chemometric analysis. *European Journal of Pharmaceutical Sciences : Official Journal of the European Federation for Pharmaceutical Sciences*, *42*(1–2), 45–54.

Wu, K. E., Li, J., Wang, W., & Winstead, D. A. (2009). Formation and Characterization of Solid Dispersions of Piroxicam and Polyvinylpyrrolidone Using Spray Drying and Precipitation with Compressed Antisolvent. *Journal of Pharmaceutical Sciences*, *98*(7), 2422–2431.

Xua, S., & Dai, W. G. (2013). Drug precipitation inhibitors in supersaturable formulations. *International Journal of Pharmaceutics*, *453*(1), 36–43.

Young, C. R., Dietzsch, C., Cerea, M., Farrell, T., Fegely, K. A., Rajabi-Siahboomi, A., & McGinity, J. W. (2005). Physicochemical characterization and mechanisms of release of theophylline from melt-extruded dosage forms based on a methacrylic acid copolymer. *International Journal of Pharmaceutics*, *301*(1–2), 112–120.

Yu, L. (2001). Amorphous pharmaceutical solids: Preparation, characterization and stabilization. *Advanced Drug Delivery Reviews*, *48*(1), 27–42.

Yuan, X., Sperger, D., & Munson, E. J. (2013). Investigating miscibility and molecular mobility of nifedipine-PVP amorphous solid dispersions using solid-state NMR spectroscopy. *Molecular Pharmaceutics*, *11*(1), 329–337.

Zajc, N., & Srčič, S. (2004). Binary melting phase diagrams of nifedipine-PEG 4000 and nifedipine-mannitol systems. *Journal of Thermal Analysis and Calorimetry*, *77*(2), 571–580.

Zhang, S., Lee, T. W. Y., & Chow, A. H. L. (2016). Crystallization of Itraconazole Polymorphs from Melt. *Crystal Growth and Design*, 16(7), 3791-3801.

Zhang, T., & Jiang, G. (2011). Impurity Profiling of Carbamazepine by HPLC / UV. *Thermo Scientific*.

Zhou, D., Zhang, G. G. Z., Law, D., Grant, D. J. W., & Schmitt, E. A. (2002). Physical stability of amorphous pharmaceuticals: Importance of configurational thermodynamic quantities and molecular mobility. *Journal of Pharmaceutical Sciences*, *91*(8), 1863–1872.

Zhu, Q., Harris, M. T., & Taylor, L. S. (2012). Modification of crystallization behavior in drug/polyethylene glycol solid dispersions. *Molecular Pharmaceutics*, *9*(3), 546–553.

Zhu, Q., Taylor, L. S., & Harris, M. T. (2010). Evaluation of the microstructure of semicrystalline solid dispersions. *Molecular Pharmaceutics*, *7*(4), 1291–1300.

Zhu, Q., Toth, S. J., Simpson, G. J., Hsu, H., Taylor, L. S., & Harris, M. T. (2013). Crystallization and Dissolution Behavior of Naproxen / Polyethylene Glycol Solid Dispersions. *Journal of Physical Chemistry B*, *117*(5), 1494–1500.